STUDIES ON THE ROLE OF ATOMISATION IN AQUEOUS TABLET FILM COATING

ANDREW M. TWITCHELL

A thesis submitted in partial fulfilment of the requirements of the Council for National Academic Awards for the degree of Doctor of Philosophy

September 1990

Leicester Polytechnic in collaboration with Colorcon Ltd.

ABSTRACT

Studies on the role of atomisation in aqueous tablet film coating

A.M. Twitchell

This study evaluates the role of the atomisation stage of the aqueous tablet film coating process in determining the mechanisms of film formation and the properties of the resulting film.

The rheological behaviour and surface activity of aqueous film coating formulations based on hydroxypropyl methylcellulose (HPMC) were studied in order to elucidate their influence on atomisation and the behaviour of droplets once impinged on a substrate surface. Relationships between coating formulation rheology and polymer solution concentration and temperature were quantified and the effect of polymer batch variation and commonly used formulation additives determined. Equations were generated which allow the prediction of the surface tension of atomised film coating solution droplets of different size and composition. It was postulated that droplet surface tension may increase as droplet size decreases and it may be considerably higher than that of the bulk solution from which it was generated.

A detailed examination of the atomisation process was undertaken using a variety of spray guns and coating formulations typical of commercial coating processes. The role of the spray gun design in determining the spray characteristics, the distribution of droplet sizes and the behaviour of the droplets after leaving the gun was elucidated. Of prime importance was the design of the spray gun air cap, which determined i) the velocity of the air exiting the annulus around the liquid nozzle (a major determinant of atomised droplet size), ii) the volume of air accompanying the droplets to the substrate surface, iii) the spray shape and iv) the droplet distribution within the spray. The effect of coating formulation viscosity and spray rate on mean atomised droplet sizes was determined. Droplet size distributions within the sprays were found to fit the Mugele and Evans upper-limit log probability relationship.

The role of atomisation conditions and droplet properties on the process of film formation and resultant film properties was examined. The behaviour of the atomised droplets upon impingement onto the substrate surface was shown to govern the density, thickness, surface characteristics and mechanical properties of the film. The factors responsible for some common film coat defects were determined and data generated which indicated how manipulation of the coat application conditions may influence coat properties and the production of a coated product with the desired appearance and performance characteristics.

ACKNOWLEDGEMENTS

I would like to express my gratitude to all my friends and colleagues who have contributed to the completion of this thesis. In particular I would like to acknowledge the help and support of the following people:

Dr Michael E. Aulton, for his guidance, encouragement and patience throughout the course of this work.

Dr John E. Hogan, for his interest, helpful discussions and organisation of the financial support from Colorcon Ltd.

Dr Ali Hamidi, University of Sheffield, for his expert guidance on the use of the Malvern Droplet Size Analyser.

Finally I would like to thank my wife Liz for her understanding, support and patience.

CONTENTS

CHAPTER 5: THE INFLUENCE OF ATOMISATION AND PROCESS CONDITIONS ON THE PROPERTIES OF AQUEOUS FILM COATED TABLETS

CHAPTER 1

GENERAL INTRODUCTION AND SCOPE OF THE THESIS

Aqueous film coating is a process which involves the deposition of a polymer film (typically 10μm to 100μm thick) onto the surface of a pharmaceutical dosage form. This film is applied by spraying atomised droplets of the various coat components, dissolved or dispersed in an aqueous solvent system, onto a moving bed of tablets or granules using one of the many pieces of equipment designed for the purpose.

Aqueous film coating is now the preferred method for coating pharmaceutical solid dosage forms. Its advantages over sugar coating and organic film coating are well documented (eg Porter, 1979; Hogan, 1982 and Cole et al., 1983)

Ideally the aqueous film coating process should economically and reproducibly result in a coat of even thickness and an aesthetically pleasing high-quality product. To achieve this it is necessary to understand how the many factors involved in aqueous film coating influence the coating process and the quality and properties of the final product.

At present the atomisation stage of the aqueous film coating process is poorly understood with the choice of spray gun and atomisation conditions tending to be empirical. The aim of the work in this thesis was therefore to investigate the effect of the atomisation conditions on the process of film formation and quality of tablet film coats, with a view to optimising the spray application conditions to produce dosage forms possessing the desired characteristics.

In order to achieve these objectives the work aimed to investigate three key inter-related factors.

1. The physical properties of film coating solutions and suspensions, so that their influence on the atomisation process and behaviour at the tablet surface could be identified.
2. The atomisation process, to elucidate the properties of the atomised droplets at the point of impingement on the tablet surface.
3. The effect of the coat application conditions on the process of film formation and film properties, to aid in the selection of appropriate conditions to achieve the desired end product properties.

CHAPTER 2

MATERIALS

The following materials were used for the preparation of the film coating solutions and the placebo tablets used in this work.

2.1 FILM COAT COMPONENTS

Many different polymers are currently used to film coat tablets. These are either applied dissolved in water or organic solvents or as latex/pseudolatex aqueous dispersions. They can act as taste-masking or odour-masking agents, enhance tablet appearance, aid tablet packaging or confer modified release characteristics to the tablets. The polymers most frequently used are the cellulose and acrylate derivatives, either used alone or in combination. The cellulose derivatives include ethylcellulose (EC), methylcellulose (MC), hydroxypropylcellulose (HPC), hydroxypropyl methylcellulose (HPMC), cellulose acid phthalate (CAP) and hydroxypropyl methylcellulose phthlate (HPMCP). Of the three water-soluble polymers, namely HPC, MC and HPMC, the latter is the most widely used in aqueous film coating and was the film-forming polymer used during this work. The commonly used acrylate derivatives are available as the Eudragit range of products (Röhm Pharma, West Germany).

2.1.1 HYDROXYPROPYL METHYLCELLULOSE

HPMC is the film-forming polymer of choice for non-modified release coatings because it has excellent film-forming ability and possesses suitable solubility characteristics over a wide pH range, thus ensuring the coating has minimal effect on drug release. HPMC has a long history of safe usage in the food and pharmaceutical industries. It gives clear, tough, chip resistant, flexible, tasteless, odourless, non-tacky

films which are stable to heat, light, air and a reasonable amount of moisture. The films can be easily overprinted and can coat tablets of a variety of shapes including those possessing logos or intagliations.

In powder form, HPMC is white to off-white, odourless, tasteless and hygroscopic with a fibrous or granular texture. It is derived from cellulose and hence possesses a polymer backbone based on a basic repeating structure of anhydroglucose units as shown below in Figure 2.1.

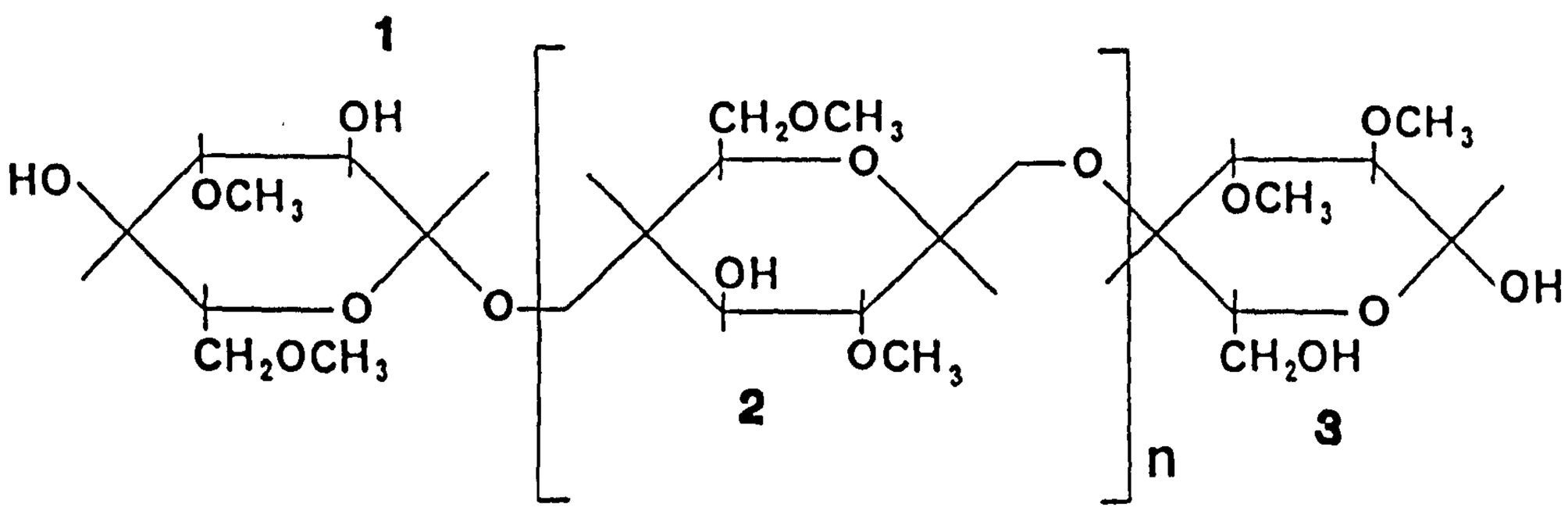

Figure 2.1: STRUCTURE OF HYDROXYPROPYL METHYLCELLULOSE

Each of these units has three possible positions (numbered one to three in Figure 2.1) where the substitution of the hydroxyl group with methyl or hydroxypropyl groups can occur. The average number of these substituent groups on the anhdroglucose unit is designated the degree of substitution (DS). If all three groups on each unit were substituted for example the degree of substitution would be 3.

HPMC is available in a wide range of grades. It is characterised both by the DS value for methyl and hydroxypropyl substitution and by the viscosity of a 2%w/v solution in water at 20°C, the latter being measured using either an Ubbelohde U-tube viscometer in accordance with

A.S.T.M. standards 1347-72 and D2363-72 (United States Pharmacopeia) or a rotating viscometer at a shear rate of $10s^{-1}$ (European Pharmacopoeia). The viscosity is dependent on the average degree of polymerisation of the anhydroglucose units and their dispersity.

The grade of polymer used in this work was Methocel E5 Premium (Colorcon Ltd., Orpington) which will be referred to hereafter as HPMC E5. This grade has nominal DS values for methoxyl and hydroxypropoxyl substitution of 1.88 and 0.20 respectively and a nominal viscosity for a 2%w/v aqueous solution at 20°C of 5mPa s (5cP). It conforms to the standards specified in the United States Pharmacopeia (USP) and European Pharmacopoeia (EP).

HPMC E5 and Pharmacoat 606 (Shin-Etsu Chemical Co. Ltd., Japan, which has a nominal viscosity designation of 6mPa s) are the most commonly used HPMC grades for non-modified release aqueous film coating. They provide a suitable compromise between the increased mechanical strength of films produced from higher grade polymers (Rowe, 1980a) and the reduced process times possible due to the increased amounts of polymer which can be incorporated into the coating solution before it becomes too viscous for satisfactory coating to be achieved.

HPMC E5 is freely soluble in cold water but insoluble in hot water. Gradual heating of solutions of HPMC E5 causes the formation of a gel network, a process known as thermal gelation. This is reported to occur between 58°C and 64°C for a 2%w/v solution (manufacturer's literature) and between 40°C and 50°C for 7.5%w/v to 20%w/v solutions (Prater, 1982). The process of thermal gelation is reported to be fully reversible on cooling.

HPMC E5 is hygroscopic, the amount of moisture absorbed being dependent on atmospheric temperature and relative humidity. It should therefore be protected from atmospheric moisture by being kept in airtight containers until just prior to use. The pharmacopoeial moisture limits (as determined by loss on drying measurements) are ‹5% (USP) and ‹10% (EP). HPMC E5 is supplied by the manufacturers with a moisture content of ‹3%

The specification of HPMC E5 allows a variation in the nominal viscosity of ±20%, this complying with the requirements of the USP. A given batch of HPMC E5 could therefore have a viscosity between 4mPa s and 6mPa s for a 2%w/v aqueous solution at 20°C. Thus in order to minimise any potential effect due to polymer batch to batch variation, any work investigating the aqueous film coating process which involves HPMC, should use either the same batch throughout the work or one of a similar nominal viscosity specification.

2.1 2 PLASTICISERS

Plasticisers are included in aqueous film coating formulations based on HPMC in order to modify the physical properties of the film and to improve the film-forming characteristics. They are usually relatively low molecular weight structures of low volatility which impart flexibility to the polymer film. It has been postulated that they reduce the build up of stresses during the application of the film and therefore reduce the incidence of bridging of the intagliations (Rowe and Forse, 1981). To be effective it is thought that the plasticiser molecules must interpose themselves between the polymer chains and interact with the forces which normally hold the chains together, thereby extending and softening the polymer matrix (Entwistle and

Rowe, 1979).

Plasticisers suitable for aqueous film coating solutions based on HPMC are limited to those which are water-soluble, non-toxic and compatible with the polymer. The plasticisers investigated in this study were those commonly used commercially and include; Glycerol BP (British Drug House Chemicals Ltd. (BDH)), Propylene glycol BP (BDH) and polyethylene glycol (PEG) of grades with nominal molecular weights of 200, 400, and 1500 (BDH). With the exception of PEG 1500, which is a waxy solid, all the plasticisers used are clear, colourless, viscous liquids. All are hygroscopic and were therefore kept in well closed containers. Each plasticiser was used as received.

Water acts as a plasticiser for HPMC because of its high affinity for the polymer (Abdul-Razzak, 1982). Any water remaining in the film after coating will exert a plasticising action and this may be sufficient such that plasticisers are not required in the coating formulation.

In addition to compatibility problems, care must be taken in the use of plasticisers since they may have detrimental effects on the properties of the film (Hawes, 1976).

2.1.3 OPACIFIERS AND COLOURING AGENTS

Opacifiers and colouring agents are included in coating formulations to aid product identification and to improve their aesthetic appearance. They may also usefully contribute to the total coating solids and aid in minimising the moisture permeability of the film coat. Those used predominantly in aqueous film coating can be divided into two groups namely aluminium lakes and inorganic pigments.

Aluminium lakes

Aluminium lakes are insoluble in water and possess good colouring and hiding properties. They are produced by adsorbing the dye onto hydrated

alumina and then converting the dye to the aluminium salt. Aluminium lakes are used in preference to water soluble dyes, since, with the latter, there is a tendency for colour migration to occur during film drying, with the resultant colour differences causing considerable intra- and inter-batch variations. In addition adverse effects on polymer dissolution caused by water-soluble dyes have been reported (Prillig, 1969).

Aluminium lakes of many different different dyes are available and are used widely in practice. They are available in regular or high tint (HT) forms the latter having 1.1-1.5 times the colour strength, this arising from the reduced average lake particle size.

As well as being used alone and in combination with inorganic pigments, aluminium lakes are also used in colouring dispersions e.g. Opaspray (Colorcon Ltd.) and as a constituent of Opadry (Colorcon Ltd.), a ready mixed dry powder coating formulation.

The aluminium lakes used in this work were; indigo carmine aluminium lake (FD&C Blue No.2 aluminium lake), erythrosine aluminium lake (FD&C Red No.3 aluminium lake), brilliant blue aluminium lake (FD&C Blue No.1 aluminium lake), sunset yellow aluminium lake (FD&C Yellow No.6 aluminium lake) and FD&C Yellow No.10 aluminium lake. All were of the high tint (HT) form and obtained from Colorcon Ltd.. They were used either alone or as a constituent of the pre-prepared products Opaspray and Opadry. All were used as received.

Inorganic pigments

Those inorganic pigments commonly used in aqueous film coating include, the iron oxides, titanium dioxide, talc and calcium carbonate. In this study the inorganic pigments used were titanium dioxide, calcium carbonate and talc. These all conformed to British Pharmacopoeial specifications and were used as received. Talc and titanium dioxide

were obtained from Colorcon Ltd. and calcium carbonate from BDH.

Titanium dioxide is a white amorphous, odourless, tasteless powder used in film coating because of its extreme whiteness and very good opacifying properties. It is widely used either alone to give a white coating or in combination with other colouring agents.

Calcium carbonate is a fine, white, odourless, tasteless powder. Although possessing little opacifying power it is used as a filler and has been utilised in the production of tablets coats with highlighted intagliations (Rowe, 1983a and Rowe and Forse, 1983a).

Talc is a very fine, white-to-greyish, odourless, crystalline powder which is also used as a filler and, in common with the two pigments mentioned above, is used to reduce the tackiness of the film during the coating process.

The abiltiy of these inorganic pigments to confer colour and opacity is dependent on their particle size and refractive indices. This has been discussed by Rowe and Forse (1983a) and Rowe (1983c and 1984a)

2.1.4 COLORANT DISPERSIONS AND READY MIXED POWDER COATING FORMULATIONS

The colorant dispersion Opaspray type M-1 (Colorcon Ltd.) was used in this project. This is an opaque, pre-milled, colour concentrate which consists of a suspension of an aluminium lake, titanium dioxide and HPMC E5 (included as a suspending agent) in water and alcohol. It is intended to be added to a polymer solution usually with the inclusion of a plasticiser and requires only hand stirring to give an even colour dispersion. The product studied in this work included indigo carmine aluminium lake (FD&C Blue No.2 aluminium lake) as the colouring agent.

An increasingly commercially important range of products for aqueous film coating are those which contain all the ingredients for producing

the film coat in a ready mixed dry-powder form. They need only be added to water and mixed over a relatively short period (the manufacturers recommend less than an hour) to obtain a useable coating suspension and thus offer the advantage of considerably reduced coating suspension preparation times. These ready-prepared dry powder formulations are available as the Opadry range of products (Colorcon Ltd.). In this work types OY-Opadry and OY-D Opadry were used, these being based on HPMC E5 and HPMC E3 respectively. Both products contained PEG 400 as a plasticiser and titanium dioxide as an opacifying agent. Two batches of the type OY-Opadry were studied, these containing either indigo carmine aluminium lake or a combination of indigo carmine, brilliant blue, sunset yellow and FD&C Yellow No.10 aluminium lakes as the colouring agents. The OY-D Opadry batch used was coloured with indigo carmine aluminium lake.

Typical concentrations recommended for use in aqueous film coating are 15%w/w for the OY-Opadry products and 25%w/w for the OY-D Opadry products.

2.1.5 SURFACE ACTIVE AGENTS

The two surface active agents used in this study were sodium lauryl sulphate and polysorbate 20.

Sodium lauryl sulphate is a white-to-pale yellow powder or crystalline substance with a slight characteristic odour and is an anionic surface active agent. Polysorbate 20 is a viscous, yellow oily liquid and a non-ionic surface active agent. Both surface active agents used were of BP quality and were obtained from BDH.

2.2 PLACEBO TABLET COMPONENTS

The components of the placebo tablets used in the investigation of the coating process (Chapter 5) are detailed below. Their role in influencing both the mechanism by which the film is formed and the properties of the film is discussed in Chapter 5.

2.2.1 MICROCRYSTALLINE CELLULOSE NF

Microcrystalline cellulose is a white, tasteless, odourless, hygroscopic, crystalline powder composed of porous particles. It is a commonly used tablet disintegrant or filler. The microcrystalline cellulose used in this work was obtained from Colorcon Ltd. and conformed to the specification in the United States National Formulary (NF).

2.2.2 STARCH 1500 (PREGELATINIZED STARCH NF)

Starch 1500 is a fine, white-to-off-white powder which is odourless and has a slight characteristic taste. It is used as a tablet binder, diluent or disintegrant. Starch 1500 was obtained from Colorcon Ltd. and conformed to the United States National Formulary monograph on pregelatinised starch.

2.2.3 STEARIC ACID BPC 1973

Stearic acid is either a hard white/yellowish white crystalline solid or a white/yellowish white powder with a slight odour and taste. It is a mixture of stearic acid and palmitic acid of which the content of each is not less than 40% and the sum of the two not less than 90%. It is used as a tablet lubricant. The stearic acid used in this work was obtained from Colorcon Ltd. and conformed to the specification in the British Pharmaceutical Codex 1973.

CHAPTER 3

THE PHYSICAL PROPERTIES OF FILM COATING SOLUTIONS AND SUSPENSIONS

3.1 INTRODUCTION

The physical properties of film coating solutions and suspensions can potentially exert an influence at many stages during the film coating process. These stages include delivery to and droplet production at the atomising device, travel to the tablet surface and the wetting, spreading, penetration, evaporation and adhesion of the atomised formulation at the tablet surface.

It is therefore important to determine the physical properties of the coating solutions and suspensions that are to be used in the film coating process, so that their influence on the appearance and properties of the final film coat can be appreciated.

The following discussion reviews the areas where the physical properties of the coating solution may be of importance during the coating process.

3.1.1 ATOMISATION

No work has been published to date on the effect of solution physical properties on the droplet size distribution or spray shape produced during atomisation of aqueous film coating solutions. Schæfer and Wørts (1977), when studying the fluidised-bed granulation process, found that with aqueous granulating fluids based on gelatine, methylcellulose, carboxymethylcellulose and polyvinylpyrollidone (PVP), the higher the solution viscosity, the larger were the droplets formed on atomisation. Banks (1981) however found with aqueous solutions PVP K30 that increasing the concentration from 5%w/v to 10%w/v did not produce a

significant change in droplet size, the effect of the viscosity increase being overridden by other process variables. The same author also demonstrated that the addition of sodium lauryl sulphate in increasing quantities to PVP granulating fluids caused both an increase in the diameter of the spray cone produced on atomisation and a reduction in the distance from the spray gun at which the spray maintained its general shape and pattern. These effects were attributed to the lower surface tension produced by the addition of the surfactant.

Although no published research of direct relevance to aqueous film coating has been carried out to elucidate the importance of the physical properties of the formulation on the atomisation process, work carried out with a variety of other materials and processes has yielded various equations describing how changes in viscosity, surface tension and density affect the quality of the atomised solution. These predictive equations which are described in detail in Chapter 4, show a wide divergence of findings on the relative importance of the aforementioned variables. This is presumably due to the wide variety in atomiser designs used in the experiments, each equation being valid for the test conditions studied but failing when extrapolated to other systems.

For airless (hydraulic) atomisation (where the process is not complicated by the volume, velocity and density of the atomising fluid as it is with airborne (pneumatic) atomisation), Fair (1974) suggested the use of Equation 3.1 as a guide to the effect of solution properties on the average droplet diameter produced during atomisation.

$$\frac{Dvm\ soln}{Dvm\ solvent} = \left[\frac{\gamma soln}{\gamma solvent}\right]^{0.6} \times \left[\frac{\mu soln}{\mu solvent}\right]^{0.2} \times \left[\frac{\rho solvent}{\rho soln}\right]^{0.3}$$

Equation 3.1

In this equation Dvm is the volume mean droplet diameter and γ, μ and ρ the surface tension, viscosity and density of the solution being sprayed.

More complex equations have been developed for predicting droplet sizes produced by pneumatic atomisation. An often quoted example is that of Nukiyama and Tanasawa (1939) an adapted form of which is shown below (Equation 3.2).

$$Ds = \left[\frac{585 \times 10^3}{v}\right] \times \left[\frac{\gamma}{\rho}\right]^{0.5} + 1683\mu^{0.45}\,[\gamma \times \rho]^{-0.225} \left[\frac{1000}{J}\right]^{1.5}$$

Equation 3.2

Here Ds is the surface mean diameter of the droplets (μm), v is the velocity of air relative to liquid at the atomiser nozzle exit (ms^{-1}), γ is the liquid surface tension (Nm^{-1}), ρ is the liquid density (kgm^{-3}), μ is the liquid viscosity (Pa s) and J is the air/liquid volume ratio at the air and liquid orifices.

Both these equations indicate that the solution physical properties of viscosity, surface tension and density will influence the atomisation process and therefore could potentially affect the quality of the final film coat.

3.1.2 DROPLET TRAVEL TO THE TABLET BED

Once atomised, the physical properties of the droplets may influence their behaviour during passage to the tablet bed. The viscosity of the droplet may affect the evaporation rate, with droplets of higher viscosity exhibiting reduced evaporation. Similarly any surface active components may form a surface layer which could serve to retard evaporation. The surface tension and viscosity of the droplet may also affect the tendency of the airborne droplets to coalesce, an increased

likelihood of coalescence occurring as the surface tension increases and the viscosity decreases.

3.1.3 DROPLET BEHAVIOUR AT THE TABLET SURFACE

Once the atomised droplets have impinged on the tablet surface, they may adhere, wet, spread, coalesce and penetrate. The extent to which these occur may depend on many factors including the viscosity and surface tension of the formulation, the conditions of atomisation and the nature of the solid surface.

The relationship between surface forces for a droplet placed onto an insoluble non-porous surface and left to reach equilibrium has been summarised by Young's equation (Equation 3.3):

$$\frac{\gamma_{sv} - \gamma_{sL}}{\gamma_{LV}} = \cos\theta \qquad \text{Equation 3.3}$$

where γ_{LV} is the liquid surface tension, γ_{sL} is the interfacial tension between the liquid and the solid, γ_{sv} the surface tension of the solid against vapour and θ the angle formed when a tangent is drawn at the point of contact between solid, liquid and vapour. This is represented in the diagram below.

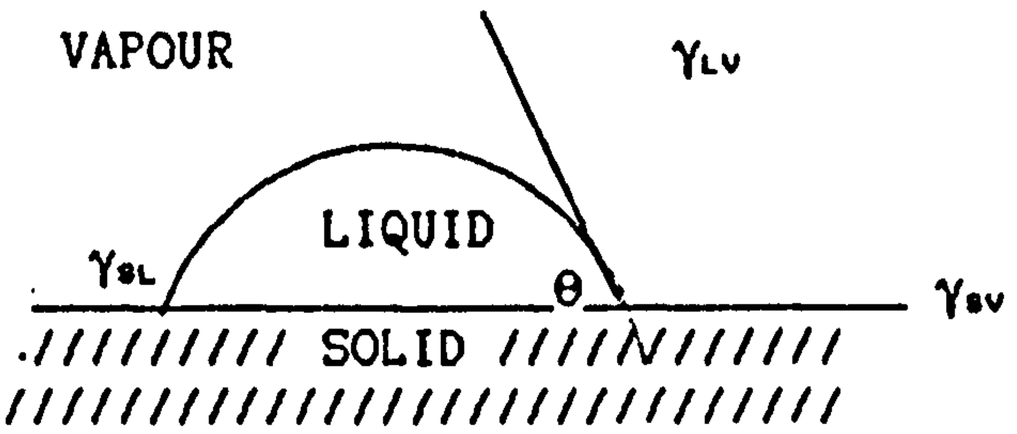

If the value of $\cos\theta$ is equal to 1 (ie $\theta=0°$) then the surface is completely wetted. The contact angle increases and therefore the degree of wetting decreases as $\cos\theta$ tends to 0 ($\theta=90°$) and on to -1 ($\theta=180°$).

From this it can be concluded that any factors which influence the

surface tension of the formulation and/or the interfacial tension will influence the degree of wetting. Surface active agents for instance may decrease both γ_{LV} and γ_{SL}, the latter arising from their adsorption at the solid-liquid interface. Banks (1981) suggested that the large increases in granule size which resulted from the inclusion of high surfactant concentrations in an aqueous PVP granulating fluid, could have arisen from the improved spreading of atomised droplets at the granule surface and a reduction in the value of γ_{SL}.

Young's equation relies strictly on surface forces to determine the tendency to spread and will give equilibrium contact angles for drops placed carefully on the surface. During aqueous film coating however there is a very short time period between the droplet hitting the surface and a film being produced. There may therefore be insufficient time for equilibrium values of γ_{SL} and γ_{LV} to be reached and equilibrium contact angles may not be achieved if spreading is slow due to a high droplet viscosity. The potential for the latter effect to occur was illustrated by Zografi (1985) who showed that for a series of polydimethylsiloxones on metal surfaces, the time taken for the equilibrium contact angle of 0° to be reached increased markedly as the liquid viscosity increased.

Droplets contacting tablet surfaces do not do so gently, but impinge with a relatively high velocity, the kinetic energy being derived from the atomising air. Data gathered from studies on spontaneous spreading may therefore not be applicable to droplet spreading during the actual coating process. Zografi (1985) reported that droplets forced to move across a surface at higher velocities exhibited larger dynamic contact angles. He concluded that forced spreading may therefore induce ordinarily good wetting systems to have less wetting power during a process like film coating.

A practical consequence of poor spreading properties of film coating solutions is manifest in a film defect known as "orange peel" where the surface is rough and has the characteristic appearance of an orange or lemon skin.

Pharmaceutical tablets will consist of pores through which the applied film coating solutions may penetrate. This penetration has been demonstrated to closely follow Equation 3.4 which was developed by Alkan and Groves (1982) from the earlier work of Washburn (1921).

$$\frac{l}{t} = \frac{1}{4}\left[\frac{2\pi}{3Vv}\right]^{2/3} x \left[\frac{\cos\theta.\gamma}{\mu}\right] x \left[\varepsilon^{2/3}.D\right] \qquad \text{Equation 3.4}$$

where D is the mean pore diameter, Vv is the void volume of the penetrated space, ε is the porosity of the powder bed, θ is the solid/liquid contact angle and μ and γ the viscosity and surface tension of the solution respectively.

Since the volume of liquid which passes into the bed will be the same as the void volume, it can be seen that the rate of penetration of a film coating solution will be dependent on its viscosity, surface tension and interaction with the solid surface.

The validity of this equation was confirmed by the authors by following the depth of penetration into a tablet with respect to time of an organic film coating solution based on HPMC.

The concept of different rates of penetration into tablet surfaces by solutions of different viscosities was utilised by Fisher and Rowe (1976b) to explain the variation in film adhesion between formulations of different grades of HPMC. The authors postulated that the increased rate and depth of penetration of solutions prepared from the lower

molecular weight grades of HPMC resulted in an increase in the effective area of coating-to-tablet contact and therefore higher adhesion.

3.1.4 COATING SOLUTION TACKINESS

The tackiness of a liquid can be defined as the impulse per unit area necessary to separate two planes initially in contact through an intervening liquid. Chopra and Tawashi (1982, 1984 and 1985) in a series of articles investigated the effects of different coating formulations on tack values. They demonstrated that with aqueous solutions of HPMC E5 at concentrations up to 20%w/w, the increase in tack (ft) with increasing viscosity (μ) followed Equation 3.5:

$$ft \propto \mu^{0.67} \qquad \text{Equation 3.5}$$

Thus solutions got more tacky as their concentration and therefore viscosity increased. At concentrations above 20%w/w, more complex relationships were identified which were related to the visco-elastic nature of the polymer.

If the above equation was followed when finely divided solids were added to the formulations, then it would be expected that the tack values would increase due to an increase in viscosity. This was indeed found to be the case with titanium dioxide and FD&C Blue No.2 aluminium lake when added to 10%w/w solutions of HPMC E5. In contrast talc was found to decrease tack. At high concentrations (65%w/w) of PVP all three additives were found to decrease tack values. The observations reported were explained in relation to the additive's effect on the way that the solution behaved during the separation process and differences in their particle size distributions.

3.1.5 ADHESIVE BEHAVIOUR OF TABLET FILM COATS

The adhesion of film coats to a tablet substrate is of importance if coating defects such as bridging of the intagliations are to be avoided (Rowe, 1981c). The extent of film adhesion will be dependent both on the properties of the tablet and those of the coating formulation when it contacts the tablet surface. In order to assure good adhesion, there should be both good intrinsic bonding between the chemical groups of the polymer and solid and a maximal true area of contact. The presence of gaps or air pockets between the polymer and solid will tend to weaken the adhesive strength.

The work of adhesion (W_A) between a solid and a liquid can be defined as the energy per unit area required to separate molecules bonding across the interface. It is described by the Young-Dupré equation (Equation 3.6):

$$W_A = \gamma_{LV} (1 + \cos\theta) \qquad \text{Equation 3.6}$$

where γ_{LV} is the solution surface tension and θ the equilibrium contact angle formed when a drop is placed on the tablet surface.

Thus, an increase in the coating solution surface tension or a decrease in the contact angle formed, should in principle promote adhesion. Maximum attractive forces between a liquid and solid should occur when $\cos\theta = 1$, ie when the contact angle θ is zero. In this case, the forces of attraction between the liquid and solid are greater than the cohesive forces of the liquid and $W_A = 2\gamma_{LV}$.

Nadkani et al. (1975) investigated the effect of solution surface tension and contact angle formed on various substrates when coating with poly(methyl vinyl ether/maleic anhydride) plasticised with glyceryl triacetate and dissolved in a variety of solvents. They found that in accordance with the theory of the Young-Dupré equation, the film adhesion of sprayed coats was greatest with solution/substrate systems

exhibiting the lowest contact angles and with solutions of the highest surface tension, although they reported that the latter result was contrary to expectations.

Fisher and Rowe (1976b) found that increasing the viscosity of an organic film coating solution, by increasing the HPMC concentration, led to a decrease in the measured adhesion of the film coat. They attributed this to the reduced penetration of the more viscous solutions into the tablet surface with the resultant reduction in the effective area of solid-liquid contact. No significant effect was found when various plasticisers were included in the formulation, but the inclusion of titanium dioxide reduced the measured adhesion. The latter effect was attributed to interference with the hydrogen bonding between the polymer film and tablet substrate.

3.1.6 GLOSS AND FILM SURFACE ROUGHNESS

Tablet gloss can be defined as the attribute of the surface which causes it to have a shiny or lustrous appearance.

Rowe (1985a) determined gloss values of film coats by measuring light specularly reflected at 60° by flat-faced film-coated tablets. It was reported that with organic solutions of HPMC, increasing polymer concentration and thus viscosity, caused a reduction in the gloss of the coat. This was attributed to the increase in roughness of the coat. It was shown for the coating conditions used in the study that tablet gloss and surface roughness could be related directly by a power-law equation.

Relland and Eber (1986) investigated the effects of formulation variables on the surface texture of film coated tablets when applying aqueous gloss solutions of HPMC. The gloss coats were sprayed over previously coated tablets in a spray box designed to mimic industrial coating conditions. They found that increasing the concentration of

HPMC from 2%w/v to 5%w/v did not have a significant effect on tablet gloss or film surface roughness. However using concentrations above 5%w/v resulted in an appreciable increase in roughness and decrease in gloss. The addition of the surfactant Brij 30 was not found to exert a significant effect on either measured parameter.

3.1.7 THERMAL GELATION

HPMC exhibits the property of thermal gelation, that is if a HPMC solution is heated above a certain temperature, a gel network is formed. For E grades of HPMC this occurs between 58°C and 64°C for a 2%w/v solution (manufacturer's literature). It is therefore important to be aware of the gelation temperatures of the HPMC solutions used in aqueous film coating and how they are affected by the addition of commonly used formulation additives, so that factors leading to the phenomenon occurring in practice can be avoided. Reduction of the gelation temperature, to 37°C or below for example, has been associated with the reduction in release rate from coated tablets (Schwartz and Alvino, 1976).

3.1.8 BRIDGING OR FOAM INFILLING OF TABLET INTAGLIATIONS

Down (1982) reported the phenomenon of bridging or foam infilling of tablet intagliations experienced during aqueous film coating with a HPMC based suspension in an air suspension column. He stated that one method of overcoming this defect was by the addition of alcohol to the formulation. This was said to improve the situation by simultaneously reducing the surface tension and viscosity of the formulation.

3.1.9 SCOPE OF THE CHAPTER

The work described in this chapter was aimed at elucidating the physical properties of a variety of aqueous film coating formulations, including those which were to be used in the atomisation and coating studies detailed in Chapters 4 and 5. It was intended to determine the role of formulation concentration, batch-to-batch variation of the HPMC E5, polymer moisture content, formulation temperature and the inclusion of various commonly used formulation additives. It was hoped that the information gained from this work would help in obtaining a clearer understanding of the importance of the solution physical properties on the coating process and would assist in determining ways in which the problems encountered in practice during aqueous film coating may be overcome.

3.2 EXPERIMENTAL

3.2.1 THE PREPARATION OF FILM COATING SOLUTIONS FOR VISCOSITY, SURFACE TENSION AND DENSITY MEASUREMENTS

Unless otherwise stated in the results section of this chapter, and with the exception of the Opadry preparations, all solutions used for determination of viscosity, surface tension and density values were prepared by the following method:

About half of the required amount of twice-distilled water was heated to about 80°C in a suitably cleaned weighed glass beaker. The HPMC E5 was added with gentle stirring until it was completely wetted and dispersed. A further quarter of the water at room temperature was added, the beaker was then placed in ice to hasten solvation and the dispersion gently stirred until solvation was complete. Any required additives were incorporated at this stage (soluble additives being dissolved in water prior to addition), the preparation made up to the desired weight, and

the solution stirred until homogeneous. Care was taken throughout to avoid the incorporation of air bubbles.

The moisture content of the HPMC E5 samples used to prepare these solutions was between 2.55%w/w and 2.65%w/w unless otherwise stated (see section 3.2.2 for method of determination).

Since HPMC E5 solutions have been shown to support microbial growth (Banker et al., 1982) which may affect their physical properties, solutions not used on the day of preparation were stored in a refrigerator and no solution was kept for more than 48 hours.

Preparation of Opadry suspensions

The total quantity of twice-distilled water required was placed without heating into a suitably sized clean glass beaker. A vortex was created in the water into which the Opadry powder was slowly added over a period of a few minutes (without the incorporation of air if possible). Once the powder was completely wetted and dispersed, the dispersion was stirred for at least a further 60 minutes to ensure polymer hydration was complete. High speed agitation was avoided to minimise aeration of the suspension.

The effect of coating solution preparation method and storage conditions on the solution properties

There are many different methods by which HPMC E5 solutions can be prepared (manufacturers' literature). These include dispersing the polymer in the total weight of either hot or cold water, and replacing a portion of the cold water with ice in order to hasten polymer solvation. In addition a variety of different qualities of water (eg distilled, de-ionised or potable water) may be used instead of twice-distilled water. Methyl cellulose solutions have been shown to exhibit different properties depending on the temperature at which they are stored (Neely, 1963). For these reasons HPMC E5 solutions were prepared and stored in

a number of different ways (see below) in addition to the standard method detailed above. The solutions prepared at a concentration of 9%w/w using these alternative methods were analysed using a suspended level viscometer (see section 3.2.3.2) to determine whether the method of preparation and storage had affected their physical properties.

Alternative solution preparation methods

1. The polymer was dispersed in the total weight of water at approximately 90°C, stirred until wetted and dispersed and then allowed to cool to room temperature with gentle agitation. The solution was analysed immediately.

2. The solution was prepared as in 1., but stored covered at room temperature for 24 hours before readings were taken.

3. The solution was prepared as in 1. but stored for 24 hours in a refrigerator and allowed to equilibrate to room temperature before analysis.

4. The polymer was dispersed in the total volume of cold water (20°C) and gently agitated until solution was complete. Solutions were left for 24 hours at room temperature before commencing measurement.

5. The solution was prepared as in 4., but stored for 24 hours in a refrigerator and equilibrated to room temperature before analysis.

6. The polymer solution was prepared using the standard method except that the cold water used to make up to weight was replaced with ice. The solution was left for 24 hours at room temperature before commencing measurement.

7. The solution was prepared as in 6., but left for 24 hours in a refrigerator before analysis.

8. The polymer solution was prepared as in the standard method except that the twice-distilled water was replaced by potable water. The solution was left at room temperature for 24 hours before being

measured.

9. The polymer solution was prepared as in the standard method, with the final solution being agitated with a high shear Ultra-Turax mixer for fifteen minutes and left to de-aerate before analysing.

3.2.2 DETERMINATION OF THE MOISTURE CONTENT OF HPMC E5 SAMPLES AND ITS EFFECT ON SOLUTION VISCOSITY

The moisture content of samples of HPMC E5 was calculated from the average weight lost from five 5g samples after heating at 60°C for 24 hours over phosphorus pentoxide.

In order to determine the influence of storage conditions on the moisture content, samples were placed in desiccators containing various saturated salt solutions and the desiccators stored at a controlled temperature of 20°C for a period of seven days, after which time the moisture content was determined as described above. The salts used to prepare the saturated salt solutions and the corresponding environmental relative humidities produced are shown in Table 3.1. All salts were of reagent grade and the solutions were prepared in twice-distilled water.

Table 3.1

SATURATED SALT SOLUTION	EQUILIBRIUM RELATIVE HUMIDITY PRODUCED (%) AT 20°C
LITHIUM CHLORIDE	11
MAGNESIUM NITRATE	53
SODIUM CHLORIDE	76
POTASSIUM NITRATE	95

Data from Nyqvist (1985)

Solutions of HPMC E5 were prepared from samples stored at conditions of differing relative humidity and their viscosity determined as described in section 3.2.3.2.

3.2 3 VISCOSITY AND ITS MEASUREMENT

3.2.3 1 VISCOSITY

The viscosity of a liquid is a measure of the internal resistance offered to the relative motion of different parts of the liquid. Viscosity is defined as the shearing force required to produce a velocity of $1ms^{-1}$ between two parallel planes of liquid each of $1m^2$ in area and separated by a distance of 1m. It has units of Pa s, with 1mPa s being equivalent to 1cP (centipoise).

The force per unit area producing the shear is called the shear stress (τ) and has units of Nm^{-2} (or Pa). The velocity gradient produced is called the shear rate (dv/dr) and has units of s^{-1}. Viscosity can therefore also be defined as the ratio of the shearing stress to the rate of shearing. This can be represented as:

$$\tau = \mu \cdot \frac{dv}{dr} \qquad \text{Equation 3.7}$$

where μ is the viscosity (or apparent viscosity) at the particular shear rate used.

If the value of μ is the same at all shear rates (assuming streamline flow and a constant temperature), then the liquid under test is said to possess Newtonian viscosity. This type of behaviour is common to most pure liquids and many solutions and dispersions.

Liquids exhibiting different viscosities at different shear rates are said to possess non-Newtonian behaviour. The main causes of non-Newtonian behaviour are the formation of a structure throughout the system or the orientation of asymmetric particles under the influence of

the velocity gradient. Types of non-Newtonian behaviour of importance to polymer solutions include pseudoplastic and thixotropic behaviour.

Pseudoplastic behaviour (shear thinning)

Pseudoplastic behaviour is characterised by a gradual decrease in the apparent viscosity with increasing shear rate. This can arise from a number of causes, including the breakdown of particle aggregates and the alignment of particles as the shear rate increases.

If pseudoplastic behaviour is exhibited then the apparent Newtonian viscosity may be obtained from the power-law equation:

$$\tau = \mu_N \times D^N \qquad \text{Equation 3.8}$$

where τ is the shear stress (Pa), μ_N is the apparent Newtonian viscosity (Pa s), D is the shear rate (s^{-1}) and N is the index of non-Newtonian behaviour.

Taking logs the equation becomes:

$$\log \tau = \log\mu_N + N\log D \qquad \text{Equation 3.9}$$

Thus if log τ versus log D is plotted and a straight line relationship exists, the slope will be equal to the index of non-Newtonian behaviour and the apparent viscosity can be derived from the intercept. If $N < 1$ then the liquid exhibits pseudoplastic behaviour. A value of $N = 1$ indicates Newtonian behaviour.

Thixotropy

A system is described as thixotropic, if, when sheared at a constant rate, it exhibits a time-dependent reduction in apparent viscosity which continues until a balance between structural breakdown and reformation is reached. On standing such a system will regain its original structure only after a finite period of time.

Solutions of high molecular weight polymers tend to be thixotropic to a certain extent. On shearing, intermolecular attractions and

entanglements are overcome and the extent of solvent immobilisation is reduced. Brownian movement restores the system to its original condition when it is left to stand.

3.2.3.2 VISCOSITY MEASUREMENT

Liquid viscosity measurements are mainly determined using either capillary flow or rotational methods. In this study both methods were employed, the former using a suspended level viscometer and the latter a cup and bob viscometer.

Haake Rotovisco RV2

The Haake Rotovisco RV2 (Gebruder Haake, West Germany) is an example of a rotational (cup and bob) viscometer. It measures the viscous drag or retarding force exerted by a liquid when a rotating body is immersed in it. The test liquid is placed in a stationary cup and is subjected to shear between the walls of the cup and those of a rotating bob. The shear rate exerted is dependent on the speed of rotation of the bob used and the geometry of the cup and bob system. The shear stress is measured from the torque exerted on the rotating bob and is dependent on the shear rate, geometry of the system and the properties of the liquid under test.

The advantage of this system is that the shear stress can be monitored at a variety of shear rates, and viscosities covering a wide range can be measured by the selection of different cup and bob systems.

The Rotovisco RV2 viscometer used in this work was fitted with a MK500 measuring head. The MV1 cup and bob sensor system was used for viscosities from 30mPa s up to 500mPa s, the MV2 sensor system for viscosities between 500mPa s and 1500mPa s and the MV3 sensor system for viscosities above 1500mPa s. Temperature was controlled using a

thermostated temperature vessel. For measurement temperatures of 45°C or below, each formulation to be studied was equilibrated to the appropriate temperature in a water bath before being placed in the measuring vessel and left for a further 10 minutes before measurement was commenced. For higher measurement temperatures (approaching and above the thermal gelation temperature), the formulation was pre-heated to 45°C, placed in the measuring vessel and left for 30 minutes before being measured. These procedures were designed to overcome any problems associated with liquid expansion on heating and enabled the formulation to be left unagitated for a minimal period before measurement. The measuring vessel was equipped with a closely fitting cover which ensured that no significant evaporation occurred over the test period.

The maximum speed of bob rotation was set at 512min^{-1}, equivalent to shear rates of 1198s^{-1}, 461s^{-1}, and 225s^{-1} for the MV1, MV2 and MV3 systems respectively. The time taken for the bob to accelerate from 0min^{-1} to 512min^{-1} and to decelerate from 512min^{-1} back to 0min^{-1} was set to eight minutes. The process was controlled with a Haake PG142 programmer and the results recorded as a shear stress versus shear rate rheogram. Viscosity values were calculated from the rheograms of at least five separately prepared solutions for each formulation tested.

To determine whether a batch of HPMC complies with the viscosity specification of the European Pharmacopoeia, the viscosity of a 2%w/v solution should be measured at 20°C using a rotational viscometer with a shear rate of 10s^{-1}. The Rotovisco system used in this work however was not capable of determining viscosity values at these low shear rates.

Suspended level viscometers

Suspended level viscometers are the instruments designated by the United States Pharmacopeia (USP) to measure the viscosity of 2%w/v aqueous solutions of HPMC, in order to test whether they comply with the

monograph specification. Although capable of very accurate measurement, these instruments suffer from the disadvantage of only measuring the viscosity at a single shear rate, this being dependent on the capillary diameter of the tube being used and the viscosity of the liquid tested. Suspended level viscometers cannot therefore give a viscosity profile over a range of defined shear rates and will only give meaningful results for Newtonian liquids. They are however relatively cheap to purchase and are available with a variety of capillary bore diameters to cover a wide range of viscosities, typically from about 2mPa s to 100,000mPa s.

In this work suspended level viscometers were used to determine the viscosity of 2%w/v solutions as specified by the USP, to measure the viscosity of solutions which could not be measured satisfactorily with the Rotovisco rotational viscometer and to allow a comparison of the results obtained from the two different instruments.

Viscosity measurements were determined using pre-calibrated Technico Ubbelohde suspended level viscometers (Gallenkamp Ltd.). Each viscometer was thoroughly cleaned before use, rinsed with twice-distilled water and dried with acetone. The viscometers were placed in a thermostated water bath at 20°C, the liquid carefully added to avoid the incorporation of air bubbles, and then left to equilibrate for at least 15 minutes. Measurements were taken in accordance with British Standard Specification 188 (1977). The liquid flow times were sufficiently long such that no adjustment was needed to compensate for the kinetic energy of efflux. For each formulation studied, measurements were taken from at least three separately prepared solutions. Viscosity readings were accepted when three consecutive readings for any one solution were within ± 0.2%.

3.2.4 SURFACE TENSION AND ITS MEASUREMENT

The surface tension (γ_{LV}) or surface free energy of a liquid surface, is equal to the work required to increase the area of the surface isothermally and reversibly by a unit amount. It is a measure of the resistance to the formation of new surface and is dependent on the molecular forces acting within the liquid. The SI unit of surface tension is Nm^{-1}, with 1 mNm^{-1} being equal to the cgs unit of 1 dyne cm^{-1}.

Many methods are available for the measurement of surface tension. These can be classified as static (capillary rise method), detachment (Wilhelmy plate and ring methods) or dynamic (drop volume, drop weight and oscillating jet methods).

In this study surface tension values were determined by a ring detachment method using a surface tension torsion balance with a platinum ring assembly (White Electrical Instruments Ltd.). This instrument measures the force required to detach a platinum ring from the surface of the test liquid. The force is supplied by means of a torsion wire attached to a scale calibrated directly in units of surface tension.

An accuracy check on the tensiometer and ring assembly was made by measuring the surface tension of twice-distilled water. A reading of 72.70 ± 0.05 mNm^{-1} was obtained, this being in agreement with the literature value of 72.75mNm^{-1} (Weast, 1988).

The platinum ring used had a circumference of 40mm giving an average radius, R, of 6.37mm. The mean diameter of the wire of the platinum ring was obtained from ten micrometer readings taken at various points around the ring circumference. From these readings the average radius of the wire, r, was found to be 0.153mm.

A glass measuring dish having a diameter of approximately 90mm was used to hold the test liquid. This was chosen so that the curvature of the

surface of the liquid contained in the dish, did not affect the shape of the liquid surface supported by the ring, and hence the value of the measured surface tension (Harkins and Jordon, 1930).

All glassware used for solution preparation and measuring of the surface tension was soaked in Teepol, thoroughly rinsed with tap water and finally rinsed with twice-distilled water. The platinum ring assembly was cleaned by flaming and immersion in twice-distilled water.

Temperature control

The glass vessel in which the liquid under study was contained was fitted with a glass heat exchanger. Water from a constant temperature water bath was circulated through this heat exchanger to ensure that the liquid in the measuring vessel remained at a constant temperature. Any vibrations set up in the liquid due to the circulation of the water through the heat exchanger were found not to alter the surface tension readings obtained. The glass vessel was fitted with a perspex cover to minimise evaporation and the entry of airborne contamination. Each test liquid was equilibrated by storing it in a separate glass vessel in a water bath before transferring it to the temperature controlled vessel.

Measurement procedure

Measurement of surface tension values with the tensiometer were made in accordance with the manufacturer's instructions and with particular attention being paid to the following points.

1. The volume of the test liquid was kept constant at 100ml.

2. The plane of the platinum ring was checked to ensure it was horizontal, since a ring not in the horizontal plane will yield an artificially low value for the surface tension.

3. The platinum ring, Perspex cover and glass dish were rinsed thoroughly with twice-distilled water after obtaining five replicate readings of the surface tension of each liquid under study. The surface

tension of twice-distilled water was then determined to verify that rinsing had removed all traces of the liquid.

4. In each case the clean glass measuring dish was rinsed with the liquid to be tested before commencing measurement, so that any residual twice-distilled water was removed.

5. The mean surface tension was calculated for each solution type from five replicate readings each from at least three separately prepared solutions. The value obtained was then corrected to give the true surface tension value using the correction factors of Harkins and Jordon (1930) as detailed below.

Determination of surface tension correction factors

In order to determine the value of the correction factor (F) and thus the true surface tension reading, the values of R/r and R^3/V were required to be known, where R is the average radius of the platinum wire ring, r is the radius of the wire of the ring and V is the volume of liquid raised above the level of the surface of the liquid under study by the maximum pull of the ring. The value of R/r is constant for a particular ring and in the case of this study was found to be 41.6.

Although the value of R^3 is constant for a particular ring, the value of V depends on the density and surface tension of the liquid under study. The value of R^3/V can be determined from the equation:

$$\frac{R^3}{V} = \frac{R^2.\rho.g}{4\pi.\gamma} \qquad \text{Equation 3.10}$$

where: ρ = density of the test liquid, g = acceleration due to gravity and γ = the uncorrected surface tension value.

Thus by determining the values of ρ and γ for any test liquid, the value of R^3/V can be calculated, and this then used along with the value of

R/r to determine the correction factor using the tables of Harkins and Jordan (1930).

Surface tension values were determined both for a range of HPMC E5 solution concentrations from 2 x 10^{-6}%w/w to 12%w/w and for HPMC E5 solutions containing either plasticisers, the colouring dispersion Opaspray or the surfactants sodium lauryl sulphate and polysorbate 20.

For HPMC E5 solutions of concentrations above approximately 5 x 10^{-3}%w/w and those containing additives, equilibrium surface tension values were found to be reached during the time taken to perform the analysis. The surface tension of these solutions could therefore be determined immediately after placing the solutions in the measuring vessel.

For dilute HPMC E5 solutions below approximately 5 x 10^{-3}%w/w equilibrium values were only reached after a period of time had elapsed. To determine the equilibrium surface tension values and the surface tension/time profile of these solutions, it was therefore necessary to undertake surface tension measurements at various time intervals after placing the solution in the measuring vessel. To achieve this, HPMC E5 solutions of the concentration of interest were placed into five different constant temperature measuring vessels. After a certain time had elapsed (this period varying depending on the solution concentration investigated) a surface tension measurement was made on the solution in the first vessel and the contents discarded. After the next time period, measurement was performed on the solution in the second vessel and the contents discarded. This process was repeated until readings had been taken from all vessels. The procedure was then repeated using different time intervals until sufficient data had been generated. This method was adopted in preference to taking readings from a single vessel for two reasons. Firstly it avoided disturbing the surface a number of times and possibly altering the course of the reduction of surface

tension with time, and secondly because detaching the measuring ring from the solution would remove a portion of the test liquid which would contain HPMC molecules and therefore potentially alter the equilibrium surface tension value obtained.

In order to check that the reduction in surface tension over the period of the test was a true property of the HPMC E5 solution, control experiments using twice-distilled water in the measuring vessels were performed.

3.2.5 COATING SOLUTION DENSITY

Knowledge of the coating solution density is required in order to calculate the correction factors needed for the determination of surface tension values when using the tensiometer and to convert the kinematic viscosity values generated from the suspended level viscometers into dynamic viscosity values.

Coating solution density has also been shown to influence the droplet size distribution produced upon atomisation (see section 3.1.1).

Density measurements in this work were determined with a density bottle using standard procedures.

3.3 RESULTS

3.3.1 THE RHEOLOGICAL BEHAVIOUR OF HPMC E5 SOLUTIONS

Viscosity values for the two batches of HPMC E5 used for the majority of the experimental work in this thesis are shown in Table 3.2 and Figure 3.1. Batch 1 (Colorcon batch MM8305156E) was used for the experimental work detailed in this chapter and batch 2 (Colorcon batch MM8305153E) for the atomisation and coating studies described in Chapters 4 and 5.

Rheograms generated by the continuous shear viscometer for HPMC E5 solutions prepared from both of these two batches, showed that at

VISCOSITY OF HPMC E5 SOLUTIONS AT 20° C

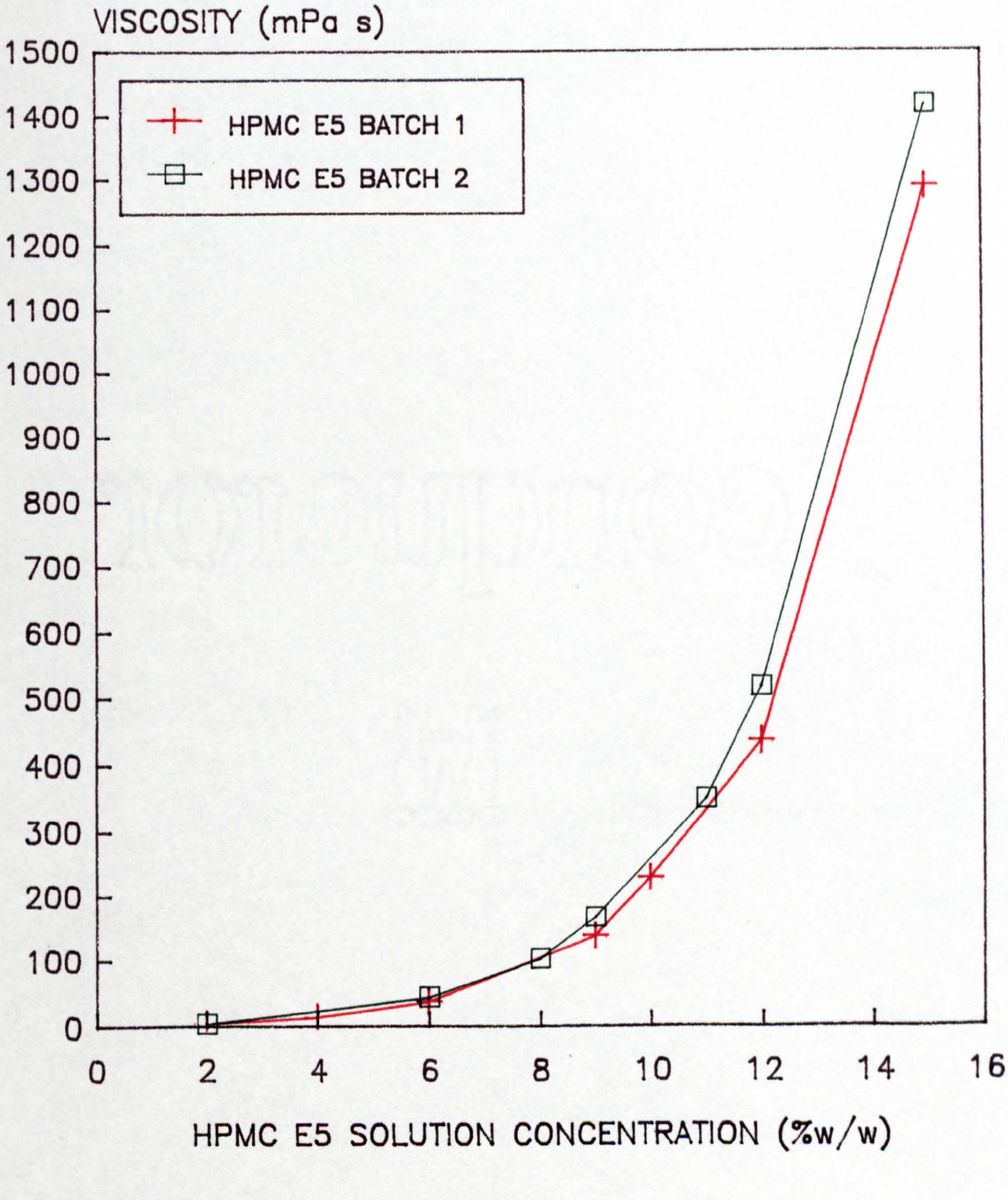

FIGURE 3.1

TABLE 3.2: THE VISCOSITY OF HPMC E5 SOLUTIONS

HPMC E5 CONCENTRATION		BATCH NUMBER	VISCOSITY (mPa s) ; MEAN ± SD		INDEX OF NON-NEWTONIAN BEHAVIOUR
			SUSPENDED LEVEL VISCOMETER	CONTINUOUS SHEAR VISCOMETER	
%w/w	%w/v				
2.0	2.01	1	4.61 ± 0.14		
4.0	4.03	1	14.03 ± 0.17		
6.0	6.08	1	37.79 ± 0.53	37.25 ± 0.90	1.000
9.0	9.19	1	136.78 ± 1.18	137.00 ± 2.43	1.000
10.0	10.23	1	228.98 ± 2.96	226.42 ± 5.03	1.000
12.0	12.34	1	439.60 ± 4.29	434.42 ± 6.50	1.000
15.0	15.45	1		1287.26 ± 41.23*	0.992
19.0	19.87	1		4304.92 ± 167.70*	0.970
2.0	2.01	2	4.82 ± 0.18		
6.0	6.08	2		44.92 ± 1.43	1.000
8.0	8.15	2		103.06 ± 2.31	1.000
9.0	9.19	2	165.83 ± 1.24	166.29 ± 3.41	1.000
11.0	11.29	2		350.35 ± 5.27	1.000
12.0	12.34	2		519.53 ± 11.14	1.000
15.0	15.45	2		1417.10 ± 39.82*	0.986

Viscosity values determined at a temperature of 20°C.

*Apparent Newtonian viscosity values determined using the power-law equation.

concentrations up to 12%w/w there was a linear increase in shear stress with increasing shear rate, this being indicative of Newtonian behaviour. This is substantiated by the values for the index of non-Newtonian behaviour, these being found to be equal to 1 for concentrations up to 12%w/w. A comparison of results obtained from the suspended level viscometers and the continuous shear viscometer (Rotovisco RV2) showed the mean viscosity values not to be statistically

different ($p<0.01$). The reproducibility of the results from the suspended level viscometers was superior to that from the continuous shear viscometer. This probably reflects the greater accuracy to which time measurements could be determined in comparison with the reading of values from the rheograms. In every case however the coefficients of variation for the viscosity values were less than 4%.

For both batches of HPMC E5 tested, deviation from Newtonian behaviour occurred at concentrations above 12%w/w and in these cases therefore the viscosity values quoted in Table 3.2 are those of the apparent Newtonian viscosity derived from the power-law equation (see section 3.2.3.1).

It can be seen from Table 3.2 and Figure 3.1 that there is not a linear increase in solution viscosity with increasing solution concentration. For example for batch 2, a 2%w/w increase in concentration from 6%w/w to 8%w/w caused a viscosity increase of 58.14mPa s, whereas a similar increase from 9%w/w to 11%w/w caused an increase of 184.06mPa s. The difference in viscosities between the two batches was also shown to widen as the concentration increased, this being 0.21mPa s for the 2%w/w solutions and 129.84mPa s for the 15%w/w solutions.

Pickard (1979), Delporte (1980) and Prater (1982) in attempting to determine a relationship between viscosity and HPMC E5 solution concentration found that a plot of log viscosity versus solution concentration was not linear. Philippoff (1936) however had demonstrated for methylcellulose that if the eighth root of viscosity was plotted against concentration (%w/v) a straight line resulted. This latter relationship was also found to be applicable for the two batches of HPMC E5 used in this work, see Figures 3.2 and 3.3. From these figures the equations describing the relationship between viscosity at 20°C and HPMC E5 solution concentration were calculated to be:

GRAPH OF THE EIGHTH ROOT OF VISCOSITY AGAINST CONCENTRATION FOR AQUEOUS SOLUTIONS OF HPMC E5 (BATCH 1) AT 20°C

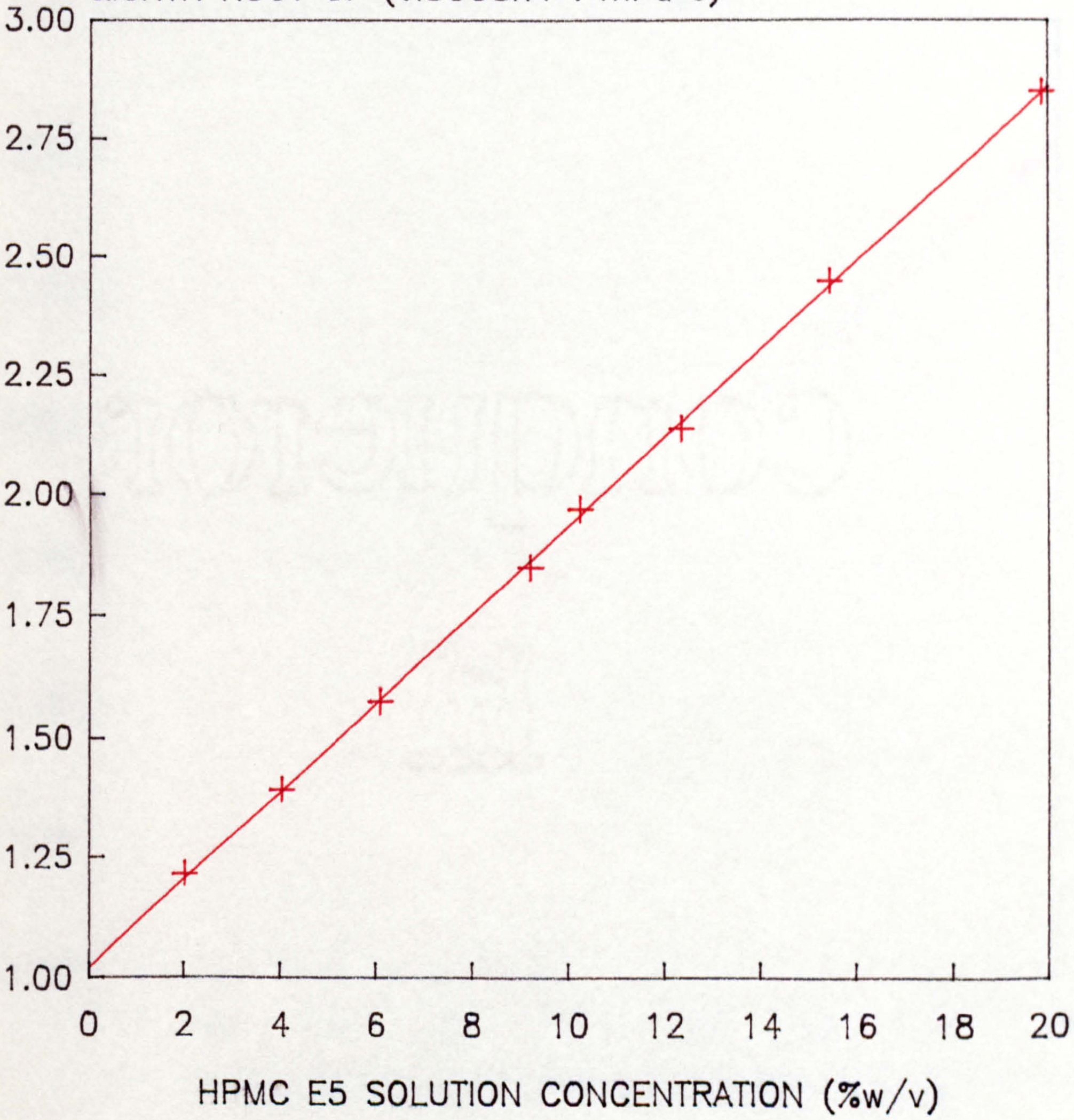

FIGURE 3.2

GRAPH OF THE EIGHTH ROOT OF VISCOSITY AGAINST CONCENTRATION FOR AQUEOUS SOLUTIONS OF HPMC E5 (BATCH 2) AT 20°C

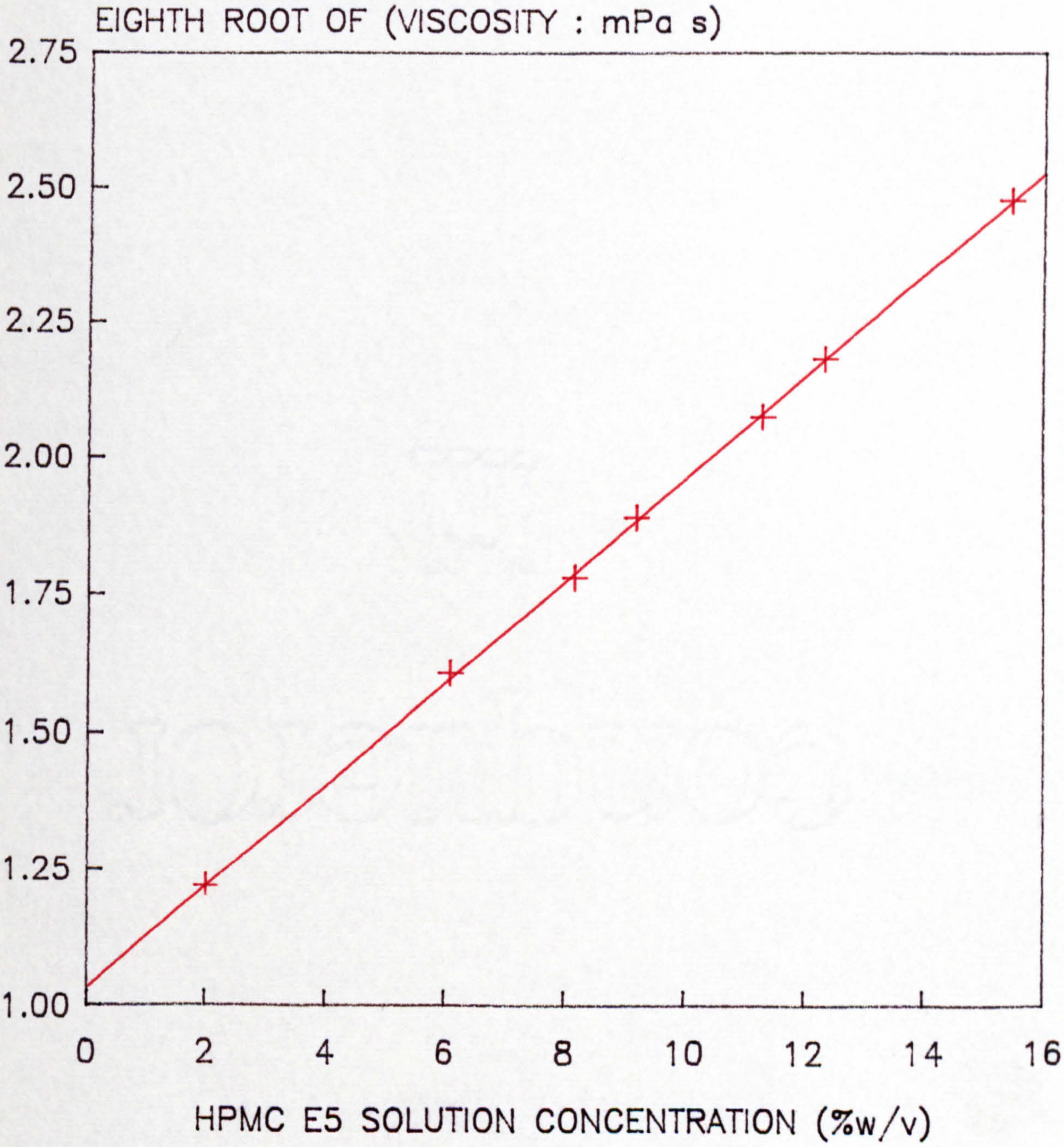

FIGURE 3.3

$$\text{Batch 1 : } \mu^{1/e} = 0.09185\ C + 1.0190$$

$$\text{Batch 2 : } \mu^{1/e} = 0.09338\ C + 1.0320$$

where μ is the solution viscosity at 20°C (mPa s) and C is the HPMC E5 concentration (%w/v). The correlation coefficients for these relationships were 0.9998 and 0.9999 respectively (giving values of $p<0.001$ in each case).

The viscosity data illustrated in Table 3.2 and plotted in Figures 3.1, 3.2 and 3.3 is that of solutions of HPMC E5 prepared from samples possessing a moisture content of 2.60%w/w. Moisture levels of commercial samples are typically of this order and therefore the data are representative of the practical situation. If the data are re-plotted with the solution concentrations altered to take into account the presence of moisture in the sample, the equations become:

$$\text{Batch 1 : } \mu^{1/e} = 0.09428\ C + 1.0190$$

$$\text{Batch 2 : } \mu^{1/e} = 0.09589\ C + 1.0320$$

with the correlation coefficients also being 0.9998 and 0.9999 respectively ($p<0.001$ in both cases).

When the data given by Prater (1982) for HPMC E5 aqueous solutions at 29°C were plotted in a similar way, it was found that the Philippoff relationship again applied. The appropriate equation in this latter case is;

$$\mu^{1/e} = 0.0920\ C + 1.002$$

with the correlation coefficient being 0.9993 ($p<0.001$)

The values for the intercept of the Philippoff plots should be representative of viscosity of water at the temperature studied.

However in this work the viscosities at the intercept were found to be 1.163mPa s and 1.287mPa s for batches 1 and 2 respectively (expected value 1.002mPa s) and for the data taken from Prater (1982) the intercept viscosity was calculated to be 1.016mPa s (expected value 0.8148mPa s).

The relationship between HPMC E5 solution temperature and solution viscosity for three different concentrations prepared using polymer batch 1 is shown in Figure 3.4. Increasing solution temperature was found to produce a reduction in viscosity, this effect being more pronounced at lower temperatures and with higher solution concentrations. A temperature increase from 10°C to 20°C resulted in a viscosity decrease of 17mPa s for a 6%w/w solution, 66mPa s for a 9%w/w solution and 216mPa s for a 12%w/w solution. A temperature increase from 20°C to 30°C however resulted in falls of only 10mPa s, 35mPa s and 115mPa s respectively.

At temperatures below approximately 50°C the solutions were found to behave as Newtonian liquids. Once the temperature was raised above 50°C however a change in the shape of the rheological profile was noted. Deviation from linearity occurred and evidence of pseudoplasticity was seen. At approximately 52°C, thixotropic behaviour was apparent for each of the solution concentrations, the solutions exhibiting different viscosities at the same shear rate when measured on the up and down curves of the rheogram. Plots of log shear stress versus log shear rate were non-linear at this temperature and therefore no values for the apparent Newtonian viscosity could be determined. Any viscosity value quoted for this temperature would therefore be meaningless since it would depend entirely on the conditions of measurement used.

The thermal gelation temperature of HPMC E5 is often taken as the temperature at which the trend of decreasing viscosity with increasing

THE EFFECT OF SOLUTION TEMPERATURE ON THE VISCOSITY OF AQUEOUS HPMC E5 SOLUTIONS OF DIFFERENT CONCENTRATIONS

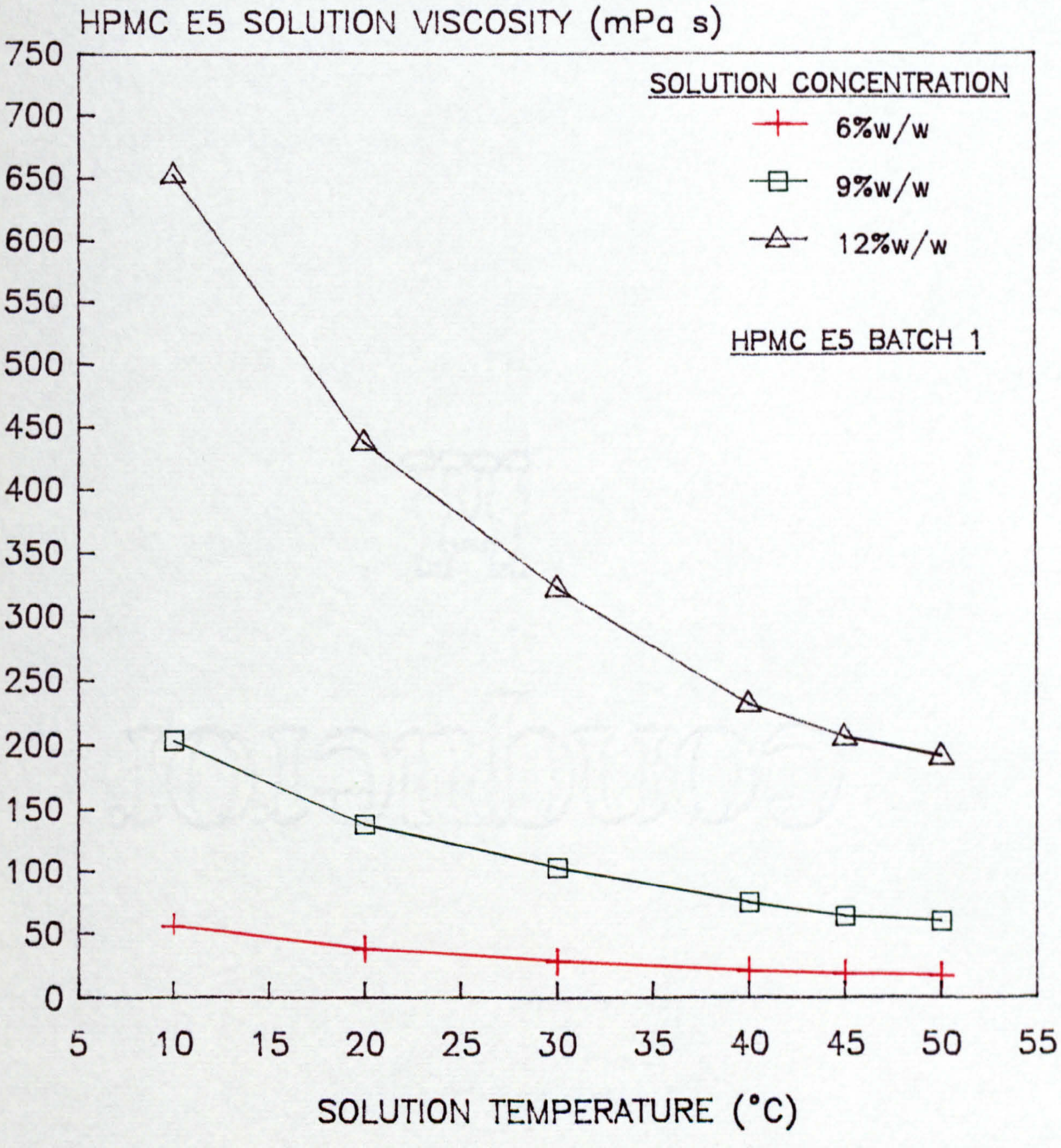

FIGURE 3.4

temperature is reversed (Prater, 1982). This definition will however generate markedly different values of the gelation temperature depending on the shear rate at which the apparent viscosity is measured. Indeed it was found when examining the rheograms in this study, that if a sufficiently high shear rate was used, the apparent viscosity continued to fall irrespective of how high the solution temperature was raised. In this work therefore the thermal gelation temperature was taken as that temperature at which thixotropic behaviour was first noted, since this is indicative of the formation of a gel structure and its breakdown on the application of shear forces. For the HPMC E5 solutions studied (see Figure 3.4), there was found to be no detectable differences in the thermal gelation temperature, this being 52°C ± 1°C in each case.

Heating the HPMC E5 solutions to temperatures above approximately 60°C resulted in the precipitation of the polymer.

Solutions which had undergone thermal gelation were found to revert to their original rheological behaviour on cooling to 20°C, with no detectable differences in viscosity being apparent.

The reduction in viscosity with increasing temperature is often described by the Andrade-Gauzman relationship (Equation 3.11), this being derived from the Arrhenius equation.

$$\ln\mu = \frac{E}{RT} + \ln A \qquad \text{Equation 3.11}$$

where μ is the solution viscosity (Pa s), E is the activation energy for viscous flow, R is the gas constant ($8.314 J mol^{-1} K^{-1}$), T is the absolute temperature (K) and A is a constant.

If this relatioship holds for HPMC E5 solutions, a plot of $\ln\mu$ versus 1/T would yield a straight line.

Andrade-Gauzman plots for 6%w/w, 9%w/w and 12%w/w solutions of HPMC E5

from batch 1 are shown in Figure 3.5. It would appear from these plots that the relationship holds for temperatures up to about 40°C to 45°C but at temperatures above this deviations from linearity occur.

The effect of HPMC E5 batch variation on solution viscosity

The USP allows the viscosity of commercially available grades of HPMC E5 to vary from between 80% to 120% of the stated nominal value. The EP allowable limits range from between 75% to 140% of the stated nominal viscosity. Batches of HPMC E5 conforming to USP and EP standards may therefore be available with viscosities in the range 4mPa s to 6mPa s and 3.5mPa s to 7mPa s respectively for 2%w/v aqueous solutions.

It has been shown previously (Table 3.2) that even if there are only small differences in the viscosity of 2%w/v aqueous solutions between two different batches, large differences may result at higher solution concentrations. This phenomenon is further illustrated in Table 3.3, which details the viscosity of 2%w/w, 9%w/w and 12%w/w solutions prepared from five different batches of HPMC E5. Batches 1 and 2 in the table are those batches whose viscosity behaviour is reported in Table 3.2. Batches 3 and 5 were specially selected to represent batches close to the bottom and top of the USP viscosity specification. It can be seen that not only may the viscosity of one batch be more than twice that of another at a solution concentration of 12%w/w and yet both conform to the USP specification, but also that some batches towards the top of the viscosity specification may exhibit non-Newtonian behaviour at a concentration of 12%w/w.

In order to gain an appreciation of the typical batch variation in viscosity which is likely to occur in practice, viscosity values of 30 representative batches of HPMC E5 were obtained from Colorcon Ltd. Table 3.4 shows a statistical analysis of these values.

It can be estimated that the viscosities of the above batches may range

ANDRADE–GAUZMAN PLOTS FOR HPMC E5 SOLUTIONS OF VARIOUS CONCENTRATIONS

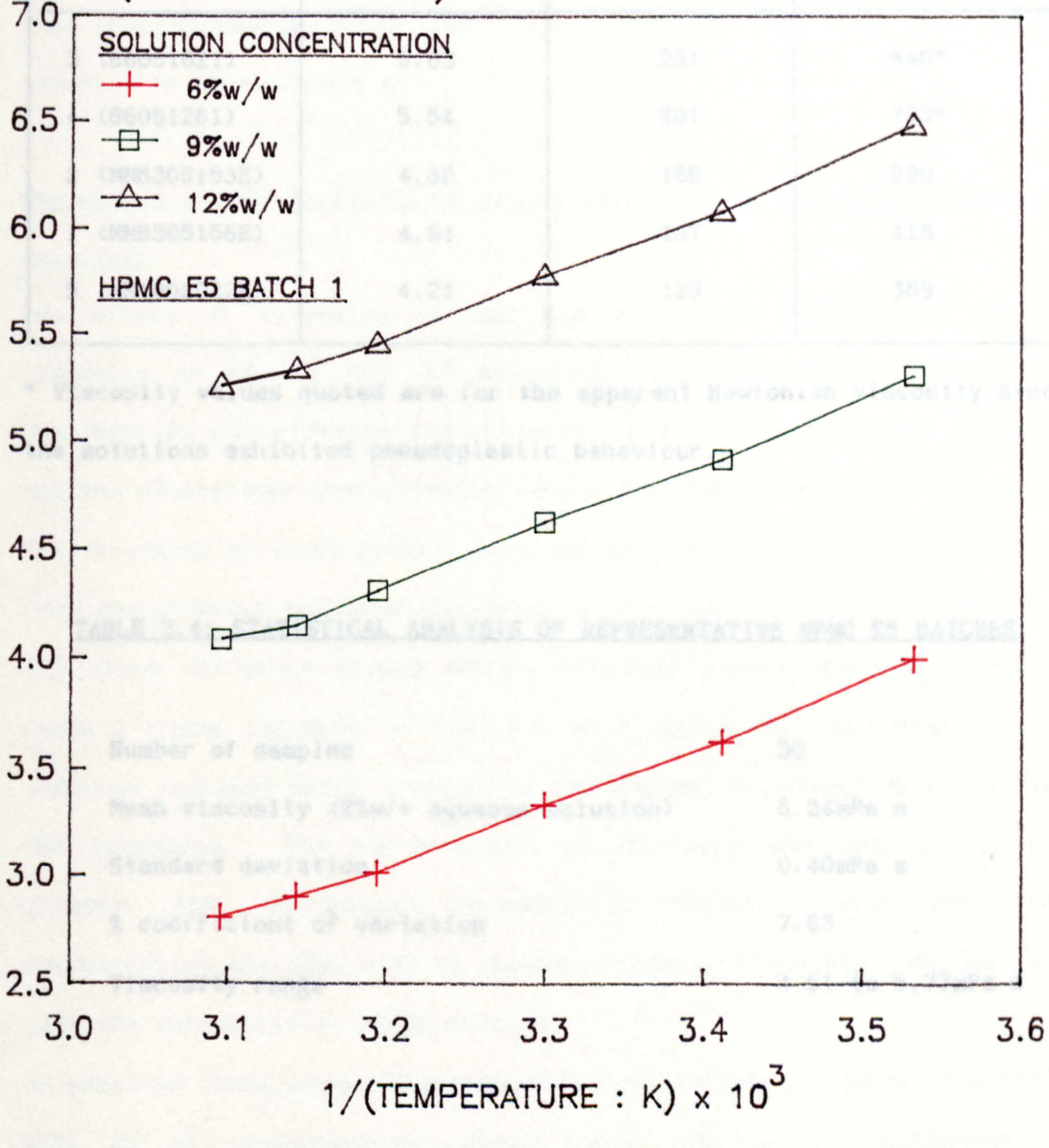

FIGURE 3.5

TABLE 3.3: THE EFFECT OF HPMC E5 BATCH VARIATION ON SOLUTION VISCOSITY

HPMC E5 BATCH (COLORCON BATCH)	VISCOSITY (mPa s)		
	2%w/w SOLUTION	9%w/w SOLUTION	12%w/w SOLUTION
3 (86051621)	5.83	231	840*
4 (86051281)	5.54	201	723*
2 (MM8305153E)	4.82	166	520
1 (MM8305156E)	4.61	137	418
5 (MM1002022E)	4.21	129	359

* Viscosity values quoted are for the apparent Newtonian viscosity since the solutions exhibited pseudoplastic behaviour.

TABLE 3.4: STATISTICAL ANALYSIS OF REPRESENTATIVE HPMC E5 BATCHES

Number of samples	30
Mean viscosity (2%w/v aqueous solution)	5.24mPa s
Standard deviation	0.40mPa s
% coefficient of variation	7.63
Viscosity range	4.51 to 5.77mPa s

from approximately 130mPa s to 215mPa s for a solution concentration of 9%w/w and 400mPa s to 800mPa s for 12%w/w solutions.

Similar estimations for batches at the extremes of the USP viscosity limits suggest that they may possess solution viscosities ranging from approximately 110mPa s to 250mPa s for 9%w/w solutions and from

approximately 300mPa s to 900mPa s for 12%w/w solutions.

It is more difficult to estimate the possible viscosity ranges exhibited by batches at extremes of the EP viscosity specification since they are well outside those encountered in this study. However it is probable that the viscosity range for 9%w/w solutions may vary from below 100mPa s to above 350mPa s.

The effect of the inclusion of plasticisers on the viscosity of HPMC E5 solutions

The effect of including various commonly used plasticisers on the viscosity of aqueous HPMC E5 solutions is illustrated in Figure 3.6. The HPMC E5 concentration was constant at 9%w/w for each test solution and the plasticiser concentration ranged from 0%w/w to 5%w/w.

The inclusion of these plasticisers was not found to cause any deviation from the original Newtonian behaviour of the solution.

The three different grades of polyethylene glycol (PEG) appeared to cause a linear increase in viscosity with increasing concentration, the observed increase being greater as the average molecular weight of the PEG increased. The non-polymeric plasticisers propylene glycol and glycerol gave non-linear increases in viscosity with increasing concentration and gave rise to smaller rises in viscosity than the PEGs over the concentration range studied.

In practice these plasticisers would be unlikely to be added to a 9%w/w HPMC E5 at concentrations above 3%w/w due to the occurrence of incompatibilities once the film coat has formed. Typical solution concentrations which would be used in practice lie between 1%w/w and 2%w/w. At these latter levels the viscosity increases caused by the plasticisers studied would range from approximately 4mPa s to 20mPa s representing an approximate increase of between 3% and 15%.

THE EFFECT OF PLASTICISER ADDITION ON THE VISCOSITY OF AN AQUEOUS 9%w/w HPMC E5 SOLUTION

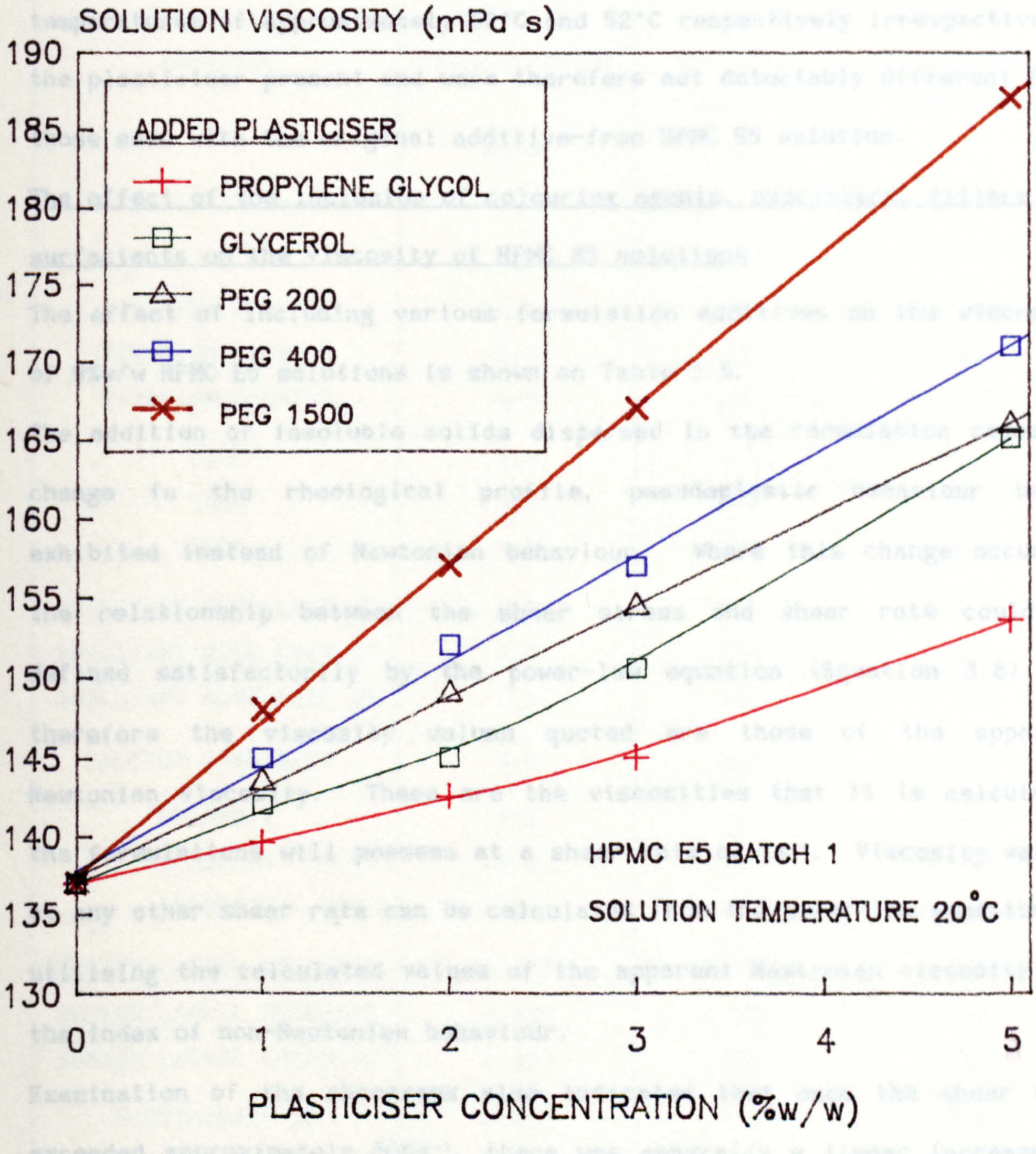

FIGURE 3.6

The relationship between solution viscosity and solution temperature for 9%w/w HPMC E5 solutions containing 2%w/w of various plasticisers was found to be similar to that observed when no plasticisers were present. The onset of pseudoplastic and thixotropic behaviour occurred at temperatures of approximately 50°C and 52°C respectively irrespective of the plasticiser present and were therefore not detectably different from those seen with the original additive-free HPMC E5 solution.

<u>The effect of the inclusion of colouring agents, opacifiers, fillers and surfactants on the viscosity of HPMC E5 solutions</u>

The effect of including various formulation additives on the viscosity of 9%w/w HPMC E5 solutions is shown on Table 3.5.

The addition of insoluble solids dispersed in the formulation caused a change in the rheological profile, pseudoplastic behaviour being exhibited instead of Newtonian behaviour. Where this change occurred the relationship between the shear stress and shear rate could be defined satisfactorily by the power-law equation (Equation 3.8) and therefore the viscosity values quoted are those of the apparent Newtonian viscosity. These are the viscosities that it is calculated the formulations will possess at a shear rate of $1s^{-1}$. Viscosity values at any other shear rate can be calculated from the power-law equation by utilising the calculated values of the apparent Newtonian viscosity and the index of non-Newtonian behaviour.

Examination of the rheograms also indicated that once the shear rate exceeded approximately $600s^{-1}$, there was generally a linear increase in shear stress with increases in shear rate, this being indicative of the existence of a Newtonian region at these shear rates.

It can be seen in Table 3.5 that the values for the index of non-Newtonian behaviour are generally close to 1 indicating that the deviation from Newtonian behaviour is not large. Over the concentration

TABLE 3.5: THE EFFECT OF THE INCLUSION OF FORMULATION ADDITIVES ON THE VISCOSITY OF A 9%w/w HPMC E5 SOLUTION

FORMULATION ADDITIVE	ADDITIVE CONCENTRATION %w/w	APPARENT NEWTONIAN VISCOSITY mPa s	INDEX OF NON-NEWTONIAN BEHAVIOUR
-	0.0	137	1.000
TITANIUM DIOXIDE	2.0	180	0.985
TITANIUM DIOXIDE	3.0	196	0.981
TITANIUM DIOXIDE	4.5	225	0.965
TALC	2.0	171	0.982
TALC	3.0	184	0.986
TALC	4.5	212	0.982
BRILLIANT BLUE LAKE HT	2.0	183	0.977
BRILLIANT BLUE LAKE HT	3.0	199	0.981
BRILLIANT BLUE LAKE HT	4.5	251	0.970
CALCIUM CARBONATE	4.5	209	0.977
OPASPRAY	7.5	188	0.986
OPASPRAY	15.0	247	0.980
OPASPRAY	20.0	388	0.945
SODIUM LAURYL SULPHATE	0.125	153	1.000
SODIUM LAURYL SULPHATE	0.250	179	1.000
SODIUM LAURYL SULPHATE	1.000	268	1.000
POLYSORBATE 20	0.500	141	1.000
POLYSORBATE 20	1.000	144	1.000
POLYSORBATE 20	2.000	154	1.000

The HPMC E5 solution concentration was 9%w/w in each case and all viscosity values were determined at 20°C.

ranges studied, the value for the index of non-Newtonian behaviour did not appear to be related to the concentration of insoluble additive used. The inclusion of the water-soluble solid surfactant sodium lauryl sulphate or the liquid surfactant polysorbate 20 were not found to give rise to pseudoplastic behaviour.

It can be seen that all the additives studied caused an increase in the viscosity of HPMC E5 solutions, although the extent of the increase varied depending on the additive used and will differ at different shear rates.

It is recommended that for HPMC-based systems, a suitable polymer to pigment ratio in the film coat is 2:1. This corresponds to 4.5%w/w of solids being incorporated into a 9% HPMC E5 solution. At this concentration it can be seen that viscosity increases of up to approximately 80% may be encountered.

The thermal gelation temperature of the formulations which included Opaspray was found to occur at approximately 52°C, this being no different from the additive-free HPMC E5 solution.

<u>The viscosity of Opadry formulations</u>

The influence of concentration on the rheological behaviour of the two Opadry type OY formulations based on HPMC E5 is shown in Table 3.6 and the batch based on HPMC E3 (type OY-D) in Table 3.7. These formulations include PEG 400 and various colouring agents in addition to HPMC. They were found to exhibit pseudoplastic bahaviour at all the concentrations studied and the relationship between shear stress and shear rate could be represented in each case by the power-law equation (Equation 3.8). The rheological behaviour is therefore represented by values for the index of non-Newtonian behaviour and the apparent Newtonian viscosity. Despite the presence of plasticiser and colouring components the relationship between the apparent Newtonian viscosity (μ_N) and

TABLE 3.6: VISCOSITY VALUES FOR OPADRY TYPE OY FORMULATIONS

OPADRY CONCENTRATION (%w/w)	OPADRY CONCENTRATION (%w/v)	BATCH NUMBER	APPARENT NEWTONIAN VISCOSITY (mPa s)	INDEX OF NON-NEWTONIAN BEHAVIOUR
9.00	9.31	1	99	0.952
10.00	10.33	1	116	0.959
13.00	13.55	1	254	0.963
15.00	15.77	1	390	0.975
17.00	18.04	1	680	0.950
20.00	21.57	1	1271	0.973
9.00	9.31	2	93	0.961
13.00	13.55	2	243	0.959
15.00	15.79	2	379	0.971
17.00	18.08	2	620	0.969
20.00	21.61	2	1192	0.963

TABLE 3.7: VISCOSITY VALUES FOR OPADRY TYPE OY-D FORMULATIONS

OPADRY CONCENTRATION (%w/w)	OPADRY CONCENTRATION (%w/v)	APPARENT NEWTONIAN VISCOSITY (mPa s)	INDEX OF NON-NEWTONIAN BEHAVIOUR
10	10.34	40	0.941
15	15.84	131	0.948
20	21.60	321	0.942
25	27.45	809	0.938

concentration (C) was found to follow the Philippoff relationship, the equations describing the relationships being;

Opadry type OY — Batch 1 : $\mu_N^{1/\theta} = 0.05540\ C + 1.2481$

Batch 2 : $\mu_N^{1/\theta} = 0.05426\ C + 1.2509$

Opadry type OY-D : $\mu_N^{1/\theta} = 0.04178\ C + 1.1621$

with correlation coefficients of 0.9991, 0.9997 and 0.9993 respectively ($p<0.01$ in each case).

The influence of storage conditions on the viscosity of HPMC E5 solutions

The moisture content of samples of HPMC E5 from Batch 1 after 7 days storage at 20°C and different relative humidities is shown in Table 3.8, along with the corresponding viscosities of solutions prepared from those samples.

It is apparent that the moisture content of HPMC E5 increases as the storage relative humidity increases, this effect being particularly marked at a relative humidity of 95%. These results are similar to those reported by Callahan et al. (1982) for HPMC, although these

TABLE 3.8: THE INFLUENCE OF STORAGE CONDITIONS ON HPMC E5 SOLUTION VISCOSITY

STORAGE RELATIVE HUMIDITY (%)	MOISTURE CONTENT (%w/w)	SOLUTION VISCOSITY (mPa s)	
		9%w/w SOLUTION	12%w/w SOLUTION
11	2.1	151	479
53	5.6	127	411
76	9.9	109	344
95	22.6	65	178

authors did not specify which grade of HPMC was studied.

As the moisture level of the sample increases, the relative proportion of HPMC E5 present decreases and the viscosity of the resultant solutions also decreases. If the presence of adsorbed water is not taken into account when preparing HPMC E5 solutions then it is clear that solution viscosity may vary considerably, with some solutions being over 2.5 times more viscous than others. These data illustrate the importance of ensuring that HPMC is stored correctly in airtight containers and not exposed to conditions of elevated relative humidity prior to use.

The influence of solution preparation method on the viscosity of HPMC E5 solutions

Table 3.9 details the viscosity values of 9%w/w HPMC E5 solutions prepared and stored as described in section 3.2.1. The viscosity values were determined using a suspended level viscometer and were not found to

TABLE 3.9

PREPARATION/STORAGE METHOD (see section 3.2.1)	9%w/w HPMC E5 SOLUTION VISCOSITY (mPa s)
1	137.46 ± 2.15
2	135.67 ± 1.23
3	137.03 ± 1.08
4	136.74 ± 1.34
5	136.23 ± 2.01
6	137.22 ± 1.77
7	135.81 ± 1.69
8	136.03 ± 1.23
9	135.98 ± 1.64

be statistically different from each other. This indicates that for a particular polymer batch, provided the solutions are prepared accurately their viscosity is likely to be the same irrespective of the preparation method.

3.3.2 THE SURFACE TENSION OF HPMC E5 SOLUTIONS

HPMC E5 solutions at concentrations of approximately 5 x 10^{-3}%w/w or less were found to take a considerable time to reach their equilibrium surface tension values. This time-dependent reduction in surface tension is illustrated in Figures 3.7 and 3.8. It can be seen that the time taken for the equilibrium surface tension to be reached decreases as the concentration increases and that for concentrations below 5 x 10^{-4}%w/w time periods in excess of 30 minutes were required under the conditions of test. At least 900 minutes was required before the 2 x 10^{-6}*%w/w solution attained equilibrium. Controls carried out with twice-distilled water showed no reduction in surface tension over a similar 900 minute period. Solution concentrations in excess of approximately 5 x 10^{-3}%w/w were found to attain their final surface tension value in the time taken to carry out the analysis.

Figure 3.9 illustrates the surface tension/concentration profile exhibited by HPMC E5 solutions at equilibrium. There is a linear decrease in equilibrium surface tension with increasing concentration up to a concentration of approximately 2 x 10^{-5}%w/w after which there is an abrupt change in the gradient of the line and the surface tension falls far less steeply with increasing concentration. The point of intersection between the extrapolated straight lines on either side of the break in the curve is analogous to the critical micelle concentration commonly shown by surface active materials.

Table 3.10 shows the surface tension of much more concentrated HPMC E5 solutions between 1%w/w and 12%w/w. It can be seen that within this

THE RELATIONSHIP BETWEEN SURFACE TENSION AND TIME FOR AQUEOUS HPMC E5 SOLUTIONS OF VARIOUS CONCENTRATIONS

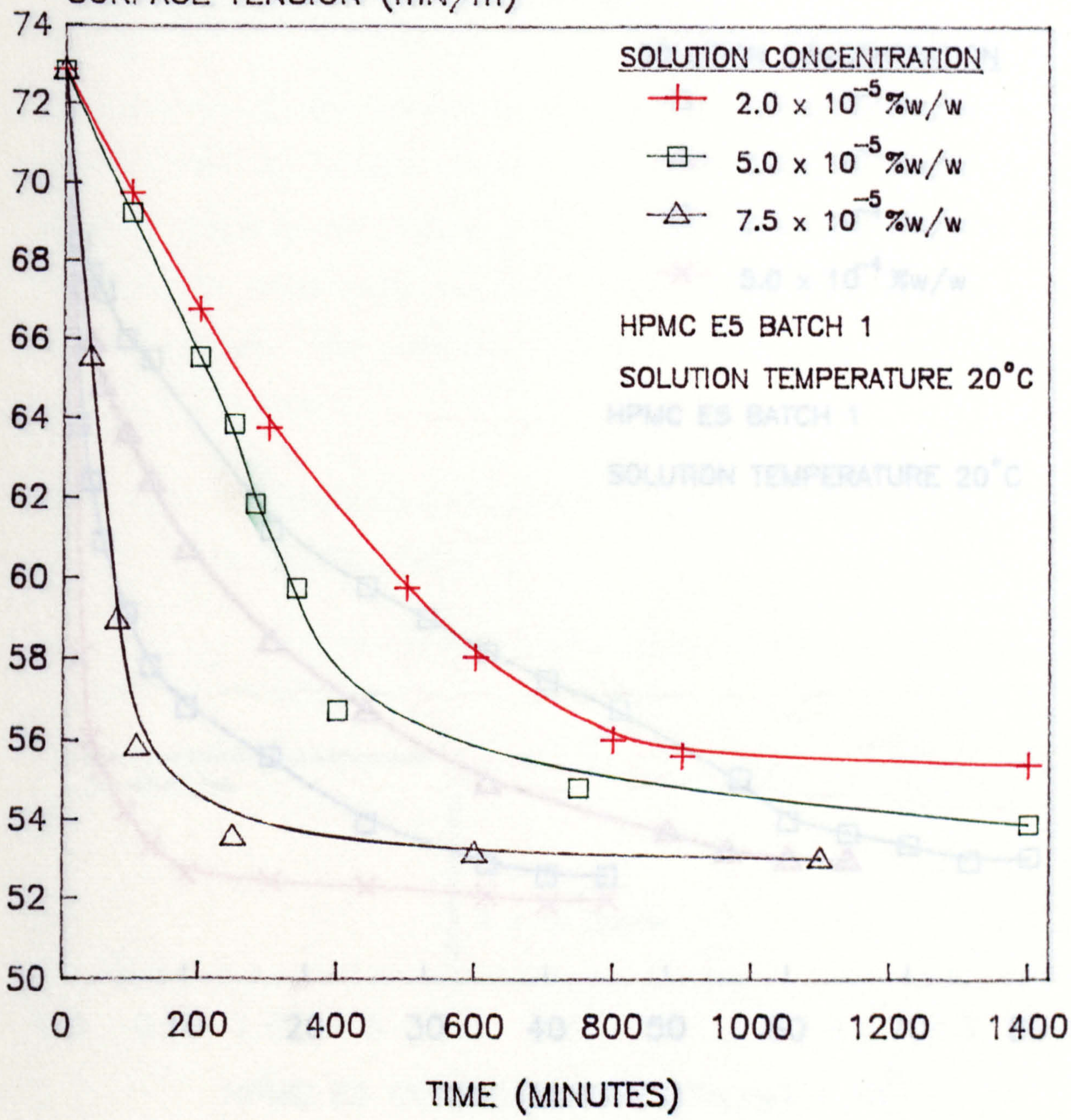

FIGURE 3.7

THE RELATIONSHIP BETWEEN SURFACE TENSION AND TIME FOR AQUEOUS HPMC E5 SOLUTIONS OF VARIOUS CONCENTRATIONS

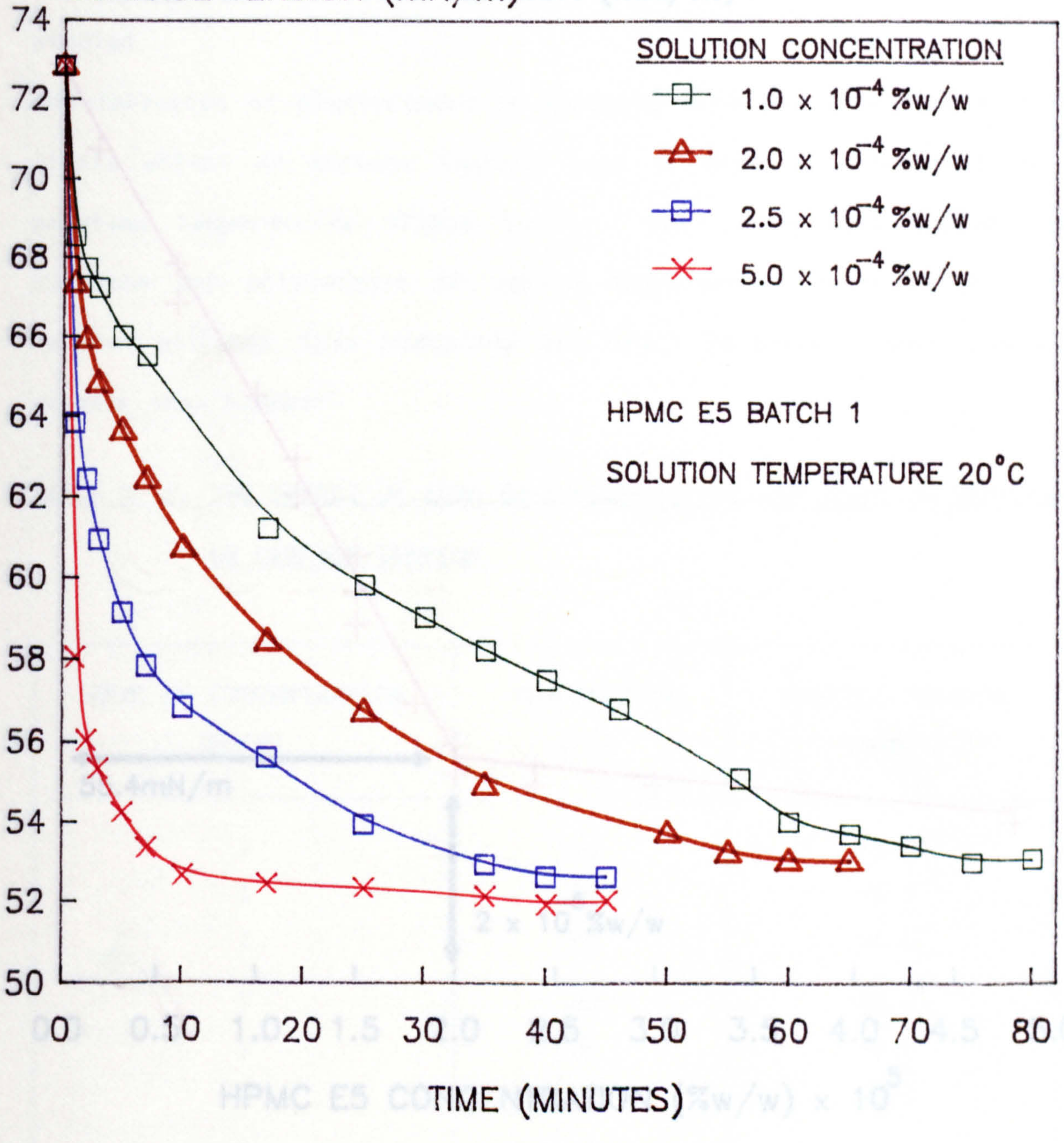

FIGURE 3.8

THE RELATIONSHIP BETWEEN HPMC E5 CONCENTRATION AND EQUILIBRIUM SOLUTION SURFACE TENSION

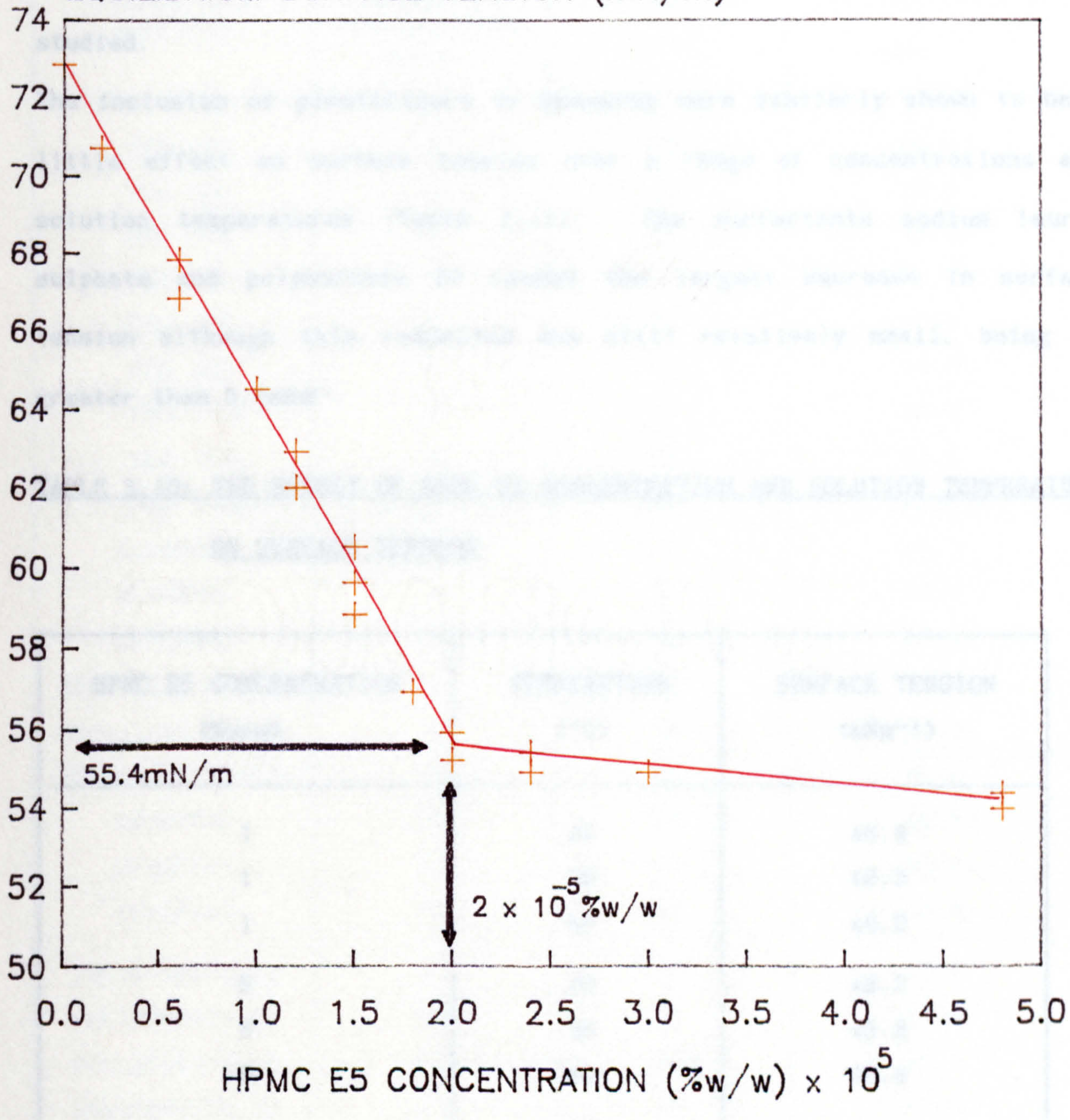

FIGURE 3.9

concentration range, which is that likely to be encountered in practice, there is very little variation in surface tension values. Table 3.10 also shows that increasing solution temperature has minimal effect on surface tension, the reduction measured on increasing the temperature from 20°C to 40°C being less than 1.2mNm^{-1} at each concentration studied.

The inclusion of plasticisers or Opaspray were similarly shown to have little effect on surface tension over a range of concentrations and solution temperatures (Table 3.11). The surfactants sodium lauryl sulphate and polysorbate 20 caused the largest decrease in surface tension although this reduction was still relatively small, being no greater than 5.8mNm^{-1}.

TABLE 3.10: THE EFFECT OF HPMC E5 CONCENTRATION AND SOLUTION TEMPERATURE ON SURFACE TENSION

HPMC E5 CONCENTRATION (%w/w)	TEMPERATURE (°C)	SURFACE TENSION (mNm^{-1})
1	20	46.8
1	30	46.3
1	40	46.0
5	20	46.2
5	30	45.8
5	40	45.6
9	20	45.7
9	30	44.8
9	40	44.5
12	20	44.5
12	30	44.1
12	40	43.9

TABLE 3.11: THE EFFECT OF VARIOUS FORMULATION ADDITIVES ON THE SURFACE TENSION OF 9%w/w HPMC E5 SOLUTIONS OVER A RANGE OF TEMPERATURES

FORMULATION ADDITIVE	ADDITIVE CONCENTRATION (%w/w)	TEMPERATURE (°C)	SURFACE TENSION (mNm^{-1})
PEG 200	3	20	45.6
PEG 200	3	30	45.0
PEG 200	3	40	44.9
PEG 400	3	20	45.6
PEG 400	3	30	45.2
PEG 400	3	40	44.7
PEG 1500	3	20	45.6
PEG 1500	3	30	44.9
PEG 1500	3	40	44.8
GLYCEROL	3	20	45.7
GLYCEROL	3	30	45.5
GLYCEROL	3	40	45.0
PROPYLENE GLYCOL	3	20	45.7
PROPYLENE GLYCOL	3	30	45.0
PROPYLENE GLYCOL	3	40	44.9
OPASPRAY	15	20	46.9
OPASPRAY	15	30	45.2
OPASPRAY	15	40	45.0
POLYSORBATE 20	0.5	20	42.1
POLYSORBATE 20	0.5	40	40.8
POLYSORBATE 20	1.0	20	41.2
POLYSORBATE 20	1.0	40	40.3
Na LAURYL SULPHATE	0.5	20	41.3
Na LAURYL SULPHATE	0.5	40	40.5
Na LAURYL SULPHATE	1.0	20	39.9
Na LAURYL SULPHATE	1.0	40	39.4

3.4 DISCUSSION

3.4.1 THE RHEOLOGICAL PROPERTIES OF HPMC E5 SOLUTIONS

The rheological properties of a polymer solution depend mainly on the following parameters :-

1. Polymer size and shape,
2. Polymer-polymer and polymer-dispersion medium molecular interactions,
3. Polymer concentration,
4. Solution temperature, and
5. Viscosity of the dispersion medium.

It is important to assess how these factors influence the rheological profiles of formulations based on HPMC E5 in order to gain an understanding of how formulations may behave during the film coating process.

Commercial grades of HPMC are not mono-disperse, but are known to contain polymer molecules covering a wide range of degrees of polymerisation and hence chain lengths (Rowe, 1980a; Tufnell et al., 1983; Davies, 1985). Molecular weight fractions between 10^3 and 10^6Da (Rowe, 1980a) and 10^2 and 10^6Da (Davies, 1985) have been found to exist. The molecular weight distribution of a polymer can be described by characteristic molecular weight averages. These include number-average molecular weights, M_N, and weight-average molecular weights, M_w where :

$$M_N = \frac{\sum n_i M_i}{\sum n_i} \qquad \text{Equation 3.12}$$

and

$$M_w = \frac{\sum n_i M_i^2}{\sum n_i M_i} \qquad \text{Equation 3.13}$$

and there are n_i molecules of molecular weight M_i.

Examination of these equations indicates that the value of M_N is particularly influenced by the presence of small amounts of low molecular weight fractions of the polymer and M_w by small amounts of

high molecular weight fractions. It can also be calculated that M_w is always $\geq M_n$.

The degree of polydispersity of a grade of HPMC can be defined by the polydispersity index (Q) where :

$$Q = \frac{M_w}{M_n} \qquad \text{Equation 3.14}$$

If the polymer is monosize then $M_w = M_n$ and $Q = 1$.

The average molecular weight and molecular weight distribution of HPMC are important factors in the coating process since they will influence not only solution viscosity, but also the mechanical properties of the final film coat (Rowe, 1976a).

Several authors have attempted to characterise the molecular weight of HPMC (Rowe, 1980a; Tufnell et al., 1983; Davies, 1985). Absolute methods of analysis, such as light scattering, which allow molecular weights to be determined directly from experimental data have been found not to be suitable for HPMC (Tufnell et al., 1983; Davies, 1985). The technique that has been used is that of gel permeation chromotography (GPC) which allows the determination of M_n, M_w and the degree of polydispersity for polymers having a wide range of molecular weights. GPC however suffers from the disadvantage that since there are no monodisperse fractionated samples of HPMC available, the gel bed has to be calibrated with other standards, eg dextrans. The molecular weight values derived for HPMC must therefore be expressed as values equivalent to the standard molecule used. Since the hydrodynamic volume of an HPMC molecule may be different to that of the standard molecule and will vary depending on the solvent used, the molar mass expressed as an equivalent to a standard molecule is likely to be different to the absolute molecular weight. Different GPC systems have been shown to produce different molecular weight values for the same HPMC sample (Davies,

1985).

Analysis of the molecular weight distribution by Rowe (1980a) and Davies (1985) illustrates the polydispersity of HPMC E5, the average values of Q being found to be 17.5 and 28.9 respectively. Rowe (1980a) reported average values of M_w of 2.94 x 10^5 and M_n of 1.95 x 10^4 from GPC studies using diethylacetamide as the solvent and polystyrene as the standard. Davies (1985) found values of 8.8 x 10^4 and 3.1 x 10^3 with aqueous HPMC E5 solutions referenced to dextran standards. Both authors demonstrated that samples of the same nominal viscosity but from different batches possessed markedly different molecular weight distributions and average molecular weight values.

It can be seen from its structure (Figure 2.1) that HPMC E5 is a polar compound with primary and secondary hydroxyl groups and ether linkages. When dispersed in water the polar groups will hydrate due to hydrogen bonding with the oxygen and hydrogen atoms of water and thus will have associated water molecules. Water however has four sites for possible strong hydrogen bond interaction and, as a result, it tends to form clusters. These clusters have a very short lifetime and are continually decomposing and reforming under thermal agitation (Pickett, 1977). The resultant solution of HPMC E5 will therefore consist of polymer "strands" surrounded by a multiple layer of water molecules, these water molecules being in dynamic equilibrium with the surrounding solvent. The surface area and spacial requirement of HPMC E5 molecules in water will therefore be markedly increased since the solvent acts kinetically as part of the polymer. This, along with the associated reduction in the water available as a dispersion medium causes an increase in the solution viscosity.

The configuration which HPMC molecules adopt in a solvent can be

estimated from the Mark-Houwink equation:

$$[\mu] = K \cdot M^{\alpha} \qquad \text{Equation 3.15}$$

where $[\mu]$ is the intrinsic viscosity, M is the molecular weight and K and α are constants characteristic of the polymer/solvent system and its temperature.

The value of α in this equation corresponds to the configuration of the polymer molecule in solution. Davies (1985) determined the molecular weight and intrinsic viscosity values for a number of HPMC polymer grades and calculated the value of α for dilute aqueous solutions of HPMC E5 to be 0.77. This indicates that in an aqueous solution, HPMC E5 molecules exist as unbranched, non-draining, randomly orientated flexible coils with an excluded volume. The excluded volume is the volume from which a given molecule excludes all others, and is essentially a result of the repulsion between polymer molecules arising from the spatial requirements. The presence of an exclusion volume and the relatively high value of α both imply that water is a good solvent for HPMC. The open and expanded coil structure formed in water reflects the large degree of hydrogen bond interaction between the water molecules and the hydroxyl groups of HPMC. The open coil structure is promoted by the presence of the cellulose rings in the polymer backbone, these decreasing the flexibility of the polymer chain.

The preceding discussion suggests that HPMC E5 in dilute aqueous solution consists of randomly orientated and randomly extended coils of hydrated molecules of a wide range of sizes, with the solvation and configuration changing continuously due to random bombardment by solvent molecules. Each molecule will tend to act as a single entity with little or no intra- or inter-molecular interactions. This would explain why dilute aqueous solutions of HPMC E5 exhibit Newtonian behaviour.

It is apparent from Table 3.2 that there is a very large increase in viscosity as increased concentrations of HPMC E5 are dissolved in water, a 12%w/w solution for example being around 500 times more viscous than water alone. One contributing factor to this is the large hydrodynamic volume of the coiled polymer chains and their associated hydrogen bonded water molecules. These large flow units increase the resistance to flow and thus viscosity. The work of Davies (1985) suggests that, in addition, there is a significant amount of water located within the random coil which is not attached to the polymer. With HPMC E5 molecules this is thought to be non-draining, the water being mechanically trapped within the polymer coil and dragged along with the macromolecule during flow. This further increases resistance to flow and also decreases the amount of remaining free solvent.

As previously explained, commercial grades of HPMC are polydisperse in nature, consisting of a wide range of molecular weight fractions. Of these, the larger molecular weight fractions contribute to the viscosity to an extent which is disproportionate to their concentration on a weight basis. Thus a HPMC molecule with a degree of polymerisation of 200 will produce a viscosity far higher than if the 200 individual units were present. This occurs since the cooperative nature of the flow of the 200 unit chain and its accompanying water molecules, must move together resulting in a very large flow unit. It would seem reasonable therefore to expect the weight average molecular weight to give the best indication of solution viscosity. The work of Davies (1985) appears to support this although the data from Rowe (1980a) shows there to be no correlation between the viscosity at 2%w/v and the value of the weight average molecular weight.

Table 3.2 illustrates the influence of HPMC E5 solution concentration on the resultant viscosity in water. It is apparent that the increase in

viscosity with increasing solution concentration is not linear, with considerably larger changes in viscosity being encountered as the solution concentration is increased. It is considered that this behaviour results from the simultaneous increase in the number of polymer molecules present and the reduction in the number of free water molecules. These two factors combined result in the relative concentration (the weight of polymer and associated water divided by the weight of free water) increasing at a greater rate than the stated concentration and thus to a non-linear viscosity/concentration profile.

HPMC E5 solutions studied in this work using a continuous shear rotational viscometer were found to be Newtonian in character up to viscosities of at least 520mPa s, corresponding to HPMC E5 concentrations of between about 11%w/w and 13%w/w depending on the batch. Use of the suspended level viscometer, which subjects the solutions to very low shear rates, was found to produce viscosity values which were not significantly different from those from the rotational viscometer (Table 3.2), this providing further evidence of the Newtonian nature of the solutions. This would suggest that, for HPMC E5 solutions at and below the concentration and viscosity values stated above, there is little or no reversible interaction or entanglement between the polymer chains or that they are instantaneously overcome at very low shear rates and therefore are not detected. It would also seem likely that HPMC E5 is existing as single molecules rather than there being any cross linking occurring between chains due to hydrogen bonding. This may be due to the steric size of the hydroxypropoxyl group preventing intimate contact and the high tendency for the hydroxypropoxyl group to hydrate with water. It would also suggest that the coiled chains do not uncoil at the shear rates used in this work, since this would both

decrease the disturbance of flow and release entrapped solvent.

At a viscosity of between approximately 520mPa s and 723mPa s (11%w/w to 14%w/w) deviation from Newtonian behaviour was noted. This is illustrated in Tables 3.2 and 3.3 where the values for the index of non-Newtonian behaviour are seen to be < 1. At these values therefore the viscosity will be dependent on the shear rate and will decrease as the shear rate increases. It is thought that the increased forced proximity of the hydrated polymer chains and the increased competition for the remaining "free" water leads to both entanglement of the polymer chains and possibly interactions between the polymer molecules themselves by hydrogen bonding. Under conditions of increased shear, the polymer chains become progressively untangled and the hydrogen bonds may be broken resulting in a reduction in the polymer dimensions and the release of any entrapped solvent, and thus a reduction in the disturbance to flow.

During the film coating process it is likely that the formulations will encounter a wide range of shear rates. These range from the low values in the tubing delivering solutions to the spray gun, to values of around $300s^{-1}$ to $20,000s^{-1}$ as they pass through the liquid spray nozzle (see Henderson et al., 1961) and to highly variable shear rates due to the high velocity atomising air at the droplet production stage. Once impinged on the tablets, the shear rate encountered will be dependent on the atomisation conditions and the tumbling action and separation of tablets occurring in the coating pan. The Newtonian solutions are likely to exhibit the same rheological behaviour at all stages of the coating process irrespective of the shear rate encountered. It is probable however that solutions which exhibit non-Newtonian behaviour may vary in viscosity at various stages during the coating process and when different coating conditions and coating equipment are used.

However, since the HPMC E5 solutions studied were found to follow the power-law equation (Equation 3.8), it is possible to estimate the viscosity of the solutions at any specified shear rate. The viscosity behaviour of a 19%w/w HPMC E5 solution prepared from batch number 1 was for example shown to follow the equation (see Table 3.2):

$$\tau = 4.305\ D^{0.97}$$

At a shear rate of $1s^{-1}$ the apparent viscosity would be 4305mPa s (4.305Pa s), this reducing to 3750mPa s at $100s^{-1}$ and to 3500mPa s and 3266mPa s at shear rates of $1,000s^{-1}$ and $10,000s^{-1}$ respectively.
Thus even if the solutions do not exhibit Newtonian behaviour it is possible to estimate their viscosity under a variety of conditions provided the shear rate encountered is known.

Philippoff (1936) demonstrated that the relationship between solution concentration and viscosity for methylcellulose solutions could be represented by the equation:

$$\frac{\mu}{\mu_o} = \left(1 + \left([\mu].\frac{C}{8} \right) \right)^8 \qquad \text{Equation 3.16}$$

where μ is the apparent viscosity, μ_o is the solvent viscosity, $[\mu]$ is the intrinsic viscosity (dl/g) and C the solution concentration (%w/v).
With measurements made at 20°C in water this equation becomes:

$$\mu'^{/8} = 1 + KC \qquad \text{Equation 3.17}$$

where $K = [\mu]/8$. Thus for methylcellulose, a plot of $\mu'^{/8}$ against concentration yields a straight line, the intercept being 1.
A straight line relationship between $\mu'^{/8}$ and concentration was also found to occur for the two batches of HPMC E5 used in this work, as illustrated in Figures 3.2 and 3.3, with the two representative equations being:

$$\text{For batch 1 : } \mu'^{/8} = 0.09185C + 1.0190$$

For batch 2 : $\mu'^{*} = 0.09338C + 1.0320$

Thus by assessing the viscosity of a range of HPMC E5 concentrations from these particular batches, and by plotting graphs of μ'^{*} against C, equations can be generated which allow the viscosity for any chosen concentration to be calculated. Similarly, the HPMC E5 concentration required to provide a solution of any required viscosity can be determined, 300mPa s viscosity solutions for example resulting from 11.12%w/v and 11.05%w/v solutions for batches 1 and 2 respectively. It should be noted that at concentrations above ≈ 12%w/w the viscosity values calculated will be those of the apparent Newtonian viscosity as derived from the power-law equation and the actual viscosity may vary at different points in the coating process depending on the shear rate to which the solution is subjected. The rheological profile of these solutions would need to be examined before these varying viscosity values could be calculated.

The differences in viscosity that may be obtained when making solutions up to volume rather than weight may also be estimated from the above relationships. This difference is minimal at low solution concentrations but rises as the solution concentrations increase. From the equations above,. 9%w/w solutions are likely to be ≈ 10mPa s more viscous than 9%w/v solutions and 12%w/w solutions at least 50mPa s more viscous than 12w/v solutions.

The Philippoff plots also allow the intrinsic viscosity values (the capacity of the polymer to enhance viscosity) for the aqueous HPMC E5 solutions from the two batches to be determined (see Equation 3.17). In this experimental work the values of $[\mu]$ for the two batches used were found to be 0.73dl/g and 0.75dl/g. These are in agreement with the value of 0.79dl/g reported by Tufnell et al. (1983) who determined the intrinsic viscosity using an alternative method. Davies (1985) however

reported a range of values between 1.011dl/g and 1.123dl/g, these being dependent on the method of analysis used. He also found that at concentrations between 0.4%w/v and 1.3%w/v, the Philippoff equation produced decreasing values for [μ] as the solution concentration increased. He therefore concluded that the Philippoff relationship did not hold for HPMC E5 solutions over the concentration range that he studied and that the equation was not a suitable method of calculating [μ]. The latter conclusion is in disagreement with the results in this study obtained using HPMC E5 solutions of higher concentrations (see Figures 3.2 and 3.3). In addition if the data reported by Prater (1982) is subjected to the Philippoff analysis it too is found to conform. A possible explanation for these discrepancies becomes apparent if the values of the intercept in the Philippoff equation are examined. It would be expected that for aqueous solutions the intercept would be equal to the viscosity of water at the temperature studied eg 1mPa s at 20°C. In this work however, intercepts corresponding to 1.163mPa s and 1.287mPa s were found for solutions at 20°C, and from the work of Prater (1982), an intercept of 1.016mPas was calculated for solution temperatures of 29°C (expected value 0.815mPa s). In both these studies therefore the intercept values are above those that would be expected. These findings, along with those of Davies (1985) would seem to indicate that the Philippoff relationship is not followed at low concentrations below about 2%w/v. It would seem appropriate therefore to use solution concentrations of 2%w/v or above (as in this work) when generating equations for predicting the viscosity of HPMC film coating solutions using the Philippoff relationship.

It can be seen from Table 3.2 that at the higher HPMC E5 concentrations, small changes in concentration result in relatively large increases in viscosity. For example the viscosity of an 11%w/w solution is 350mPa s whereas a 12%w/w solution has a viscosity of 520mPa s. This concept may be of importance in relation to any evaporation that occurs from atomised droplets before thay impinge on the tablet surface. If for example 20% of the water is lost from the droplets during their passage to the tablet bed, as suggested by Yoakam and Campbell (1984), then solutions initially of 6%w/w and having a viscosity of 45mPa s would hit the tablet with a concentration of 7.39%w/w and a viscosity of approximately 81mPa s. Similarly, droplets from 9%w/w and 12%w/w solutions may increase in viscosity from 166mPa s to 360mPa s and from 519mPa s to 1265mPa s respectively. In the case of the 12%w/w solution this is likely to be accompanied by a change in the rheological nature of the solution from Newtonian to pseudoplastic. Large differences may therefore potentially exist between the viscosity of the droplets and that of the bulk solution, with this effect becoming considerably greater as the solution concentration increases. The extent to which these changes in viscosity may occur during the coating process will be dependent on factors such as the temperature and humidity of the drying air, the droplet size and the time taken to reach the tablet surface.

<u>The effect of temperature on the rheological properties of HPMC E5 solutions</u>

The effect of solution temperature on the viscosity of HPMC E5 solutions can be seen in Figure 3.4. A temperature rise from 20°C to 40°C resulted in an approximate halving of the viscosities of the three concentrations studied. It has been suggested that this behaviour could be exploited during the film coating process, since if HPMC E5 solutions were heated prior to use, then a greater solids loading could be

achieved for a particular viscosity value, leaving atomisation unchanged and the coating process time reduced (Hogan, 1982). This suggestion however has yet to be proved practically.

Increasing the temperature of HPMC E5 solutions to ≈ 50°C gave rise to a change in their rheological profile, the solutions exhibiting pseudoplastic behaviour. Further temperature increases to ≈ 52°C resulted in the solution gelling and becoming thixotropic.

If the viscosity decrease with increasing temperature was attributed wholly to the reduction in viscosity of the solvent, then it would be expected that the ratio of solution to solvent viscosity (the relative viscosity, μ_r) would be constant (Batdorf and Francis, 1963). This however was not the case with the HPMC E5 solutions in this study, as shown in Table 3.12. The reduction in μ_r with increasing temperature can be attributed both to the dehydration or desolvation of the polymer chains with its associated reduction in the hydrodynamic volume, and to the tendency for the polymer to adopt a less open coil structure since water is not such a good solvent for the dehydrated chains (Moore, 1971). The effect of a temperature increase is thus to both

TABLE 3.12

TEMPERATURE (°C)	VISCOSITY OF A 9%w/w AQUEOUS HMPC E5 SOLUTION (mPa s)	VISCOSITY OF WATER (mPa s)	RELATIVE VISCOSITY (μ_r)
10	203	1.307	155
20	137	1.002	138
30	102	0.798	125
40	74	0.653	113
45	63	0.592	106
50	59	0.547	107

reduce the viscosity of the water and to alter the polymer dimensions. The decrease in viscosity with increasing temperature has been shown previously to follow the Andrade-Gauzman equation (Abdul-Razzack, 1979; Prater, 1982). A plot of $\ln\mu$ versus 1/T is shown in Figure 3.5 for 6%w/w, 9%w/w and a 12%w/w solutions of HPMC E5 prepared from batch 1. It can be seen that there appears to be a linear relationship between $\ln\mu$ and 1/T up to a temperature of approximately 45°C. At temperatures above 45°C deviation from linearity was observed. These findings are probably associated with the changing of rheological behaviour as the solution temperature approaches 50°C. Around this temperature, the extent of the de-solvation of the polymer is such that polymer-water bonds are replaced by polymer-polymer bonds resulting in associations between polymer chains and restriction of the flow of the continuous phase. When the solution is sheared, the chains become more linearly orientated and any structure formed may be broken, this resulting in a decrease in apparent viscosity. A small further increase in temperature to about 52°C results in the formation of a structured gel network (thermal gelation) in which the solvent is entrapped between chains of hydrogen bonded polymer. The viscosity at low shear rates at this temperature is thus considerably increased. With increasing shear rates the apparent viscosity falls as the structure is broken and solvent liberated. Thixotropic behaviour is noted, since the reformation of the gel structure on the removal of the shear stress is not instantaneous. In this work the thermal gelation temperature was taken as the temperature where thixotropic behaviour was first apparent and not as previously suggested (Prater, 1982) as the temperature where the trend for a decrease in viscosity with increasing temperature is reversed. This is because it was observed in this work that if the gel structure was sheared at a high enough rate, the viscosity values determined could

always be found to decrease with increasing temperature and thus a gelation temperature would never be reached.

It would follow from the above discussion that increasing polymer concentration would cause gelation to occur at a lower temperature, since there would be a greater number of molecules present, a reduced amount of water and an increase in the proximity of polymer molecules, all of which would tend to lead to earlier polymer-polymer interactions. The difference between the thermal gelation temperatures of solutions in the concentration range 6%w/w to 12%w/w for the batch of HPMC E5 tested was however was found to only be approximately 1°C.

In order to avoid changes in rheological behaviour and the problems associated with thermal gelation when aqueous film coating, it is important that HPMC E5 solutions are not subjected to temperatures over approximately 45°C at any point in the coating process. Similarly it should be remembered that the viscosity of a coating solution may vary considerably (Figure 3.4) at different points in the coating process if it is subjected to fluctuating temperatures. These temperature changes may occur in the coating solution holding vessel, during passage to the spray gun, at the spray gun itself, during passage to the tablet surface or at the tablet surface.

<u>HPMC interbatch variability</u>

In order to comply with the specifications set by the United States Pharmacopeia (USP), the viscosity of 2%w/v aqueous solutions of HPMC at 20°C should not deviate by more than ± 20% from the stated nominal viscosity. The European Pharmacopoeia (EP) states that the viscosity should not be less than 75% and not more than 140% of the stated nominal viscosity. The USP therefore allows the viscosity of the 2%w/v solutions of HPMC E5 to vary between 4mPa s and 6mPa s and the EP between 3.75mPa s and 7mPa s. It is conceivable that solutions of

markedly different viscosities may therefore be produced from different HPMC batches of the same nominal viscosity, with these differences potentially being greater if the batch only has to comply with the EP viscosity specification rather than the USP specification. To test the likely extent of this batch variation in practice, the viscosity of 2%w/v solutions of thirty representative batches of HPMC E5 were obtained from the manufacturer (Colorcon Ltd.), the statistical analysis of these values being shown in Table 3.4. In addition, viscosities of the five batches of HPMC E5 available in the laboratory were analysed, the concentrations studied being 2%w/w, 9%w/w and 12%w/w (Table 3.3). In all cases the viscosity of the 2%w/v solutions of HPMC E5 fell well within both the USP and EP viscosity specification limits. Only relatively small variations in viscosity were noted at this concentration, the maximum difference being 1.42mPa s, although the most viscous solution did have a viscosity which was 30% higher than the least viscous. Examination of the results for the five batches studied at concentrations of 9%w/w and 12%w/w however shows both vastly increased differences in the viscosity range encountered and a greater percentage difference between batches. At a 9%w/w concentration, viscosities in the range of 129mPa s to 231mPa s were found and at 12%w/w the range was 359mPa s to 840mPa s. In the latter case two of the solutions were found to exhibit non-Newtonian behaviour. These viscosity values are however for batches which are well within both the USP and EP viscosity specifications. If batches which only just complied with the specifications were used, it is estimated that the viscosities may vary from between 110mPa s and 250mPa s for 9%w/w solutions and 300mPa s and 900mPa s for 12%w/w solutions when using the USP limits, and by considerably greater amounts when using the EP limits. Variations in the distribution of the molecular weight

fractions present in HPMC have been reported by Rowe (1980a) and Davies (1985) and it is this variation which is thought to be responsible for the differing viscosity values between batches.

The possible wide variations in solution viscosity between different HPMC E5 batches may potentially affect the coating process by influencing the droplet size distribution produced upon atomisation and the droplet behaviour at the tablet surface. This is examined in Chapters 4 and 5.

Since the viscosity limits set in the Pharmacopeoia are applicable to other grades of HPMC, then the problem of large batch to batch viscosity variation is equally applicable to the other sources of HPMC which may be used in aqueous film coating.

The role of HPMC E5 moisture content

HPMC is known to absorb moisture when stored in conditions of high relative humidity (manufacturers literature, Callahan et al., 1982) and has been described as moderately hygroscopic (Callahan et al (1982). The moisture content of samples of HPMC from the batch designated as batch 1, after storage at 20°C and various relative humidities is detailed in Table 3.8. It can be seen that the moisture content (the amount of moisture present expressed as a percentage of the total sample weight) varied from 2.1%w/w when storage was at 11% relative humidity to 22.6%w/w when storage was at 95% relative humidity. These results are similar to those reported by Callahan et al. (1982) for an unspecified grade of HPMC. Table 3.8 also shows the viscosity of 9%w/w and 12%w/w solutions of HPMC E5 prepared from samples stored at the various conditions. It is apparent that if the moisture content of the sample is not controlled then large variations in the solution viscosity may result, with nearly a three-fold difference in viscosity being encountered between the 12%w/w solutions. This phenomenon is likely to

be more pronounced as the batch viscosity approaches the top of the viscosity specification and the solution concentration increases. It should be noted that since the manufacturer's specification for HPMC E5 moisture content is <3%, problems associated with differing moisture levels are only likely to occur after inappropriate storage. To ensure problems do not occur, HPMC E5 should be stored in air-tight containers and conditions of high humidity avoided. In addition, samples should be routinely checked to determine if their moisture content has changed. If changes have occurred, then in order to ensure the solution viscosity is constant the concentration of HPMC should be altered by an appropriate amount. For instance for the sample stored at 95% relative humidity to produce the same solution viscosity as the sample stored at 11% relative humidity, the concentration would need to be a factor of 1.26 higher. Thus similar solution viscosities would be produced by 15.1%w/w and 12%w/w solutions respectively.

If a Philippoff type relationship has been determined for a batch of HPMC, then an estimation of the viscosity that will be produced by samples of differing moisture content can be obtained by inserting an appropriate value for the solution concentration into the generated equation.

<u>HPMC solution preparation methods</u>

There are a plethora of methods in which HPMC solutions can be prepared and stored before use, all of which result in the formation of a clear solution. In industrial film coating procedures or experimental work involving HPMC solutions, it is likely that many of these different processes may be encountered. It is therefore important to determine that the rheological properties of the solution are independent of the method of preparation and storage. It was found in this work (Table 3.9) that there was no significant difference in final solution

viscosity with different methods of preparation, although the ease and speed of preparation varied markedly. Unlike methylcellulose solutions, where time-dependent polymer de-aggregation and viscosity differences were shown to occur after storage at a temperature of 4°C (Neely, 1963), solutions of HPMC E5 were found not to be influenced by storage in a refrigerator. Thus, it can be concluded that as long as solutions are prepared accurately and stored correctly (so that minimal bacterial growth occurs), any recommended method of solution preparation will yield an identical viscosity from the same batch of material.

The effect of plasticisers on the rheological behaviour of HPMC solutions

The effect of added plasticisers on the viscosity of 9%w/w HPMC E5 solutions is shown in Figure 3.6. All the plasticisers studied caused an increase in solution viscosity. There appeared to be a linear relationship between the increase in viscosity and the concentration of plasticiser added for the three different molecular weight grades of polyethylene glycol (PEG) used, although this was not found to be the case for the non-polymeric plasticisers glycerol and propylene glycol.

Due to problems associated with incompatibility in the film after coating, the maximum concentration of the five plasticisers studied that would be included in a formulation containing 9%w/w HPMC is approximately 2%w/w. At this concentration the percentage increase in viscosity was found to range between 4% when propylene glycol was used to 15% for PEG 1500.

It has been shown by Okhamafe and York (1983) that the addition of PEG 400 and PEG 1000 to aqueous solutions of HPMC of low concentrations (0.05%w/v to 0.5%w/v), resulted in a decrease in the value of the intrinsic viscosity. They attributed this decrease to an interaction between PEG and water, which was postulated to remove the water

associated with HPMC and thereby reduce its molecular dimensions. If this was the case however, it would be expected that PEG 400 being more hydrophilic than PEG 1000 would give rise to a greater reduction in intrinsic viscosity. The reverse was however observed by Okhamafe and York (1983). A minimum was observed in the intrinsic viscosity values at a PEG 1000 concentration of 50%w/w and a PEG 400 concentration of 60%w/w, these concentrations being relative to the amount of HPMC E5. It was postulated that above these concentrations some of the PEG was interacting with the HPMC leading to an increase in the molecular dimensions and thus a viscosity increase, although it should be noted that PEG would not be used at these concentrations in tablet coating formulations due to film compatibility problems.

The effect of added plasticisers on the viscosity of HPMC E5 solutions is likely to be influenced by several factors. Firstly, all of the plasticisers when added to water will cause an increase in its viscosity. At concentrations of 5%w/w the rank order was found to be PEG 1500 (1.40mPa s), PEG 400 (1.21mPa s), PEG 200 (1.18mPa s), propylene glycol (1.17mPa s) and glycerol (1.13mPa s). In the absence of any other interactions the viscosities of the HPMC E5 solutions would therefore be expected to be increased by an appropriate multiple. Thus, with the addition of 5%w/w PEG 1500 one would expect the viscosity to increase by a factor of 1.40 to 192mPas. Although this relationship was found to be approximately correct for the three molecular weights of PEG studied, it did not hold for the addition of glycerol and propylene glycol, the addition of glycerol causing a greater than expected increase in viscosity and propylene glycol causing a less than expected increase.

A second factor that may influence viscosity arises from the fact that all the plasticisers used are poor solvents for HPMC E5 compared with

water, HPMC E5 for example being virtually insoluble in glycerol at all temperatures. Their addition may therefore render the solvent system less favourable to the formation of a random, opened coiled structure and thus cause a reduction in the hydrodynamic volume of the polymer. This would be reflected by a reduction in the value of α in the Mark-Houwink equation (Equation 3.15). A consequence of the altered polymer dimensions would be a reduction in the values of intrinsic and actual viscosity and could explain the observations of Okhamafe and York (1983) with regard to the reduced intrinsic viscosity values observed when plasticisers were added.

A further contributing factor is the possibility that the plasticisers are either interacting with the polymer itself, or more likely the water sheath surrounding the polymer, thereby altering the polymer dimensions. This interaction may either increase the dimensions of the polymer unit due to the association of the plasticiser with it, or decrease the dimensions by competing for and removing the attached water molecules. The latter effect would be more liable to occur with glycerol and propylene glycol since they are far more hydrophilic than the PEGs.

In practice it is probable that there is a combination of these three factors influencing the viscosity, with the relative magnitude being different for each plasticiser.

Schwartz and Alvino (1976) demonstrated that if the thermal gelation temperature of a film coat approached 37°C then problems with tablet dissolution may result. Care must therefore be taken to ensure any additives included in the coating formulation do not adversely reduce the gelation temperature. It has been shown by Levy and Schwarz (1958) that glycerol can cause a reduction in the gelation temperature of methylcellulose whereas propylene glycol and PEG 400 can cause an

increase. Prater (1982) found the inclusion of propylene glycol at a concentration of 20%w/w to have a minimal effect on the gelation temperature of 5%w/v solutions of HPMC E5. In this work, the inclusion of the five plasticisers studied at a solution concentration of 2%w/w (the maximum at which they are likely to be used practically) in a 9%w/w HPMC E5 solution, was found to have no effect on the shape of the viscosity/temperature profile and no detectable influence on the gelation temperature.

The effect of other formulation additives on the rheological behaviour of HPMC solutions

The effect of various formulation additives on the rheological properties of HPMC E5 solutions is shown in Table 3.5. It can be seen that with the exception of polysorbate 20, all the additives studied caused a significant increase in viscosity at concentrations likely to be used practically. The inclusion of non-soluble components also caused a change in rheological behaviour from Newtonian to pseudoplastic, this arising from disturbances to the flow pattern, and orientation of asymmetric particles as the shear rate increased. The extent of this change was dependent on the material used and generally was found to increase with increasing additive concentration. Formulations including these additives may therefore exhibit differing viscosities at different stages in the coating process. The extent to which this may occur can be calculated from values of the apparent Newtonian viscosity and index of non-Newtonian behaviour detailed in Table 3.5, in conjunction with the power-law equation (Equation 3.8).

Of the four insoluble additives studied, the greatest increase in apparent Newtonian viscosity was caused by the brilliant blue HT aluminium lake followed by titanium dioxide, talc and calcium carbonate, with viscosity increases of over 80% (from 137mPa s to 251mPa s) being

possible in the practical situation. The differences in the viscosity enhancing effect of the non-soluble additives will be dependent on complex relationships between factors such as the particle size, shape, density, particle-particle interaction and degree of agglomeration. Chopra and Tawashi (1985) for example showed that as the mean volume diameter of talc decreased from 39μm to 16μm, so the ability to enhance viscosity markedly increased. Substances such as talc, which have a flake like structure, would (all other factors being equal) be expected to cause a greater deviation from Newtonian behaviour than substances like titanium dioxide which is more rounded. Increasing density may be expected to reduce the degree of viscosity enhancement due to a reduction in the surface area available for disturbance of the flow patterns.

Since there is likely to be considerable variation in the physical properties of most of these additives depending on their source, then it follows that the viscosity changes caused by their addition is also likely to vary. The rank order of viscosity enhancing ability may therefore not always be that demonstrated in Table 3.5.

Addition of the colorant dispersion Opaspray (which contains 30%w/w solids) to a solution of HPMC E5 also imparted pseudoplastic behaviour, this being due to the titanium dioxide and aluminium lake included in its formulation. At the recommended concentration of 15%w/w with a 9%w/w HPMC E5 solution (giving a film polymer:pigment ratio of 2:1) Opaspray caused a viscosity increase of 109mPa s (+79%).. A further increase in Opaspray concentration to 20%w/w more than doubled the viscosity increase to 250mPa s (+181%)

The inclusion of the surface active agents sodium lauryl sulphate (SLS) and polysorbate 20 at the concentrations detailed in Table 3.5 did not cause the 9%w/w HPMC E5 solution to deviate from Newtonian behaviour.

However there was a large difference in their effect on the solution viscosity, with SLS causing nearly a doubling of viscosity from 137mPa s to 268mPa s when included at a concentration of 1%w/w and polysorbate 20 having only a minimal effect at concentrations up to 2%w/w. The inclusion of SLS at a concentration of 1%w/w was found to cause a similar relative increase in the viscosity of a 12%w/w solution of HPMC E5 from 437mPa s to 821mPa s. This coupled with the fact that a 1%w/w solution of SLS was found to possess a viscosity of 1.86mPa s, suggests that the increases seen in the viscosity of the HPMC solutions is in effect due to an increase in the viscosity of the solvent rather than SLS interacting with the HPMC E5 molecules or their associated water sheath. In the absence of any difference in the effect of these suface active agents on the surface tension of HPMC solutions, it would seem sensible to use polysorbate 20 instead of SLS, since this may reduce any potential problems arising from increased viscosity values.

The rheological properties of Opadry suspensions

Two types of Opadry were studied in this work, type OY based on HPMC E5 and type OY-D based on HPMC E3. As would be expected, they both exhibited non-Newtonian viscosity behaviour due to the presence of dispersed insoluble . colouring agents in the formulation. Their viscosity was therefore expressed in terms of the index of non-Newtonian behaviour and apparent Newtonian viscosity (see Tables 3.6 and 3.7). Like HPMC E5 solutions, the increase in viscosity with increasing concentration became more pronounced as the concentration increased. Despite the presence of a plasticiser and colouring agents in the formulation, the viscosity/concentration relationship could still be represented by Philippoff relationship (Equation 3.17), thus enabling the estimation of the viscosity of any desired concentration and the preparation of suspensions of a specified viscosity. Although the two

batches of the Opadry type OY studied contained different colouring agents, the difference in their viscosity profiles was relatively small, especially at concentrations of 15w/w and below.

The manufacturers recommend that Opadry OY and Opadry OY-D formulations are used at concentrations of 15%w/w and 25w/w respectively. These concentrations are likely to produce apparent Newtonian viscosities in the order of 385mPa s for the type OY Opadry and 809mPa s for the type OY-D Opadry. These are approximately equivalent in viscosity to 11.5%w/w and 14%w/w solutions of HPMC E5 respectively.

3.4.2 THE SURFACE TENSION OF HPMC E5 SOLUTIONS

It has been shown that HPMC E5 is surface active in aqueous solution, with solution concentrations of between 1%w/w and 12%w/w (those likely to be used practically for aqueous film coating) reducing the surface tension at 20°C from 72.8mNm^{-1} (water alone) to between 46.8mNm^{-1} and 44.5mNm^{-1} (Table 3.10). Although a considerable reduction in surface tension resulted from the addition of 1%w/w HPMC E5, minimal further reduction was seen with an additional twelvefold increase in concentration. Any reduction in surface tension, in the absence of other changes in physical properties, would be expected to favour droplet formation and aid in solution spreading on a tablet surface. Examination of the results in Table 3.10 would however appear to indicate that any effects caused by the reduction in surface tension with increasing concentration are likely to be minimal.

At very low concentrations of HPMC E5 (<5 x 10^{-3}%w/w) the surface tension was shown to be time-dependent, a phenomenon known as *surface ageing*. The has also been reported for high molecular weight hydroxypropylcellulose samples at concentrations of 2 x 10^{-5}%w/w and below (Zografi, 1985), although no experimental details of how the study

was undertaken were given. Surface ageing arises since when a fresh surface is formed it will be free of actively adsorbed HPMC molecules. This however is not the equilibrium state. There will be a gradual diffusion of solute molecules from the bulk of the solution to the surface and orientation of the molecules once at the surface, until an equilibrium situation is achieved. The wide distribution of molecular weight fractions in HPMC E5 (Rowe, 1980a; Davies, 1985) is likely to contribute to the time-dependent nature of the suface tension, with the larger molecules diffusing less rapidly and being more sterically hindered. The attainment of the equilibrium surface tension will correspond to that of equilibrium adsorption, this being a dynamic state with molecules continuously leaving and entering the surface layer. The time-dependent non-equilibrium surface tension is referred to as the *dynamic surface tension*.

Non-ionic surface active agents, into which category HPMC E5 can be classed, tend to exhibit marked surface activity at considerably lower concentrations than ionic ones with identical hydrophobic groups. If the surfactants form micelles, this leads in turn to a tendency for lower values of the critical micelle concentration. The attainment of equilibrium surface tension values at concentrations below the critical micelle concentration has been found to be considerably slower with non ionic surfactants, and for a specific surfactant to be slower for lower concentrations (Lange, 1971; Wan and Lee, 1974). This latter effect was observed for HPMC E5 in this work as demonstrated in Figures 3.7 and 3.8. At concentrations below the point of inflection in the surface tension/concentration curve (Figure 3.9), it can be considered that the surface can accommodate all the HPMC moleclues in the solution, and thus before the equilibrium surface tension is reached these molecules must make their way to the surface. As the solution

concentration increases there becomes an excess of molecules over those which can be accommodated at the surface. Since the molecules are distributed randomly initially, the molecules which are required to reach the surface have on average a shorter distance to travel and thus equilibrium is attained more quickly. HPMC E5 solutions with a concentration greater than approximately 5 x 10^{-3}%w/w were found to have attained equilibrium surface tension values sufficiently quickly such that no time-dependent reduction in surface tension could be detected.

It should be realised that the equilibrium times quoted for the different HPMC E5 concentrations are only applicable for the apparatus and sample volumes used in this study. They do however serve to illustrate that when there are only just sufficient molecules to saturate the liquid surface, there may be a considerable time-period before the equilibrium surface tension values are reached.

Estimation of the surface tension of droplets atomised from HPMC E5 solutions

HPMC E5 was shown to exhibit a linear decrease in equilibrium surface tension with increasing solution concentration up to a concentration of 2 x 10^{-5}%w/w. Above this concentration there was a sharp change in gradient of the slope and the surface tension was seen to fall more slowly with increasing concentration. The point of intersection between the extrapolated straight lines of the surface tension/concentration profie is often associated with the formation of micelles of some form and is referred to as the critical micelle concentration. HPMC E5 has not however been demonstrated to form micelles and evidence from intrinsic viscosity measurements indicates that the molecules exist as single entities at low concentrations (Davies, 1985). The size of the HPMC E5 molecules, the presence of the heterocyclic ring structure and the absence of specific hydrophobic and hydrophilic "ends" are all

factors which tend to reduce the possibility of micelle formation. It is assumed therefore that at the point of inflection in Figure 3.9, the surface is saturated with HPMC molecules and that any additional molecules will remain as single units in the solution bulk. The point of intersection in Figure 3.9 will therefore be refered to as the *critical surface tension.* In this work this was found to have a value of 55.4mNm^{-1}. The importance of the surface ageing phenomenon and the apparent critical surface tension may at first seem of little relevance to film coating, since the practically used concentrations are far in excess of those required to reach the critical surface tension or those at which surface ageing is detectable. The potential importance of these factors will however become apparent if the following hypothesis is considered:

The area occupied by each molecule at the liquid surface at the critical surface tension can be calculated from the Gibbs adsorption equation:

$$\Gamma = - \frac{C}{RT} \times \frac{d\gamma}{dC} \qquad \text{Equation 3.18}$$

where Γ is defined as the surface excess concentration (concentration at the surface - concentration in the bulk) in mol m^{-2}, C is the overall concentration in mol dm^{-3}, R is the gas constant, T is the absolute temperature and $d\gamma/dC$ is the slope of the surface tension/concentration curve at concentration C.

Utilising the information from Figure 3.9, the surface excess concentration can be calculated as:

$$\frac{C}{8.314 \times 293} \times \frac{17.4 \times 10^{-3}}{C} = 7.14 \times 10^{-6} \text{ mol m}^{-2}$$

If at the critical surface tension the HPMC molecules are assumed to be entirely at the surface, then the number of molecules per m^2 can be

calculated as:

$$\Gamma \times \text{Avogadros number} = 7.14 \times 10^{-6} \times 6.023 \times 10^{23}$$

$$= 4.30 \times 10^{18} \text{ molecules } m^{-2}.$$

Each molecule will on average occupy an area equivalent to the reciprocal of this value ie $2.32 \times 10^{-19} m^2$.

To produce a surface tension of $55.4 mNm^{-1}$ therefore 4.30×10^{18} molecules are required for every m^2 of surface produced.

If we now consider an individual atomised droplet we can calculate its weight in grams (assuming it is spherical) as:

$$\frac{4\pi r_d^3}{3} \times \rho_d$$

where r_d and ρ_d are the radius (m) and density ($g\ m^{-3}$) of the droplet respectively.

The number of molecules in a droplet can therefore be calculated as:

$$\frac{4\pi r_d^3 \rho_d}{3} \times \frac{C}{100} \times \frac{6.023 \times 10^{23}}{\text{molecular weight}}$$

where C is the solution concentration (%w/w).

The number of molecules available per m^2 of surface generated can therefore be calculated for any droplet size by assuming that the surface area of the droplet = $4\pi r_d^2$.

As discussed previously, the value for the molecular weight of HPMC E5 remains uncertain and has been found to vary markedly between batches and on the method of analysis used. The value used in this work is the weight average molecular weight of $2.94 \times 10^6 Da$ determined by Rowe (1980a). By substituting this value in the above equation and simplifying, the number of molecules available per m^2 surface in any particular sized atomised droplet can be calculated as:

$$\frac{d_d \times \rho_d \times C \times 2.05 \times 10^{16}}{6}$$

where d_d is the droplet diameter (m).

It has already been determined that 4.30×10^{18} molecules per m^2 of surface are required to give a surface tension of $55.4mNm^{-1}$. Thus for any desired solution concentration, the droplet diameter which will give a surface tension value of $55.4mNm^{-1}$ can be calculated, if it is assumed that all the molecules are at the droplet surface and the solution density is known. These droplet diameters are shown in Table 3.13 for various HPMC E5 solution concentrations.

TABLE 3.13

HPMC E5 CONCENTRATION (%w/w)	DROPLET DIAMETER POSSESSING A SURFACE TENSION OF $55.4mNm^{-1}$ (μm)
6	207
9	137
12	102

As the droplet size gets smaller, its surface area to volume ratio will increase. Droplets of diameters smaller than those shown in Table 3.13 may therefore exhibit surface tension values greater than $55.4mNm^{-1}$. On atomising a 6%w/w HPMC E5 solution, all droplets smaller than 210μm may thus potentially have a surface tension greater than $55.4mNm^{-1}$.

The number of molecules needed per m^2 to produce the surface tensions above $55.4mNm^{-1}$ can be calculated using the Gibbs adsorption equation in the same manner as illustrated above. This then enables the surface tension of any droplet size below those shown in Table 3.13 to be

estimated for different solution concentrations.

Since the relationship between surface tension and solution concentration was found to be linear (Figure 3.9) at values below the critical surface tension and the increase in the ratio of surface area to volume for a spherical droplet is proportional to $1/d_d$, then the increase in droplet surface tension (γ_d) with decreasing droplet diameter will also be linear. Some of the equations describing these linear relationships are shown in Table 3.14. The limiting droplet diameters are those diameters calculated for Table 3.13. At diameters above these limiting values the equations do not hold since surface tension behaviour is outside the scope of Gibbs adsorption equation (Equation 3.18).

Table 3.14

HPMC E5 CONCENTRATION (%w/w)	EQUATION FOR CALCULATING DROPLET SURFACE TENSION	LIMITING DROPLET DIAMETER (μm)
6	$\gamma_d = 72.8 - 0.084d_d$	207
9	$\gamma_d = 72.8 - 0.127d_d$	137
12	$\gamma_d = 72.8 - 0.171d_d$	102

Based on these equations, a 50μm diameter droplet would have surface tension values of 68.6mNm^{-1}, 66.5mNm^{-1} and 64.3mNm^{-1} for 6%w/w, 9%w/w and 12%w/w solutions of HPMC E5 respectively. Simlarly a 10μm droplet would have values of 72.0mNm^{-1}, 71.6mNm^{-1} and 71.1mNm^{-1} and a 100μm droplet values of 64.4mNm^{-1}, 60.1mNm^{-1} and 55.7mNm^{-1}. These equations therefore

indicate that any droplets in the order of 10μm may possess surface tension values which approach those of water and that there may be significant differences in droplet surface tension depending on the solution concentration from which they were generated.

It should be noted that these equations assume that all the HPMC E5 molecules are present at the droplet surface. It has been shown under laboratory conditions however that considerable time periods may be required for equilibrium surface tension values to be reached when there is not an excess of HPMC moleclues over the amount required to "saturate" the surface. In a practical coating situation not only is there a large amount of "fresh" surface generated after atomisation, but there is also considerably less than a second between the time of droplet formation and the point of impingement on the tablet surface. It is conceivable therefore that there may be insufficient time for the HPMC E5 molecules to migrate to the droplet surface (albeit a very small distance) and the equilibrium surface tension values to be reached. Droplet surface tension values may therefore be even higher than those generated from the equations in Table 3.14 which will represent the minimum calculated surface tension values.

The use of the Gibbs adsorption equation to estimate droplet surface tensions is limited to surface tension values at or above the critical surface tension value of 55.4mNm^{-1}. This is however still significantly higher than the surface tensions that would be expected of the coating solutions which would be used practically, which were shown to possess values of between 44.5mNm^{-1} and 46.8mNm^{-1}. Thus even droplets of diameters greater than the limiting diameters shown in Table 3.14 are likely to have surface tension values which are considerably higher than those envisaged from measurement of the surface tension of the solutions from which they were generated.

The factors discussed above will be equally applicable to HPMC of other grades and possibly other coating polymers. Use of a higher grade material will be likely to exacerbate the potential problem, since the concentrations used will be lower and the average molecular weight will be higher.

It is realised that the above calculations are based on an ideal situation and that in practice there may be other influencing factors. These may include solvent evaporation during travel to the tablet bed, polymer polydispersity, polymer batch to batch variation and the inclusion of formulation additives. The above discussion does however illustrate that the surface tension of droplets of HPMC E5 solutions hitting the tablet surface may be considerably greater than that predicted from measuring the surface tension of the bulk solution, this effect being more pronounced with smaller droplets and less concentrated solutions and potentiated by the time taken for HPMC molecules to reach the droplet surface. The extent to which this phenomenon may occur during film coating will be dependent on how the coating solutions are atomised and the actual size of the droplets produced. This is examined and discussed in Chapters 4 and 5.

<u>The effect of solution temperature and formulation additives on the surface tension of HPMC E5 solutions</u>

The addition of plasticisers was found to have a minimal effect on the surface tension of 9%w/w HPMC E5 solutions. This is perhaps not surprising since the surface tension of 2%w/w solutions of the plasticisers were found to be above 66mNm^{-1} in each case. The inclusion of colouring agents and opacifiers similarly had little effect on the solution surface tension. Sodium lauryl sulphate and polysorbate 20 although highly surface active when alone in solution, only caused a relatively small reduction in surface tension when added to 9%w/w HPMC

E5 solutions. In order to estimate the effects of these surfactants on the atomised droplet surface tension, appropriate surface tension/concentration profiles and surface ageing characteristics would need to be identified.

If the addition of a surfactant to HPMC E5 solutions was required, the data in this chapter suggest that it may be preferable to use polysorbate 20 rather than SLS, since the latter may cause significant increases in solution viscosity.

Increasing the temperature of a 9%w/w solution of HPMC E5 from 20°C to 40°C was found to result in a reduction in surface tension of approximately $1mNm^{-1}$. Water over the same temperature range would be expected to exhibit a reduction in surface tension of about $4mNm^{-1}$ (Bikerman, 1970) this being due to the gradual reduction in intermolecular cohesive forces as the temperature increases (the surface tension will be zero at some finite temperature). The difference in behaviour between HPMC E5 solutions and water probably results from the non-volatile nature of HPMC with the situation being complicated by the differing levels of solvation at different temperatures.

3.4.3 CONCLUSIONS

From the results presented and discussed in this chapter it is apparent that the physical properties of HPMC E5 based solutions used in aqueous film coating may vary markedly and therefore potentially influence the coating process at a number of stages.

The main variable factor potentially influencing the atomisation stage would appear to be the solutions rheological properties, with the range of surface tension and density values which may be encountered seeming unlikely to exert any significant effects. Variation in the rheological

properties may arise from a variety of causes including the solution concentration and temperature, material batch variation, inappropriate storage conditions and whether plasticising or colouring agents are present. In addition, some formulations may exhibit pseudoplastic behaviour which may give rise to variable values of viscosity at the point of atomisation, these being dependent on the shear conditions encountered.

It has been demonstrated that the surface tension of the droplets produced on atomising film coating solutions may vary depending on their droplet size (and thus the rheological properties of the solution from which they were produced), the concentration of HPMC E5 present and the time taken to travel to the tablet surface. Differences in droplet size, surface tension and viscosity may in addition influence the degree of evaporation and coalescence which occurs before the droplets impinge on the tablet which in turn may further influence the rheological properties.

Once impinged on the tablet surface, the large variations in droplet viscosity and surface tension which may exist may affect the ability of the droplets to adhere, wet, spread, coalesce and penetrate. This in turn may lead to differences in the occurrence of film coat defects, the adhesion to the tablet core and the gloss and roughness of the coat.

The extent to which the physical properties of the film coating solutions affect the various stages of the coating process will become clearer after examination of the actual droplet sizes produced during film coating and the properties of film coats produced in a practical situation. These two factors are examined in Chapters 4 and 5.

CHAPTER 4

THE ATOMISATION STAGE OF AQUEOUS FILM COATING

4.1 INTRODUCTION

4.1.1 GENERAL INTRODUCTION

Atomisation is the process whereby a liquid is broken up into a spray of droplets. It is employed in a wide range of industrial processes including paint application, air conditioning humidification, fuel ignition, spray drying, fluidised-bed granulation and film coating. In aqueous film coating the utilisation of atomisation techniques enables the coating polymer to be efficiently applied to a granule or tablet core surface. Atomised droplets hitting the tablet during film coating should be in such a state that they spread evenly over the surface and form a smooth continuous film of even thickness. The atomisation stage of the coating process will therefore encompass all factors which influence the state at which the droplets arrive at the tablet surface and their behaviour once there. Inadequate control of the atomisation process may result in film coat defects such as picking, sticking and orange peel (roughness).

Although much research has been carried out in recent years into various aspects of the film coating process, characterisation of the atomisation stage and its influence on the final film properties has been largely ignored. Satisfactory film coats have been achieved in the pharmaceutical industry using atomisation techniques arising from a combination of trial and error and previous experience. If however the operator had knowledge of how the coating formulation, spray gun type and operating parameters influenced the atomisation process and the resulting film properties, a more rational approach could be adopted to predict the conditions likely to produce a satisfactory end product.

4.1.2 METHODS OF ACHIEVING ATOMISATION

Many different methods of atomising solutions are available. They all tend to produce a distribution of droplet sizes and all, except those using ultrasonic energy, tend to be relatively inefficient; the energy required to produce the increase in surface area is typically less than 1% of the total energy consumption (Masters, 1976).

Methods of achieving atomisation include:

Ultrasonic atomisation

Ultrasonic atomisers form droplets by subjecting the fluid to intense high frequency vibrations. They have not been used for tablet film coating to date, since those available are either incapable of coping with the flow rates required for either organic or aqueous film coating, produce droplets which do not possess sufficient momentum or have nozzles which are easily fouled.

Hydraulic (airless) atomisation

In a hydraulic atomiser, droplets are produced by forcing a liquid under pressure through a small orifice. The form of the resulting liquid can be varied by changing the pressure used, by altering the direction of flow into the orifice or by the use of different nozzles. Flat or conical spray patterns may be produced. Hydraulic atomisation is the system of choice when organic solvents are used to dissolve the film forming polymer, since premature drying is inhibited as air is not used to produce and shape the spray. The high pressures needed to produce adequate atomisation of viscous coating solutions however demand that even with very small orifice diameters the flow rates produced are relatively high. This is acceptable with highly volatile organic solvents, but when water is used as is the current trend in pharmaceutical tablet coating, the ability of the coating equipment to evaporate the solvent satisfactorily may be overcome and the tablet bed

overwetted, resulting in poor quality coatings.

Pneumatic atomisation

This is the method of choice for aqueous film coating. The energy for atomisation is derived from a high-speed air stream which impinges on the solution to be atomised. In order to produce droplets this air stream has to both accelerate the liquid above a critical speed whereby it becomes unstable, and provide energy to overcome the viscous and surface tension forces resisting droplet formation. Since air has a low density, a comparitively large volume moving at high speed is required to impart a portion of its energy to heavy viscous materials such as film coating solutions. Each part of the solution that leaves the spray gun is thus accompanied by a high proportion (relative to liquid) of fast flowing air. The droplets in this stream move with and are propelled by the expanding stream of atomising air towards the tablet surface. The correct balance between atomising air and fluid flow is essential for correct droplet formation.

4.1.3 PNEUMATIC ATOMISER DESIGN

Pneumatic atomisers are available in many different designs and for many different purposes, however the same basic principles of operation apply to each.

Each atomiser consists of a liquid nozzle and an air nozzle (air cap) and many contain a fluid control assembly. A simple form of pneumatic atomiser is shown in Figure 4.1.

Liquid nozzle

The liquid nozzle provides control for metering material delivery, serves to direct the liquid into the atomising air stream and provides a seat (where applicable) for the liquid needle which shuts off liquid flow.

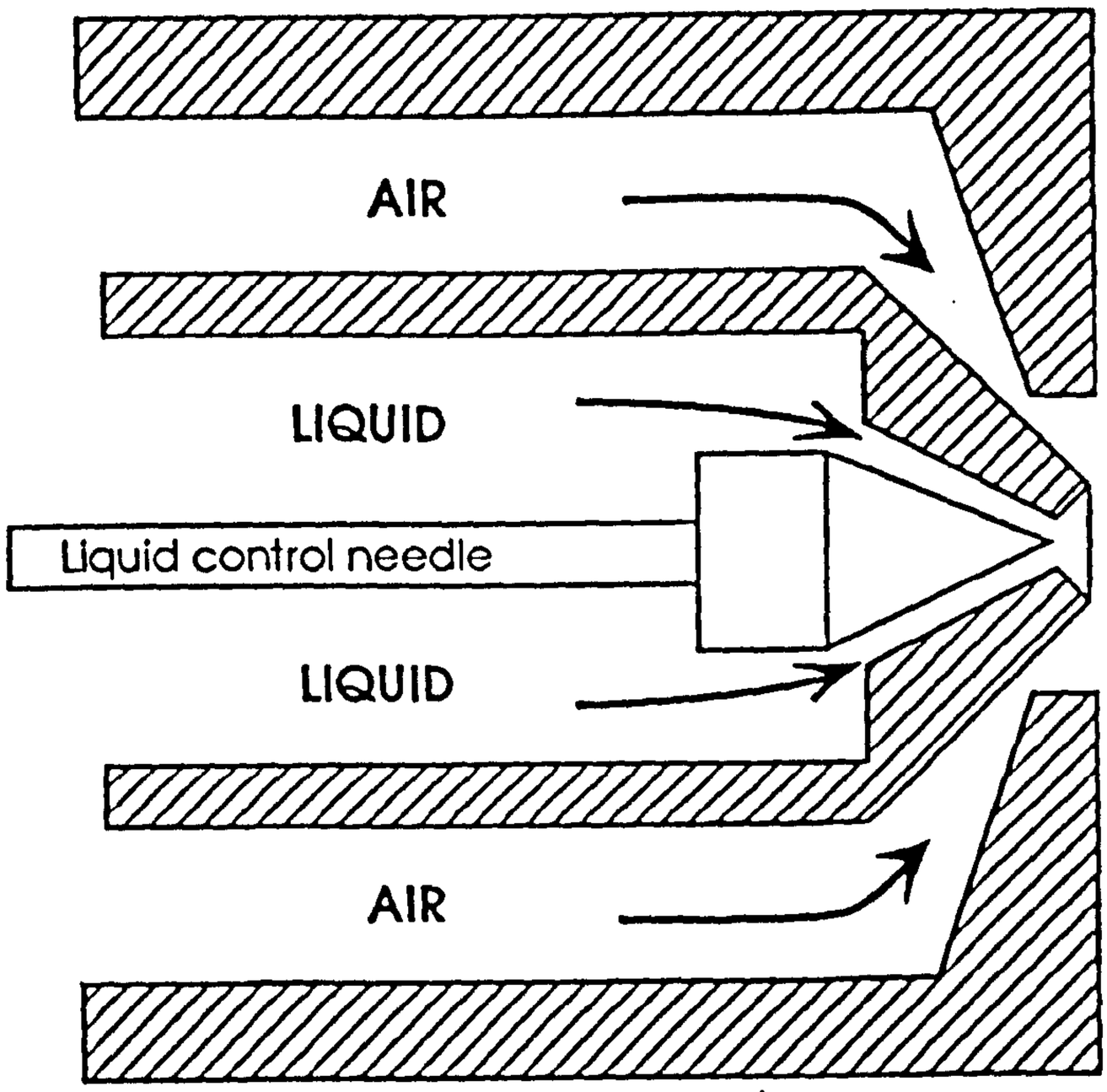

FIGURE 4.1: A SIMPLE PNEUMATIC ATOMISER

Liquid nozzles are manufactured with a variety of orifice diameters. The required orifice size for a liquid nozzle will be determined by the viscosity of the material, the flow rate required, the volatility of the solvent, the solids content and the method used to deliver the liquid to the nozzle. If the diameter is too small it may become blocked during atomisation, especially if volatile solvents are used or there is a high proportion of solids in the formulation. Additionally use of smaller orifices requires an increase in the pressure needed to force the liquid through the nozzle and leads to the liquid being emitted from the nozzle at a greater velocity. If this velocity is too great, the atomising air may be prevented from attacking the liquid stream efficiently, resulting in poor quality atomisation.

The orifice diameter of liquid nozzles utilised in the spray guns used

for aqueous film coating usually ranges between 0.5mm and 1.8mm.

Of equal importance to the orifice diameter is the outer diameter of the liquid nozzle. This, along with the inner diameter of the air cap defines the area of the annulus through which the atomising air passes, and thus influences its kinetic characteristics.

Air cap

The air cap serves to direct the jets of air used to atomise the liquid, determines the spray shape and influences the degree of momentum imparted to the atomised droplets.

Air caps fall into two main categories, external or internal mix. In an internal mix system, liquid is emitted inside the air cap, mixed with the air and atomised before being released to the atmosphere. Internal mix air caps usually have either a round hole or a slot from which the spray is ejected which controls the spray shape. In order to function efficiently this system requires the air and liquid pressure to be approximately equal. In aqueous film coating since liquid flow rates used are fairly low (20gmin^{-1} to 100gmin^{-1}) the corresponding pressures required to deliver the liquid to the nozzles also tend to be low (<69kPa (10psi)), even when the orifice diameter is small. However the air pressures required in order to atomise viscous film coating solutions are in the order of 207kPa to 552kPa (30psi to 80psi). This large pressure differential negates the use of these systems since any attempted compromise by increasing liquid pressure or decreasing atomising air pressure results in unacceptable atomisation.

The system used for aqueous film coating usually therefore involves external mix air caps with which the liquid and air do not come into contact until after thay have left their respective nozzles.

External mix air caps of the type used in aqueous film coating have one or more of the design features shown in Figure 4.2.

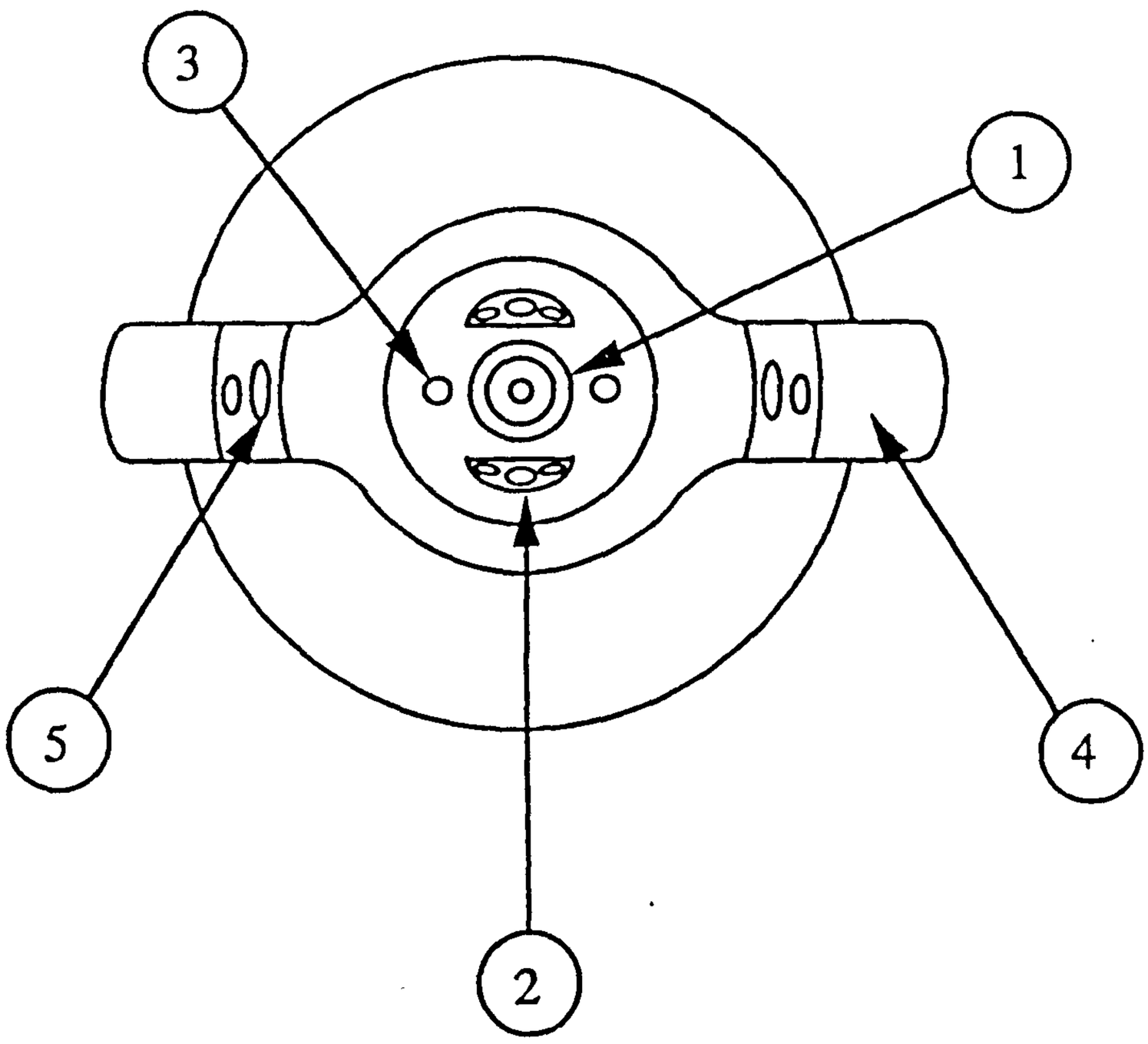

1. ANNULAR RING AROUND LIQUID NOZZLE TIP
2. ANGULAR CONVERGING HOLES
3. CONTAINMENT HOLES
4. ANGULAR PROJECTING LUGS
5. SIDE-PORT HOLES

Figure 4.2: Design features of an external mix air cap.

As the liquid being sprayed leaves the liquid nozzle it is immediately surrounded by an envelope of pressurised air emitted from the annular ring (1) around the liquid nozzle tip. The liquid expands into the hollow column of air and the resulting turbulence mixes the liquid with the air, accelerates the liquid above a speed at which the stream is stable and supplies energy to overcome the viscous and surface tension forces resisting droplet formation. This is called *the first stage atomisation* and is where the majority of the atomisation occurs. The size of the annular ring (1) will influence the volume and velocity of the atomising air as it leaves the spray gun, which in turn will affect the liquid/air shear forces and thus the extent of atomisation.

In some air caps there may be two sets of angular converging holes (2) which may also cause turbulence and possibly a degree of atomisation (*second stage atomisation*). They may also help to keep the face of the air cap clean. The containment holes (3) (if present) serve to reduce the degree of spray expansion, help direct it and aid in reducing air cap fouling. The angular projecting lugs (4) (also known as horns, ears or wings) on the edges of the air cap base contain the passage-ways for the side port air jets (5). There are typically one or two passage-ways in each projecting lug. The air emitting from the side ports changes the shape of the spray from that of a cone to a more elongated eliptical form. Additional turbulence may occur at this stage as may potentially a small amount of atomisation (*third stage atomisation*). The spray pattern width and elongation can be adjusted in many spray guns by controlling the amount of air allowed to enter the side port holes. In other guns this spray-shaping air cannot be controlled and the spray shape is dependent on both the angle of the air as it emits from the side ports and the atomising air pressure.

As the cross-section of the spray changes from a circular to an

eliptical shape, the surface area covered by the spray increases, and thus the amount of coat deposited per unit area decreases. This effect is shown in Figure 4.3. An eliptical or flat spray is usually adopted for aqueous film coating, since it provides a more even coverage and therefore both an increased likelihood of an even coat thickness and a reduced possibility of localised overwetting.

Liquid control assembly

The liquid control assembly has two main functions; to shut off liquid flow to prevent dripping and to provide extra control over the rate of liquid flow. It usually consists of a needle whose movement is controlled by a spring under the influence of pressurised air. This pressurised controlling air may be fed to the spray gun separately from the atomising air. At rest the spring causes the control needle to be seated in the liquid nozzle so as to prevent flow. When air at a certain pressure is introduced, the pressure of the spring is overcome and liquid flow is allowed. When the air supply to the assembly is switched off the needle closes under pressure from the spring and liquid flow is halted. This process eliminates any "tailing off" of the feed rate or dripping from the gun.

The position of the needle during operation can often be varied to give a fine adjustment of liquid throughput.

4.1.4 FACTORS AFFECTING THE SIZE DISTRIBUTIONS OF DROPLETS PRODUCED BY PNEUMATIC ATOMISATION

Droplets produced during pneumatic atomisation will be spherical but not monosize; they will exist in a range of diameters. In order to characterise fully the spray and to assess the influence of the atomisation stage on the properties of the resulting film coat, it is necessary to analyse the droplet size distributions produced under

EVOLUTION OF SPRAY PATTERN FROM
A CONE TO A FLAT SPRAY SHAPE

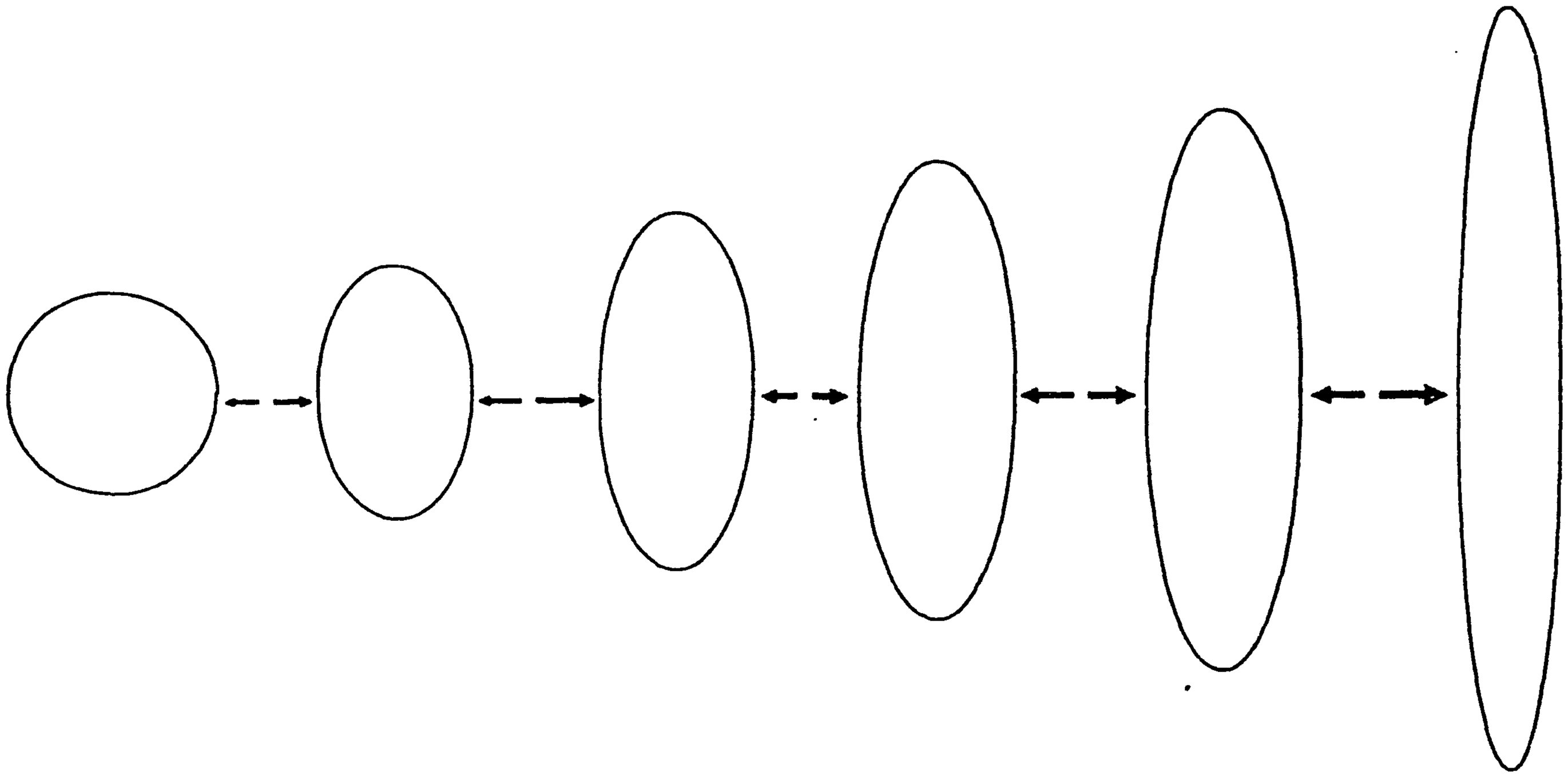

INCREASING VOLUME OF AIR INTO SIDE-PORT HOLES

FIGURE 4.3

defined atomisation conditions. The data obtained can then be examined to determine whether the droplet sizes fit mathematically defined distribution patterns and characteristic mean droplet diameters can be calculated.

Research to date on the factors influencing atomisation has largely been in the fields of mechanical engineering and fuel technology and has involved a wide range of atomiser designs, liquids and atomisation parameters. Because of this diversity of atomisation conditions, extrapolation of the results from previous work to the conditions encountered during aqueous film coating is not possible and they can only serve to give an indication of the possible influencing factors.

The majority of workers investigating the atomisation process have characterised the droplet distribution in terms of characteristic droplet diameters and presented equations to show the effect of process variables on these diameters. Although they have no fundamental meaning unless it is known that the droplets fall in a defined distribution function, characteristic droplet diameters serve as a useful and simple method of comparing large quantities of data. When expressing an average diameter, a given polysize system is replaced by either an equivalent monosize system which has the same number of droplets and one other property (such as length, surface or mass) in common, or by a system where the poly- and monosize systems do not have the same number but have other properties in common such as specific surface.

Before reviewing the literature therefore it is necessary to define these characteristic droplet diameters. Those commonly used are:

Mean length diameter

The mean length diameter (D_L), also known as the *arithmetic mean diameter*, is defined as the diameter of a monosize system having the

same number and total length as the polysize system. Thus,

$$D_L = \frac{\Sigma(x.\Delta n)}{N}$$

where Δn is the number of droplets of diameter x, and N is the total number of droplets.

Volume mean diameter

The volume mean diameter (D_{VM}) is defined as the diameter of a monosize system which has the same number and total volume as the polysize system. Thus,

$$D_{VM} = \left[\frac{\Sigma(x^3.\Delta n)}{N} \right]^{1/3}$$

Surface mean diameter

The surface mean diameter (D_{SM}), also referred to as the *Sauter mean diameter*, is the diameter of a monosize system having the same specific surface as the polysize system. Thus,

$$D_{SM} = \frac{\Sigma(x^3\ \Delta n)}{N} \div \frac{\Sigma(x^2\ \Delta n)}{N}$$

Mean evaporative diameter

The mean evaporative diameter (D_{ME}) is the diameter of a monosize system which has the same specific evaporation rate as a given polysize spray and can be calculated by,

$$D_{ME} = \left[\frac{\Sigma(x^3\ \Delta n)}{N} \div \frac{\Sigma(x\ \Delta n)}{N} \right]^{0.5}$$

Mass median diameter

The mass median diameter (D_{MM}) is the diameter above or below which lies 50% of the total mass. It can be read from a cumulative weight percentage undersize graph.

Other diameters determined by the percentage of the total mass which lies below their size include $D_{0.1}$ (10% below), $D_{0.9}$ (90% below), and the Rosin-Rammler diameter (63.2% below) (see section 4.3.13).

4.1.5 LITERATURE REVIEW

Studies investigating pneumatic atomisation have been carried out using a wide variety of spray guns, liquids and process conditions. Because of this there appears to be little correlation between results from different workers, each placing a different emphasis on the importance of the various atomisation variables. This review of the literature will therefore serve to ascertain the factors which are likely to influence the atomisation process in aqueous film coating and therefore warrant investigation.

Investigation into the droplet sizes produced during aqueous tablet film coating is limited to the work of Cole et al. (1980 and 1983). They described a photographic technique to measure the size of droplets produced from formulations based on HPMC and HPMC/HPC, plasticised with propylene glycol and containing coloured aluminium lakes. They found that when using a Walther Pilot WX/XV spray gun and liquid flow rates between $10gmin^{-1}$ and $50gmin^{-1}$, the median size of the droplets decreased on increasing the air pressure, from around 30µm at 276kPa (40psi) to 18µm at 552kPa (80psi). However the authors gave no information on the distribution of sizes encountered, the viscosity of the formulations, the spray shape used or the distance from the spray gun that measurements were taken.

One of the earliest and most quoted studies on the factors affecting atomisation was performed by Nukiyama and Tanasawa (1938). They produced the equation below from work on internal mix atomisers, to express the droplet Sauter mean diameter in terms of liquid properties

and nozzle operational variables in the ranges stated.

$$D_{SM} = \frac{585}{U_r}\left[\frac{\gamma_L}{\rho_L}\right]^{0.5} + 597\left[\frac{\mu}{(\gamma_L\rho_L)^{0.5}}\right]^{0.45}\left[\frac{Q_L.1000}{Q_A}\right]^{1.5}$$

Equation 4.1

where U_r is the velocity of air relative to liquid at the nozzle exit (up to 300ms^{-1}), γ_L the liquid surface tension (19mNm^{-1} to 73mNm^{-1}), ρ_L the liquid density (690kgm^{-3} to 1200kgm^{-3}), μ the liquid viscosity (0.3mPa s to 30mPa s) and Q_L/Q_A the air/liquid volume ratio at the air and liquid orifices respectively. Liquid feed rates up to 450cm^{3}min^{-1} were studied. The investigations showed that droplet size increased with increasing liquid viscosity and surface tension, and decreased with increasing liquid density, air/liquid relative velocity and air/liquid volume flow rates. It was concluded that at the low viscosities used, if the ratio Q_A/Q_L was greater than 5,000 then the second term in the equation became neglible and droplet size was dependent mainly on the liquid surface tension and density and the relative velocity of air to liquid. If these findings were applicable to the spray guns used in aqueous film coating, it would suggest that since solution density and surface tension vary to a minimal extent, droplet size could be regulated by controlling atomising air velocity.

Bitron (1955) demonstrated that the equation of Nukiyama and Tanasawa (1938) could be extended to cover higher relative velocities of up to 680ms^{-1}. A reduction in the size of the largest droplets was also reported as the atomising air velocity increased.

Garner and Henry (1953) investigated the droplet sizes produced by an external mix atomiser when spraying various fuels into areas of reduced atmospheric pressure. They reported a decrease in the average droplet size produced (measured 40mm from the nozzle exit) with an increase in air pressure (range 64kPa to 192kPa) and an increase in droplet size

with increasing liquid flow rate (range 0.575gmin^{-1} to 1.96gmin^{-1}) and decreasing pressure of the chamber into which the liquid was being sprayed. They found that heating the fuels prior to atomisation resulted in a finer spray, this being attributed to a reduction in fuel viscosity, surface tension and density. The different fuels studied exhibited different droplet size distributions when atomised under identical conditions. This appeared to be due to differences in their surface tension (range 20.9mNm^{-1} to 28.4mNm^{-1}), density (684kgm^{-3} to 879kgm^{-3}) and aromatic content, although the exact influence of each was not quantified. The authors concluded that the effect of viscosity under the test conditions was small (although the range studied was only between 0.695mPa s and 2.044mPa s).

Weiss and Worsham (1959) studied the droplet sizes attained when atomising molten wax (viscosity 3.25mPa s to 11.3mPa s, specific gravity 806kgm^{-3} to 828kgm^{-3} and surface tension 18.2mNm^{-1} to 22mNm^{-1}) into a hot airstream (149°C to 208°C) of sustained high velocity (61ms^{-1} to 305ms^{-1}). They found that changes in the sampling distance from the nozzle between 280mm and 1041mm did not cause a significant difference in the measured mass median diameter. The major influence on droplet size was found to be the relative velocity between the atomising air and liquid (U_r), the mass median diameter being proportional to $U_r^{-1.33}$. The physical properties of the molten wax were also found to influence atomisation with the mass median diameter determined to be proportional to $\mu^{0.24}$. The diameter of the liquid nozzle and the liquid exit velocity were found to be of least importance, especially at high atomising air velocities. The results of the work were correlated empirically by the dimensionless equation:

$$\left[\frac{D_{nn}\rho_A U_r^2}{\gamma_L}\right] = 0.61\left[\frac{U_r\mu_L}{\gamma_L}\right]^{12/3}\left[1+\frac{1000\rho_A}{\rho_L}\right]\left[\frac{W\,\rho_L\gamma_L\mu_A}{\mu_L^4}\right]^{1/12}$$

Equation 4.2

where W is the mass injection rate of the liquid and the other symbols are as previously defined.

Gretzinger and Marshall (1961) used a converging pneumatic atomiser (one which surrounds the liquid with an annulus of atomising air as with film coating spray guns) capable of using different liquid nozzles in a study of the atomisation of water. They investigated flow rates between 38gmin^{-1} and 340gmin^{-1}, atomising air pressures up to 688kPa (100psi), liquid nozzle diameters between 1.37mm and 5.51mm and air/liquid mass ratios between 0.4 and 30. Mass median droplet diameters between 5μm and 30μm were measured. The authors found that at air pressures between 552kPa and 688kPa, the liquid flow rate had relatively little effect on the air-flow pattern in the vicinity of the nozzle outlet, providing the flow was non-pulsating. Pulsating flow was found to give rise to larger droplet sizes than non-pulsating flow. The mass median diameter of the sprays was found to be reduced with increasing air/liquid mass rates, this relationship taking the shape of a hyperbola. At ratios above ≃4, little further reduction in D_{nn} was observed. Each different liquid nozzle used gave a different droplet size distribution and average droplet size, this being due to differences in their diameter and the area of the annulus through which the atomising air was flowing. Liquid nozzles of smaller internal diameter were found to give the smaller droplet sizes for a given air/liquid mass ratio. This was attributed to the more effective energy utilisation when atomising a thinner liquid film. The authors did not investigate the influence of solution physical properties.

Rizkalla and Lefebvre (1975) conducted a study of pneumatic atomisation

using a specially designed atomiser in which the liquid was first spread into a thin sheet and then exposed on both sides to high velocity air. They arrived at the dimensionless equation below to represent the influence of air and fluid properties on droplet production.

$$D_{sm}/t = A(\gamma_L\rho_L/t)^{0.5}\ (U_A\rho_A)^{-1.0}\ (1+M_L/M_A) + B(\mu_L^2/\gamma_L\rho_A t)^{0.425}\ (1+M_L/M_A)^2$$

Equation 4.3

where A and B are constants, and t is the liquid film thickness (m). The ranges studied were: air velocity (70ms^{-1} to 125ms^{-1}), air temperature (23°C to 151°C), air pressure (10kPa to 850kPa), viscosity (1mPa s to 44mPa s), surface tension (26mNm^{-1} to 74mNm^{-1}) and liquid density (780kgm^{-3} to 1500kgm^{-3}). The authors found that increasing atomising air temperature gave rise to larger droplets as did a reduced air velocity and an increased liquid flow rate. Atomisation quality was found to deteriorate when the air/liquid mass ratio fell below 4 and declined rapidly at ratios below 2. Ratios exceeding 5 only produced very slight reductions in droplet size. These latter findings are similar to those reported by Gretzinger and Marshall (1961). When atomising water and kerosine Rizkalla and Lefebvre (1975) found that the mean droplet size was inversely proportional to air pressure. Their general conclusions were that at low solution viscosities, the dominant factors were air velocity and density, D_{sm} being proportional to both. Liquid viscosity was found however to have an effect separate from air velocity, hence their equation is expressed as the product of two terms, the first dominated by air velocity and density and the second by viscosity. For low viscosity liquids the first term is postulated to predominate and droplet size increases with increasing surface tension, liquid density, liquid film thickness and liquid/air ratio, and decreases with increasing air velocity and density. With

liquids of high viscosity the second term acquires greater significance and thus variations in air velocity and density are predicted to have a smaller effect.

Hukuo et al. (1976) used sodium silicate solutions to investigate the atomisation of viscous liquids by external mix pneumatic atomisation. Liquid nozzles with diameters between 2.4mm and 4mm were used and air velocities between 50ms^{-1} and 250ms^{-1} studied. The viscosity, surface tension and density of the solutions ranged from 90mPa s to 3700mPa s, 47.7mNm^{-1} to 89.8mNm^{-1} and 1450kgm^{-3} to 1480kgm^{-3} respectively. Measurements were taken 300mm from the nozzle exit. It was found that with an air/liquid volume ratio above 10,000, the surface mean diameter was proportional to $U_r^{-0.61}$. Increasing the air/liquid volume ratio above ≈4000 caused very little decrease in droplet size and no further decrease was noted at ratios above 10,000. These factors and those accounting for the solution physical properties were embodied in the empirical equation:

$$D_{SM} = \frac{0.47(\gamma/\rho)^{0.36}}{U_r^{0.61}} + 0.14\left[\frac{\mu}{(\gamma\rho)^{0.5}}\right]^{0.43}\left[\frac{1000Q_L}{Q_A}\right]^{0.64}$$

Equation 4.4

where D_{SM} is in mm, γ in mNm^{-1}, ρ in gcm^{-3} and μ in poise.

The authors concluded that when Q_A/Q_L was large, the droplet size was mainly governed by the first term in the equation, that is surface tension, density and relative velocity were the important factors. When Q_A/Q_L was small however the mean diameter was said to be influenced mainly by the second term and the solution physical properties and the air/liquid volume ratio become important.

Kumar and Prasad (1971) proposed a theoretically based equation to predict droplet sizes produced from an external mix pneumatic atomiser which directed the atomising air towards the liquid at different angles.

They equated the forces resisting droplet formation (surface tension forces, droplet expansion forces, drag forces and viscosity) to those assisting detachment (droplet weight and the kinetic energy of both the liquid and gas). Experimental work to test the validity of the theoretical concepts was carried out with water, and mixtures of glycerol and water and glycerol and alcohol. Droplets were analysed 230mm from the atomiser. The variables studied and their ranges were: liquid viscosity 1mPa s to 230mPa s, surface tension 37mNm^{-1} to 64mNm^{-1}, liquid flow rate 24gmin^{-1} to 390gmin^{-1}, air velocity 120ms^{-1} to 240ms^{-1} liquid orifice diameter 1.6mm to 4.8mm, and nozzle angle 30° to 180°.

They found an increase in the measured volume mean diameters with increasing solution viscosity, surface tension, and liquid flow rate and a decrease with increasing air velocity. Their proposed theoretical equation (Equation 4.5) was found to be in good agreement with their experimental results.

$$\frac{(\pi r_3\ \mu_L\ Q_L\ V^{-1})}{6} + \frac{Q_L^2 \rho_L\ V^{-2/3}}{(14.5\ (Q_L\ \rho_L\ U_A\ /\ 2.5 \times 10^4)^{2/3})} = Q_A\ \rho_A\ U_A$$

Equation 4.5

where r is the radius of the constriction formed in the liquid jet (cm) and V is the droplet voloume (cm^3). The authors also compared their data with that which was predicted by the empirical expression derived by Nukiyama and Tanasawa (1938). They found good agreement at low liquid flow rates but large deviations to occur at high liquid flow rates (low air/liquid flow rate ratios).

A study of the atomising characteristics of convergent type external mix pneumatic atomisers was carried out by Kim and Marshall (1971). The liquids atomised were molten wax and melts of wax/polyethylene. Different liquid and air nozzles covering a range of annulus areas were investigated. The authors found that for a given nozzle and air flow

rate a plot of log D_{MM} versus the square root of the liquid flow rate was linear. The slopes of these lines increased as the air flow rate increased and varied between nozzle designs. The value of D_{MM} was found to decrease and approach a limiting value as the mass flow ratio of air to liquid increased. At a constant mass flow ratio increasing the atomising air velocity and decreasing fluid viscosity was found to produce smaller droplets. The authors introduced the concept of a limiting mass median diameter, this being the value obtained as M_A/M_L tended to infinity. The limiting mass median diameter was found to be a function of the dynamic force of the air ($U_A^2\rho_A$), viscosity and the total air mass flow rate. Correlation of the results led to Equation 4.6:

$$D_{MM} = \frac{249\ \gamma_L^{0.41}\ \mu_L^{0.32}}{(U_A^2\rho_A)^{0.67}\ A^{0.36}\ \rho_L^{0.16}} + 1260\left[\frac{\mu_L^2}{\rho_L\gamma_L}\right]^{0.17}\left[\frac{1}{U_r^{0.64}}\right]\left[\frac{M_A}{M_L}\right]^M$$

Equation 4.6

where M = 1.0 if M_A/M_L <3 and m = -0.5 if M_A/M_L >3. The area of the air annulus is represented by A.

This equation was valid for the following ranges of variables: U from 250ms^{-1} up to sonic, ρ_L from 800kgm^{-3} to 1041kgm^{-3}, γ_L from 0.03Nm^{-1} to 0.05Nm^{-1}, μ_L from 0.008Pa s to 0.05Pa s, M_L from 11 x 10^{-4}kgs^{-1} to 151 x 10^{-4}kgs^{-1}, M_L/MA from 0.06 to 40 and nozzle diameters from 1.4 x 10^{-3}m to 5.6 x 10^{-3}m.

Filkova and Cedik (1984) measured the droplet sizes produced when atomising a Newtonian liquid and two model pseudoplastic liquids with an external mix pnuematic atomiser. The liquid nozzle diameter used was 2.5mm and droplets measured 2m from the atomiser. They used an air pressure of 300kPa and a liquid feed rate of 0.1 lmin^{-1} to 0.3 lmin^{-1}. Their experimental data was compared with that predicted by Nakiyama and Tanasawa (1938), Gretzinger and Marshall (1961), Kim and Marshall (1971)

and Hukuo et al. (1976). They found that with water none of the equations suggested by the above authors fitted the data well, the equation of Nakiyama and Tanasawa (1938) being nearest at low flow rates and that of Hukuo et al. (1976) being best at higher flow rates. The pseudoplastic liquids used were carboxymethylcellulose solutions at concentrations of 2%w/v and 4%w/v. They possessed densities of 1021.3kgm^{-3} and 1028.3kgm^{-3}, surface tensions of 71.49 x 10^{-3}Nm^{-1} and 68.63 x 10^{-3}Nm^{-1} and apparent viscosities of 0.29Pa s and 3.6Pa s (indices of non-Newtonian behaviour were 0.73 and 0.61). With the 2% solution the sizes of the atomised droplets were found to fit almost exactly those predicted by Gretzinger and Marshall (1961), however none of the equations were suitable to describe the droplet sizes produced from the highly pseudoplastic 4%w/v solution.

Shæffer and Wørts (1977) in a series of papers examining the control of the fluidised-bed granulation process, examined the droplet sizes produced by the pneumatic atomisation of solutions of gelatine, polyvinylpyrrolidone, sodium carboxymethylcellulose and methylcellulose. The Schlick model 941-943/7 atomisers used had a liquid orifice diameter between 1.2mm and 2.3mm and a compressed air consumption of 4Nm^{3}hr^{-1} to 18.7Nm^{3}hr^{-1}. Air/liquid mass ratios between 0.86 and 25.8 were employed and the solution viscosities ranged between 2mPa s and 100mPa s. Droplet sizes were measured 450mm from the atomiser and mass median diameters from 37μm to 200μm were calculated. The authors found that D_{MM} was inversely proportional to the air/liquid mass ratio, and proportional to $\mu^{0.17}$ and $w^{0.42}$ as shown in Equation 4.7:

$$D_{MM} = \frac{852\ \mu^{0.17}}{(M_G/M_L)\ w^{0.42}} \qquad \text{Equation 4.7}$$

where w is the liquid flow rate in gmin^{-1}, μ is in cP and D_{MM} in μm. This equation was found to hold for a particular liquid and air nozzle

combination. Changes in liquid orifice diameter were not found to influence atomisation provided they permitted uniform liquid flow. The spray angle was found to affect droplet size with larger values of D_{MM} being determined in sprays with larger angles. This was attributed to differences in the intensity of contact between air and liquid. Attempts to produce smaller droplets by heating the solutions and thus reducing their viscosity proved to be inconclusive. There was no satisfactory agreement with droplet sizes calculated from the equations of Gretzinger and Marshall (1961), Nakiyama and Tanasawa (1938) and Kim and Marshall (1971).

Horvath et al. (1978) found a direct correlation between the dissolution rate of urea particles, coated using a fluidised-bed process, and the droplet size of the atomised coating solution. Particles coated with conditions producing smaller droplet sizes were found to exhibit reduced dissolution rates. The authors did not provide any details of the spray gun used and obtained their reduced droplet sizes by increasing the atomising air pressure and mass flow rate.

Arai et al. (1982) investigated the evaporation of atomised droplets from both a water and a fuel oil spray. They found that the surface mean diameter of water sprays increased with a radial increase in distance from the atomiser from 80mm to 320mm, this effect being potentiated by an increase in the ambient air temperature. They accounted for this observation by considering that the faster evaporation rate of smaller droplets meant that some droplets evaporated completely before passing the measuring device and therefore a greater emphasis was given to the larger droplets. A similar effect was noted with gasoline which was considered a highly volatile fuel. With kerosine (taken as a moderately volatile fuel) however, little difference in mean droplet diameter was noted with increasing radial

distance at 20°C. There was an initial increase in mean droplet diameter when the ambient temperature was increased to 50°C, followed by a progressive decrease with further temperature rises up to 200°C. The authors did not offer any explanation for this behaviour.

Radial differences in droplet sizes were also investigated by Prasad (1982) when atomising water with an internal mix atomiser. The mass median droplet diameter was found to increase as the distance from the nozzle increased from 150mm to 450mm, although the increase was small at distances greater than 260mm.

Meyer and Chigier (1985) investigated the atomisation of water and coal-water slurries using an external mix pneumatic atomiser which utilised atomising air both inside and outside the fluid. The slurries had an apparent viscosity of 500mPa s to 750mPa s and were fed to the atomiser at between 1.5kgmin^{-1} and 9.1kgmin^{-1}. Atomising air pressures between 70kPa and 130kPa were used and the air/fuel mass flow rate varied between 0.1 and 1.0. The authors found that the surface mean diameter and mass median diameter of the sprays increased as the distance from the nozzle increased from 100mm to 250mm. For example at liquid flow rates of 4.54kgmin^{-1} and an air/liquid mass ratio of 0.3, the D_{SM} and D_{MM} increased from 18μm to 30μm and 30μm to 50μm respectively for water and 28μm to 42μm and 50μm to 64μm for the slurry. At any one distance from the atomiser it was found that there was an axial variation in drop size, the droplets increasing in diameter as the distance from the centre of the spray increased. These observed effects were discussed in relation to evaporation and coalescence behaviour arising from velocity variations between different sized droplets.

Tambour et al. (1985) also discussed the simultaneous evaporation and coalescence processes occurring in atomised sprays. They concluded that coalescence is more likely to be dominant at the centre of the spray,

whilst at the edges evaporation is more likely to occur.

Sakai et al. (1985) investigated the atomisation characteristics of suspensions of styrene beads in water and pulverised coal in water, using an internal mix atomiser. The average diameter of the beads used was 109.8μm and the coal 67.8μm. Suspension concentrations up to 50% were studied. It was concluded both from theoretical considerations and the practical results, that the atomisation process for the suspensions proceeded as for a pure liquid, and that the size of the droplets produced from the suspensions increased over those produced from water alone by the volume of solids contained. Thus the diameter of the droplets increased by a factor of $\alpha^{-1/3}$, where α is the liquid volume fraction.

The role of surfactants in determining the size of droplets produced by a pneumatic atomiser was investigated by Winters (1989). He reported that the reduction in surface tension caused by the addition of surfactants resulted in smaller droplets being produced. The extent of the reduction in size was dependent on the diameter of the largest droplets present in the spray.

It is apparent from the literature survey, that studies into the atomisation process have encompassed a wide range of spray guns, atomisation conditions and liquids. The results from this work have often been found to only apply for the particular set of conditions used and difficulty has been encountered when trying to extrapolate results of one study to those of another. Since the atomisation process is complex with many interacting variables, prediction of the size of droplets produced on a purely theoretical basis has proved unsatisfactory to date. The conditions encountered in aqueous film coating are also quite unlike most of those detailed in earlier work.

However the survey of past work has yielded the following general conclusions about the factors most likely to influence the atomisation process during aqueous film coating:

1. The size of droplets produced during atomisation will depend on the design of the atomiser, the properties of the liquid and the conditions under which atomisation takes place.
2. Larger droplets are usually produced from liquids of increasing viscosity, surface tension and density.
3. The method of imparting the energy from the high velocity, high pressure air to the liquid is an important influencing factor.
4. The relative velocity of the atomising air to that of the liquid being atomised, and thus the shear rate produced is a major determinant of the final droplet size.
5. An increasing air/liquid mass ratio up to a value of around 4, will tend to produce smaller droplets, but further increases in the ratio are unlikely to result in any additional reduction in droplet size.
6. The liquid flow rate may influence atomisation in addition to its effect on the air/liquid mass ratio.
7. Heating the liquid to be atomised may result in a reduction in atomised droplet size.
8. There may be axial and radial differences in droplet sizes depending on the atomiser used and the extent of coalescence and evaporation.

4.1.6 DROPLET SIZE DISTRIBUTIONS

An accurate knowledge of the distribution of droplet sizes within a spray is a pre-requisite for the understanding of how the many factors involved in tablet film coating affect both the atomisation process and the resultant film coat. To fully describe the spray produced from a stated set of atomisation conditions, it is necessary to give the

number, weight or volume of droplets of a particular size or in a particular size band. In studies where a large variety of different atomisation conditions are investigated, describing the droplet sizes in this way yields a large amount of data where it is difficult to assess the relative importance of the variables involved. Consequently droplet distributions are often characterised by a single value representing a "mean diameter" as described in section 4.1.4.

An alternative approach to representing the sprays is to determine if the data can be expressed by well defined mathematical functions, as shown by Rosin and Rammler (1933), Mugele and Evans (1951), Fraser and Eisenklam (1956) and Kumar and Prasad (1971). These functions include the normal, log-normal, Rosin-Rammler and upper-limit log-normal distributions. They are empirical in nature and because of the complex liquid break-up mechanisms associated with most sprays have no theoretical basis. The selection of the function to describe a system is only dependent on its ability to fit the actual data. The advantage of characterising sprays in this way is that the entire distribution can be represented by two or three parameters, these usually describing a "mean" diameter and an indication of the dispersity of sizes.

4.1.7 METHODS OF DROPLET SIZE ANALYSIS

The ideal droplet sizing technique should:

1. Not interfere with the spray pattern and break-up process.
2. Provide for large representative samples.
3. Permit rapid sampling and counting.
4. Have good size discrimination over the entire range of droplets being measured
5. Tolerate variations in the liquid and ambient gas properties.
6. Permit determinations of both the spatial and temporal droplet size distribution.

Since it is very difficult to satisfactorily fulfil all of these criteria, the capabilities and limitations of a given technique must be recognised.

There are three main methods of characterising droplet sizes, these are:

1. Photographic

Photographic techniques utilising double flash/double image photographs are capable of measuring both droplet size and droplet velocity. Cole et al. (1978) using such a technique reported that droplets as small as 5μm could be detected. Useful information on disintegration mechanisms and the droplet formation process may also be gained. This method however suffers from some major drawbacks. It is difficult to measure very small droplets accurately, there is a limited amount of information which can be gained from each photograph and accurate analysis is both tedious and time consuming.

2. Captive techniques

Captive techniques commonly employed include impingement onto either glass slides or plates coated with a powder or high viscosity oil, or onto smoked paper. Much of the earlier research into the atomisation process relied on these captive methods for measuring droplet sizes. The methods may however interfere with the spray pattern and are time consuming and tedious to perform. They are also often inaccurate due to collection of unrepresentative samples and problems associated with evaporation and/or coalescence.

3. Optical systems

Major advances in the measurement of droplet sizes have occurred in recent years with the advent of sophisticated optical systems. Many instruments are commercially available, these being based on forward light scattering, diffraction, laser doppler velocimetry and holography.

They are invariably very quick, non-intrusive and permit coupling to a microprocesser for data analysis.

Chigier (1982) in a review of the sizing techniques available, concluded that the Fraunhofer diffraction particle sizer (Malvern Instruments Ltd.) was the simplest of the methods to use and reported that it had been extensively adopted in laboratories for testing overall spray characteristics. It was reported to provide accurate, repeatable and reliable results in a wide range of environments, but could not give information on individual droplets.

Reviews of droplet measurement techniques have been presented by Jones (1977) and Chigier (1982).

4.2 EXPERIMENTAL

4.2.1 SOLUTION PREPARATION AND STORAGE

The formulations utilised in this work were prepared and stored as described in section 3.2.1. HPMC E5 from the batch designated batch 2 (see Table 3.2) was used throughout. The viscosity and surface tension of the formulations were measured prior to use and all were found to be within ±5% of the values stated in Tables 3.2 and 3.10.

4.2.2 SPRAY GUNS

Details of the spray guns used are shown in Table 4.1. The features referred to in the end column of the table are those described in section 4.1.3 and Figure 4.2. The Schlick gun was obtained from Orthos (Engineering) Ltd., Market Harborough, the Walther Pilot gun from Manesty Machines Ltd., Liverpool, the Binks Bullows gun from Binks Bullows Ltd., Brownhills and the Spraying Systems guns from CT (London) Ltd., London.

Table 4.1

SPRAY GUN MAKE	MODEL	AIR CAP DESIGNATION	LIQUID NOZZLE DESIGNATION	LIQUID NOZZLE DIAMETER (mm)	ANNULUS AREA (mm^2)	SPRAY GUN AIR CAP FEATURES
SCHLICK	930/7-1	STANDARD	STANDARD	0,8	2,30	5
SCHLICK	931/7-1	STANDARD	STANDARD	1,2	2,30	5
SCHLICK	932/7-1	STANDARD	STANDARD	1,8	2,30	5
WALTHER PILOT	WA/WX	0,5-1,5	STANDARD	1,0	2,16	3,5
BINKS BULLOWS	540	63PB	66	1,8	3,13	2,3,5
SPRAYING SYSTEMS	1/4J SERIES	62240-60°	2850	0,71	0,68	5
		67228-45°	2850	0,71	1,01	5
		67228-45°	2050	0,51	1,01	5

The Spraying Systems guns will generally be referred to hereafter as either the Spraying Systems 45° gun (677228-45° air cap) or the Spraying Systems 60° gun (62240-60° air cap). Unless otherwise stated the 0.71mm liquid nozzle was used with the Spraying Systems guns.

In addition to the atomising air supply, the Schlick, Walther Pilot and Binks Bullows guns require a separate air supply to control the fluid delivery automatic shut off device. These three guns also allow manipulation of the spray shape (from a narrow angle solid cone to a flat spray) by controlling the amount of air passing into the side ports and side port holes of the air cap. These latter two facilities are not available on the Spraying Systems guns used, the spray shape being largely determined by the design of the air cap and the angle at which the atomising air strikes the liquid.

4.2.3 ATOMISING AIR SUPPLY

Before being fed to the spray guns, the atomising air was passed through a filter/regulator unit (Spirax-Monnier, model IP2 (Spirax-Sarco Ltd., Cheltenham)) fitted with a pressure gauge. This served to remove any particulate matter in the air and allowed the air pressure to be controlled. Air from the filter/regulator was then passed through an air volume flow meter (Brooks full-view flow meter, model 1120, fitted with a type 10-RV-15 float (Brooks Instruments, Stockport)), which allowed the monitoring of the volume (and thus mass) flow rate of the atomising air at various pressures and spray shapes. In addition use of the flow meter enabled the spray shape to be reproduced exactly at any chosen atomising air pressure.

The temperature of the atomising air was determined just prior to it entering the spray gun by a thermocouple placed in the airstream. This temperature was between 19°C and 22°C in all cases.

Reinforced safety tubing of internal diameter 10mm was used to supply the atomising air. The length of tubing between the filter/regulator and the flow meter and between the flow meter and the spray gun was kept to a minimum. Tubing of smaller internal diameter and of excessive length leads to differences between the air pressure measured by the gauge and the pressure of the air entering both the flow meter and spray gun. It can be calculated for example that air entering the tubing at a pressure of 414kPa (60psi) and flowing at a rate of 25m^3hr^{-1}, may lose approximately 3.5kPa (0.5psi) for every meter of tubing having an internal diameter of 10mm, and 138kPa (20psi) for tubing of 5mm diameter (Spirax Sarco technical literature booklet PS12 (1978)).

4.2.4 LIQUID CONTROL ASSEMBLY AIR SUPPLY

If an air supply was required to control the fluid shut-off device, this

was passed through a minature filter regulator fitted with an automatic drain and pressure gauge, before it entered the spray gun.

4.2.5 COATING SOLUTION DELIVERY TO THE SPRAY GUN

Liquid was fed to the spray guns using a peristaltic pump (Watson Marlow model 501S) and silicon tubing of external diameter 8mm and internal diameter 4mm. The delivery rate was monitored using a top pan digital balance. A pressure vessel was not used to deliver the fluid to the spray gun, since the flow rate was found to vary markedly with changes in viscosity, liquid nozzle diameter, atomising air pressure and the height of the gun above the exit port of the vessel.

The temperature of the liquid at the point of entry into the spray gun was determined by a thermocouple placed in the liquid stream.

4.2.6 DROPLET SIZE MEASUREMENT

The Malvern Droplet and Particle Size Analyser

Droplet size distributions were measured using a Malvern Droplet and Particle Size Analyser model 2600D (Malvern Instruments Ltd). The theoretical concepts utilised by the Malvern and its accuracy and limitations have been reviewed by Swithenbank et al. (1976), Negus and Azzopardi (1978), Chigier (1982), Anderson and Johnson (1983), Hirleman and Dodge (1985), Felton et al. (1985), Naining and Hongjian (1987) and Bayvel et al. (1987).

The Malvern analyser, a schematic representation of which is shown in Figure 4.4, is based on the theory of Fraunhofer diffraction. A small safe laser transmitter produces a 9mm diameter parallel beam of monochromic light (He/Ne, λ=632.8nm) through which is passed the spray to be analysed. When the light falls on the droplets a diffraction pattern is formed whereby some of the light is diffracted by an amount dependent on the size of the droplet. The diffraction angle is largest

Figure 4.4: Schematic representation of the Malvern droplet size analyser

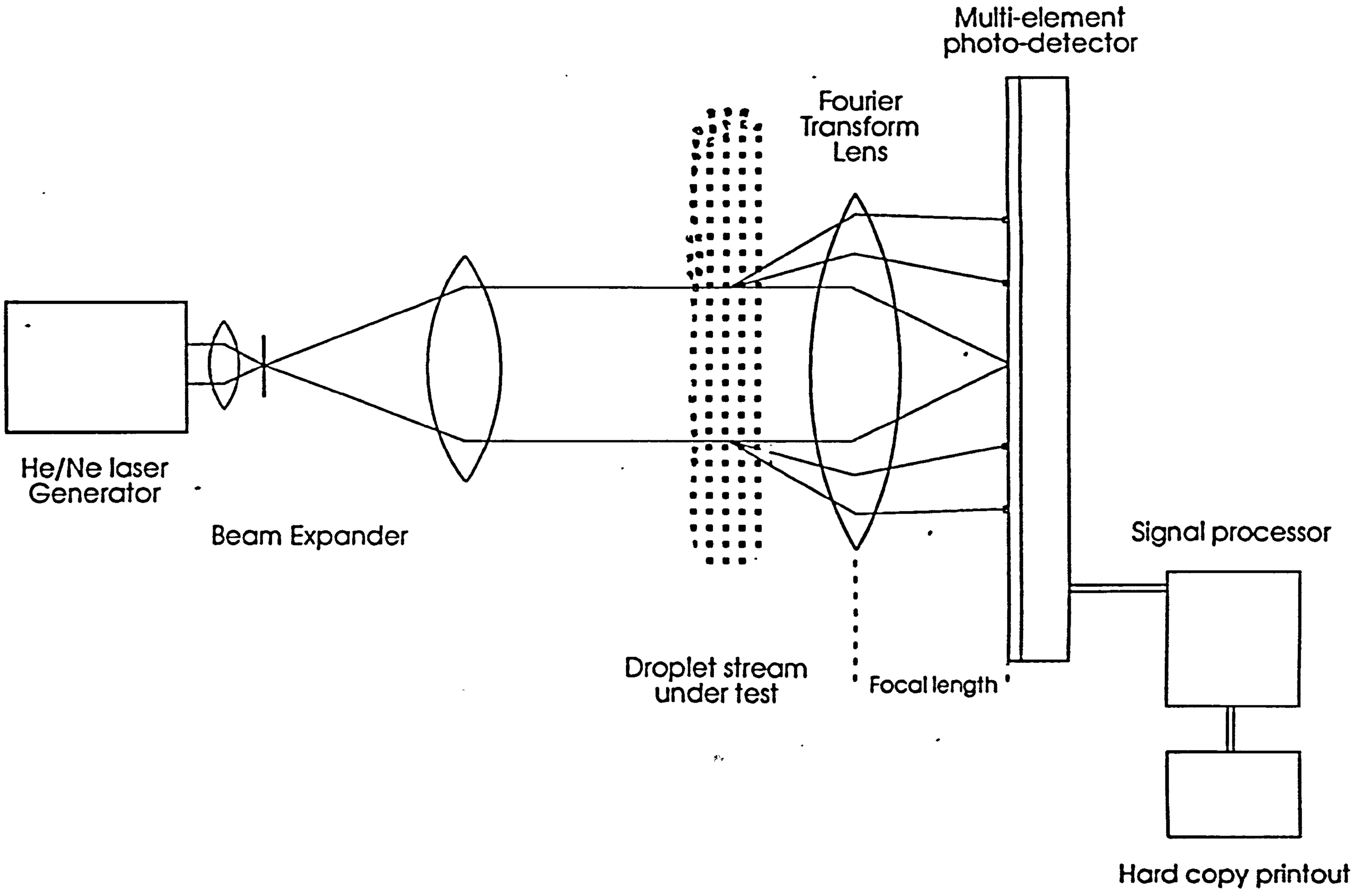

for small droplets (for example, 11° for droplets of 1μm diameter) and decreases as the droplet size increases. A Fourier transform lens is used to focus the light pattern onto a multi-element photodetector in order to measure the diffracted light energy distribution. Undiffracted light is brought to focus at a hole in the centre of the detector and the diffracted light is focussed concentrically around the central axis. The radius of the concentric rings is therefore a function of the focal length of the lens and the size of the droplet which diffracted the light, the light from larger droplets being focussed a smaller distance from the centre. The diffraction pattern generated by the droplets is independent of the position of the droplet in the beam, hence measurements can be made with droplets moving at any speed. Since the spray is not monosize, a series of concentric rings of different radii corresponding to droplets of different sizes are generated. The photodetector consists of 30 concentric, semi-circular, light sensitive ring detectors, with a hole in the centre. Behind the hole is a photodiode which is used for alignment and measuring the intensity in the centre of the pattern. Each pair of detectors corresponds to droplets of a particular diameter range (thus giving fifteen size bands), this depending on the focal length of the Fourier transform lens used. The lenses available for the Malvern had focal lengths of 63mm, 100mm and 300mm, corresponding to total droplet measuring size ranges of 1.2μm to 118μm, 1.9μm to 188μm and 5.8μm to 584μm respectively. The rings of the photodetector are scanned every 35ms, the scanning process taking 10ms. The signal from the multi-element detector is amplified, digitised and processed by a microcomputer. The data can either be presented as a best fit to a chosen mathematical function (normal, log-normal and Rosin-Rammler are available) or analysed independently (model-independent mode) using the Malvern algorithm. Results can be

stored on floppy disc and a hard copy produced. Results detailed include the percentage by weight in each of sixteen different size bands (the sixteenth being an estimation of the weight below the smallest droplet size that the machine can measure) and the cumulative weight percentages above and below the size bands (see Table 4.2). An indication of the closeness of fit of the data to the distribution function used is given by a log error value, a computation being acceptable if the log error is <4.5. A value for the obscuration is also detailed, this giving an indication of the fraction of the light which is diffracted. Obscuration values above 0.5 indicate that the results may be inaccurate due to multiple scattering effects (Felton et al., 1985). Very low obscuration values signify that only a small amount of droplets are being analysed, which can also lead to inaccurate results. Obscuration values between 0.05 and 0.50 are normally considered acceptable.

Practical use of the Malvern Droplet and Particle Size Analyser

Calibration of the Malvern droplet size analyser is not usually necessary, providing the equipment is correctly aligned. Hirleman and Dodge (1985) reported that earlier models of the Malvern deviated from independently characterised reference standards by up to 24%. Later models (one of which was used in this work) however incorporate individually determined detector correction factors and were found to be accurate to ±2.6% when applied to the same standards. Since the Malvern was removed from its optical bench in order to characterise the sprays in this work, correct alignment was confirmed before readings were taken.

The Fourier transform lens must be placed at a distance from the spray equivalent to its focal length. Preliminary studies showed lenses of focal length 63mm and 100mm to be quickly fouled by the sprays

irrespective of the spray shape or spray gun used, and thus could not be used in this work. The lens used was therefore one of focal length 300mm, capable of detecting droplets in the range 5.8µm to 584µm.

Before analysing each spray, a background reading was taken to check the alignment of the equipmemt, that there were no droplets remaining from a previous spray run and that the lens was clean. This background reading was subtracted from main reading by the software during data analysis. Each spray was analysed over a period of at least seven seconds so that the distribution pattern determined was the average of over 200 separate scans of the detector diodes. Data was computed using the model-independent mode of analysis.

Film coating solutions were sprayed vertically downwards through the laser beam, the spray guns being moved to the required position by means of calibrated vertical and horizontal spray bars. A vacuum system was utilised between each spray analysis to help remove any remaining droplets.

The reproducability of measurements was determined by performing repeat analyses over a period of days using selected atomisation conditions.

4.2.7 MODELLING OF CONDITIONS EXPERIENCED IN A MODEL 10 ACCELA-COTA

Ideally the droplet size distributions should be measured "in situ", ie inside the Accela-Cota, so that the effect of the current of hot dry air accompanying the droplets to the tablet surface can be accounted for. However consideration of the design and dimensions of both the coater and the Malvern droplet size analyser, led to the conclusion that this would be extremely difficult without major alterations to the equipment. Measurements of the velocity and temperature distributions of the drying air in the Accela-Cota were therefore undertaken, in order that these could be reproduced when analysing the sprays with the Malvern. The

properties of the drying air used in typical coating operations were determined using a Testovent 4000 combined anemometer and temperature probe (Testoterm Ltd., Emsworth). The Testovent 4000 incorporates a vane type system to monitor air velocity, whereby the rotational movement of the vanes is converted to electrical signals which are processed and displayed on a LCD. Velocity can either be displayed as an instantaneous value or one averaged over a period of 20 seconds. The latter was used in this work. The temperature sensor used was a NiCr-NiAl thermocouple which was incorporated into the vane probe. In order to monitor the air temperature and velocity, the door of the Accela-Cota was replaced with a specially designed Perspex cover. Holes were drilled into this cover in order that the temperature/velocity probe could be inserted at various chosen positions adjacent to the tablet bed and at varying distances from the tablet bed. The holes were sealed when not in use. Results from this study are shown in Tables 4.11 and 4.12.

4.2.8 ATOMISATION PARAMETERS INVESTIGATED

The parameters investigated in order to determine their influence on the atomisation process and the droplet sizes produced were:

1. Spray gun type
2. Atomising air pressure
3. Coating solution flow rate (spray rate)
4. Coating solution viscosity
5. Distance from the spray gun
6. Spray shape
7. Radial distance from the spray centre
8. Liquid nozzle diameter
9. Simulation of the drying conditions encountered in a Model 10

Accela-Cota

10. Heating the coating solutions prior to atomisation

11. Atomising air mass flow rate and velocity

The results of these studies are detailed in sections 4.3.1 to 4.3.12.

4.2.9 CHARACTERISTICS OF THE SPRAY PATTERNS GENERATED DURING THE ATOMISATION STUDIES

In order to more fully understand the influence of the atomisation parameters on the droplet size distributions measured by the Malvern analyser, it was necessary to determine the general spray patterns produced by different spray guns under a variety of conditions.

One possible method for doing this was reported by Prater (1982). This involved spraying coating solutions containing tartrazine onto polyurethane foam and analysing sections of the foam to ascertain the variation in dye concentration. This then enabled the spray droplet density to be estimated at various points within the spray. Although a quantitative estimate of the spray pattern is obtained, it would be very time consuming to evaluate all the atomisation conditions in this study using the technique. An alternative method was therefore devised which allowed both a qualitative estimation of the droplet density distribution across the spray and a visual assessment of the spray to see if the droplet sizes matched those analysed quantitatively by the Malvern. The method involved exactly reproducing sprays previously examined using the Malvern, by adjustment of the atomising air pressure and, in the case of the Schlick, Walther Pilot and Binks Bullows guns, the volume flow rate of the atomising and spray shaping air. In order that the spray patterns could be clearly seen, suspensions of Opadry were atomised. The suspension concentrations were calculated so that

they produced approximately the same viscosity as the HPMC E5 solutions or Opadry suspensions used in the atomisation studies. A piece of absorbant white card of dimensions 350mm by 300mm was placed the appropriate distance from the spray gun, this being protected by a further piece of card. The Opadry suspensions were then sprayed onto the protecting card for about 15 seconds. The protecting card was quickly removed for about three seconds to allow spraying onto the evaluating card. The protecting card was replaced and spraying ceased. Each spray pattern was examined visually. Firstly, to gain a qualitative assessment of the colour depth and droplet density across the spray and thus an indication of the spray distribution, and secondly to see if the effect of differences in droplet sizes determined by the Malvern could be observed. A more detailed study examining the actual spray dimensions is described in Chapter 5.

4.3 RESULTS

4.3.1 DATA PRESENTATION

A facsimile of the data print-out from the Malvern Droplet Size Analyser is shown in Table 4.2. This data represents the distribution of droplet sizes produced by the Schlick model 930/7-1 spray gun when atomising a 9%w/w HPMC E5 solution fed to the gun at a rate of 50gmin^{-1}. A flat spray pattern was used, utilising an atomising air pressure of 414kPa and an atomising air volume flow rate of 15.3m^{3}hr^{-1}. The solution was fed at 20°C and measurements taken at the centre of the spray, 180mm from the spray gun.

In order to represent the data generated from the Malvern analyser as fully as possible, it would be necessary to reproduce the data in the form demonstrated in Table 4.2. However because of the large volume of data generated in this study, representing the results in this way would

TABLE 4.2: FACSIMILE OF DATA PRODUCED BY THE MALVERN DROPLET SIZE ANALYSER

LOG ERROR = 3.73 OBSCURATION = 0.28

SIZE BAND UPPER (μm)	LOWER (μm)	CUMULATIVE WEIGHT BELOW (%)	WEIGHT IN BAND (%)	CUMULATIVE WEIGHT ABOVE (%)	LIGHT ENERGY COMPUTED	LIGHT ENERGY MEASURED
564.0	261.6	100.0	0.0	0.0	23	0
261.6	160.4	100.0	0.0	0.0	43	0
160.4	112.8	99.7	0.3	0.0	147	132
112.8	84.3	96.5	3.2	0.3	221	208
84.3	64.6	89.9	6.6	3.5	336	349
64.6	50.2	84.6	5.3	10.1	499	488
50.2	39.0	74.8	9.8	15.4	723	708
39.0	30.3	61.7	13.1	25.2	988	1007
30.3	23.7	49.4	12.3	38.3	1280	1259
23.7	18.5	37.0	12.4	50.6	1558	1561
18.5	14.5	28.0	9.0	63.0	1731	1726
14.5	11.4	21.8	6.2	72.0	1855	1859
11.4	9.1	16.9	4.9	78.2	1932	1906
9.1	7.2	11.8	5.1	83.1	1987	1994
7.2	5.8	6.7	5.1	88.2	2047	2047

not be conducive to easy interpretation of how the many variables of the atomisation process affect the droplet distribution.

Alternative methods of presenting the data include:

1. Graphical

Graphical representation can either be in the form of histograms plotting the relative frequency of droplets within a particular size band, or as %weight undersize curves. These methods allow easier visualisation of the data and may allow several sets of data to be

represented together. There is still however a limited amount of information which can be portrayed on a single figure, making comparisons of sprays produced under a variety of conditions difficult.

2. Mathematical

Many studies on the atomisation process, have shown that the distribution of droplet sizes produced conforms to a particular mathematical function (Rosin and Rammler, 1933; Mugele and Evans, 1955; Fraser and Eisenklam, 1956; Kumar and Prasad, 1971). In these cases the distribution can be expressed in the form of an equation usually involving two or three variable parameters, including one representing an average droplet size and one representing the degree of size distribution. A close fit of the data to these mathematical distributions enables them to be used to compare results generated under different conditions and may enable the original data to be regenerated. Many of the mathematical functions however involve complex data manipulation and have no theoretical basis.

3. Characteristic mean diameters

The most widespread method of representing the droplet distribution is by the calculation of characteristic mean diameters from the original distribution pattern. Although these have no fundamental meaning (unless it is known that the droplets conform to a defined distribution), they provide a convenient method of representing the spray by a single value and therefore allow the comparison of many different sprays within a single figure or table. Those characteristic droplet diameters commonly used have been defined in section 4.1.4. Their values for the droplet distribution pattern illustrated in Table 4.2 are shown in Table 4.3.

TABLE 4.3: CHARACTERISTIC MEAN DROPLET DIAMETERS CALCULATED FROM DATA IN TABLE 4.2

CHARACTERISTIC MEAN DIAMETER	(μm)
MEAN LENGTH DIAMETER (D_L)	3.7
VOLUME MEAN DIAMETER (D_{VM})	6.4
SURFACE MEAN DIAMETER (D_{SM})	14.3
MEAN EVAPORATIVE DIAMETER (D_{EM})	9.3
MASS MEDIAN DIAMETER (D_{MM})	24.1
$D_{0.1}$	6.7
$D_{0.9}$	64.9

Equations attempting to predict the droplet size of sprays atomised using a variety of different atomisation parameters usually do so by defining the average droplet size in terms of one or more of these characteristic diameters. The main disadvantage in expressing data in this way is that no indication of droplet size distribution is given and hence it is possible for two markedly different distributions to give the same characteristic mean diameter.

Of the droplet diameters in Table 4.3, the most commonly quoted are the volume mean diameter, surface mean diameter and mass mean diameter. In the case of the above example, the values of the mean length diameter and volume mean diameter are lower since they are affected disproportionately by the large *number* of droplets in the lowest diameter bands. Since the ability of the Malvern to determine droplet sizes is reduced at diameters of approximately 10μm and below (Weiner, 1982; Naining and Hongjian, 1986) these latter two characteristic

diameters were not used in this work.

It can be concluded from the above discussion that each of the methods of expressing the data has its advantages and disadvantages. Because of the large amount of data generated in this work, the majority of the results will be expressed in the form of characteristic droplet diameters. These will be supplemented where necessary by the use of graphical representations of the complete distribution, in order to substantiate the findings and provide further explanations of the phenomena occurring. The data will also be examined to see if they conform to any mathematical functions.

4.3.2 ESTIMATION OF THE REPEATABILITY OF MEAN DROPLET SIZE MEASUREMENTS

Values of the mass median diameter and surface mean diameter determined from sprays produced on five consecutive days using the conditions described in section 4.3.1, are detailed in Table 4.4.

Table 4.4

	MASS MEDIAN DIAMETER (μm)	SURFACE MEAN DIAMETER (μm)
DAY 1	24.1	14.3
DAY 2	22.8	13.5
DAY 3	24.5	14.0
DAY 4	25.0	14.3
DAY 5	23.6	13.8
MEAN ± SD	24.0 ± 0.76	14.0 ± 0.30
%CV	3.15	2.14

The results in Table 4.4 indicate that the characteristic mean diameters detailed hereafter are likely to be within approximately ±6% of the true mean values.

4.3.3 THE EFFECT OF SPRAY GUN TYPE AND ATOMISING AIR PRESSURE ON THE ATOMISATION OF AQUEOUS FILM COATING SOLUTIONS

Figures 4.5 to 4.10 show the influence of atomising air pressure on the mean droplet sizes produced by the Schlick model 930/7-1 spray gun when atomising HPMC E5 solutions of different concentrations fed to the gun at various flow rates. The droplet sizes were measured in the centre of the spray at a distance of 180mm from the spray gun. A flat spray shape was produced, the total atomising air flow rates (air consumption values) used being detailed in Table 4.5. It can be seen that both the mass median diameter and surface mean diameter are reduced as the atomising air pressure increases, this being apparent at all the spray rates and solution concentrations (and hence viscosities) investigated. The effect of atomising air pressure is most noticeable at pressures below 276kPa (40psi), and the quality of the atomised spray is shown to rapidly deteriorate as the pressure falls to 69kPa (10psi). At atomising air pressures above 276kPa there appears to be only a relatively small reduction in droplet size with increasing air pressure. A comparison of the effect of the atomising air pressure on the droplet sizes produced by different spray guns is shown in Figures 4.11 to 4.14. HPMC E5 solutions of 9%w/w and 12%w/w sprayed at a rate of 50gmin^{-1} were examined, droplets being measured at the centre of the flat spray at a distance of 180mm from the spray gun. Total atomising air volume flow rates and air volume flow rates through the annulus around the liquid nozzle are detailed in Table 4.5. From the figures it can be seen that different spray guns produce different mean droplet sizes under

THE EFFECT OF ATOMISING AIR PRESSURE ON THE SURFACE MEAN DIAMETER OF DROPLETS PRODUCED BY A SCHLICK MODEL 930/7-1 GUN

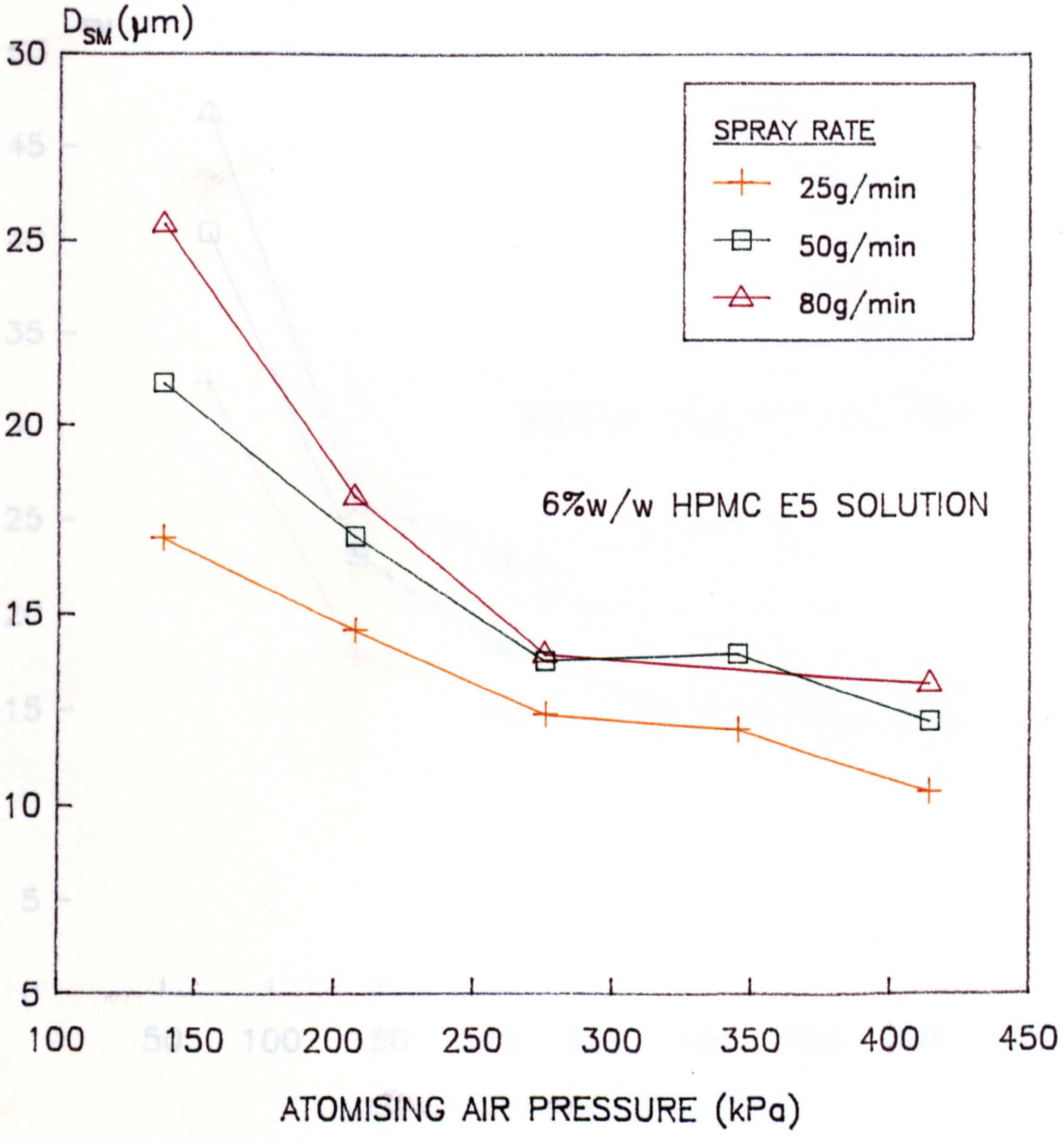

FIGURE 4.5

THE EFFECT OF ATOMISING AIR PRESSURE ON THE SURFACE MEAN DIAMETER OF DROPLETS PRODUCED BY A SCHLICK MODEL 930/7-1 GUN

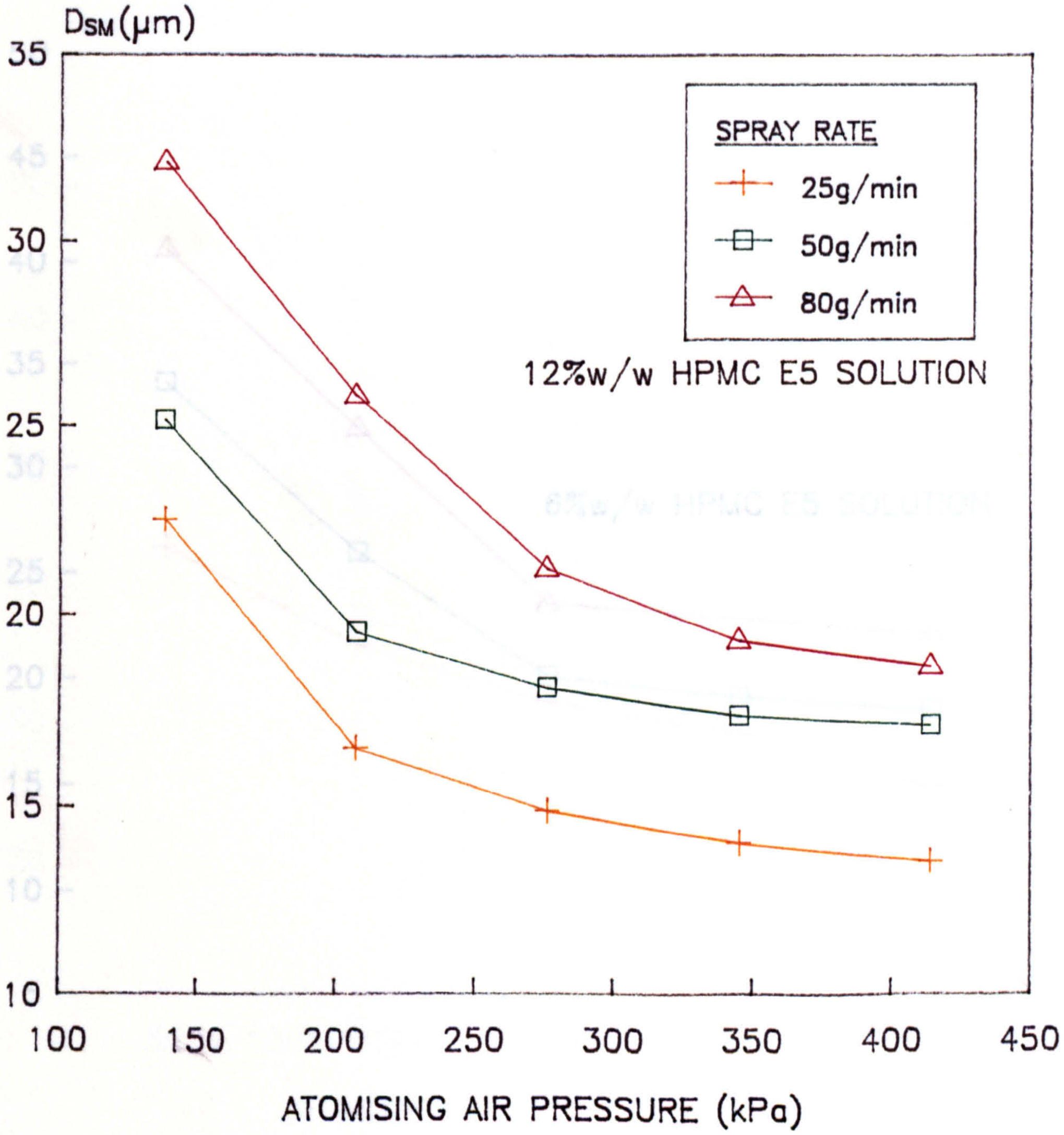

FIGURE 4.7

THE EFFECT OF ATOMISING AIR PRESSURE ON THE MASS MEDIAN DIAMETER OF DROPLETS PRODUCED BY A SCHLICK MODEL 930/7-1 GUN

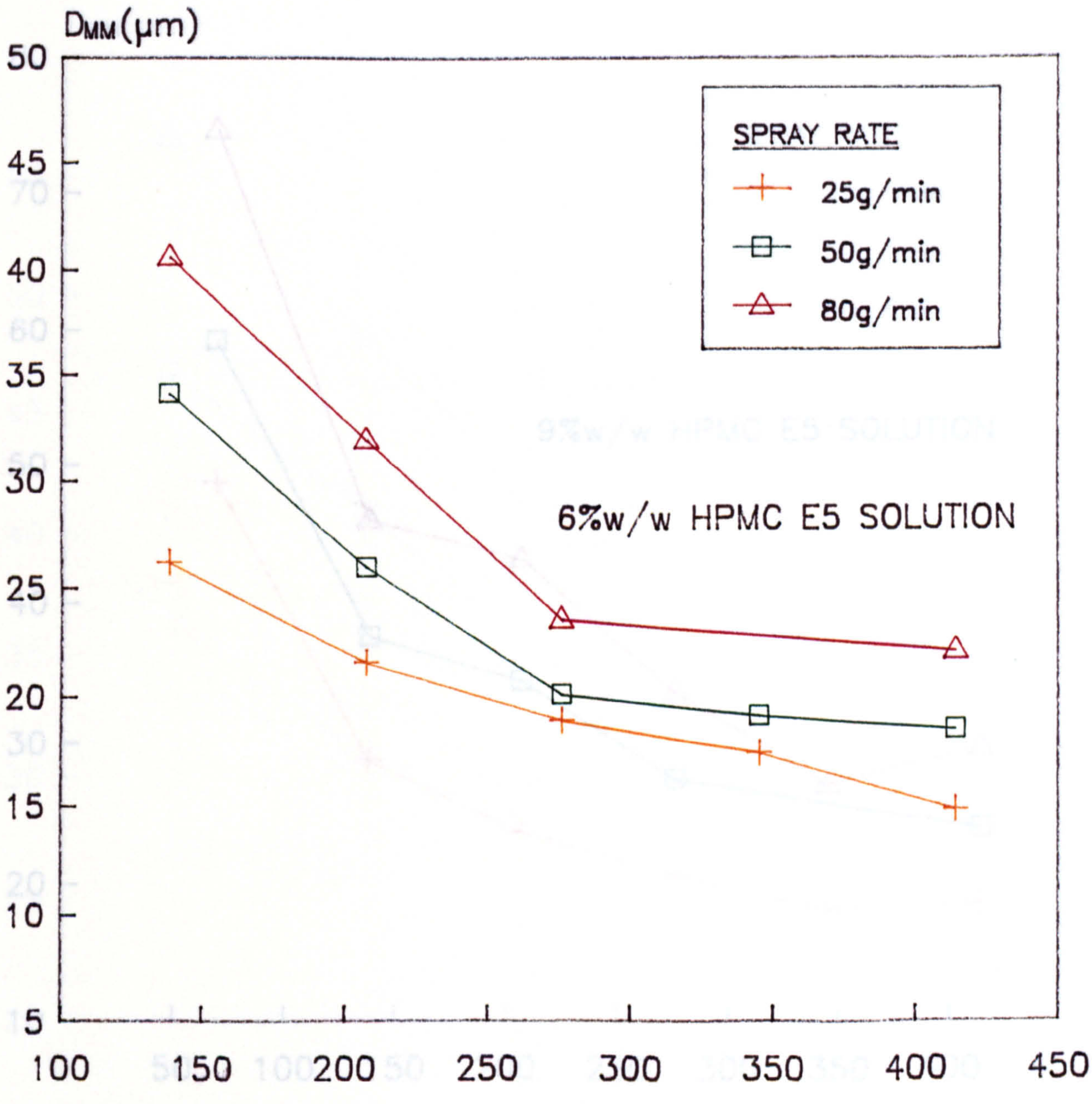

FIGURE 4.8

THE EFFECT OF ATOMISING AIR PRESSURE ON THE MASS MEDIAN DIAMETER OF DROPLETS PRODUCED BY A SCHLICK MODEL 930/7-1 GUN

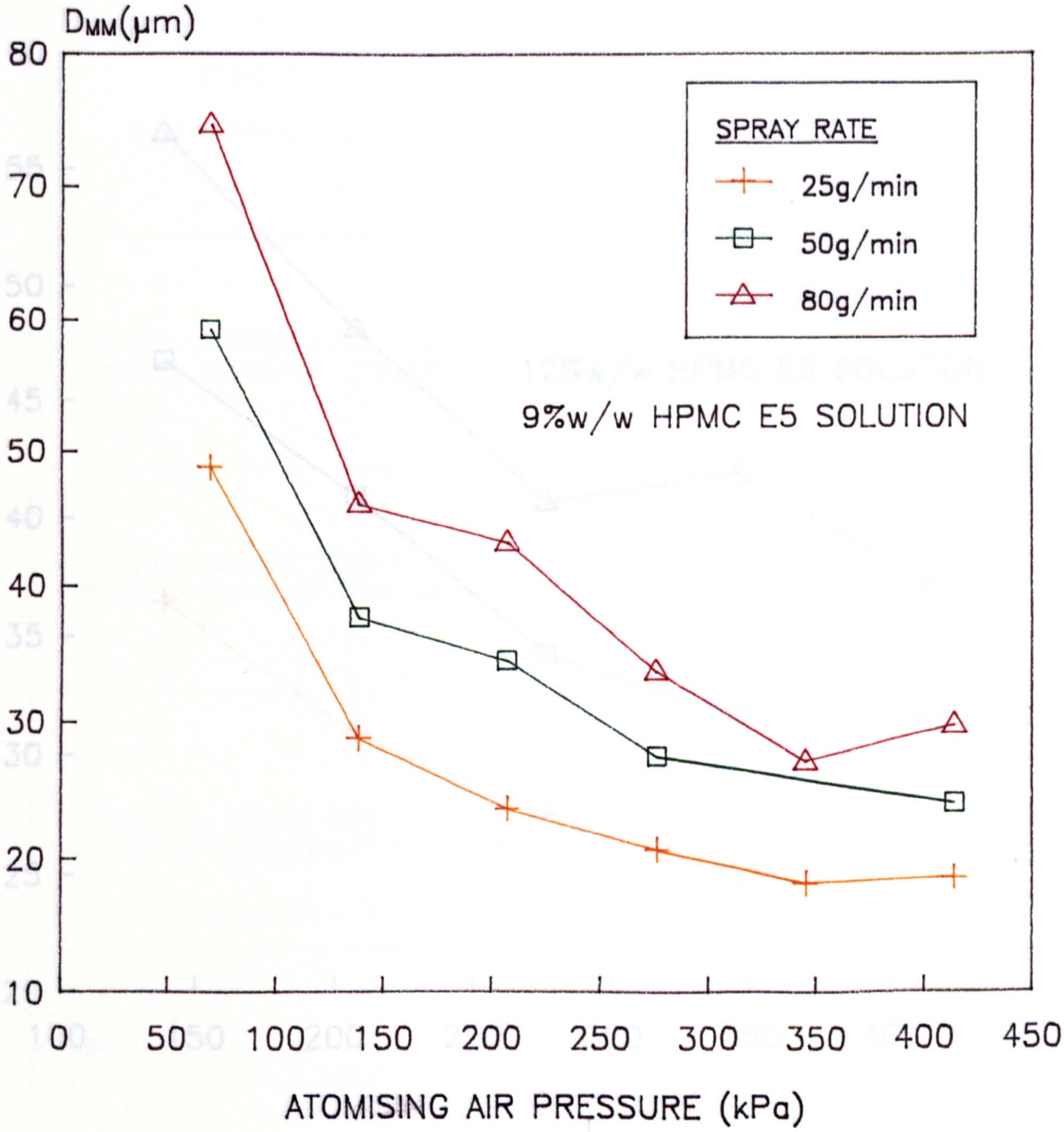

FIGURE 4.9

THE EFFECT OF ATOMISING AIR PRESSURE ON THE MASS MEDIAN DIAMETER OF DROPLETS PRODUCED BY A SCHLICK MODEL 930/7-1 GUN

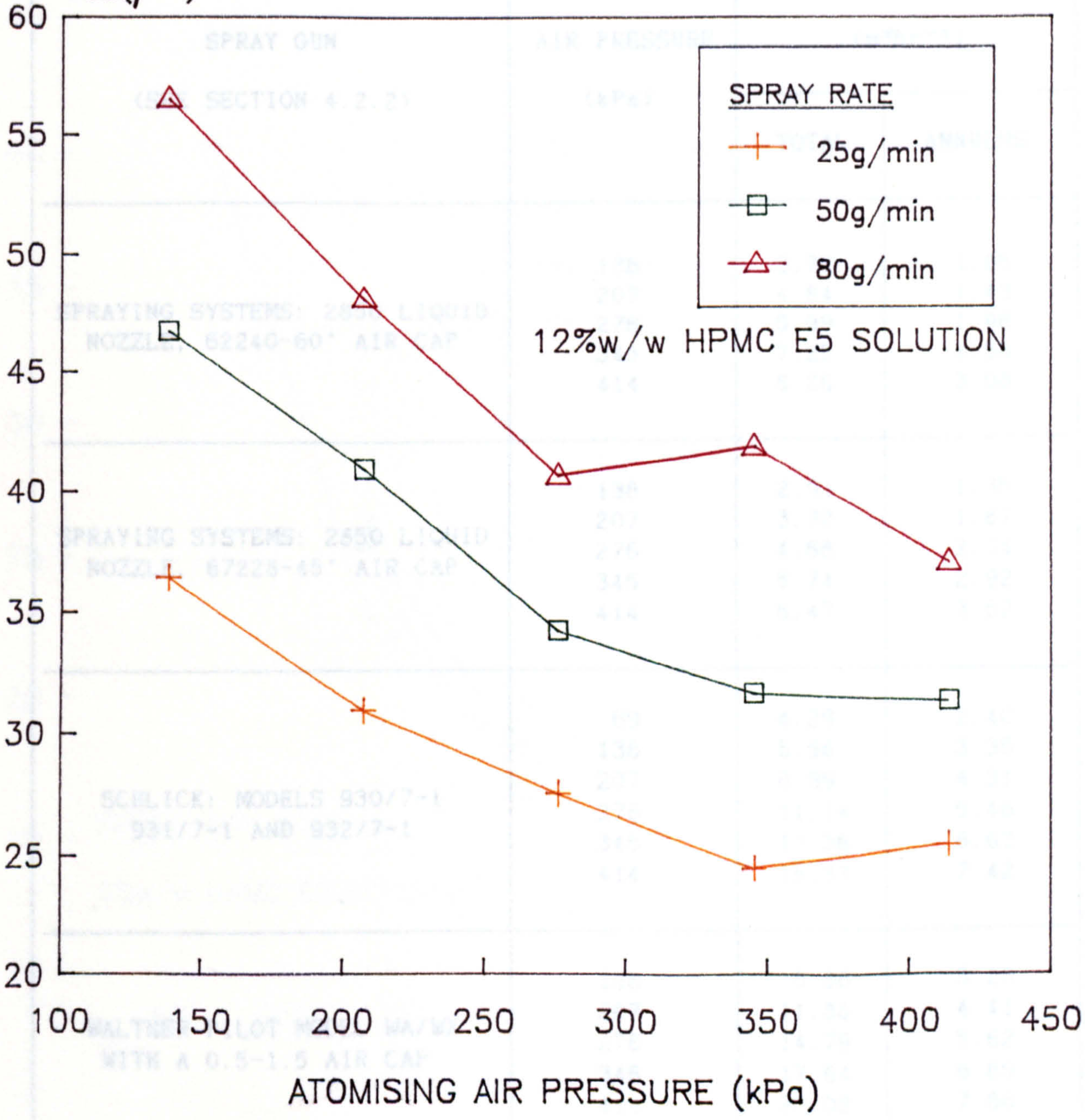

FIGURE 4.10

TABLE 4.5: ATOMISING AIR VOLUME FLOW RATES USED FOR THE PRODUCTION OF STANDARD FLAT SPRAY SHAPES

SPRAY GUN (SEE SECTION 4.2.2)	AIR PRESSURE (kPa)	ATOMISING AIR VOLUME FLOW RATE (m^3hr^{-1})	
		TOTAL	ANNULUS
SPRAYING SYSTEMS: 2850 LIQUID NOZZLE, 62240-60° AIR CAP	138	3.72	1.05
	207	4.84	1.43
	276	5.99	1.98
	345	7.25	2.58
	414	8.26	3.08
SPRAYING SYSTEMS: 2850 LIQUID NOZZLE, 67228-45° AIR CAP	138	2.91	1.35
	207	3.72	1.87
	276	4.68	2.34
	345	5.74	2.92
	414	6.47	3.52
SCHLICK: MODELS 930/7-1 931/7-1 AND 932/7-1	69	4.29	2.40
	138	6.56	3.35
	207	8.99	4.31
	276	11.14	5.46
	345	13.36	6.63
	414	15.33	7.42
WALTHER PILOT MODEL WA/WX WITH A 0.5-1.5 AIR CAP	138	8.86	3.26
	207	11.88	4.41
	276	14.79	5.62
	345	17.64	6.69
	414	20.02	7.88
BINKS BULLOWS MODEL 540 WITH A 63PB AIR CAP	207	12.46	4.76
	276	15.50	6.18
	345	18.61	7.81
	414	21.80	9.35

THE EFFECT OF ATOMISING AIR PRESSURE ON THE SURFACE MEAN DIAMETER OF DROPLETS PRODUCED BY DIFFERENT SPRAY GUNS

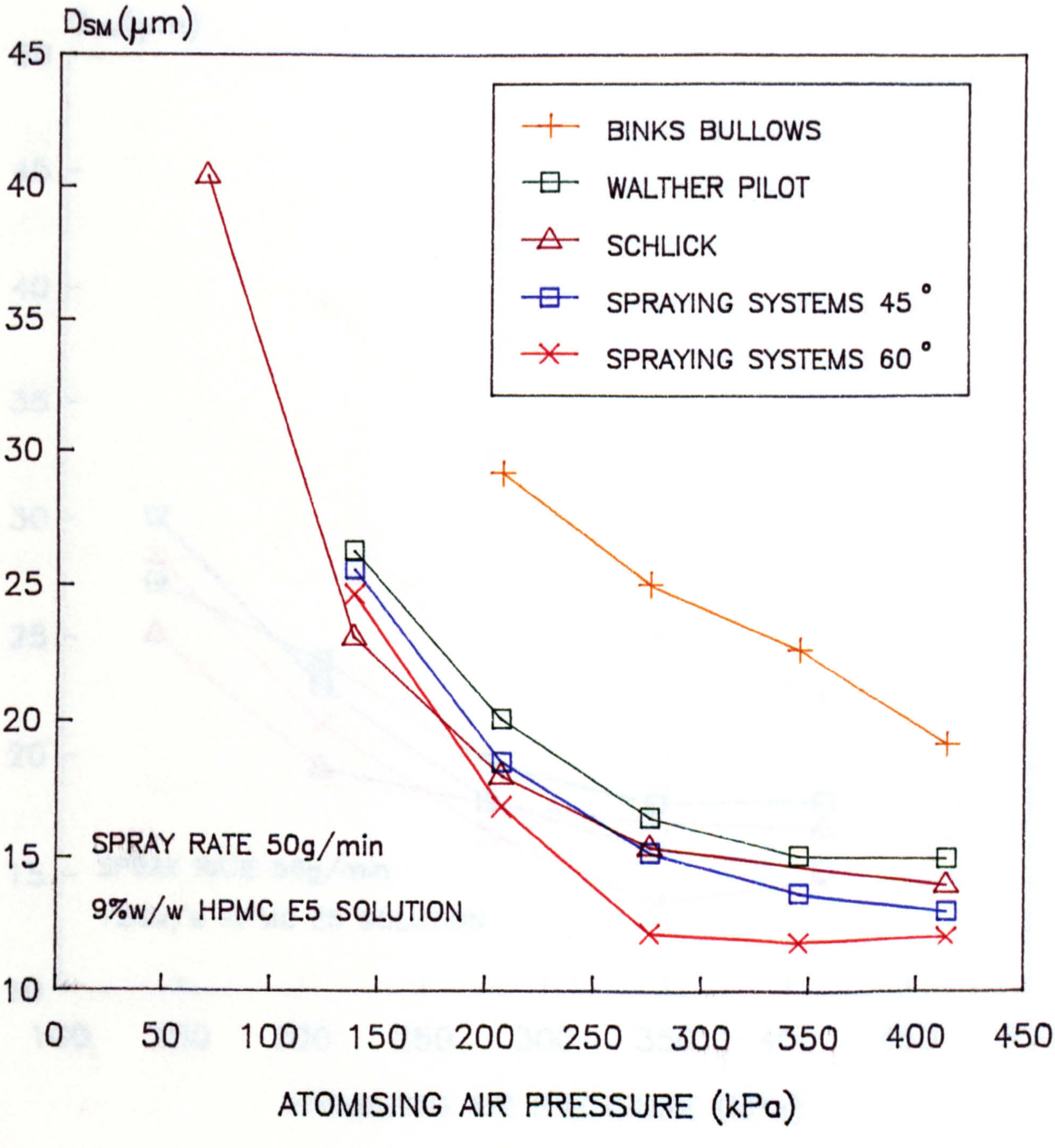

FIGURE 4.11

THE EFFECT OF ATOMISING AIR PRESSURE ON THE SURFACE MEAN DIAMETER OF DROPLETS PRODUCED BY DIFFERENT SPRAY GUNS

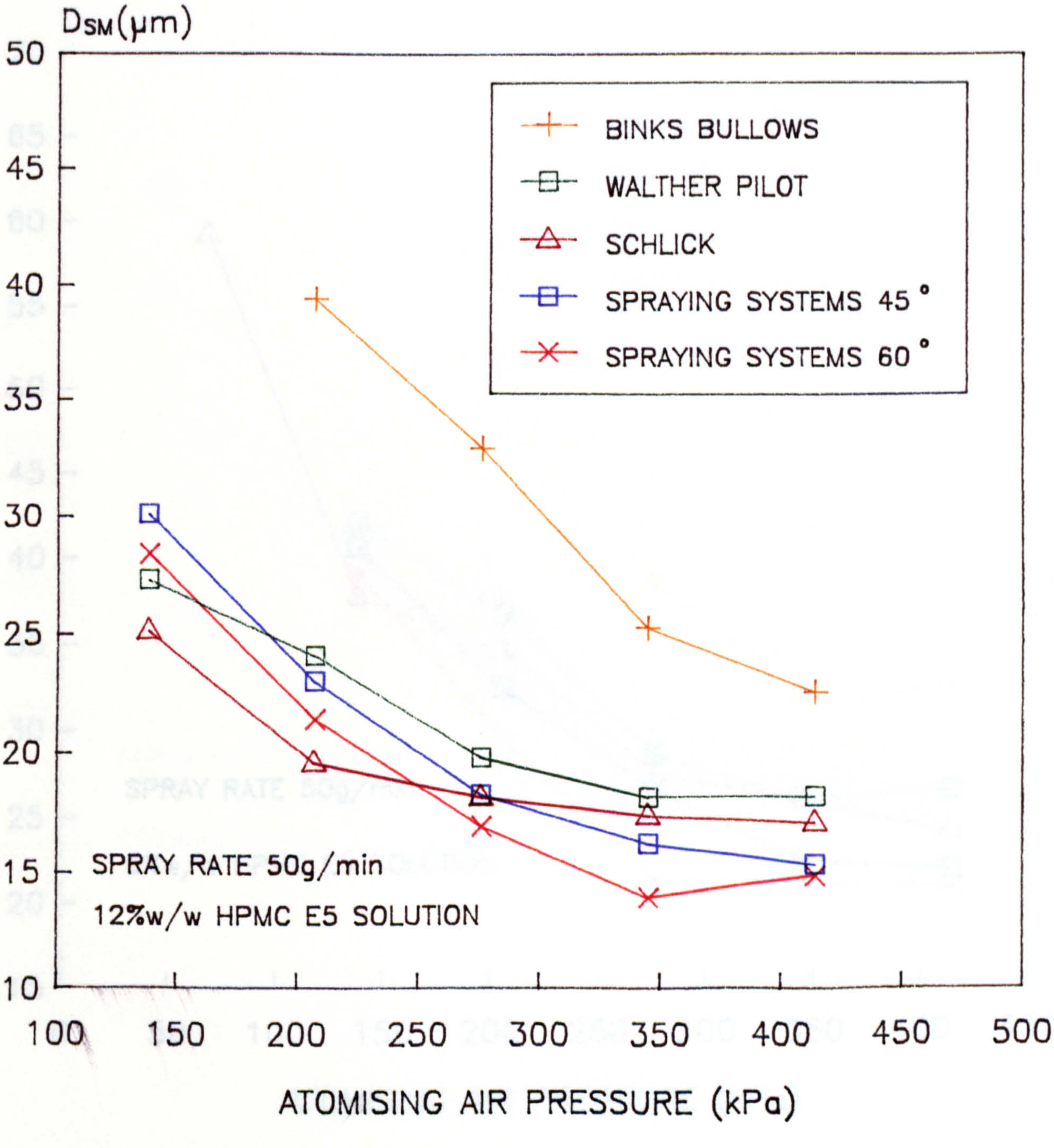

FIGURE 4.12

THE EFFECT OF ATOMISING AIR PRESSURE ON THE MASS MEDIAN DIAMETER OF DROPLETS PRODUCED BY DIFFERENT SPRAY GUNS

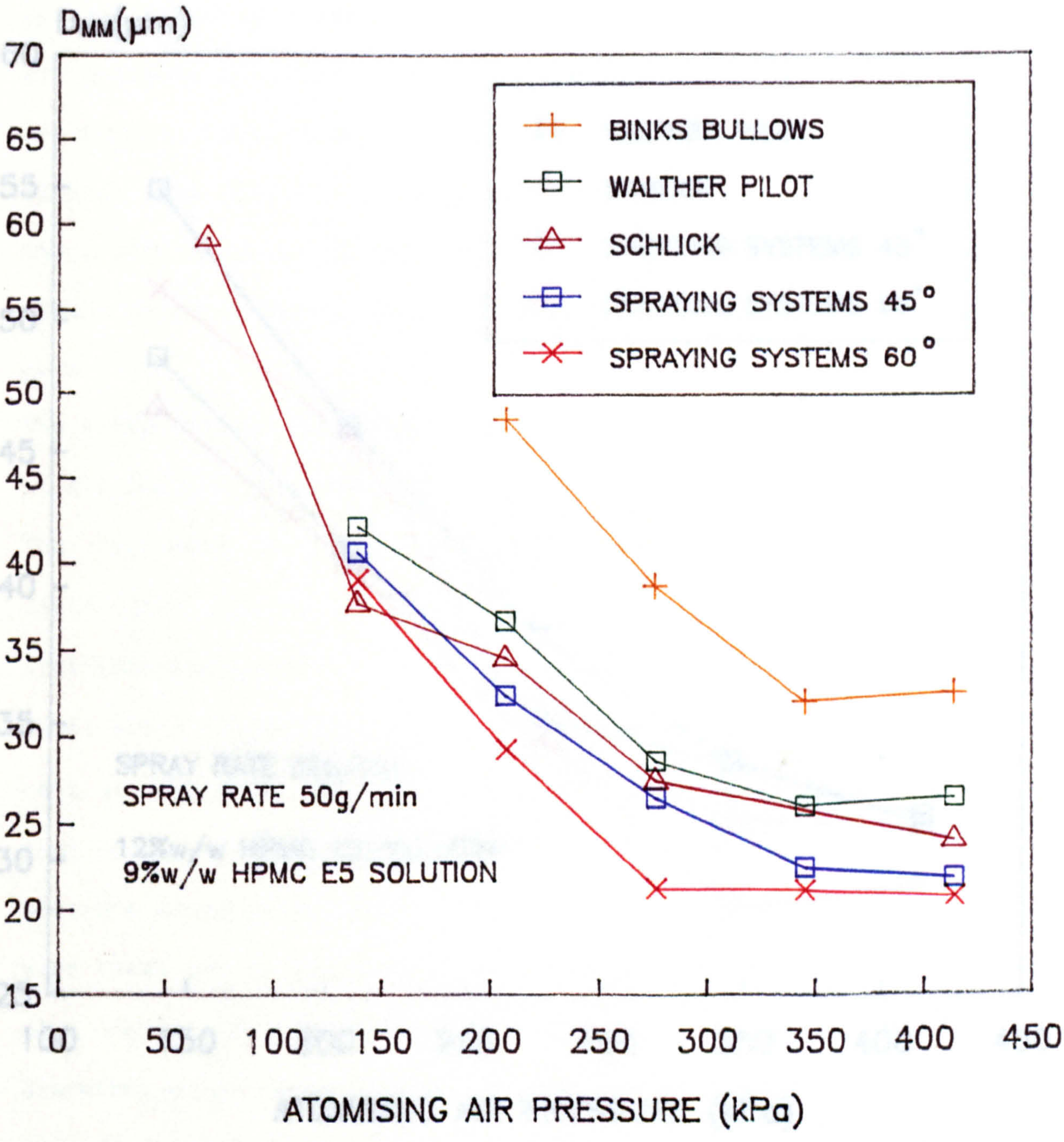

FIGURE 4.13

THE EFFECT OF ATOMISING AIR PRESSURE ON THE MASS MEDIAN DIAMETER OF DROPLETS PRODUCED BY DIFFERENT SPRAY GUNS

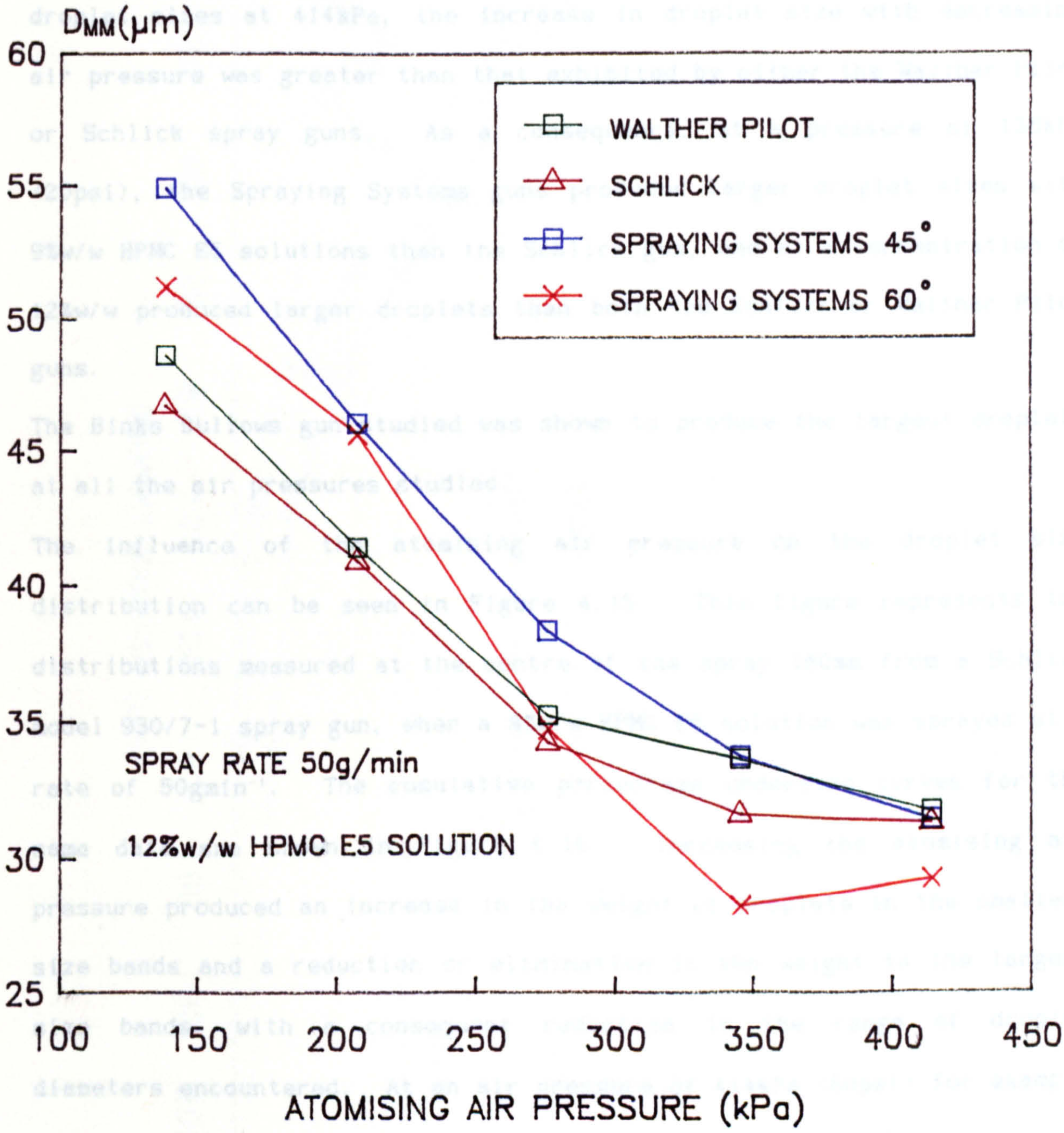

FIGURE 4.14

otherwise identical atomisation conditions. With all the spray guns studied the droplet size reduced with increasing atomising air pressure, although the extent to which this occurred appeared to vary between the guns. Although both Spraying Systems guns produced the smallest average droplet sizes at 414kPa, the increase in droplet size with decreasing air pressure was greater than that exhibited by either the Walther Pilot or Schlick spray guns. As a consequence, at a pressure of 138kPa (20psi), the Spraying Systems guns produced larger droplet sizes with 9%w/w HPMC E5 solutions than the Schlick gun, and at a concentration of 12%w/w produced larger droplets than both the Schlick or Walther Pilot guns.

The Binks Bullows gun studied was shown to produce the largest droplets at all the air pressures studied.

The influence of the atomising air pressure on the droplet size distribution can be seen in Figure 4.15. This figure represents the distributions measured at the centre of the spray 180mm from a Schlick model 930/7-1 spray gun, when a 9%w/w HPMC E5 solution was sprayed at a rate of 50gmin^{-1}. The cumulative percentage undersize curves for the same data are shown in Figure 4.16. Increasing the atomising air pressure produced an increase in the weight of droplets in the smallest size bands and a reduction or elimination in the weight in the largest size bands, with a consequent reduction in the range of droplet diameters encountered. At an air pressure of 414kPa (60psi) for example only 10.1wt% of droplets greater than 64.6µm were encountered, whereas at 69kPa (10psi) there was 55.5wt%. It can also be observed that when using the atomisation conditions stated, there is a change in the frequency distribution pattern. A much more even weight distribution is apparent as the atomising air pressure decreases with an accompanying absence of the large weight frequency of droplets below 10µm.

THE EFFECT OF ATOMISING AIR PRESSURE ON
THE DROPLET SIZE DISTRIBUTIONS PRODUCED
BY A SCHLICK MODEL 930/7-1 SPRAY GUN

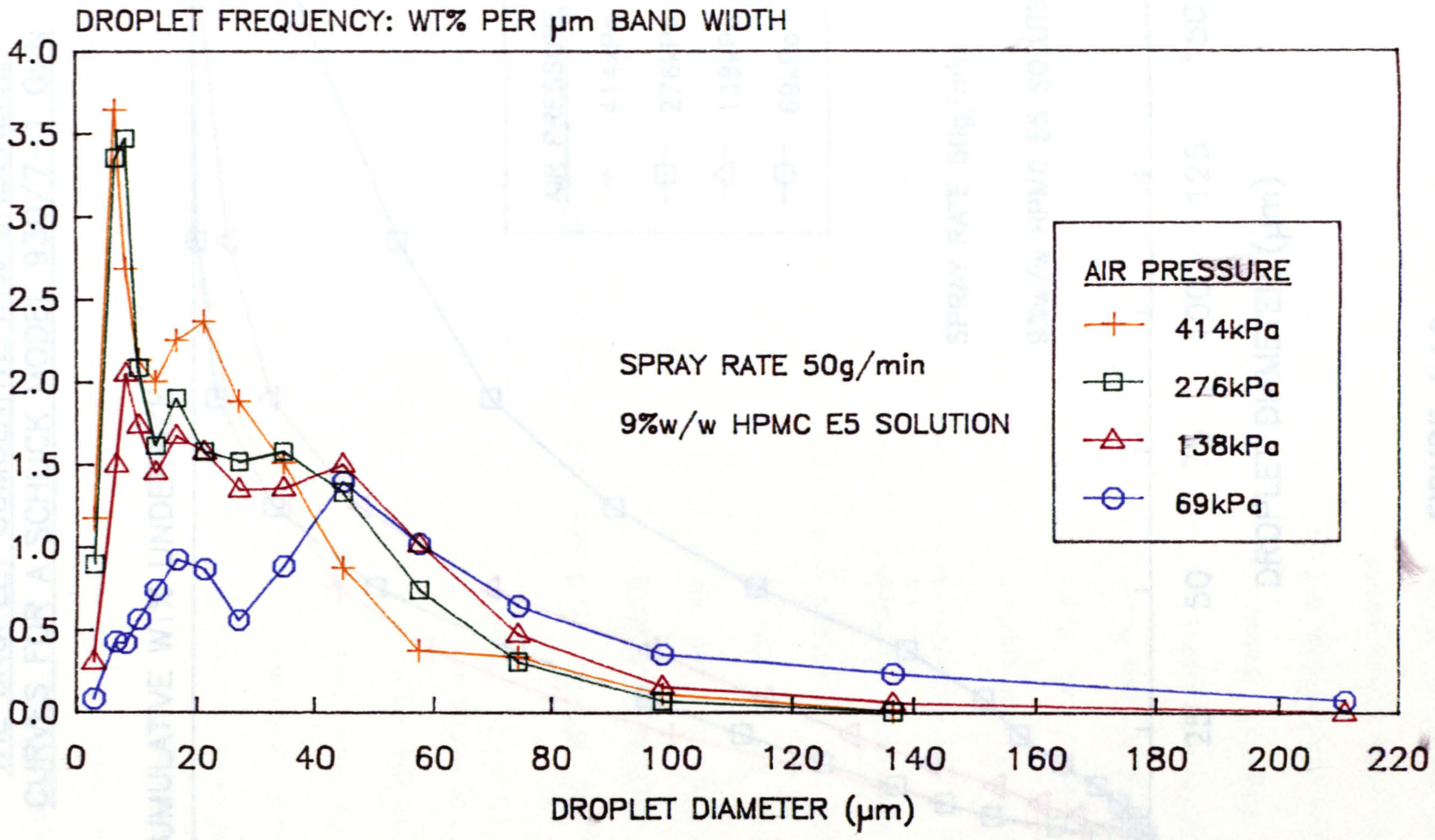

FIGURE 4.15

THE EFFECT OF ATOMISING AIR PRESSURE ON THE DROPLET CUMULATIVE WT% UNDERSIZE CURVES FOR A SCHLICK MODEL 930/7-1 GUN

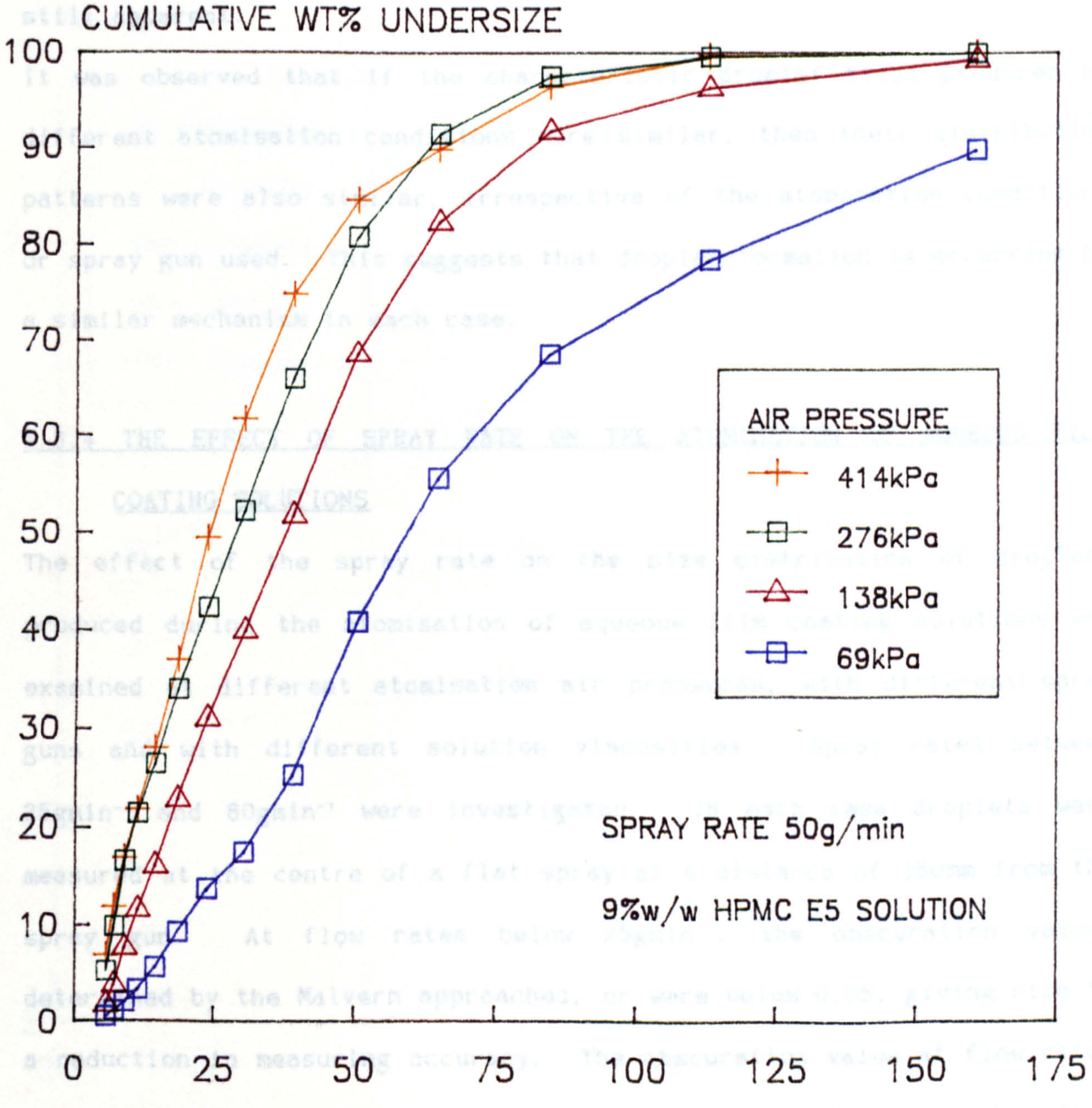

FIGURE 4.16

Although there was a tendency for only small changes in the characteristic mean diameters to occur as the atomising air pressures increased above 276kPa (40psi), the reduction in the droplet size range and increase in the weight frequency in the smallest size bands were still apparent.

It was observed that if the characteristic droplet sizes produced by different atomisation conditions were similar, then their distribution patterns were also similar, irrespective of the atomisation conditions or spray gun used. This suggests that droplet formation is occurring by a similar mechanism in each case.

4.3.4 THE EFFECT OF SPRAY RATE ON THE ATOMISATION OF AQUEOUS FILM COATING SOLUTIONS

The effect of the spray rate on the size distribution of droplets produced during the atomisation of aqueous film coating solutions was examined at different atomisation air pressures, with different spray guns and with different solution viscosities. Spray rates between 25gmin^{-1} and 80gmin^{-1} were investigated. In each case droplets were measured at the centre of a flat spray at a distance of 180mm from the spray gun. At flow rates below 25gmin^{-1}, the obscuration values determined by the Malvern approached, or were below 0.05, giving rise to a reduction in measuring accuracy. The obscuration value at flow rates above 80gmin^{-1} tended to be close to or above 0.5, indicating that multiple scattering effects may be occurring with a subsequent error in droplet size measurement.

The influence of spray rate on the droplet mass median diameter and surface mean diameter produced by the Schlick gun at different atomising air pressures is illustrated for 6%w/w, 9%w/w and 12%w/w HPMC E5 solutions in Figures 4.17 to 4.22. It can be seen that over the range

THE EFFECT OF SPRAY RATE ON THE SURFACE MEAN DIAMETER OF DROPLETS PRODUCED BY A SCHLICK MODEL 930/7-1 SPRAY GUN

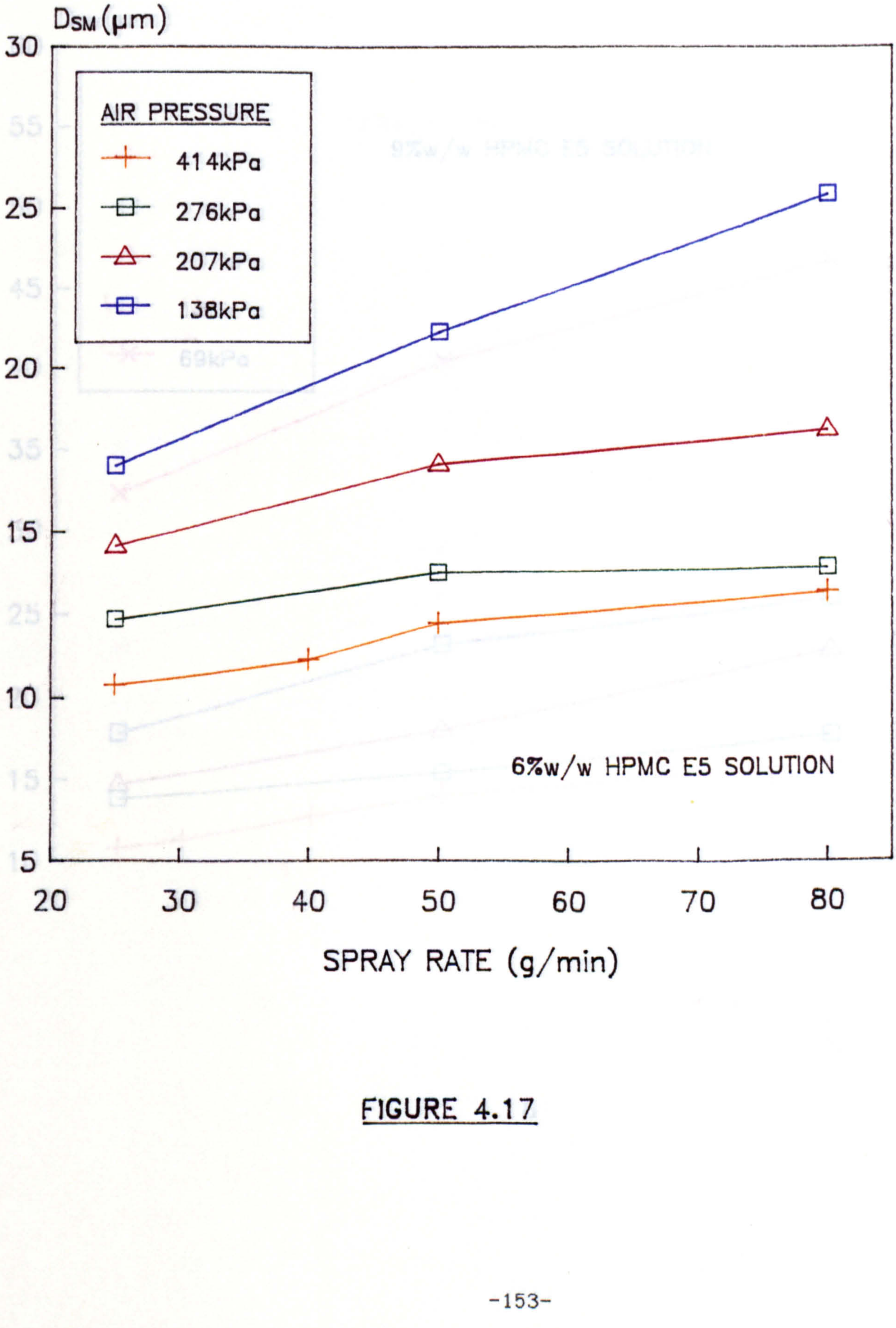

FIGURE 4.17

THE EFFECT OF SPRAY RATE ON THE SURFACE MEAN DIAMETER OF DROPLETS PRODUCED BY A SCHLICK MODEL 930/7-1 SPRAY GUN

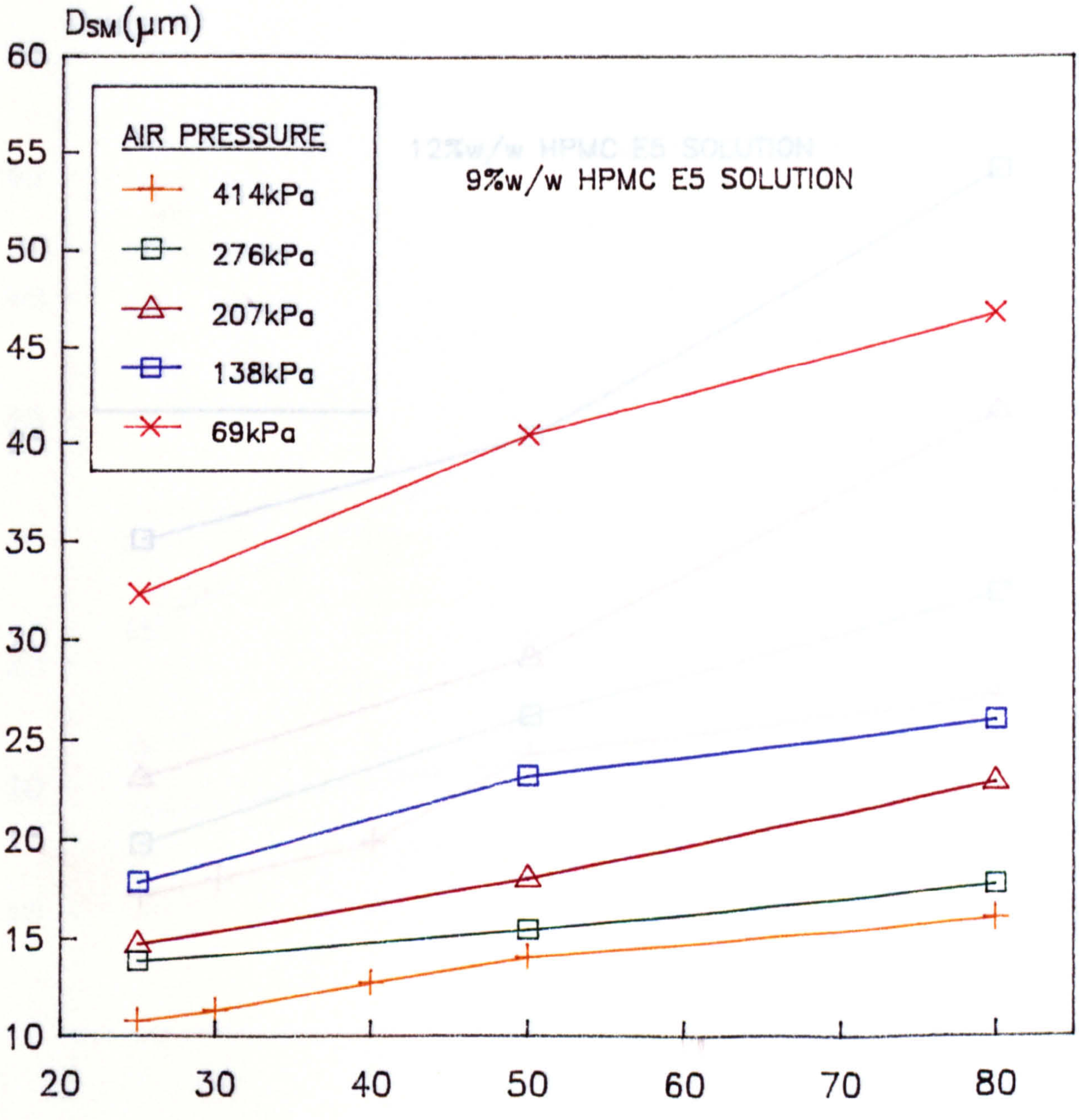

FIGURE 4.18

THE EFFECT OF SPRAY RATE ON THE SURFACE MEAN DIAMETER OF DROPLETS PRODUCED BY A SCHLICK MODEL 930/7-1 SPRAY GUN

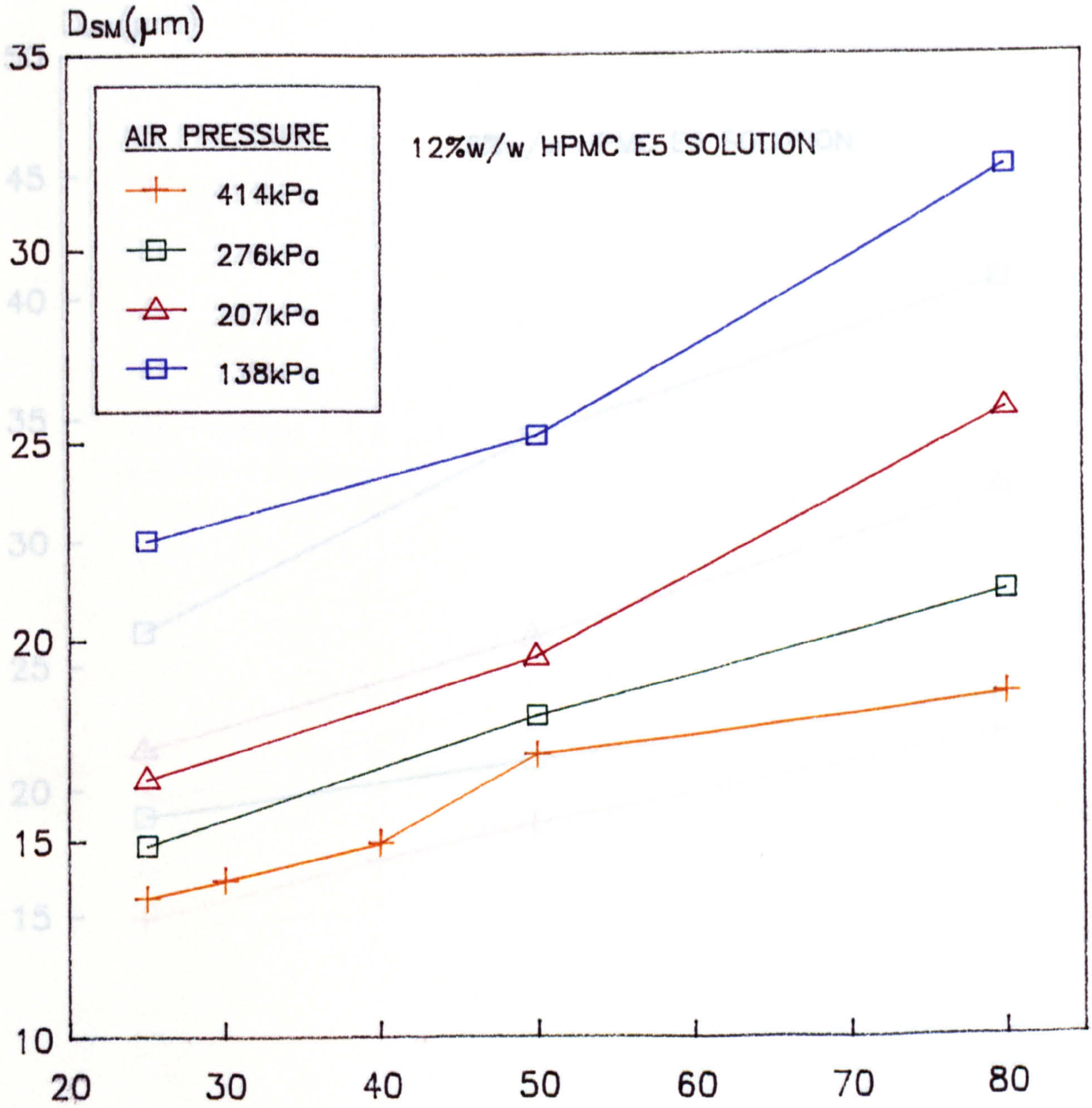

FIGURE 4.19

THE EFFECT OF SPRAY RATE ON THE MASS MEDIAN DIAMETER OF DROPLETS PRODUCED BY A SCHLICK MODEL 930/7-1 SPRAY GUN

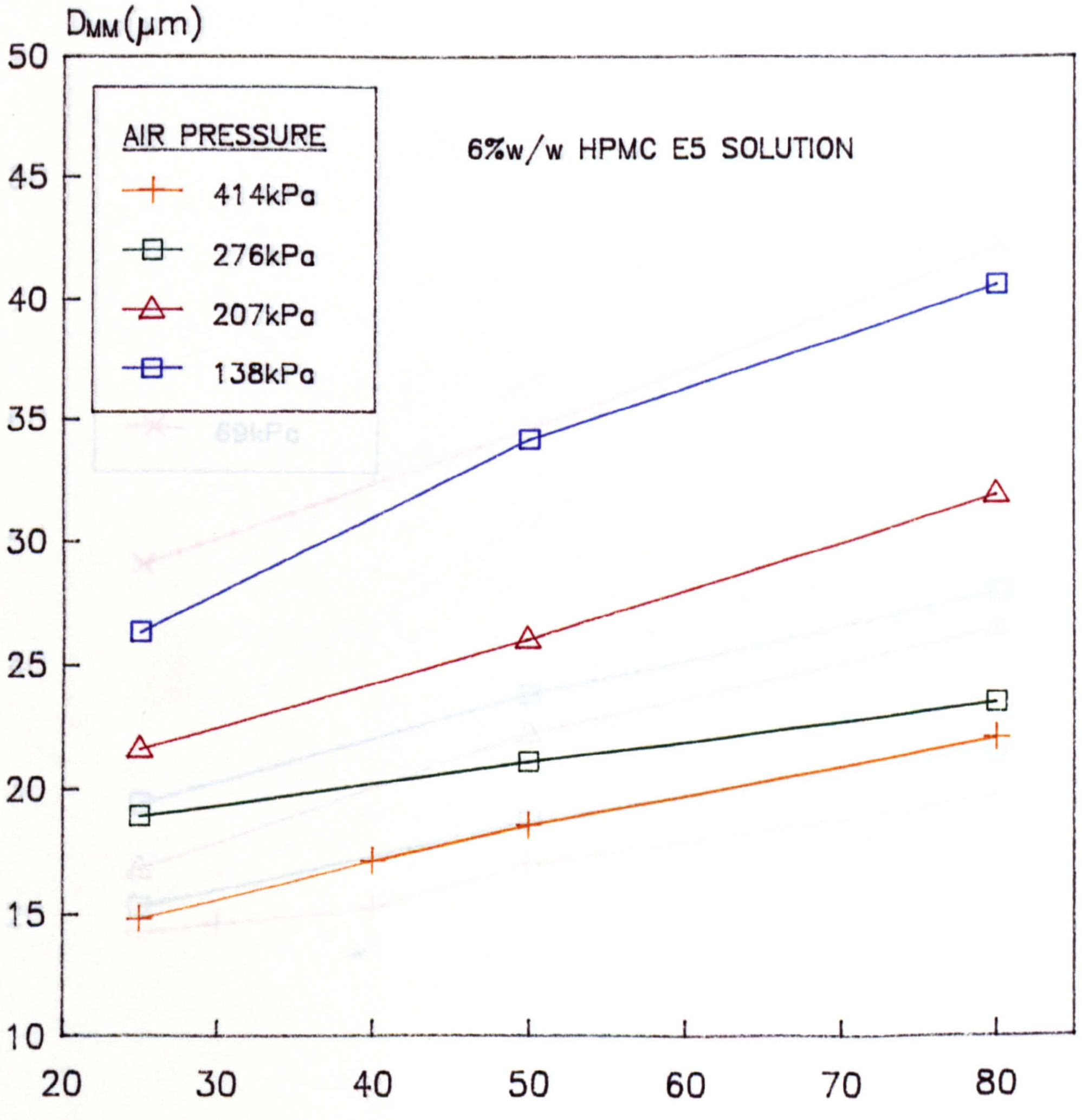

FIGURE 4.20

THE EFFECT OF SPRAY RATE ON THE MASS MEDIAN DIAMETER OF DROPLETS PRODUCED BY A SCHLICK MODEL 930/7-1 SPRAY GUN

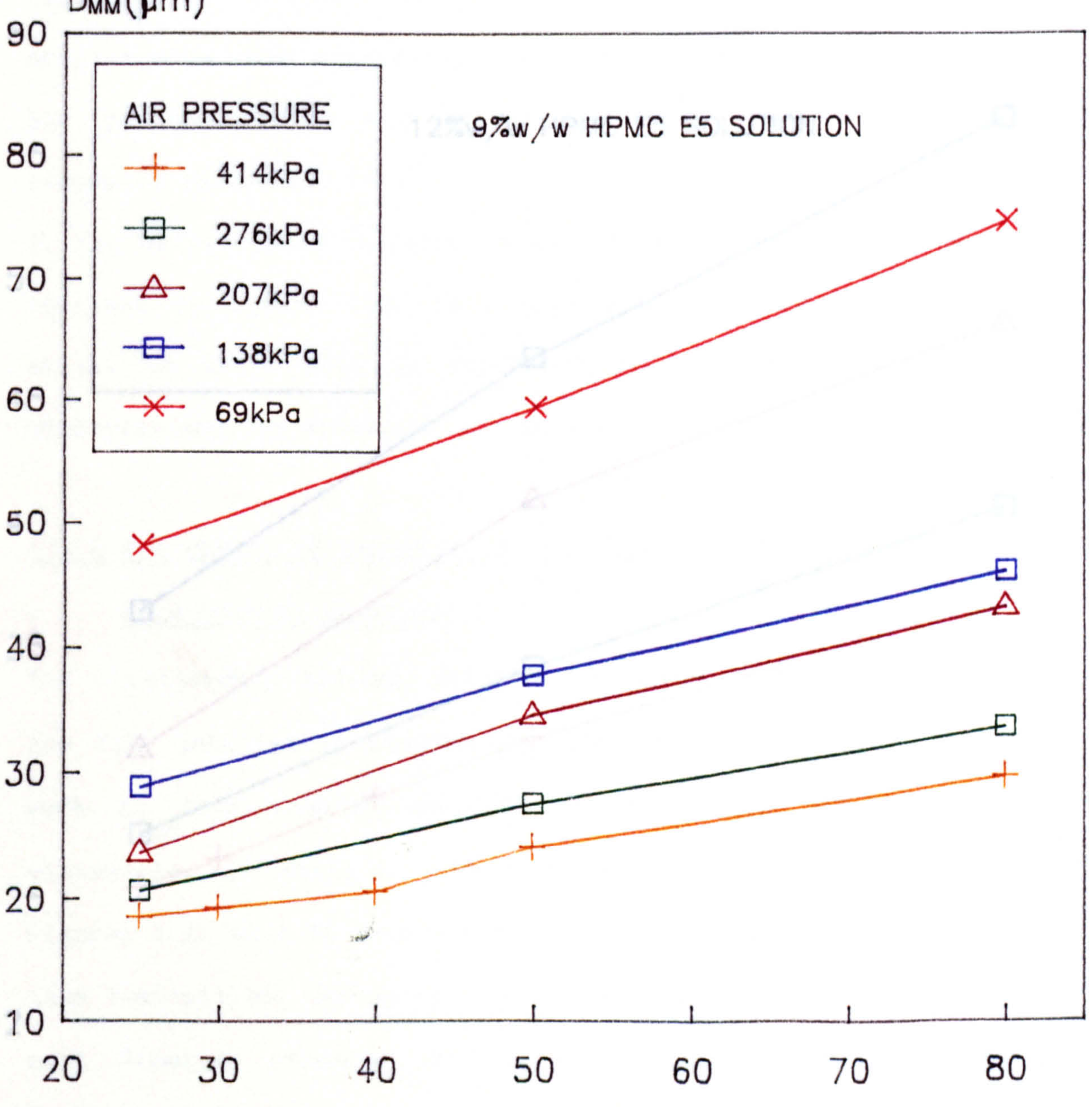

FIGURE 4.21

THE EFFECT OF SPRAY RATE ON THE MASS MEDIAN DIAMETER OF DROPLETS PRODUCED BY A SCHLICK MODEL 930/7-1 SPRAY GUN

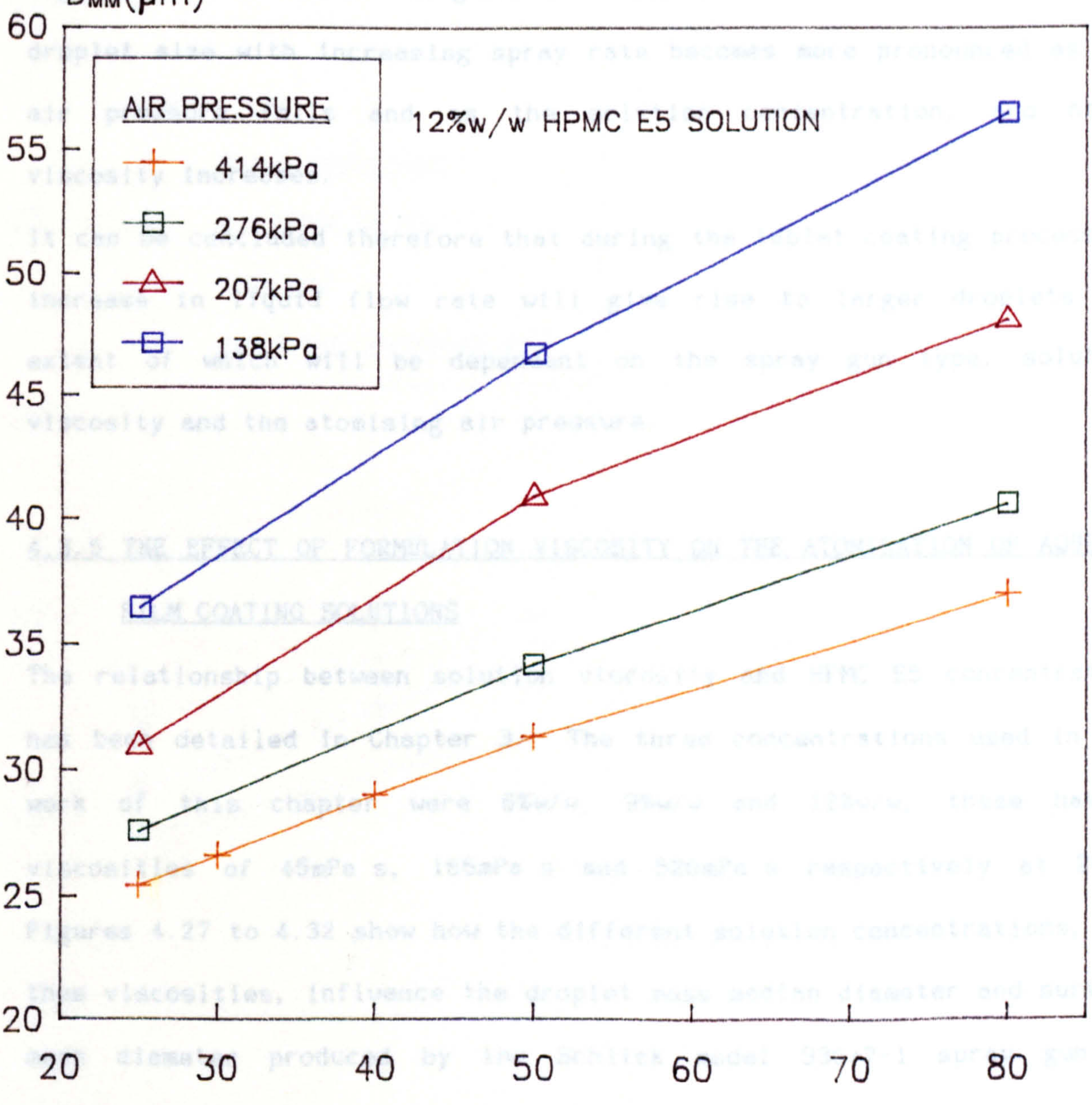

FIGURE 4.22

of air pressures studied and at each HPMC E5 concentration, an increase in flow rate produced an increase in both the droplet mass median diameter and surface mean diameter. This effect is further illustrated for the Walther Pilot, Binks Bullows and Spraying Systems guns in Figures 4.23 to 4.26. In general it can be seen that the increase in droplet size with increasing spray rate becomes more pronounced as the air pressure falls and as the solution concentration, and hence viscosity increases.

It can be concluded therefore that during the tablet coating process an increase in liquid flow rate will give rise to larger droplets the extent of which will be dependent on the spray gun type, solution viscosity and the atomising air pressure.

4.3.5 THE EFFECT OF FORMULATION VISCOSITY ON THE ATOMISATION OF AQUEOUS FILM COATING SOLUTIONS

The relationship between solution viscosity and HPMC E5 concentration has been detailed in Chapter 3. The three concentrations used in the work of this chapter were 6%w/w, 9%w/w and 12%w/w, these having viscosities of 45mPa s, 166mPa s and 520mPa s respectively at 20°C. Figures 4.27 to 4.32 show how the different solution concentrations, and thus viscosities, influence the droplet mass median diameter and surface mean diameter produced by the Schlick model 930/7-1 spray gun at different atomising air pressures and spray rates. The effect of solution viscosity on the droplet sizes produced by the other spray guns when using a variety of atomisation conditions is shown in Table 4.6. In all cases where the influence of viscosity was investigated, measurements were taken 180mm from the spray gun from the centre of a flat spray.

It can be seen that variations in the solution concentration, and thus

THE EFFECT OF SPRAY RATE ON THE SURFACE MEAN DIAMETER OF DROPLETS PRODUCED BY DIFFERENT SPRAY GUNS

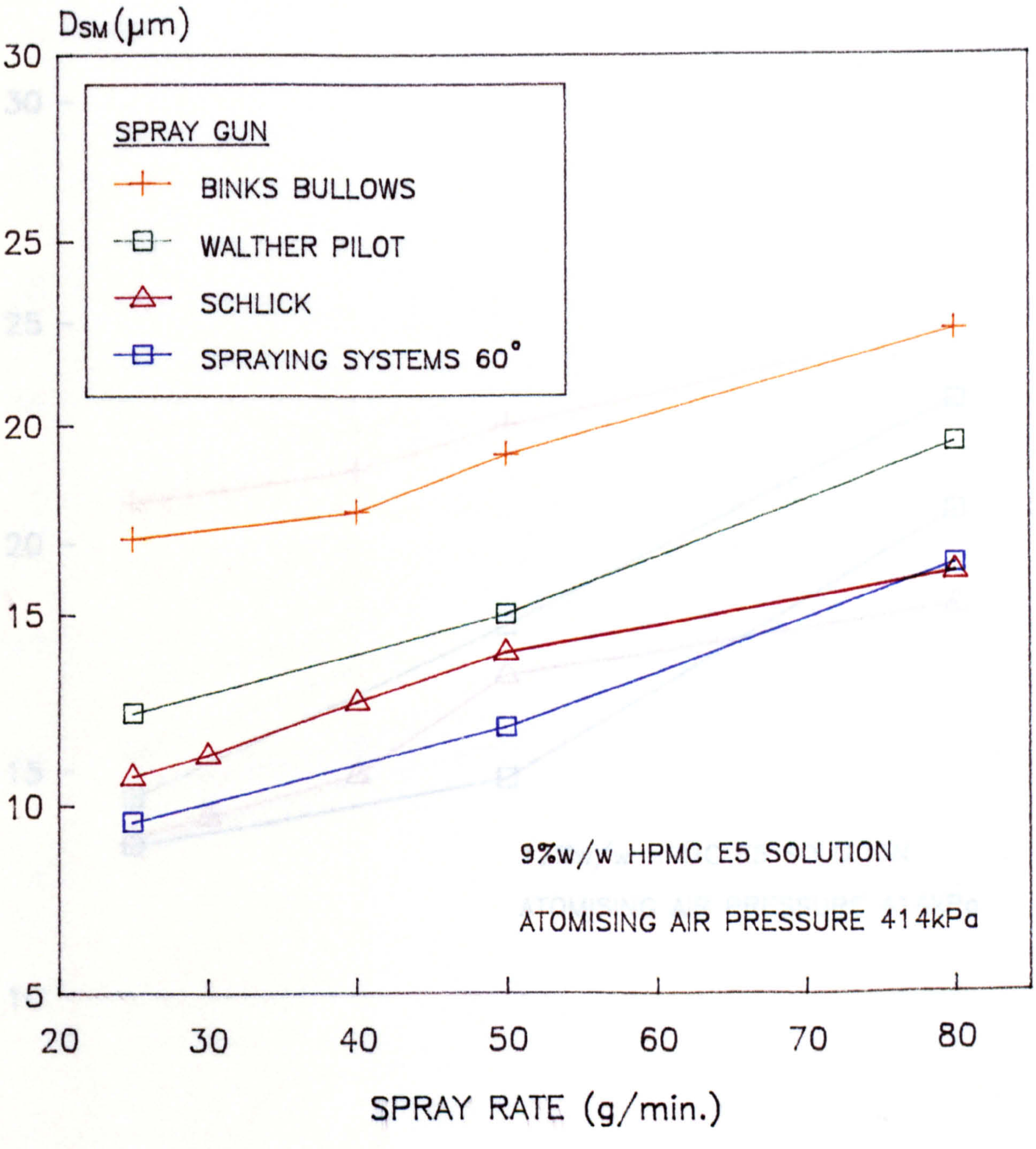

FIGURE 4.23

THE EFFECT OF SPRAY RATE ON THE SURFACE MEAN DIAMETER OF DROPLETS PRODUCED BY DIFFERENT SPRAY GUNS

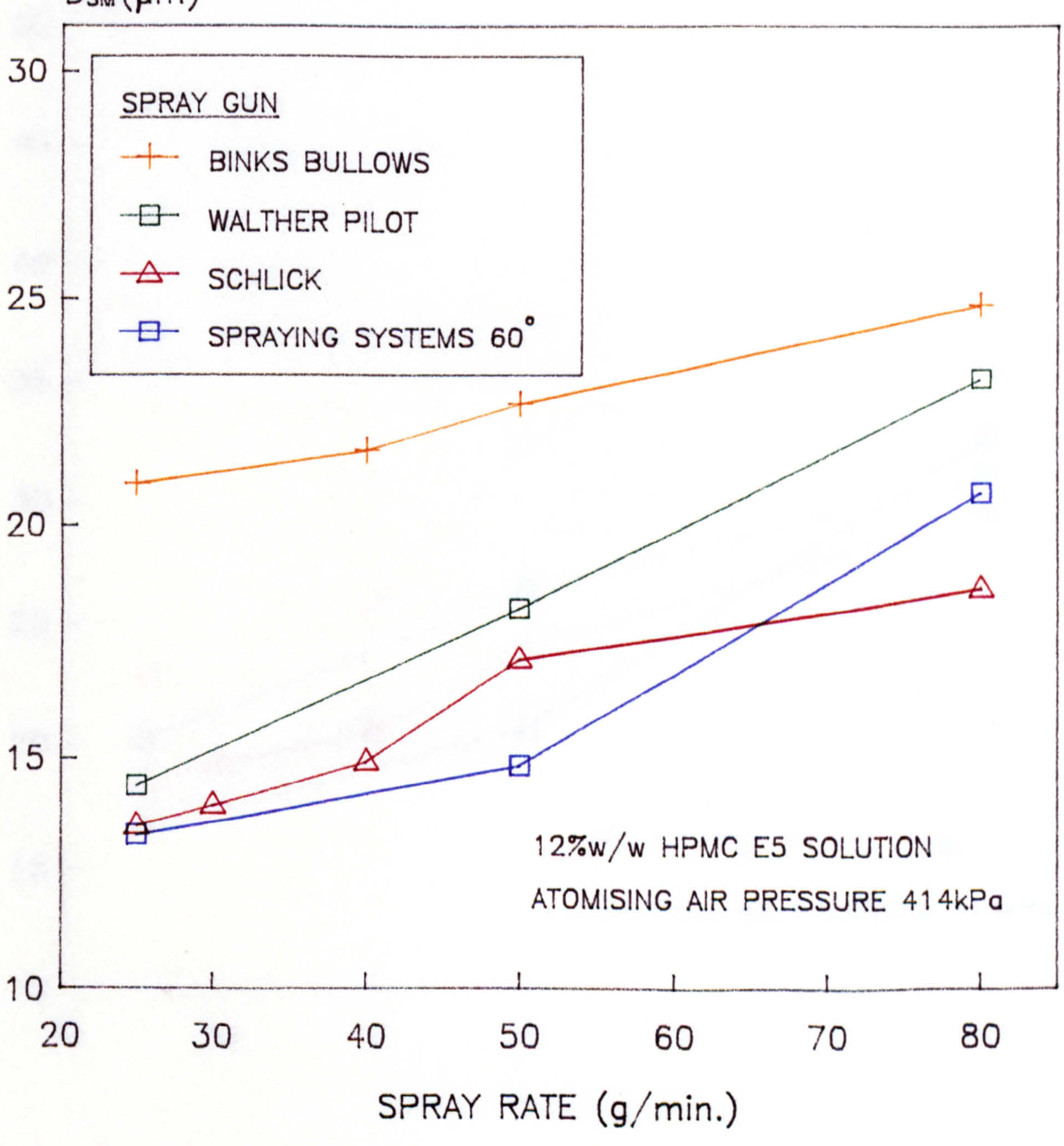

FIGURE 4.24

THE EFFECT OF SPRAY RATE ON THE MASS MEDIAN DIAMETER OF DROPLETS PRODUCED BY DIFFERENT SPRAY GUNS

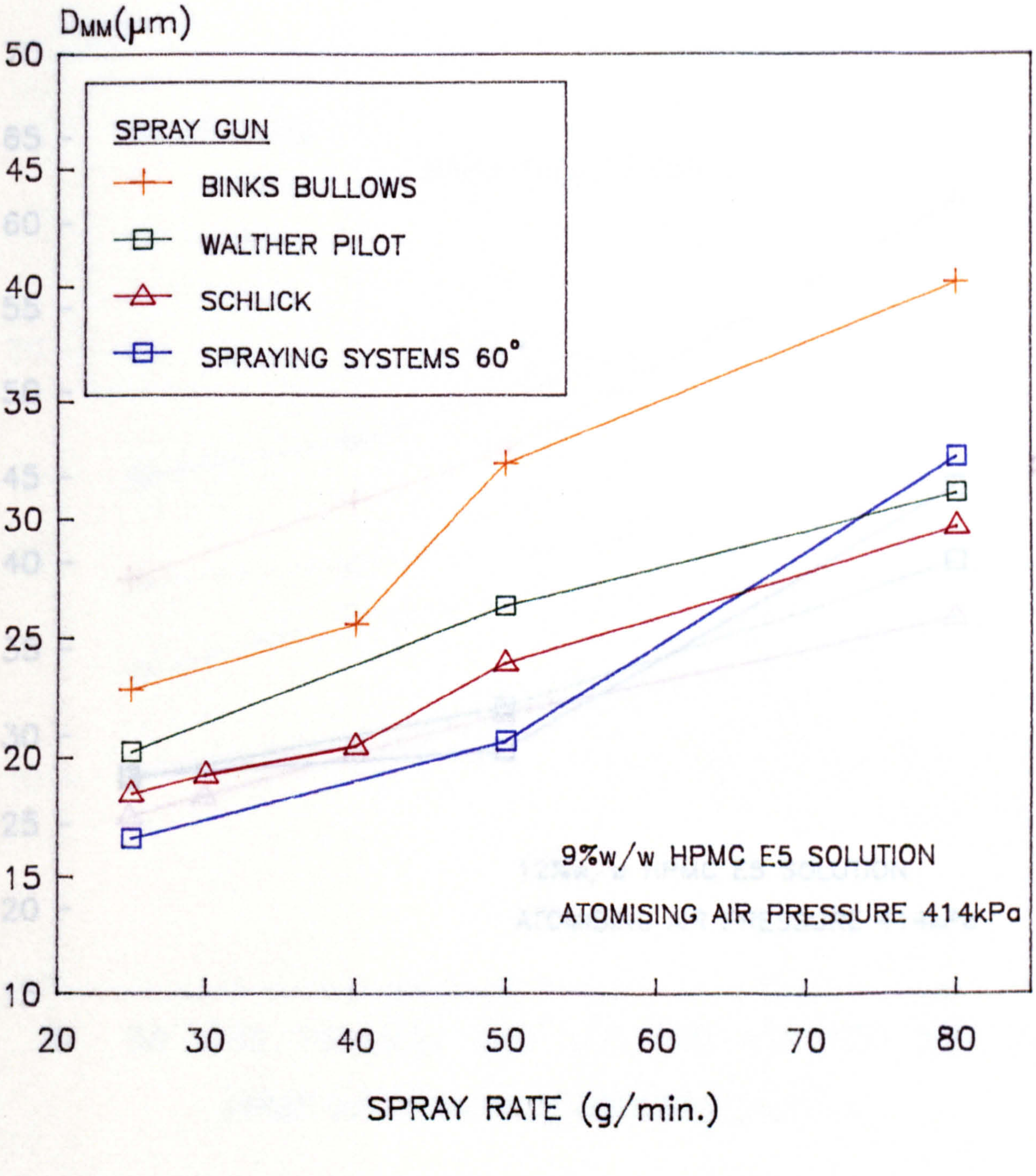

FIGURE 4.25

THE EFFECT OF SPRAY RATE ON THE MASS MEDIAN DIAMETER OF DROPLETS PRODUCED BY DIFFERENT SPRAY GUNS

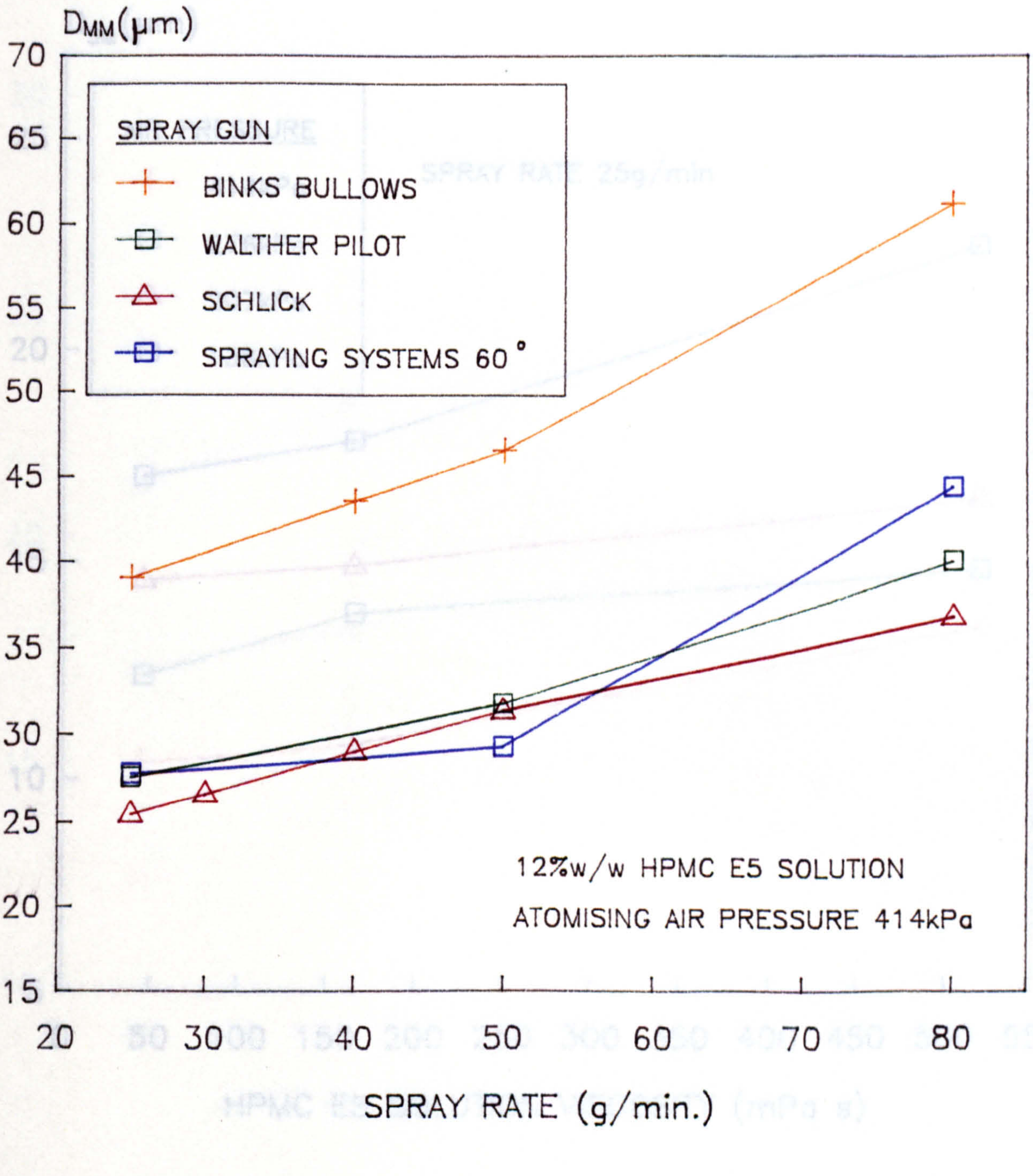

FIGURE 4.26

THE EFFECT OF HPMC E5 SOLUTION VISCOSITY ON THE SURFACE MEAN DIAMETER OF DROPLETS FROM A SCHLICK MODEL 930/7-1 SPRAY GUN

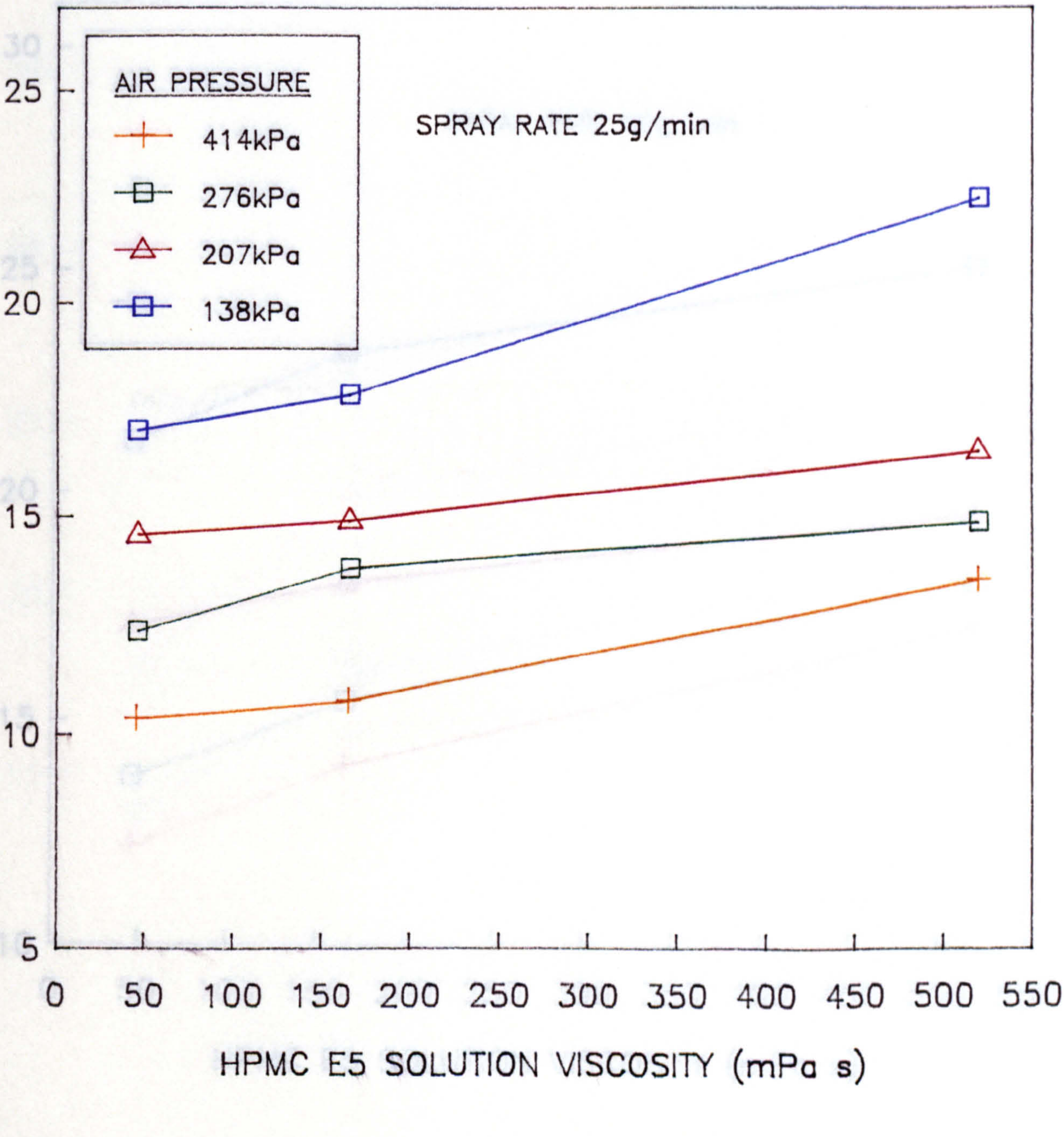

FIGURE 4.27

THE EFFECT OF HPMC E5 SOLUTION VISCOSITY
ON THE SURFACE MEAN DIAMETER OF DROPLETS
FROM A SCHLICK MODEL 930/7-1 SPRAY GUN

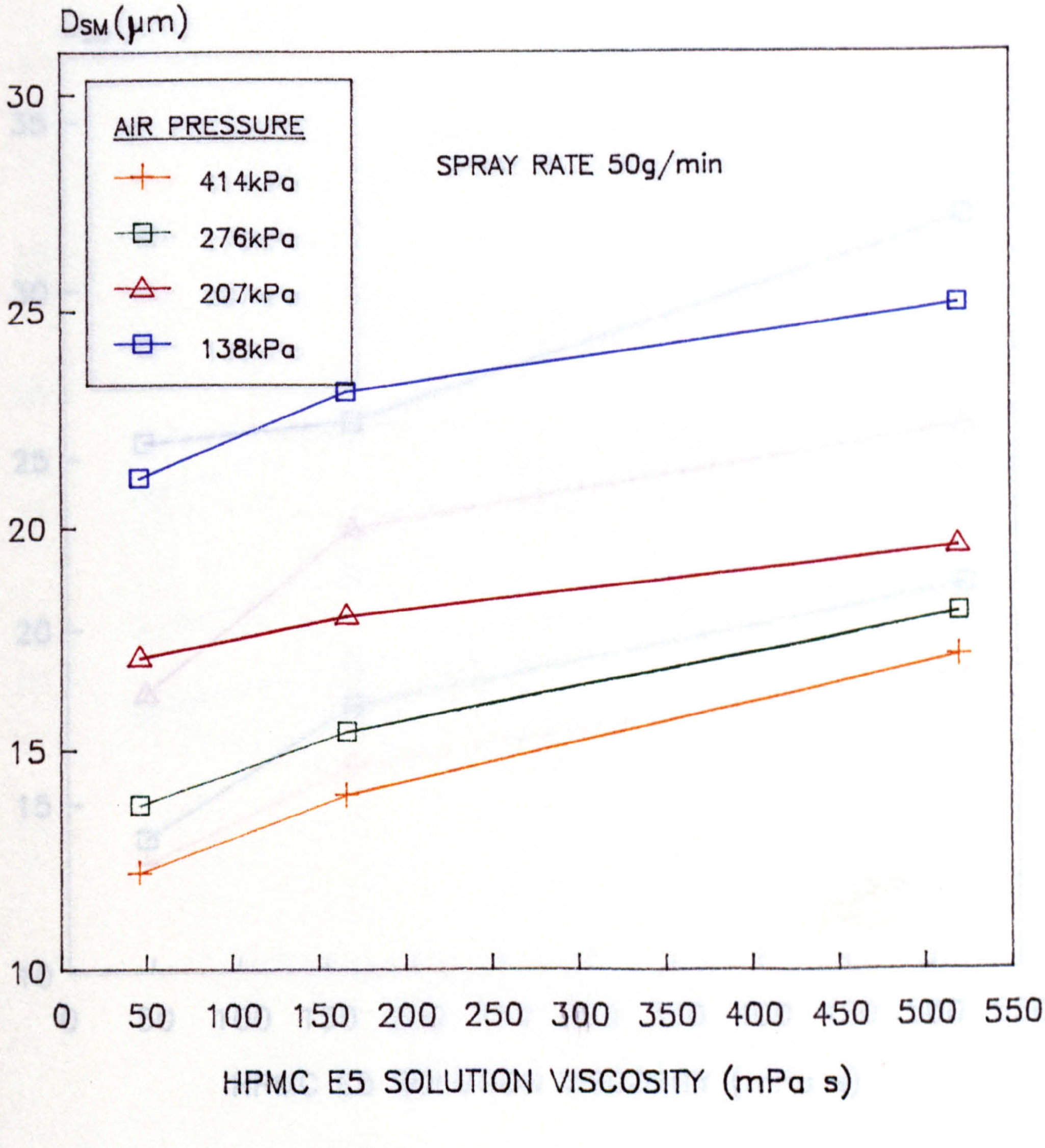

FIGURE 4.28

THE EFFECT OF HPMC E5 SOLUTION VISCOSITY ON THE SURFACE MEAN DIAMETER OF DROPLETS FROM A SCHLICK MODEL 930/7-1 SPRAY GUN

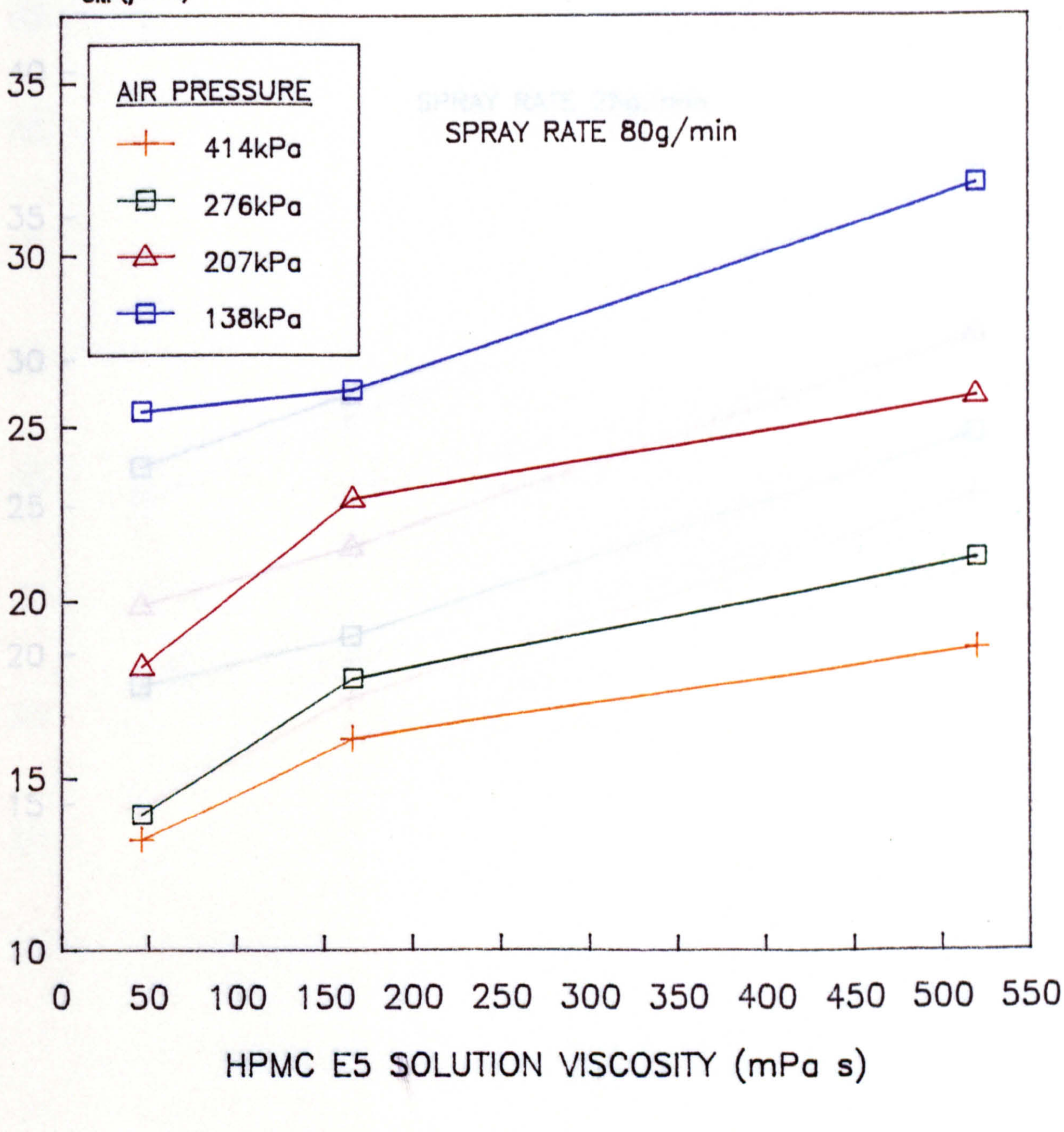

FIGURE 4.29

THE EFFECT OF HPMC E5 SOLUTION VISCOSITY ON THE MASS MEDIAN DIAMETER OF DROPLETS FROM A SCHLICK MODEL 930/7-1 SPRAY GUN

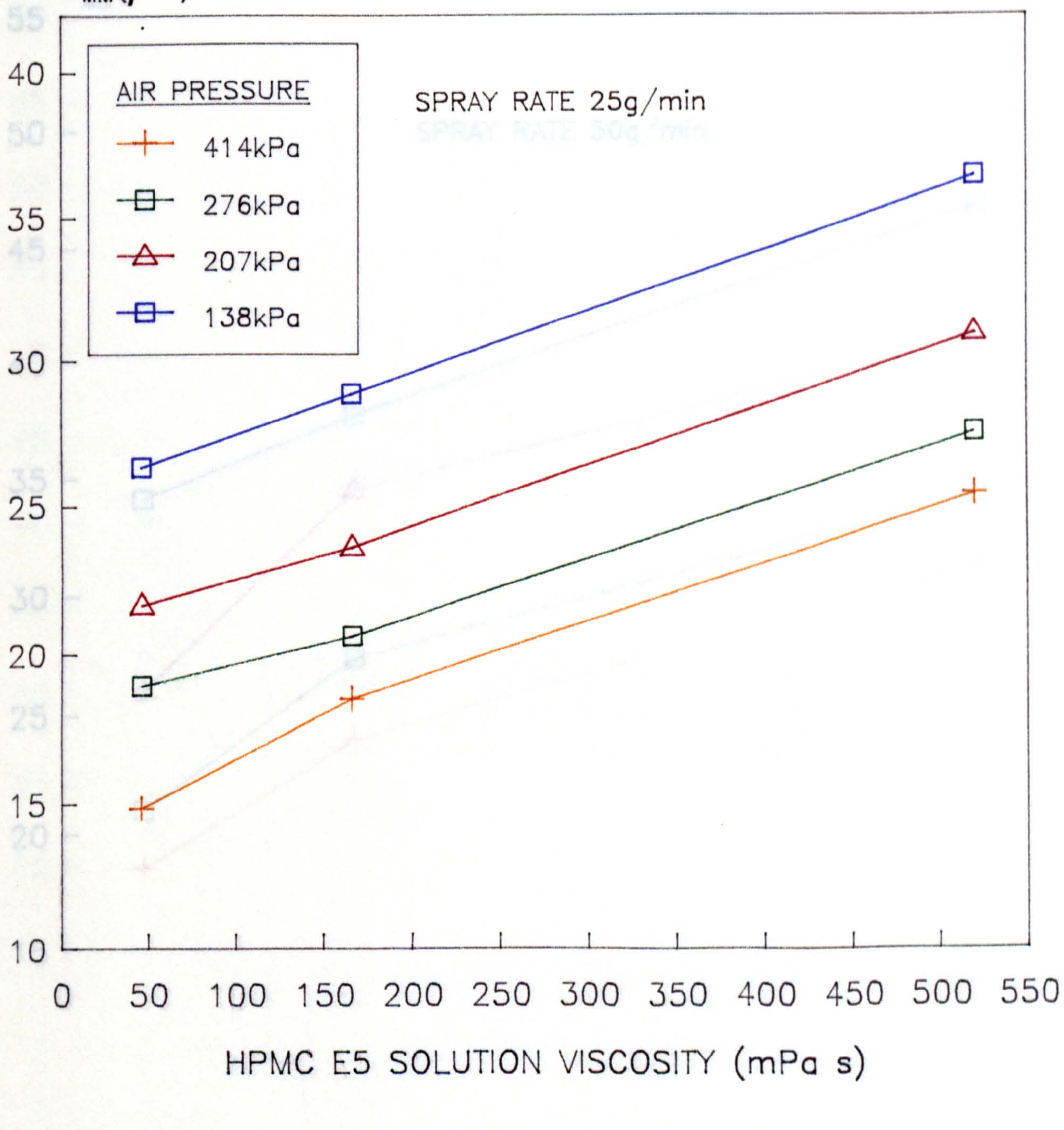

FIGURE 4.30

THE EFFECT OF HPMC E5 SOLUTION VISCOSITY ON THE MASS MEDIAN DIAMETER OF DROPLETS FROM A SCHLICK MODEL 930/7-1 SPRAY GUN

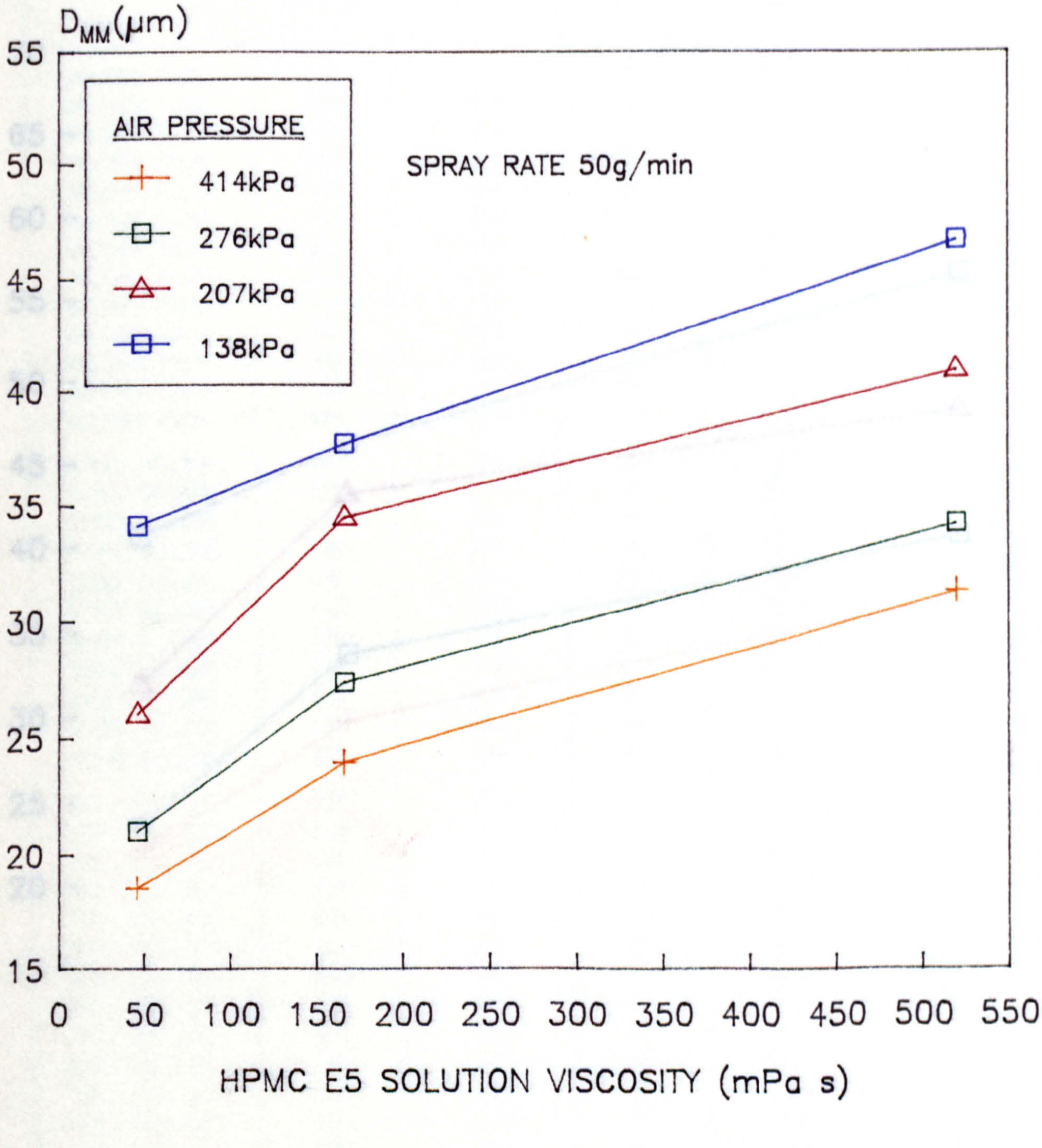

FIGURE 4.31

THE EFFECT OF HPMC E5 SOLUTION VISCOSITY ON THE MASS MEDIAN DIAMETER OF DROPLETS FROM A SCHLICK MODEL 930/7-1 SPRAY GUN

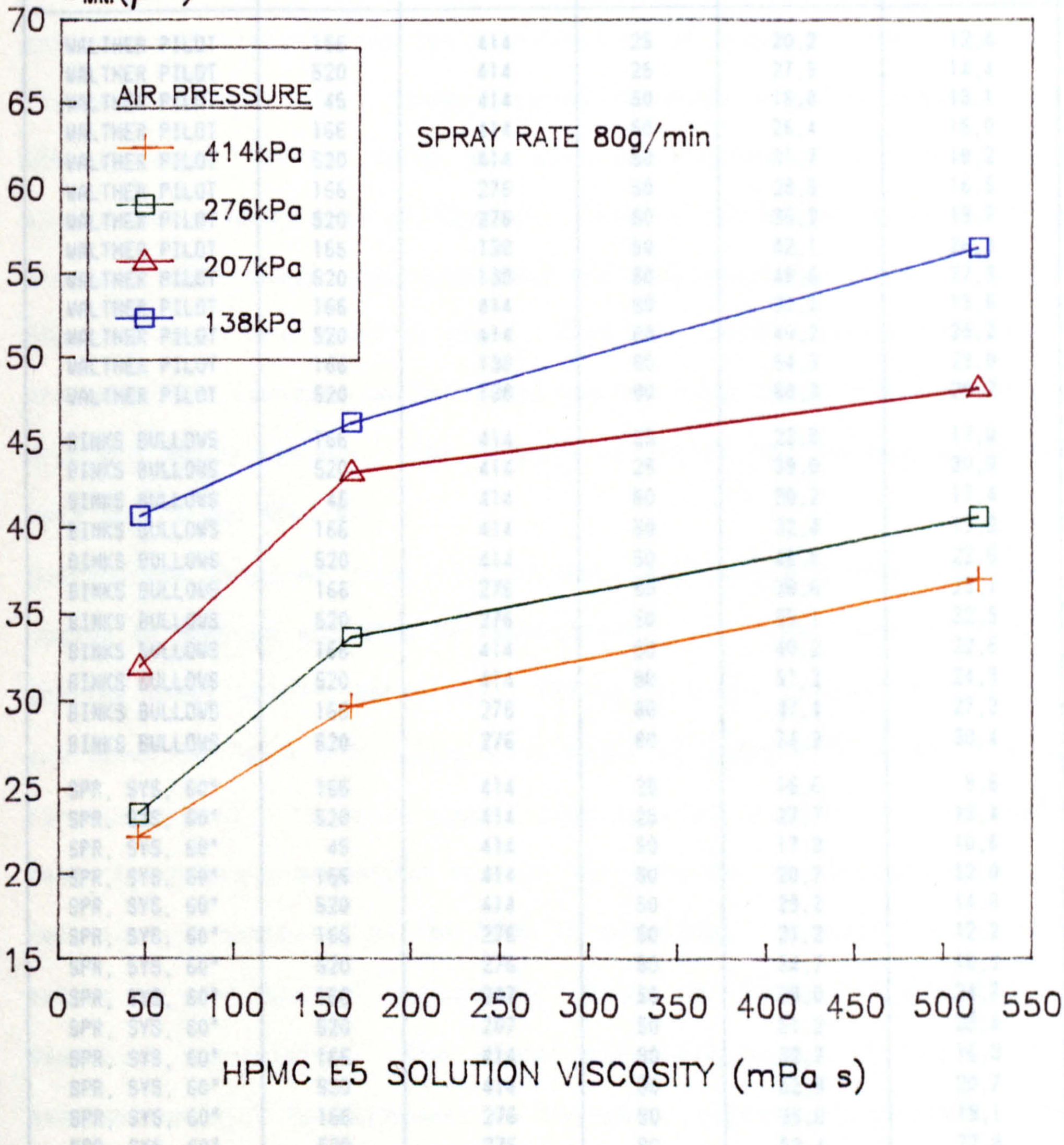

FIGURE 4.32

TABLE 4.6: THE EFFECT OF HPMC E5 SOLUTION VISCOSITY ON MEAN DROPLET SIZES PRODUCED UPON ATOMISATION

SPRAY GUN (SEE SECTION 4,2,2)	SOLUTION VISCOSITY (mPa s)	ATOMISING AIR PRESSURE (kPa)	SPRAY RATE ($gmin^{-1}$)	MASS MEDIAN DIAMETER (µm)	SURFACE MEAN DIAMETER (µm)
WALTHER PILOT	166	414	25	20,2	12,4
WALTHER PILOT	520	414	25	27,5	14,4
WALTHER PILOT	45	414	50	19,8	13,1
WALTHER PILOT	166	414	50	26,4	15,0
WALTHER PILOT	520	414	50	31,7	18,2
WALTHER PILOT	166	276	50	28,5	16,5
WALTHER PILOT	520	276	50	35,2	19,7
WALTHER PILOT	166	138	50	42,1	26,3
WALTHER PILOT	520	138	50	48,6	27,3
WALTHER PILOT	166	414	80	31,2	19,5
WALTHER PILOT	520	414	80	40,2	25,2
WALTHER PILOT	166	138	80	54,3	29,0
WALTHER PILOT	520	138	80	68,3	39,2
BINKS BULLOWS	166	414	25	22,8	17,0
BINKS BULLOWS	520	414	25	39,0	20,9
BINKS BULLOWS	45	414	50	30,2	17,4
BINKS BULLOWS	166	414	50	32,4	19,2
BINKS BULLOWS	520	414	50	46,5	22,6
BINKS BULLOWS	166	276	50	38,6	25,1
BINKS BULLOWS	520	276	50	59,1	32,9
BINKS BULLOWS	166	414	80	40,2	22,6
BINKS BULLOWS	520	414	80	61,2	24,9
BINKS BULLOWS	166	276	80	47,4	27,3
BINKS BULLOWS	520	276	80	74,2	38,4
SPR, SYS, 60°	166	414	25	16,6	9,6
SPR, SYS, 60°	520	414	25	27,7	13,4
SPR, SYS, 60°	45	414	50	17,3	10,6
SPR, SYS, 60°	166	414	50	20,7	12,0
SPR, SYS, 60°	520	414	50	29,2	14,8
SPR, SYS, 60°	166	276	50	21,2	12,2
SPR, SYS, 60°	520	276	50	34,7	16,9
SPR, SYS, 60°	166	207	50	39,0	24,7
SPR, SYS, 60°	520	207	50	51,2	28,4
SPR, SYS, 60°	166	414	80	32,7	16,3
SPR, SYS, 60°	520	414	80	52,8	20,7
SPR, SYS, 60°	166	276	80	39,0	19,1
SPR, SYS, 60°	520	276	80	53,4	27,8
SPR, SYS, 45°	45	414	50	17,9	11,5
SPR, SYS, 45°	166	414	50	21,8	13,0
SPR, SYS, 45°	520	414	50	31,4	15,3
SPR, SYS, 45°	166	276	50	26,4	15,2
SPR, SYS, 45°	520	276	50	38,3	18,2
SPR, SYS, 45°	166	138	50	40,6	25,6
SPR, SYS, 45°	520	138	50	54,9	30,1

solution viscosity will influence the size of the droplets produced upon atomisation. This is shown to be true for each spray gun studied and for a variety of spray rates and atomisation air pressures. The increase in the mean droplet diameters with increasing viscosity appears to be approximately equal for each atomising air pressure studied. The influence of viscosity on the distribution of droplet sizes is shown in Figures 4.33 and 4.34. These figures represent droplets produced by a Schlick model 930/7-1 spray gun with an atomisation air pressure of 414kPa and a spray rate of 50gmin^{-1}. When a concentration of 6%w/w was atomised under these conditions, all the droplets were found to be below 65µm and over 75wt.% below 25µm. With the 9%w/w solution 99.7%w/w of droplets were found to be below 112.8µm and with the 12%w/w solution all droplets below 160.4µm. The respective values for amounts below 25µm were 52wt.% and 40wt.%.

Suspensions prepared from type OY and OY-D Opadry powder dispersions (based on HPMC E5 and HPMC E3 respectively) were also atomised with the Schlick model 930/7-1 spray gun. The details and results of this study are shown in Table 4.7, along with those of atomised HPMC E5 solutions for comparison. It would appear from initial scrutiny of the results that the Opadry suspensions did not fit into the viscosity/droplet size relationship exhibited by the HPMC E5 solutions. However the viscosity values of the Opadry suspensions quoted in Table 4.7 are apparent Newtonian viscosities. The actual viscosity values at the point of atomisation will be dependent on the shear forces encountered. These shear forces may arise during passage through the liquid nozzle or from the high velocity atomising air. Their role and that of the suspended solid fraction are discussed in section 4.4.

THE EFFECT OF HPMC E5 SOLUTION VISCOSITY ON DROPLET SIZE DISTRIBUTIONS PRODUCED BY A SCHLICK MODEL 930/7-1 SPRAY GUN

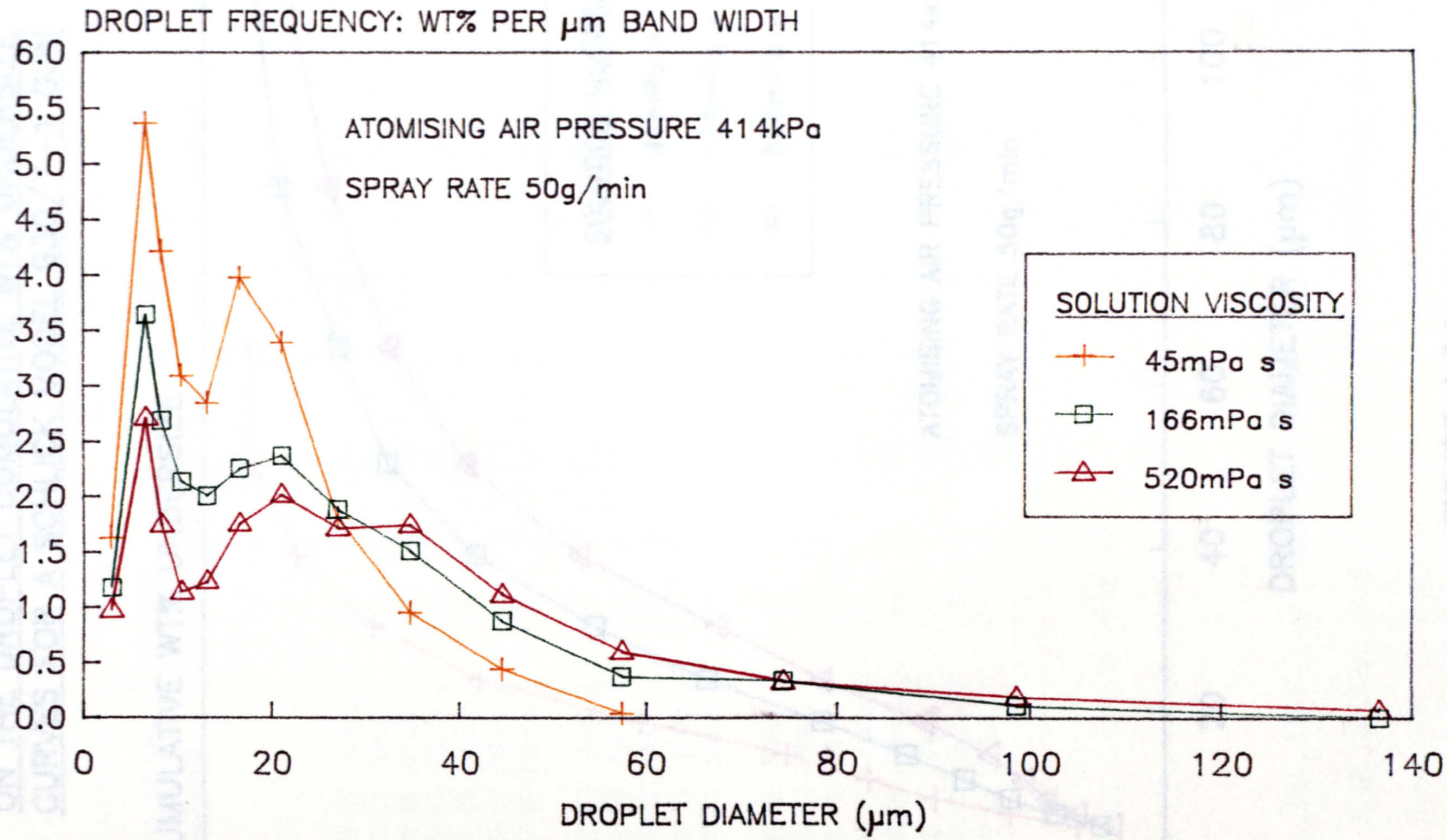

FIGURE 4.33

THE EFFECT OF HPMC E5 SOLUTION VISCOSITY ON THE DROPLET CUMULATIVE WT% UNDERSIZE CURVES FOR A SCHLICK MODEL 930/7--1 GUN

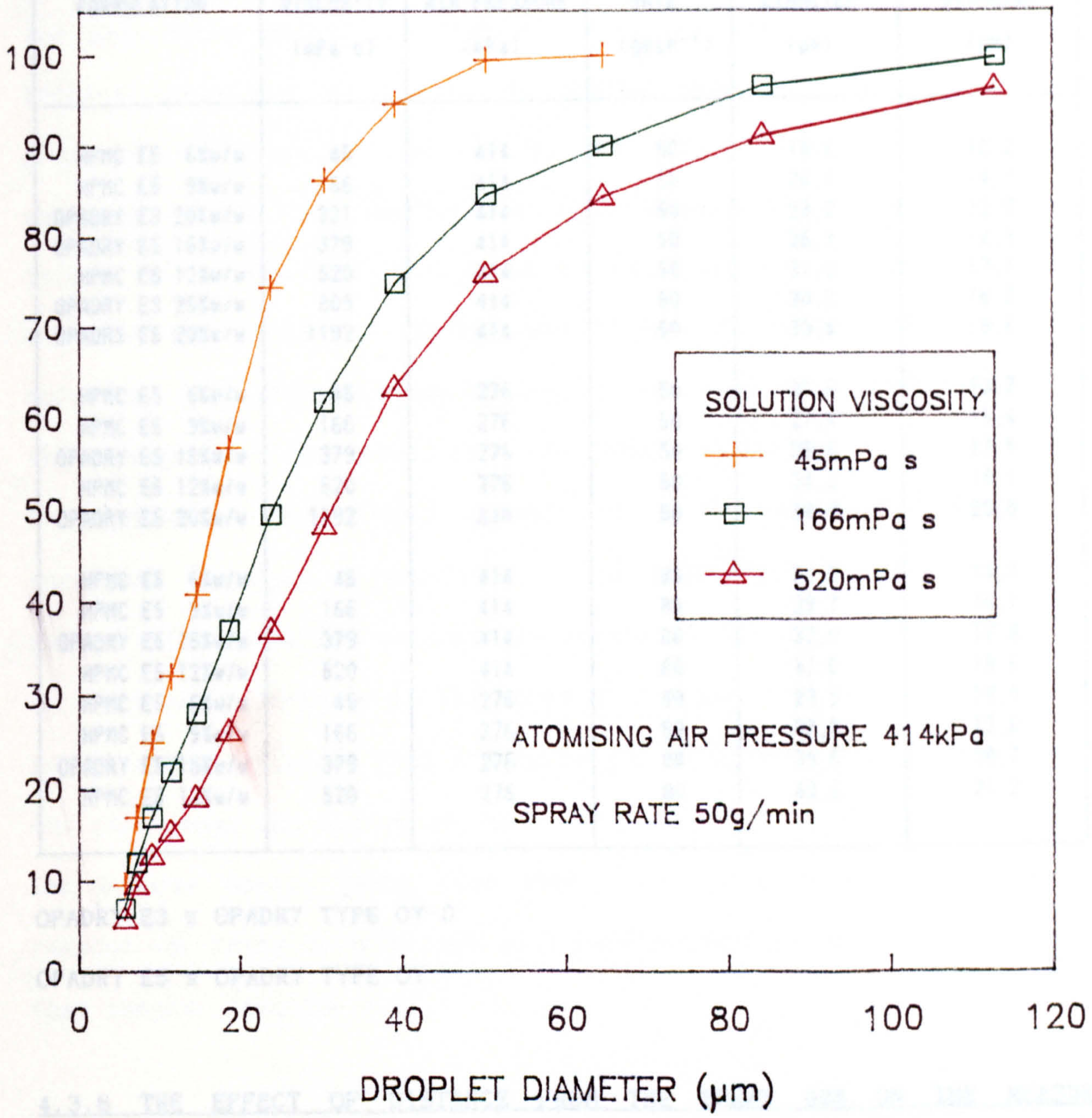

FIGURE 4.34

TABLE 4.7: THE EFFECT OF OPADRY SUSPENSION CONCENTRATION ON MEAN DROPLET SIZES PRODUCED UPON ATOMISATION

FILM COATING FORMULATION	SOLUTION VISCOSITY (mPa s)	ATOMISING AIR PRESSURE (kPa)	SPRAY RATE ($gmin^{-1}$)	MASS MEDIAN DIAMETER (µm)	SURFACE MEAN DIAMETER (µm)
HPMC E5 6%w/w	45	414	50	18.6	12.2
HPMC E5 9%w/w	166	414	50	24.0	14.0
OPADRY E3 20%w/w	321	414	50	23.2	13.0
OPADRY E5 15%w/w	379	414	50	26.3	14.3
HPMC E5 12%w/w	520	414	50	31.3	17.1
OPADRY E3 25%w/w	809	414	50	30.2	16.2
OPADRY E5 20%w/w	1192	414	50	33.4	18.6
HPMC E5 6%w/w	45	276	50	21.0	13.7
HPMC E5 9%w/w	166	276	50	27.4	15.4
OPADRY E5 15%w/w	379	276	50	29.6	17.5
HPMC E5 12%w/w	520	276	50	34.2	18.1
OPADRY E5 20%w/w	1192	276	50	34.7	20.0
HPMC E5 6%w/w	45	414	80	22.1	13.2
HPMC E5 9%w/w	166	414	80	29.7	16.1
OPADRY E5 15%w/w	379	414	80	32.0	17.8
HPMC E5 12%w/w	520	414	80	37.0	18.6
HPMC E5 6%w/w	45	276	80	23.5	13.9
HPMC E5 9%w/w	166	276	80	33.7	17.8
OPADRY E5 15%w/w	379	276	80	35.6	18.7
HPMC E5 12%w/w	520	276	80	40.6	21.2

OPADRY E3 ≡ OPADRY TYPE OY-D

OPADRY E5 ≡ OPADRY TYPE OY

4.3.6 THE EFFECT OF DISTANCE FROM THE SPRAY GUN ON THE MEASURED MEAN DROPLET DIAMETERS OF ATOMISED FILM COATING SOLUTIONS

Spray guns used in the model 10 (24") Accela-Cota are usually positioned between approximately 150mm and 200mm from the tablet bed. This is due to space constraints within the Accela-Cota, especially with the bulky Binks Bullows and Walther Pilot spray guns. It is possible with the

Schlick and Spraying Systems guns to increase the distance from the tablet bed to ≈300mm. This latter distance is also commonly encountered in the larger model Accela-Cotas (48" and 60") used for production scale film coating. Figures 4.35 and 4.36 show the variation in surface mean and mass median diameters with increasing distance from the spray gun, for both 9%w/w and 12%w/w HPMC E5 solutions fed to the Schlick model 930/7-1 spray gun at a rate of 50gmin^{-1} and atomised at 414kPa to produce a flat spray. It can be seen that there is an approximate doubling of the mass median and surface mean droplet diameters from 24.0μm to 45.4μm and 14.0μm to 29.2μm respectively for the 9%w/w solution and 31.3μm to 59.4μm and 17.1μm to 36.1μm for the 12%w/w solution. The distributrion of droplet sizes at various distances from the spray gun is shown for the 9%w/w solution in Figure 4.37. Examination of this figure shows that as the distance from the gun increases there is a reduction in the proportion of droplets in the smaller size bands and an increase in the larger size bands. There was in addition an increase in the range of droplet sizes encountered at the furthest two distances from the spray gun, droplets being encountered in the size range 160.4μm to 261.6μm. The weight of droplets in this band was however small, being less than 1% in both cases. The possible reasons for these observations will be discussed in more detail later in this chapter (section 4.4).

4.3.7 THE EFFECT OF SPRAY SHAPE ON THE MEAN DROPLET SIZES OF ATOMISED AQUEOUS FILM COATING SOLUTIONS

The droplet size results presented so far in this chapter have all been calculated from distributions measured in the centre of a flat spray shape of the type commonly employed in aqueous film coating. The Schlick, Walther Pilot and Binks Bullows guns are however capable of

THE EFFECT OF DISTANCE FROM THE SPRAY GUN ON THE MEASURED SURFACE MEAN DROPLET DIAMETER

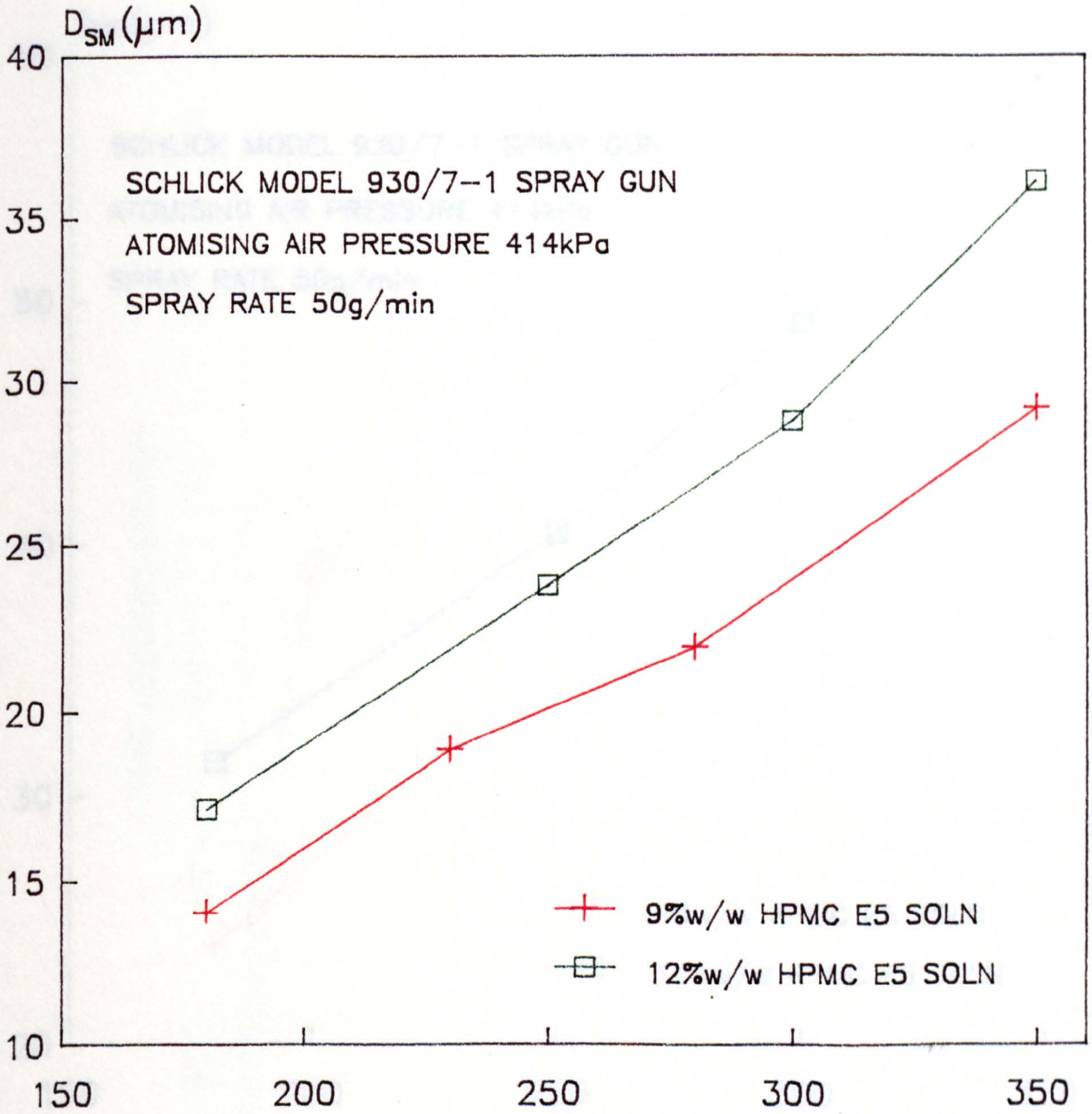

FIGURE 4.35

THE EFFECT OF DISTANCE FROM THE SPRAY GUN ON THE MEASURED MASS MEDIAN DROPLET DIAMETER

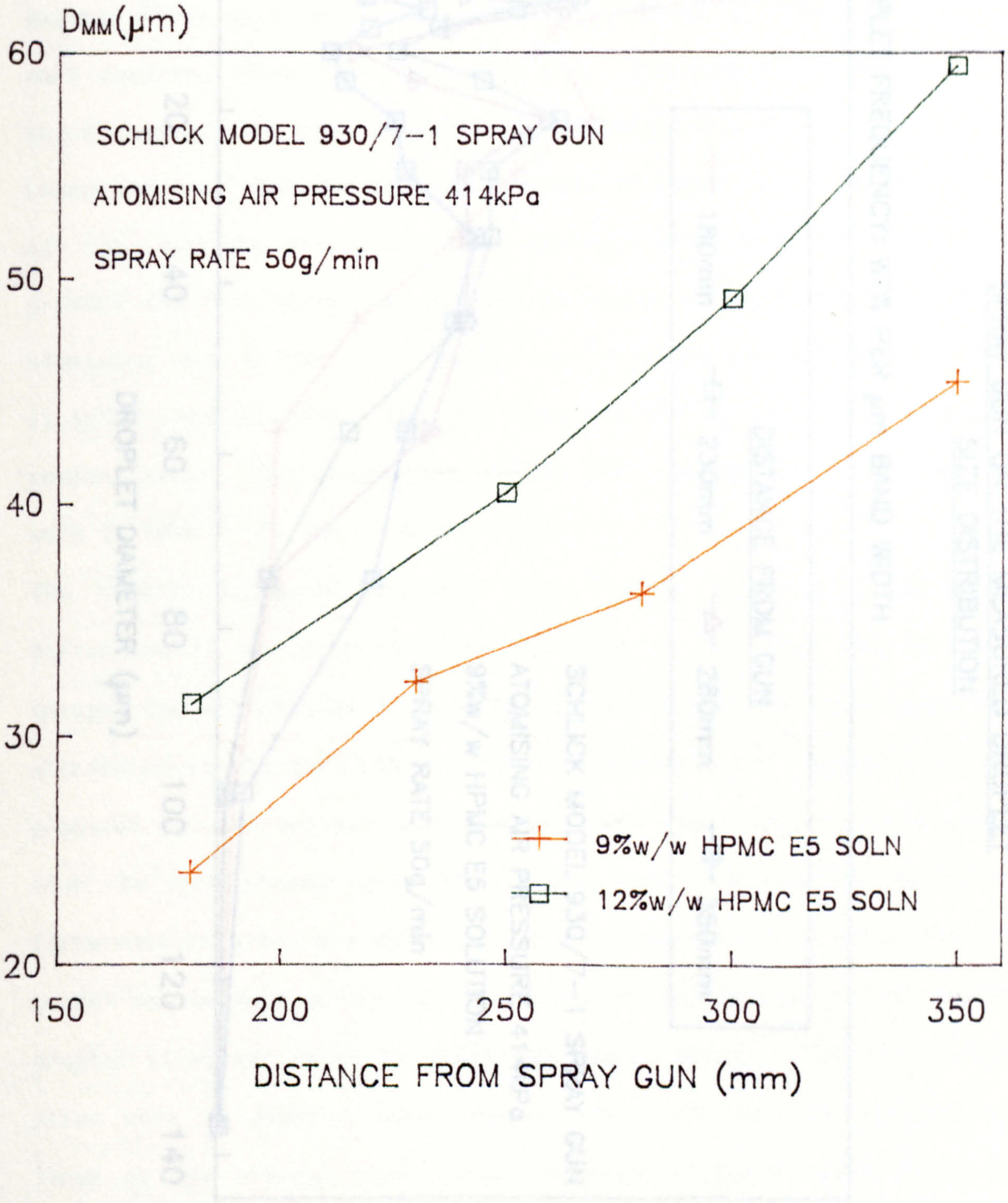

FIGURE 4.36

THE EFFECT OF DISTANCE FROM THE SPRAY GUN ON THE MEASURED DROPLET SIZE DISTRIBUTION

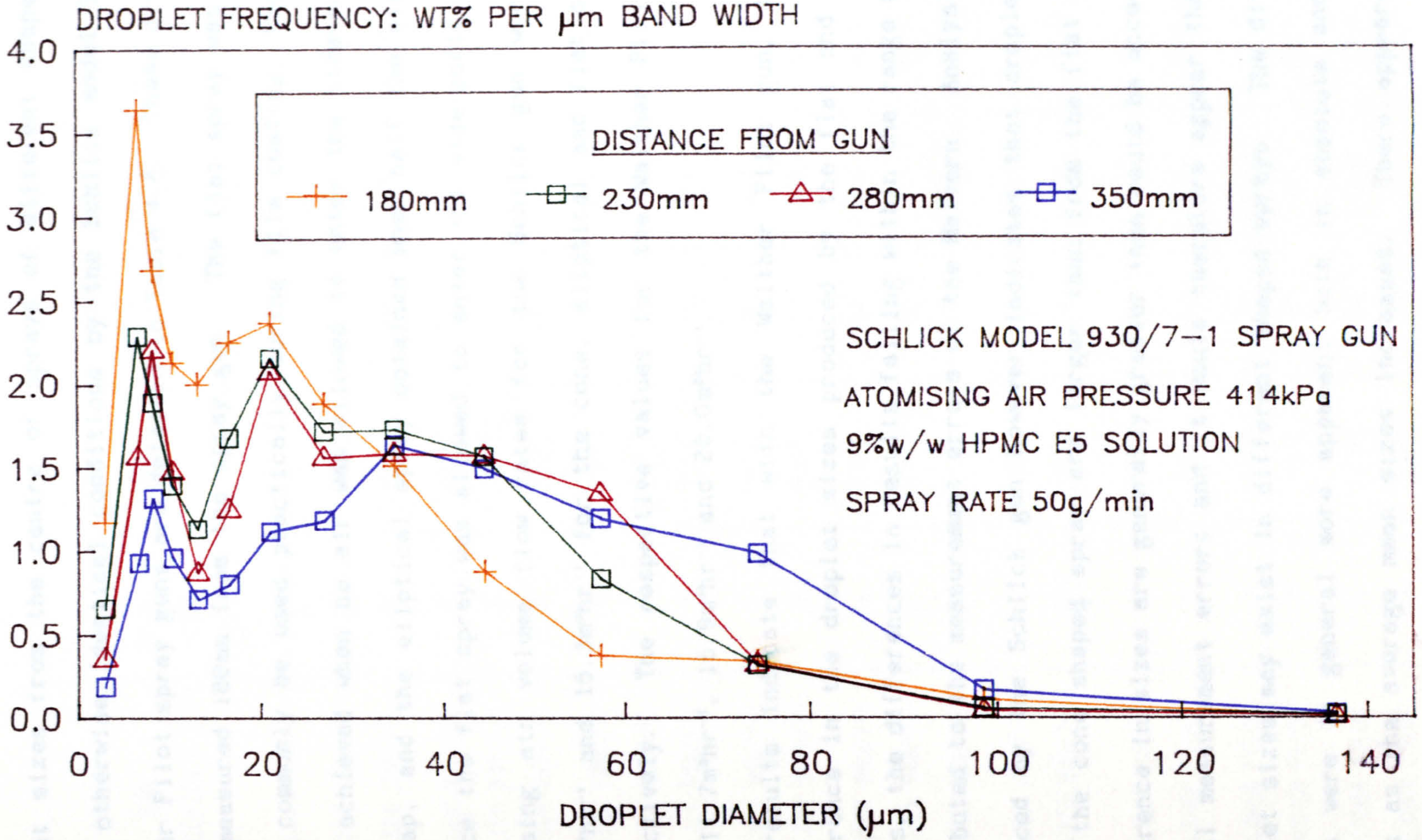

FIGURE 4.37

producing a variety of spray shapes ranging from a narrow angle solid cone (of approximately 10° exit angle) to a wide angle flat spray. Droplet sizes from the centre of sprays of different shapes produced under otherwise identical conditions by the Schlick model 930/7-1 and Walther Pilot spray guns are detailed in Table 4.8. These droplet sizes were measured 180mm from the spray gun. The flat spray was that which would commonly be used practically during film coating, the cone that shape achieved when no air was allowed to enter the side-ports of the air cap, and the eliptical spray obtained when half the air needed to produce the flat spray was allowed to enter the side-ports. The total atomising air volume flow rates for the Schlick gun were 7.4m^3hr^{-1}, 11.4m^3hr^{-1} and 15.3m^3hr^{-1} for the cone, eliptical and flat spray shapes respectively. The respective values for the Walther Pilot spray gun were 11.7m^3hr^{-1}, 15.9m^3hr^{-1} and 20.0m^3hr^{-1}.

The results indicate that with the Walther Pilot gun, there is no difference in the droplet sizes produced by the flat and cone shaped sprays, the differences in results falling within the range which may be attributed to the measurement errors of the Malvern. Analysis of sprays produced by the Schlick gun however indicates that droplets measured from the cone shaped spray are larger than from the flat spray. The difference in sizes are generally greater than could be accounted for by normal measurement errors and it would therefore appear that different droplet sizes may exist in different shaped sprays. The differences in sizes were in general more apparent both in absolute and percentage terms as the average mean sizes increased. There appeared to be no detectable differences between droplet sizes determined for the eliptical and flat spray shapes.

TABLE 4.8: THE INFLUENCE OF SPRAY SHAPE ON MEAN DROPLET SIZE

SPRAY GUN (SEE SECTION 4.2.2)	HPMC E5 SOLUTION CONC (%w/w)	SPRAY SHAPE	SPRAY RATE ($gmin^{-1}$)	AIR PRESSURE (kPa)	MASS MEDIAN DIAMETER (μm)	SURFACE MEAN DIAMETER (μm)
SCHLICK 930/7-1	6	CONE	50	414	19.3	11.2
SCHLICK 930/7-1	6	FLAT	50	414	18.5	12.2
SCHLICK 930/7-1	9	CONE	25	414	20.2	14.2
SCHLICK 930/7-1	9	ELIPTICAL	25	414	19.4	11.4
SCHLICK 930/7-1	9	FLAT	25	414	18.5	10.7
SCHLICK 930/7-1	9	CONE	40	414	23.6	13.7
SCHLICK 930/7-1	9	ELIPTICAL	40	414	20.9	12.8
SCHLICK 930/7-1	9	FLAT	40	414	20.5	12.7
SCHLICK 930/7-1	9	CONE	80	414	38.2	20.9
SCHLICK 930/7-1	9	FLAT	80	414	29.7	16.1
SCHLICK 930/7-1	12	CONE	50	414	39.3	18.6
SCHLICK 930/7-1	12	ELIPTICAL	50	414	32.5	17.0
SCHLICK 930/7-1	12	FLAT	50	414	31.3	17.1
SCHLICK 930/7-1	12	CONE	80	414	46.1	20.4
SCHLICK 930/7-1	12	FLAT	80	414	37.0	18.6
WALTHER PILOT	9	CONE	25	414	19.6	12.2
WALTHER PILOT	9	FLAT	25	414	20.2	12.4
WALTHER PILOT	9	CONE	50	414	27.5	15.3
WALTHER PILOT	9	FLAT	50	414	26.4	15.0
WALTHER PILOT	12	CONE	80	414	38.9	21.5
WALTHER PILOT	12	FLAT	80	414	40.2	23.2

4.3.8 THE RADIAL VARIATION IN MEAN DROPLET SIZES WITHIN A SPRAY

All droplet size measurements presented so far have been calculated from distributions measured at the centre of a spray at a defined distance from the spray gun. In practice however during film coating the spray width at the point the droplets contact the tablet bed can be in excess of 300mm, the actual width being dependent on both the spray shape and the distance from the spray gun. To gain an indication as to whether the droplet size varies with the radial distance across the spray, measurements were taken at 25mm intervals from the centre of a spray produced from a 9%w/w HPMC E5 solution, fed at 50gmin^{-1} to a Schlick model 930/7-1 spray gun and atomised at 414kPa. The gun was set to produce the normal flat spray pattern and measurements were taken at a central distance of 180mm from the spray gun. Results from this study are shown in Table 4.9. At radial distances above 75mm from the centre of the spray the obscuration values became too low for meaningful droplet sizes to be obtained.

The results in Table 4.9 indicate that with the atomisation conditions described, there is no detectable radial variation in droplet size at distances of up to 50mm from the spray centre. As the distance increases to 75mm however there is the suggestion that a reduction in droplet size may occur. The reasons for these observations and the likelihood of there being similar occurrences in sprays produced using alternative atomisation conditions will be discussed later in the chapter (section 4.4).

TABLE 4.9: THE RADIAL VARIATION IN MEAN DROPLET SIZES WITHIN A SPRAY

RADIAL DISTANCE FROM CENTRE OF SPRAY (mm)	MASS MEDIAN DIAMETER (μm)	SURFACE MEAN DIAMETER (μm)
0	24.0	14.0
25	22.4	13.7
50	22.8	13.3
75	21.6	12.4

4.3.9 THE EFFECT OF LIQUID NOZZLE DIAMETER ON THE ATOMISATION OF AQUEOUS FILM COATING SOLUTIONS

Pneumatic spray guns are often available with a choice of liquid nozzle diameters. It is therefore necessary to determine whether the droplet size produced by the spray guns is dependent on the liquid nozzle diameter, and if so, how the liquid nozzle influences droplet production. To investigate this, a 9%w/w HPMC E5 solution was atomised with both the Schlick and Spraying Systems spray guns, using identical conditions except for changes in the inner diameter of the liquid nozzle (NB the outer diameter of the nozzle did not change). Schlick model 930/7-1, 931/7-1 and 932/7-1 spray guns with corresponding liquid nozzle diameters of 0.8mm, 1.2mm and 1.8mm and Spraying Systems 1/4J series guns with 2850 (nozzle diameter 0.71mm) and 2050 (nozzle diameter 0.51mm) liquid nozzles were used. A flat spray was produced by the Schlick nozzle combinations, and in both cases droplets were measured at the centre of the spray, 180mm from the spray gun.

The results from this study are shown in Table 4.10. They indicate that over the range of liquid nozzle diameters studied, which covers the majority of the range available for the spray guns used in aqueous film coating, the liquid nozzle diameter has no influence on the mean droplet sizes produced upon atomisation. Examination of the distribution of droplet sizes also failed to show any detectable differences.

TABLE 4.10: THE INFLUENCE OF LIQUID NOZZLE DIAMETER ON DROPLET SIZE

SPRAY GUN	AIR CAP	LIQUID NOZZLE DIAMETER (mm)	SPRAY RATE ($gmin^{-1}$)	AIR PRESSURE (kPa)	MASS MEDIAN DIAMETER (µm)	SURFACE MEAN DIAMETER (µm)
SCHLICK 930/7-1	STANDARD	0,8	40	414	20,5	12,7
SCHLICK 931/7-1	STANDARD	1,2	40	414	21,6	13,4
SCHLICK 932/7-1	STANDARD	1,8	40	414	20,3	12,8
SCHLICK 930/7-1	STANDARD	0,8	80	414	29,7	16,1
SCHLICK 931/7-1	STANDARD	1,2	80	414	28,9	16,3
SCHLICK 932/7-1	STANDARD	1,8	80	414	30,3	17,0
SCHLICK 930/7-1	STANDARD	0,8	50	276	27,4	15,4
SCHLICK 931/7-1	STANDARD	1,2	50	276	28,9	17,1
SCHLICK 932/7-1	STANDARD	1,8	50	276	28,1	16,0
SPRAYING SYSTEMS	67228-45°	0,51	50	414	23,1	13,4
SPRAYING SYSTEMS	67228-45°	0,71	50	414	21,8	13,0
SPRAYING SYSTEMS	62240-60°	0,51	50	414	21,2	11,7
SPRAYING SYSTEMS	62240-60°	0,71	50	414	20,7	12,0

4.3.10 THE DRYING CONDITIONS WITHIN A MODEL 10 ACCELA-COTA AND THEIR POTENTIAL EFFECT ON THE ATOMISED DROPLET SIZE

Droplet size measurements detailed so far in this chapter have been produced from sprays emitted into still air at room temperature. The air inside the Accela-Cota (and other coating pans) however is not stationary and is usually above room temperature. It was considered that droplet sizes within the coating pan may therefore be different to those measured in the laboratory. From consideration of the design of both the Malvern droplet size analyser and the Accela-Cota it was concluded that measurements of droplet sizes could not be made "in situ" without major structural alterations. To examine the potential effect of the hot drying air on the droplet size in the laboratory, it was first necessary to measure both the air velocity and temperature distributions within the Accela-Cota at typical coating conditions. Details of the methods for measuring these values are given in section 4.2.7. A drying air volume flow rate of $0.13 m^3 s^{-1}$ was used, since with this volume of air, the pressure within the Accela-Cota is balanced so that during coating minimal air is either drawn in from the surroundings or emitted from the coating pan. The results of the study are shown in Tables 4.11 and 4.12. The values for the angle of maximum velocity were calculated assuming an angle of 0° when the vane was horizontal (facing the perforated periphery) and an angle of 90° when the vane was facing vertically upwards. The values for the distances of the measurement probe from the tablet bed are quoted as ranges, since the tablet flow pattern varies as the pan rotates. The values for the depth into the pan were measured from the pan door.

It is apparent from Tables 4.11 and 4.12 that a reduction in temperature of the drying air occurs between the point just prior to it entering the

TABLE 4.11: DRYING AIR VELOCITY AND TEMPERATURE VALUES WITHIN A MODEL 10 ACCELA-COTA

Operating conditions

Weight of tablets = 10kg. Pan speed = 10rpm. Drying air volume flow rate = 0.13m^3s^{-1} (275cfm). Ambient air temperature 22-24°C. Door sealed. Schlick spray gun in position (not operational).

Distance from the tablet bed

Probe position 1. 50-100mm
Probe position 2. 0-50mm
Probe position 3. 50-80mm
Probe position 4. 80-130mm
Probe position 5. 160-200mm
(position of spray gun)

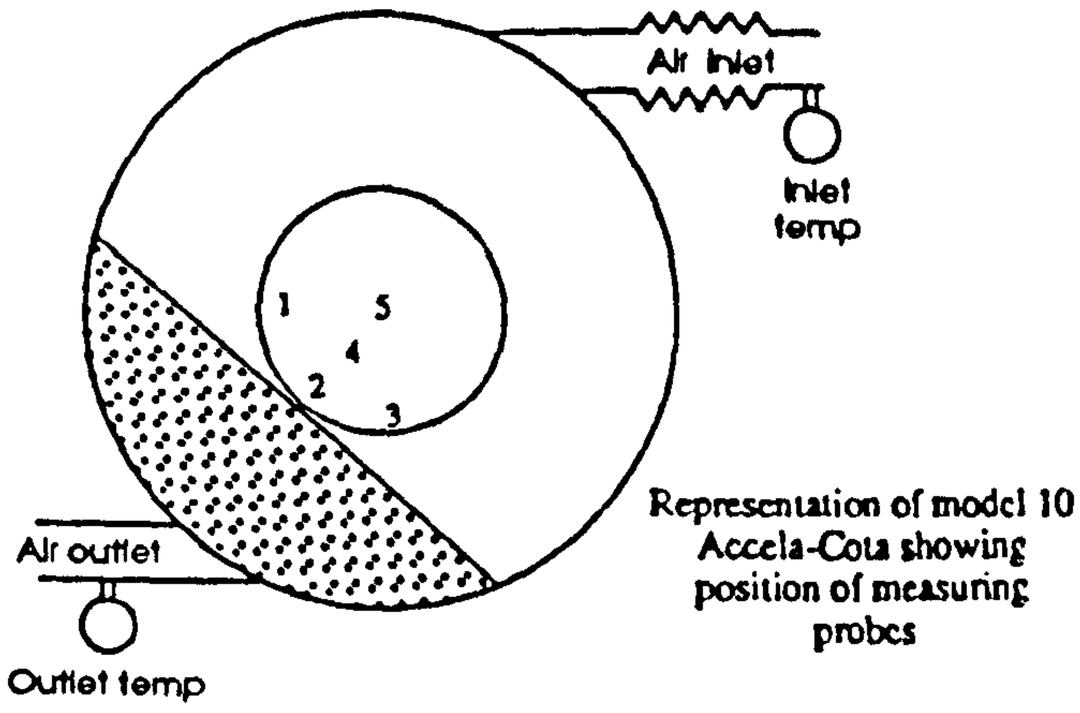

Representation of model 10 Accela-Cota showing position of measuring probes

PROBE POSITION		DEPTH INTO PAN (mm)	MAXIMIUM VELOCITY (ms^{-1})	ANGLE OF MAX. VELOCITY	TEMPERATURE (°C)
INLET	1	420	1.06	60-90	58.9
TEMP.	1	330	0.82	90	58.5
64.5°C	1	230	0.73	60-70	58.4
OUTLET	1	150	0.51	90-110	57.7
TEMP.	1	75	0.57	90-135	57.5
57.5°C					
INLET	2	420	1.25	45	57.6
TEMP.	2	330	0.78	0-60	57.3
64-65°C	2	230	0.70	45	58.3
OUTLET	2	150	0.89	0-70	59.1
TEMP.	2	75	<0.4	45	58.2
57°C					
INLET	3	420	0.57	0-90	61.1
TEMP.	3	330	<0.5	-	60.9
65°C	3	230	<0.5	-	61.7
OUTLET	3	150	0.90	40-60	61.1
TEMP.	3	75	<0.4	-	60.2
58°C					
INLET	4	420	<0.4	-	58.5
TEMP.	4	330	0.50	90	58.7
65°C	4	230	0.65	90	58.5
OUTLET	4	150	0.65	90	58.6
TEMP.	4	75	<0.4	-	57.6
58°C					

TABLE 4.12: DRYING AIR VELOCITY AND TEMPERATURE VALUES WITHIN A MODEL 10 ACCELA-COTA

Operating conditions

Weight of tablets = 10kg. Pan speed = 10rpm. Drying air volume flow rate = 0.13m^3s^{-1} (275cfm). Ambient air temperature 22-24°C. Door sealed. Spray gun absent.

Distance from the tablet bed

Probe position 1. 50-100mm
Probe position 2. 0-50mm
Probe position 3. 50-80mm
Probe position 4. 80-130mm
Probe position 5. 160-200mm
(normal position of spray gun)

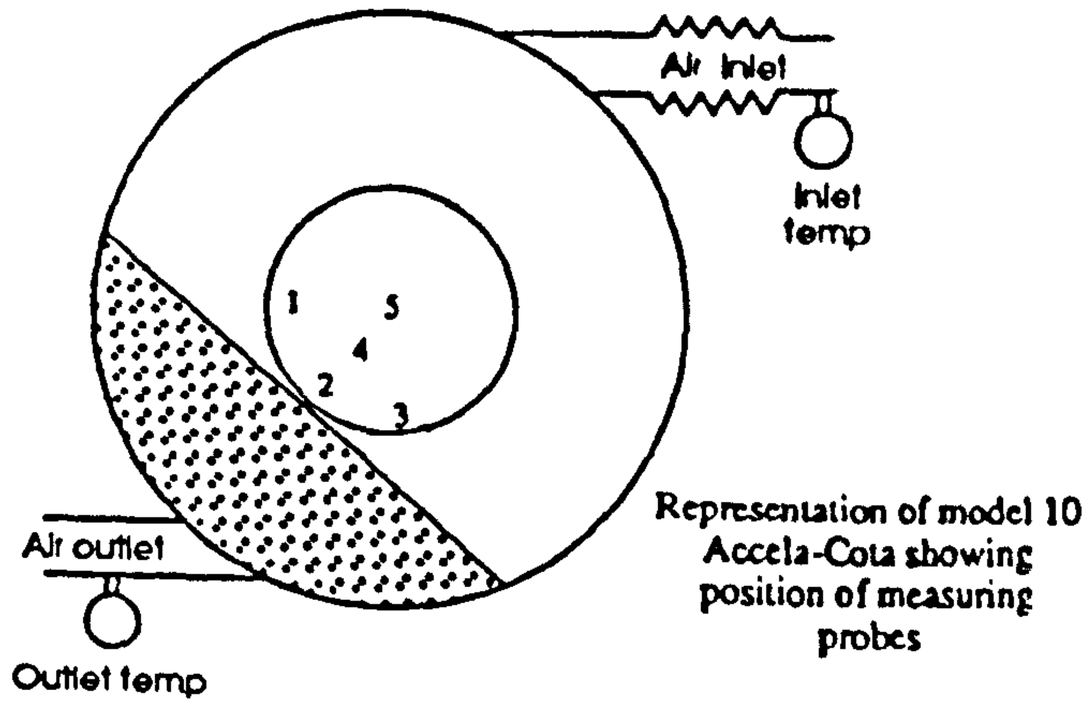

Representation of model 10 Accela-Cota showing position of measuring probes

	PROBE POSITION	DEPTH INTO PAN (mm)	MAXIMIUM VELOCITY (ms^{-1})	ANGLE OF MAX. VELOCITY	TEMPERATURE (°C)
INLET	1	420	1.16	90	46.2
TEMP.	1	330	0.99	90	46.3
52.5°C	1	230	0.70	90	46.3
OUTLET	1	150	0.60	40-60	46.0
TEMP.	1	75	0.63	90	45.4
44.5°C					
INLET	2	420	1.12	45	45.5
TEMP.	2	330	0.86	0-60	44.9
51-52°C	2	230	0.76	45	45.1
OUTLET	2	150	0.82	0-70	44.8
TEMP.	2	75	0.85	45	45.9
44°C					
INLET	3	420	0.86	0-60	47.7
TEMP.	3	330	0.77	0-70	47.0
52°C	3	230	0.78	45	47.6
OUTLET	3	150	0.83	75	47.8
TEMP.	3	75	0.54	100	46.7
44°C					
INLET	5	420	<0.4	-	48.6
TEMP.	5	330	<0.4	-	49.2
52°C	5	230	<0.4	-	49.1
OUTLET	5	150	0.72	45-90	48.7
TEMP.	5	75	0.59	45-90	48.2
44°C					

coater and when it reaches the tablet bed. This is due to heat loss to the coater and its immediate environment and was found to be in the order of 5°C for these typical coating conditions. The actual temperature and thus drying capacity of the air will therefore be less than that envisaged from the air inlet temperature measurement. The differences in air temperature between probe positions 2 and 5 in Table 4.12 suggests that there is also a reduction in the drying air temperature as it travels between the spray gun and the tablet surface.

The temperarure of the drying air is demonstrated to vary little in the vicinity of the tablet bed surface.

The velocity of the drying air when flowing at a rate of $0.13m^3s^{-1}$ is seen to range between below $0.4ms^{-1}$ (the lowest velocity the probe is capable of measuring) and $1.25ms^{-1}$. Generally air flow appeared to be fastest towards the back of the pan,

The measurements of the temperature and velocity of the drying air, determined under typical coating conditions, indicate those values which it must be attempted to reproduce, in order to ascertain the effect of the drying air on the measured droplet sizes when using the Malvern droplet analyser. After investigating various combinations of hot air driers, it was found that a Philips fan heater model HB3240 at the 2kW setting provided the closest reproduction of the drying air properties within the Accela-Cota. The air velocities and temperatures produced by this fan heater when placed 120mm behind the spray gun are shown in Table 4.13.

The use of this heater fan unit placed 120mm behind the spray gun, therefore allowed the conditions experienced by the droplets on their way to the tablet bed in the model 10 Accela-Cota to be modelled when using the Malvern droplet size analyser.

TABLE 4.13: AIR TEMPERATURE AND VELOCITY VALUES PRODUCED BY A PHILIPS MODEL HB3240 FAN HEATER

DISTANCE FROM SPRAY GUN (mm)	AIR VELOCITY (ms^{-1})	AIR TEMPERATURE (°C)
20	1.35	70
80	1.20	65
150	1.15	59
200	1.12	55
250	0.99	53
300	0.60	45

Droplets from the centre of flat shaped sprays produced by a Schlick model 930/7-1 gun were analysed by the Malvern at various distances from the spray gun, with the heater fan unit both operational and absent. A 9%w/w HPMC E5 solution was investigated, utilising a spray rate of 50$gmin^{-1}$ and various atomising air pressures. Results from this study are shown in Figures 4.38 and 4.39 and Table 4.14. The atomising air pressures were chosen to examine the effect of the heater fan over a wide range of droplet sizes.

It is apparent that the operation of the heater fan unit causes no significant difference in the measured droplet size when atomisation is carried out using the conditions stated. Examination of the droplet size distributions also showed the presence of the heater fan to cause minimal difference to both the distribution pattern and the range of droplet sizes encountered.

THE EFFECT OF SIMULATING MODEL 10 ACCELA-COTA DRYING CONDITIONS ON THE MEASURED ATOMISED DROPLET SIZE

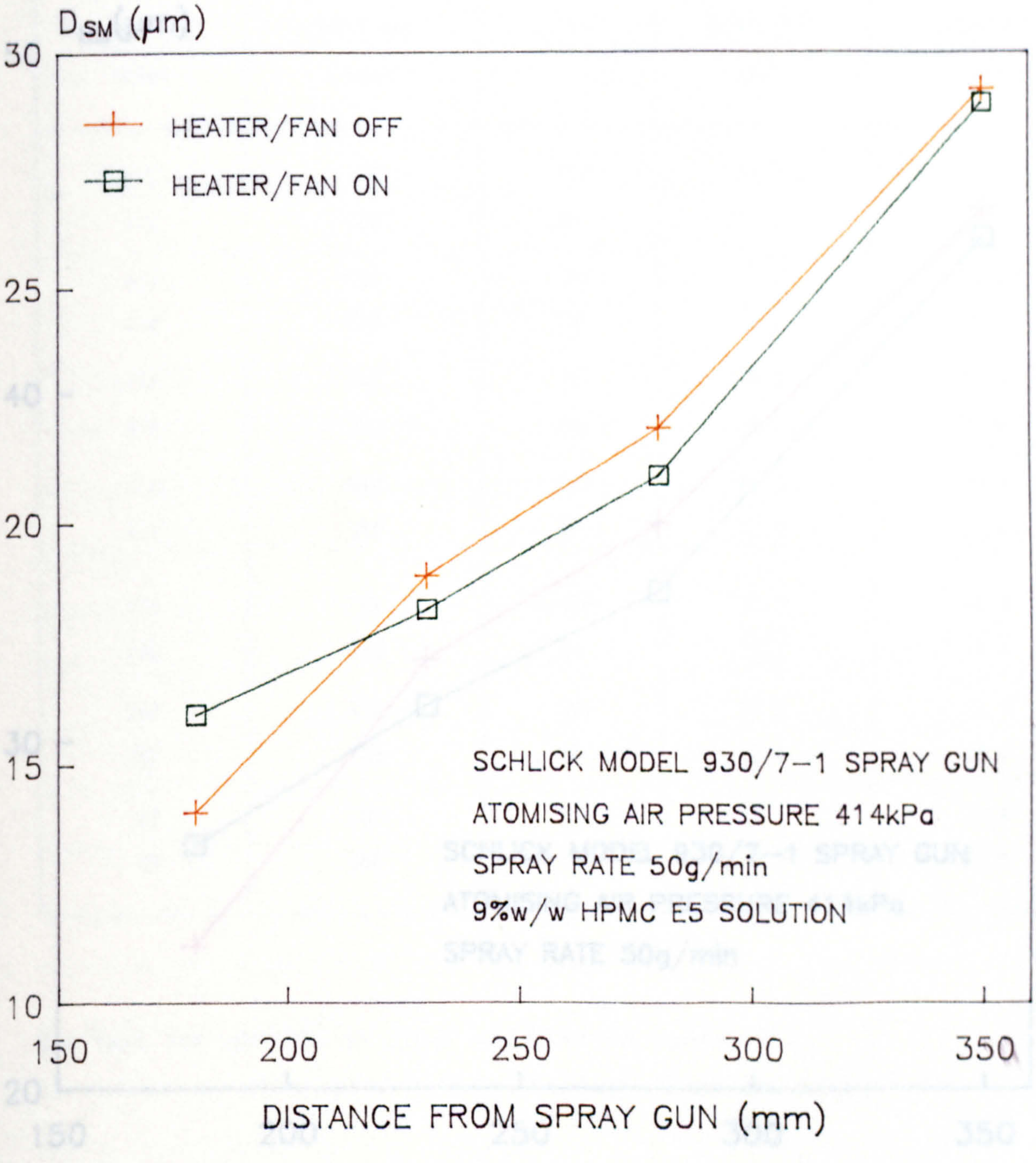

FIGURE 4.38

THE EFFECT OF SIMULATING MODEL 10 ACCELA-COTA DRYING CONDITIONS ON THE MEASURED ATOMISED DROPLET SIZE

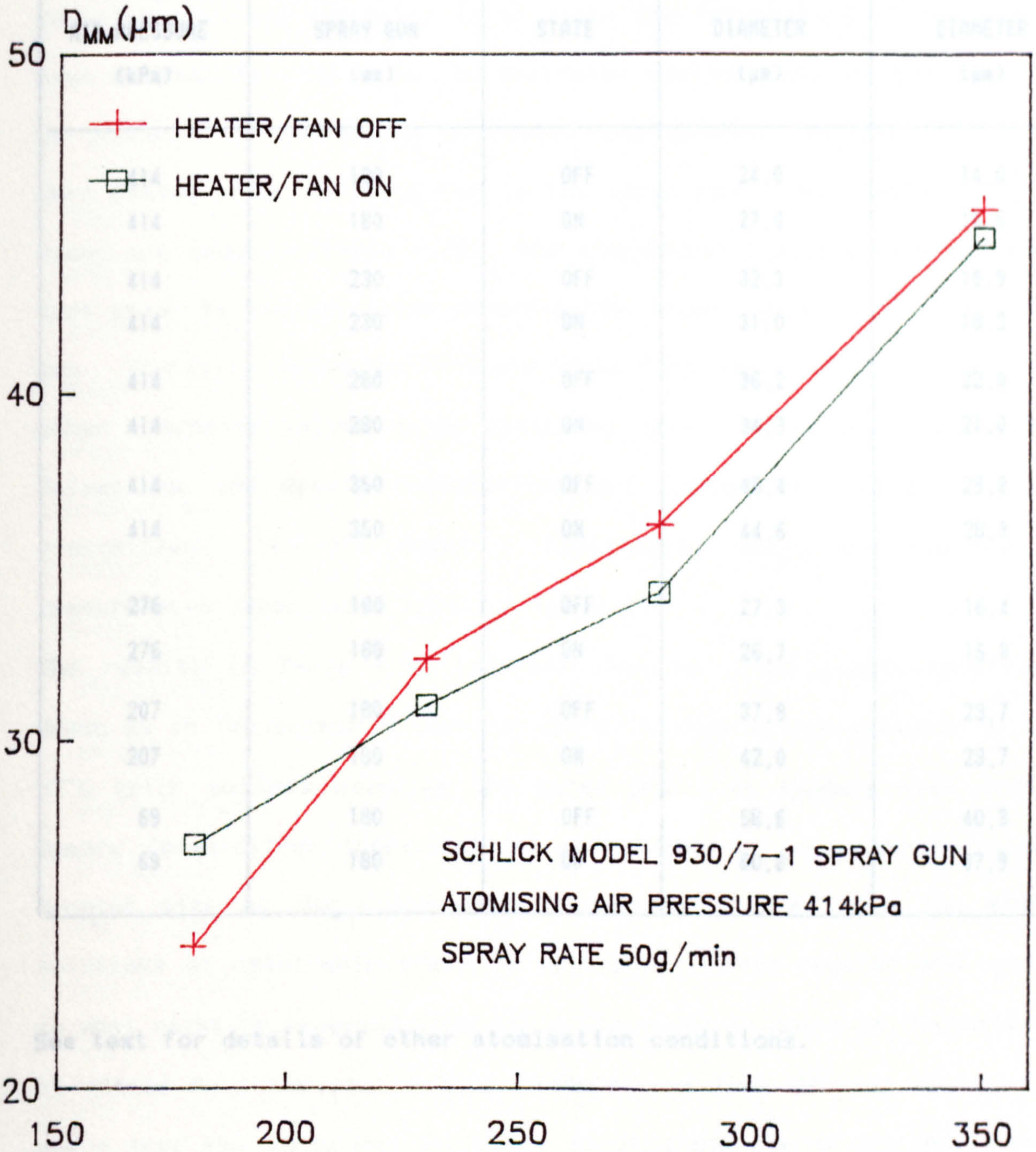

FIGURE 4.39

TABLE 4.14: THE EFFECT OF SIMULATING MODEL 10 ACCELA-COTA DRYING CONDITIONS ON THE MEASURED ATOMISED DROPLET SIZE

ATOMISING AIR PRESSURE (kPa)	DISTANCE FROM SPRAY GUN (mm)	HEATER STATE	MASS MEDIAN DIAMETER (μm)	SURFACE MEAN DIAMETER (μm)
414	180	OFF	24.0	14.0
414	180	ON	27.0	14.6
414	230	OFF	32.3	18.9
414	230	ON	31.0	18.2
414	280	OFF	36.2	22.0
414	280	ON	34.3	21.0
414	350	OFF	45.4	29.2
414	350	ON	44.6	28.9
276	180	OFF	27.3	16.4
276	180	ON	26.7	15.8
207	180	OFF	37.8	23.7
207	180	ON	42.0	23.7
69	180	OFF	58.6	40.3
69	180	ON	60.8	37.9

See text for details of other atomisation conditions.

4.3.11 THE EFFECT OF HEATING AQUEOUS FILM COATING SOLUTIONS PRIOR TO ATOMISATION ON THE RESULTANT ATOMISED DROPLET SIZE

It has been shown previously (section 4.3.5) that reducing the solution viscosity results in smaller droplets upon atomisation. One method of reducing solution viscosity is to raise the temperature of the solution (see Chapter 3). In order to determine whether smaller droplets could be produced by increasing solution temperatures, various formulations were heated prior to being fed to the spray gun. The results from this study are shown in Table 4.15. The temperatures quoted were determined just prior to the solutions entering the liquid input port of the spray gun. Viscosity values at 20°C are those detailed in section 3.3.1, with other viscosity values being estimated from information in Chapter 3. Values for the Opadry formulations are quoted as apparent Newtonian viscosities. In all cases a flat spray shape was analysed and measurements taken 180mm from the spray gun.

The results in Table 4.15 indicate that no clear conclusions can be drawn as to the effect of heating the solutions to temperatures of up to 37°C prior to them entering the spray gun. It appears that with the Opadry formulations there may be a tendency to cause an increase in droplet size as the temperature increases, whereas with the HPMC E5 solutions no detectable trend is apparent. These results are contrary to what might be expected from the differences in solution viscosity.

It should be noted that higher temperatures than 37°C at the point of entry into the spray gun could not be obtained due to the necessity to keep the solutions below their thermal gelation temperatures in the holding vessel.

TABLE 4.15: THE EFFECT OF SOLUTION TEMPERATURE ON THE ATOMISED DROPLET SIZE

FILM COATING FORMULATION	SOLUTION TEMPERATURE (°C)	SOLUTION VISCOSITY (mPa s)	AIR PRESSURE (kPa)	SPRAY RATE ($gmin^{-1}$)	MASS MEDIAN DIAMETER (µm)	SURFACE MEAN DIAMETER (µm)
OPADRY OY 15%w/w	20	379	414	50	26.3	14.3
OPADRY OY 15%w/w	30	258	414	50	26.7	14.6
OPADRY OY 15%w/w	37	223	414	50	26.1	15.0
OPADRY OY 15%w/w	20	379	276	50	29.6	17.5
OPADRY OY 15%w/w	30	258	276	50	32.0	18.4
OPADRY OY 15%w/w	37	223	276	50	32.7	19.5
OPADRY OY 15%w/w	20	379	414	80	32.0	17.8
OPADRY OY 15%w/w	37	223	414	80	38.8	20.4
HPMC E5 12%w/w	20	520	414	25	25.4	13.5
HMPC E5 12%w/w	30	380	414	25	23.7	12.9
HPMC E5 12%w/w	20	520	414	40	29.0	14.9
HPMC E5 12%w/w	30	380	414	40	26.9	14.8
HPMC E5 12%w/w	20	520	276	50	34.2	18.1
HPMC E5 12%w/w	30	380	276	50	35.0	17.9
HPMC E5 9%w/w	20	166	414	40	20.5	12.7
HPMC E5 9%w/w	30	113	414	40	20.3	12.8
HPMC E5 9%w/w	37	83	414	40	20.4	13.4
HPMC E5 9%w/w	20	166	414	80	29.7	16.1
HPMC E5 9%w/w	30	113	414	80	27.9	17.1
HPMC E5 9%w/w	37	83	414	80	26.7	16.9

4.3.12 SPRAY GUN ANNULUS ATOMISING AIR VELOCITY AND MASS FLOW RATES

It has been shown that differences exist between droplet sizes produced by different spray guns under otherwise identical conditions (section 4.3.3). These could arise from differences in the geometry of the annulus around the liquid nozzle, which may in turn lead to differences in the atomising air velocity and mass/volume flow rates. Variation in the liquid nozzle diameter itself has been shown to have no effect on the droplet size (section 4.3.9). Table 4.16 details for each gun studied, the values of the atomising air mass flow rate through the annulus around the liquid nozzle; these are derived from the measured values of the air volume flow rate and air density values. Also detailed are the values for the velocity of the atomising air as it leaves the spray gun annulus; these are determined from the annulus area, air volume flow rates and air compression ratios. For any particular gun and air cap combination used, the values remained the same regardless of the liquid nozzle used.

The results show the Binks Bullows gun to exhibit the largest air mass flow rates but the lowest air exit velocities. Values for the Walther Pilot gun are slightly higher than the Schlick gun, although with the latter the air velocity is shown to vary less with changes in atomising air pressure. The Spraying Systems guns both have considerably lower annulus atomising air mass flow rates than the other three guns. The Spraying Systems 60° gun exhibits the highest air exit velocity values. The air velocity values for the Spraying Systems 45° gun are similar to those of the Schlick and Walther Pilot guns.

Although the air exit velocity values all increase with increasing atomising air pressure, the increase is relatively small compared with the corresponding increase in air mass flow rate.

TABLE 4.16: SPRAY GUN ANNULUS ATOMISING AIR VELOCITY AND MASS FLOW RATES

SPRAY GUN	AIR CAP	ATOMISING AIR PRESSURE (kPa)	ANNULUS AIR MASS FLOW RATE ($gmin^{-1}$)	ANNULUS AIR EXIT VELOCITY (ms^{-1})
SCHLICK 930/7-1	STANDARD	69	48	173
SCHLICK 930/7-1	STANDARD	138	67	172
SCHLICK 930/7-1	STANDARD	207	87	172
SCHLICK 930/7-1	STANDARD	276	110	177
SCHLICK 930/7-1	STANDARD	345	133	182
SCHLICK 930/7-1	STANDARD	414	149	182
SCHLICK 930/7-1	STANDARD	552	197	185
WALTHER PILOT WA/WX	0,5-1,5	138	66	177
WALTHER PILOT WA/WX	0,5-1,5	207	89	186
WALTHER PILOT WA/WX	0,5-1,5	276	113	194
WALTHER PILOT WA/WX	0,5-1,5	345	134	196
WALTHER PILOT WA/WX	0,5-1,5	414	158	199
WALTHER PILOT WA/WX	0,5-1,5	552	206	205
BINKS BULLOWS 540	63PB	207	96	138
BINKS BULLOWS 540	63PB	276	124	147
BINKS BULLOWS 540	63PB	345	157	158
BINKS BULLOWS 540	63PB	414	188	159
BINKS BULLOWS 540	63PB	552	250	168
SPRAYING SYSTEMS	62240-60°	138	21	181
SPRAYING SYSTEMS	62240-60°	207	29	192
SPRAYING SYSTEMS	62240-60°	276	40	217
SPRAYING SYSTEMS	62240-60°	345	52	239
SPRAYING SYSTEMS	62240-60°	414	62	247
SPRAYING SYSTEMS	62240-60°	552	81	256
SPRAYING SYSTEMS	67228-45°	138	27	158
SPRAYING SYSTEMS	67228-45°	207	38	170
SPRAYING SYSTEMS	67228-45°	276	47	173
SPRAYING SYSTEMS	67228-45°	345	59	183
SPRAYING SYSTEMS	67228-45°	414	71	191
SPRAYING SYSTEMS	67228-45°	552	97	206

The values in Table 4.16 in conjunction with the data in Figures 4.11 to 4.14, suggest that at the higher atomising air pressures the most important factor in determining the size of droplets is not the atomising air mass flow rate, but the velocity of the air as it exits the air cap. Since with the Schlick gun the air velocity is virtually the same across the range of air pressures, the rise in droplet size with decreasing air pressure must be due to the reduction in air mass flow rate, with its accompanying reduction in the air to liquid mass ratio.

The resultant droplet size is therefore likely to be dependent on a complex relationship between the air velocity and mass flow rate. This is illustrated in Figures 4.11 to 4.14 which show a cross-over of some of the profiles as the air pressure changes and thus the relative effects of air velocity and mass flow rate change.

4.3.13 CORRELATION OF DROPLET SIZE DISTRIBUTIONS WITH MATHEMATICAL FUNCTIONS

The droplet size distributions produced by the spray guns studied in this work have been shown not to follow a normal distribution pattern (see Figures 4.15, 4.33 and 4.37). Three sets of representative data covering a wide range of average droplet sizes were therefore analysed to determine if they could be described by any alternative mathematical functions. The conditions which produced these data were;

Spray 1. Walther Pilot WA/WX spray gun, 12%w/w HPMC E5 solution, flow rate 80gmin^{-1}, atomising air pressure 276kPa, flat spray measured 180mm from the spray gun.

Spray 2. Schlick model 930/7-1 spray gun, 9%w/w HPMC E5 solution, flow rate 50gmin^{-1}, atomising air pressure 414kPa, flat spray measured 180mm from the spray gun.

Spray 3. Spraying Systems gun with a 2850 liquid nozzle and a 62240-60° air cap, 9%w/w HPMC E5 solution, flow rate 25gmin^{-1}, atomising air pressure 414kPa, droplets measured 180mm from the spray gun.

A log normal function, as used for example by Fraser and Eisenklam (1956) and Matsumoto and Takashima (1971) was found not to satisfactorily describe the droplet sizes within these sprays. This is demonstrated in Figure 4.40 where non-linear plots are apparent when the logarithm of the droplet diameter is plotted against the % weight oversize on a probability scale. Similarly, the non-linearity of Figure 4.41 shows the data not to fit a square root normal function.

The Rosin-Rammler function (Rosin and Rammler, 1933), which was the sole distribution function used by the original model of the Malvern analyser is described by Equation 4.8:

$$R = e^{-(D/D_{RR})^q} \qquad \text{Equation 4.8}$$

where R is the weight fraction of droplets greater than diameter D and D_{RR} and q are characterising parameters, namely the Rosin-Rammler mean droplet diameter and a dispersion coefficient. The data would comply with this function if a plot of ln(1/R) on a logarithmic scale against logD was linear. Figure 4.42 shows this function to more closely describe the sprays produced in this work. However there was a tendency for deviation to occur at the largest and smallest droplet sizes.

The main fault of the three distribution functions mentioned above is that they assume that extremely large droplets exist, albeit in small quantities. Actual droplets produced during atomisation will however have a maximum size which is stable under the atomising conditions used. In order to take this into account Mugele and Evans (1951) proposed a

LOG NORMAL PLOTS FOR DROPLET DISTRIBUTIONS PRODUCED FROM ATOMISED AQUEOUS FILM COATING SOLUTIONS

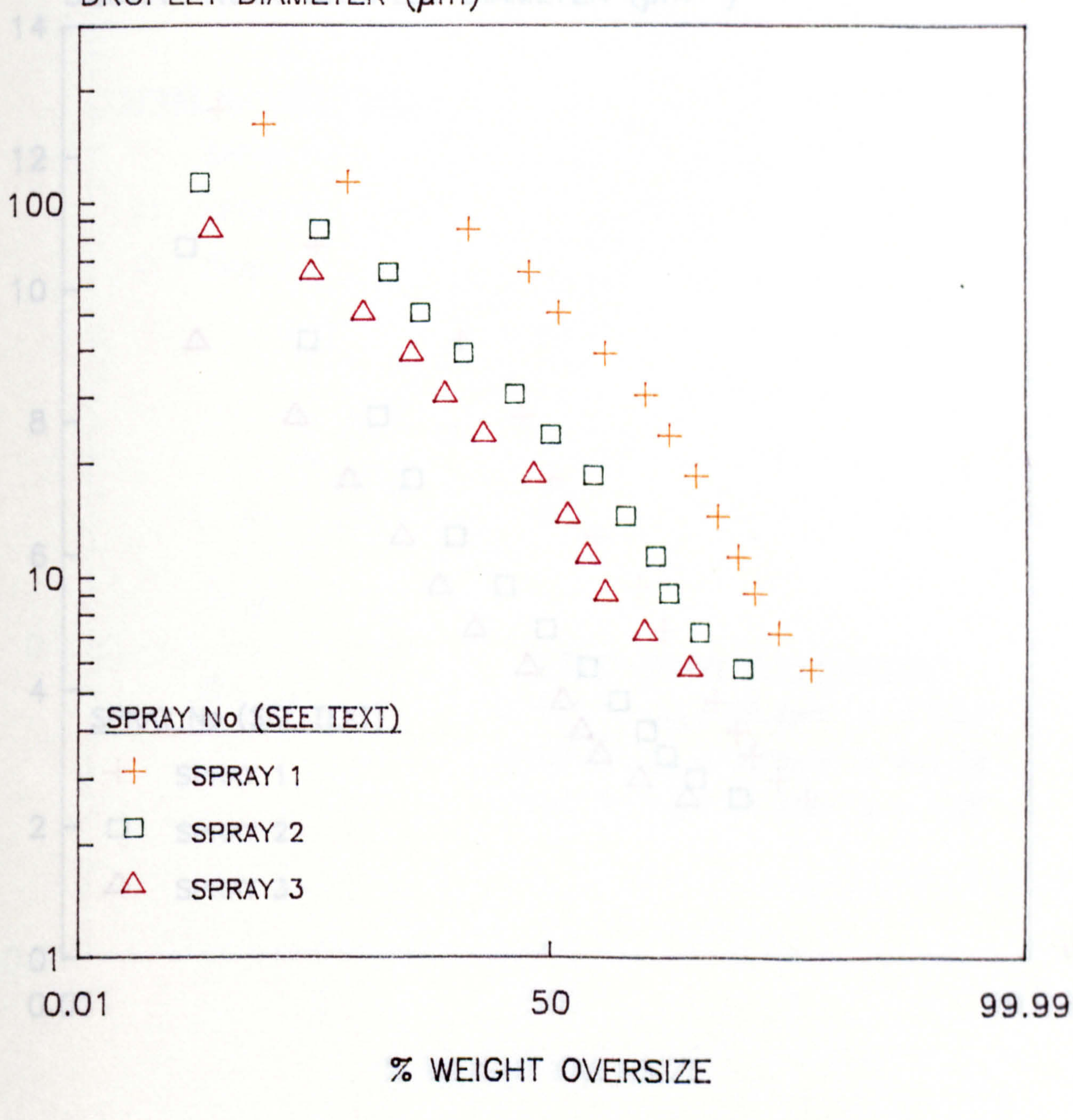

FIGURE 4.40

SQUARE ROOT NORMAL PLOTS FOR DROPLET DISTRIBUTIONS PRODUCED FROM ATOMISED AQUEOUS FILM COATING SOLUTIONS

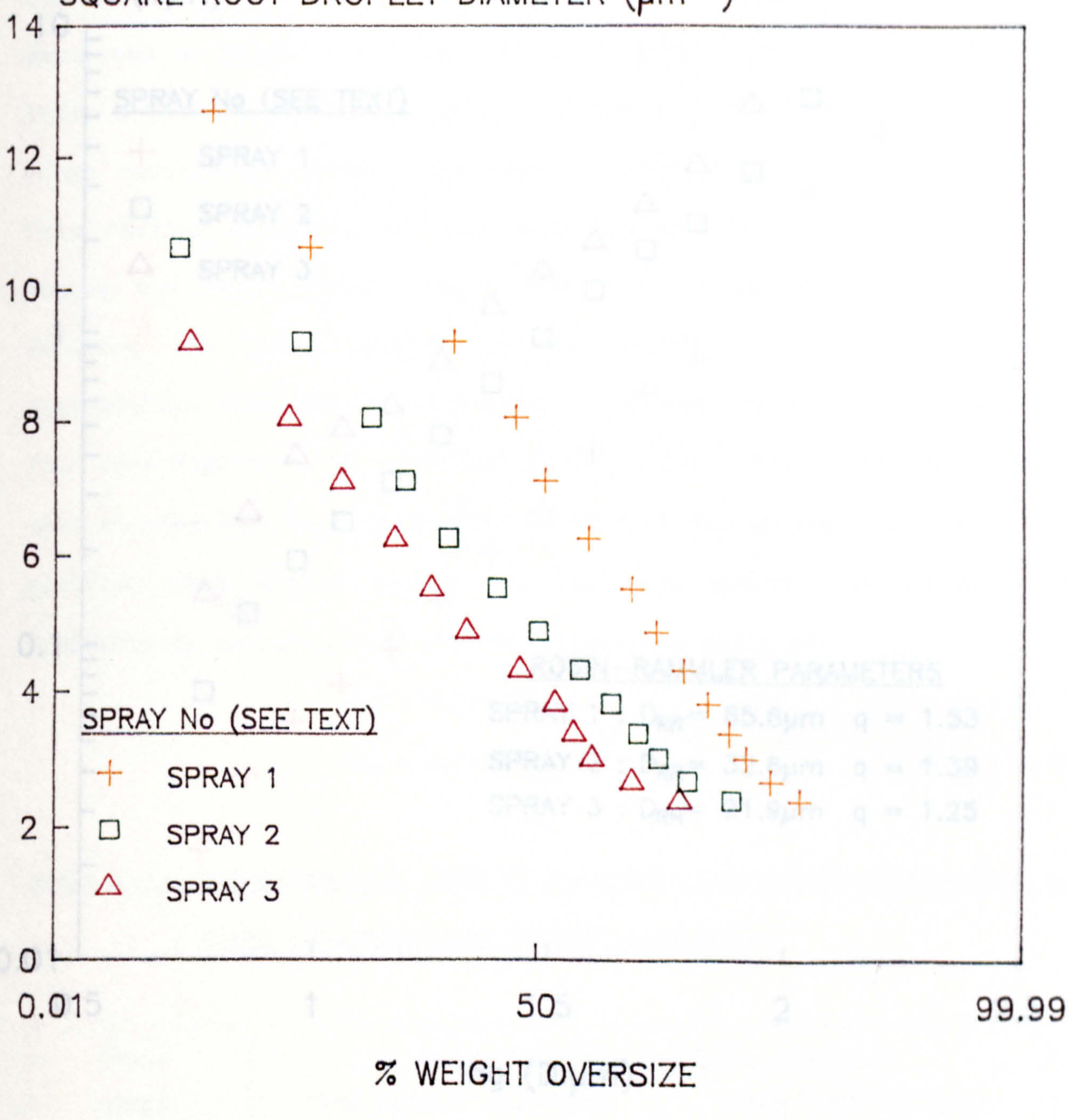

FIGURE 4.41

ROSIN–RAMMLER PLOTS FOR DROPLET DISTRIBUTIONS PRODUCED FROM ATOMISED AQUEOUS FILM COATING SOLUTIONS

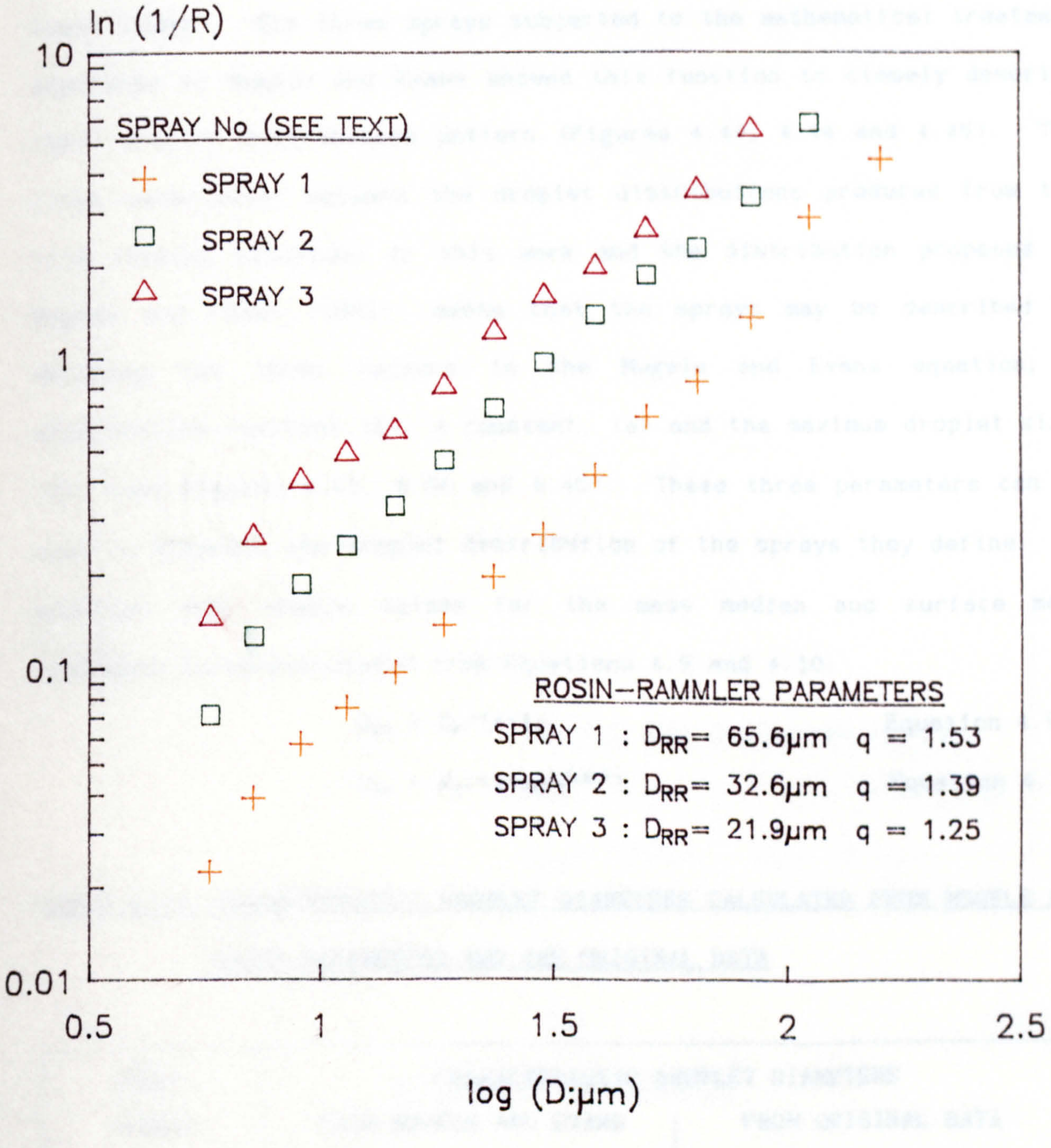

FIGURE 4.42

modified version of the log-probability distribution which they called the special upper limit function. This mathematical function includes a term for the maximum droplet size in the spray which can be estimated either from the Malvern data or calculated as described by Mugele and Evans (1951). The three sprays subjected to the mathematical treatment described by Mugele and Evans showed this function to closely describe their droplet distribution pattern (Figures 4.43, 4.44 and 4.45). The close association between the droplet distributions produced from the film coating solutions in this work and the distribution proposed by Mugele and Evans (1951), means that the sprays may be described by defining the three factors in the Mugele and Evans equation; a distribution function (δ), a constant, (a) and the maximum droplet size, (X_M) (see Figures 4.43, 4.44 and 4.45). These three parameters can be used to generate the droplet distribution of the sprays they define. In addition they enable values for the mass median and surface mean diameters to be calculated from Equations 4.9 and 4.10:

$$D_{MM} = X_M/(a+1) \qquad \text{Equation 4.9}$$

$$D_{SM} = X_M/(1+ae^{1/4\delta^2}) \qquad \text{Equation 4.10}$$

TABLE 4.17: CHARACTERISTIC DROPLET DIAMETERS CALCULATED FROM MUGELE AND EVANS PARAMETERS AND THE ORIGINAL DATA

SPRAY NUMBER	CHARACTERISTIC DROPLET DIAMETERS			
	FROM MUGELE AND EVANS		FROM ORIGINAL DATA	
	D_{MM}	D_{SM}	D_{MM}	D_{SM}
1	48.4	28.6	46.7	27.2
2	23.9	14.4	24.1	14.3
3	15.8	9.4	16.6	9.6

MUGELE AND EVANS PLOT OF THE DROPLET DISTRIBUTION OF SPRAY 1 (SEE TEXT FOR ATOMISATION PARAMETERS)

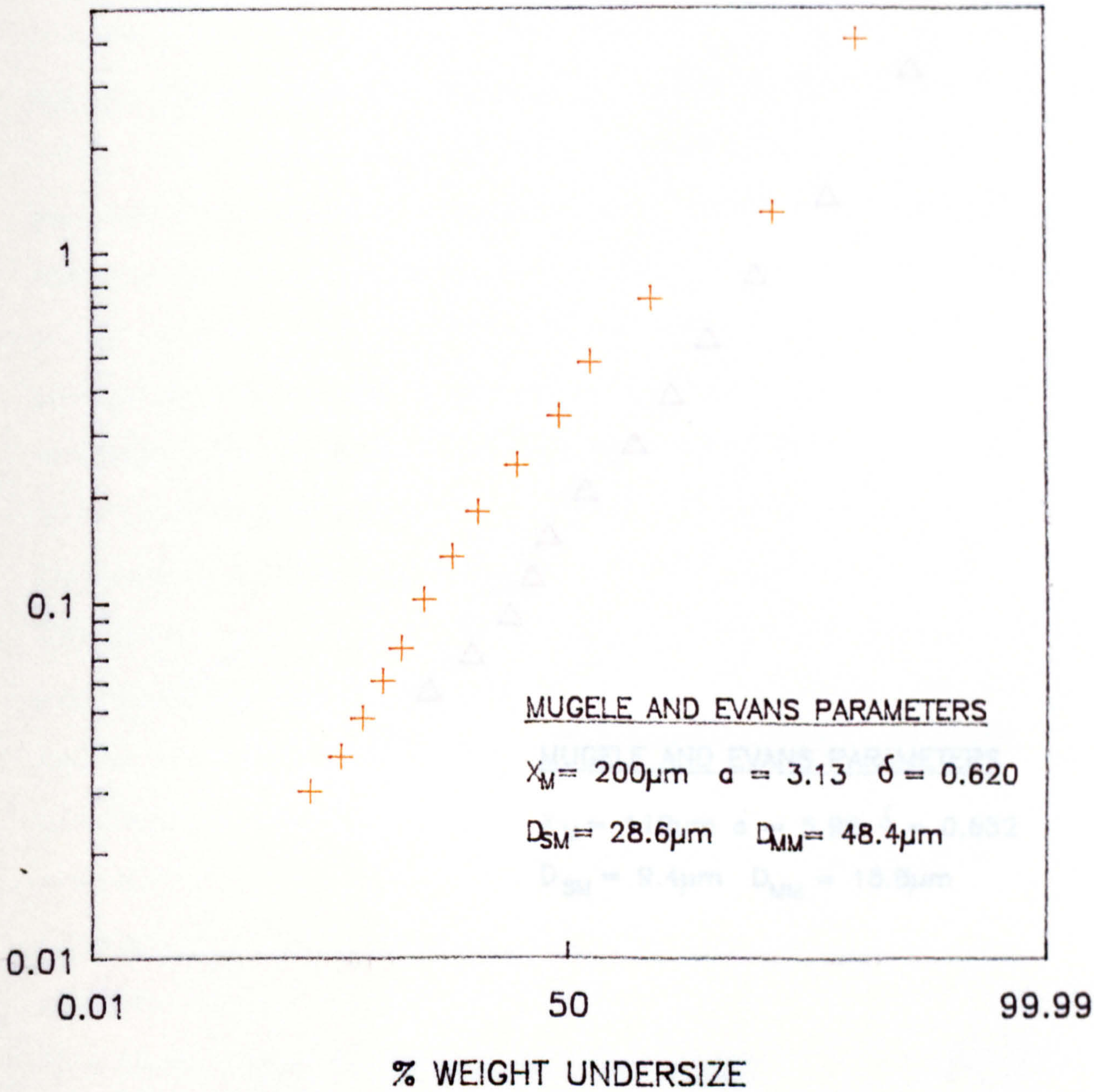

FIGURE 4.43

MUGELE AND EVANS PLOT OF THE DROPLET DISTRIBUTION OF SPRAY 3 (SEE TEXT FOR ATOMISATION PARAMETERS)

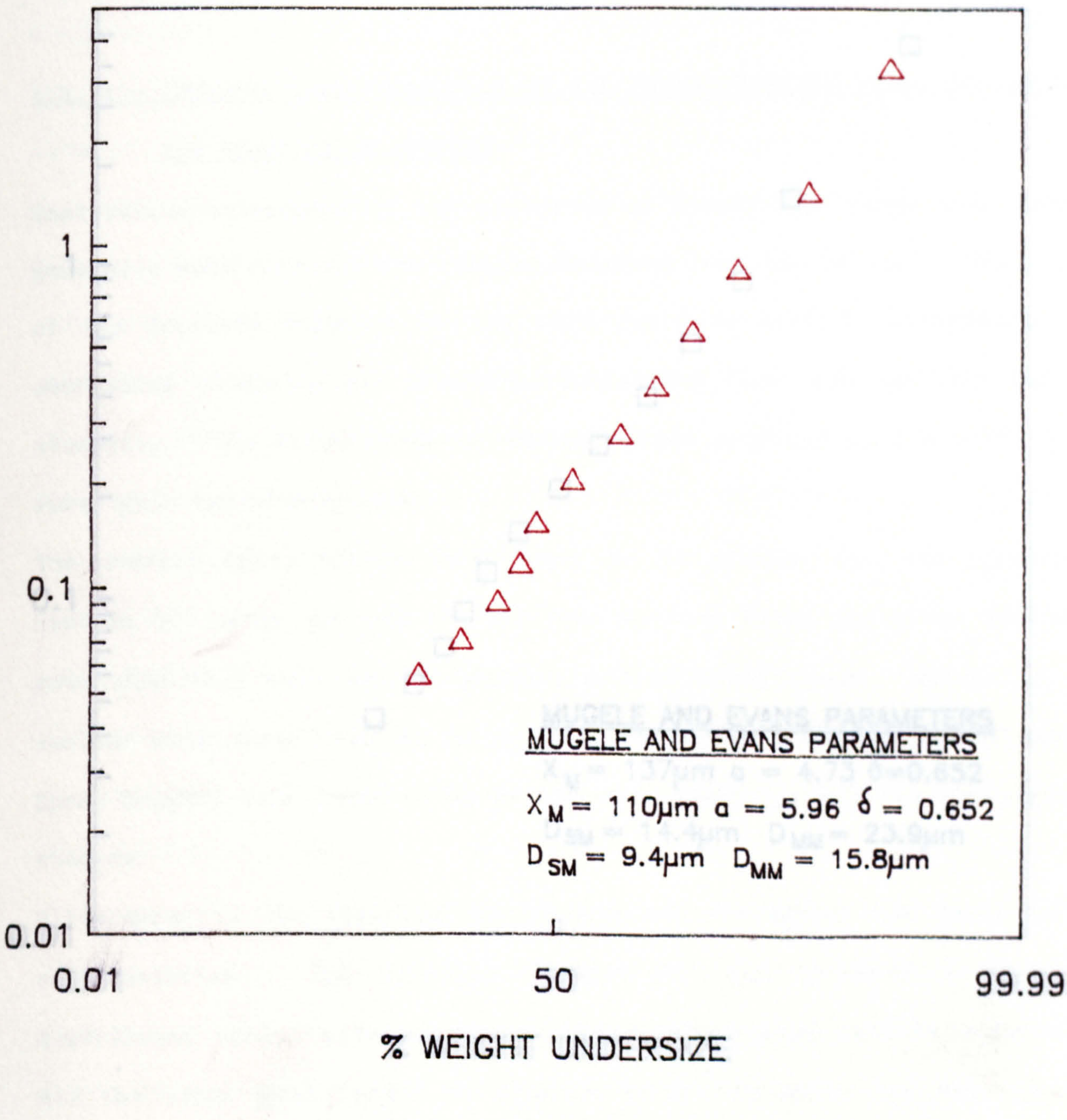

FIGURE 4.45

MUGELE AND EVANS PLOT OF THE DROPLET DISTRIBUTION OF SPRAY 2 (SEE TEXT FOR ATOMISATION PARAMETERS)

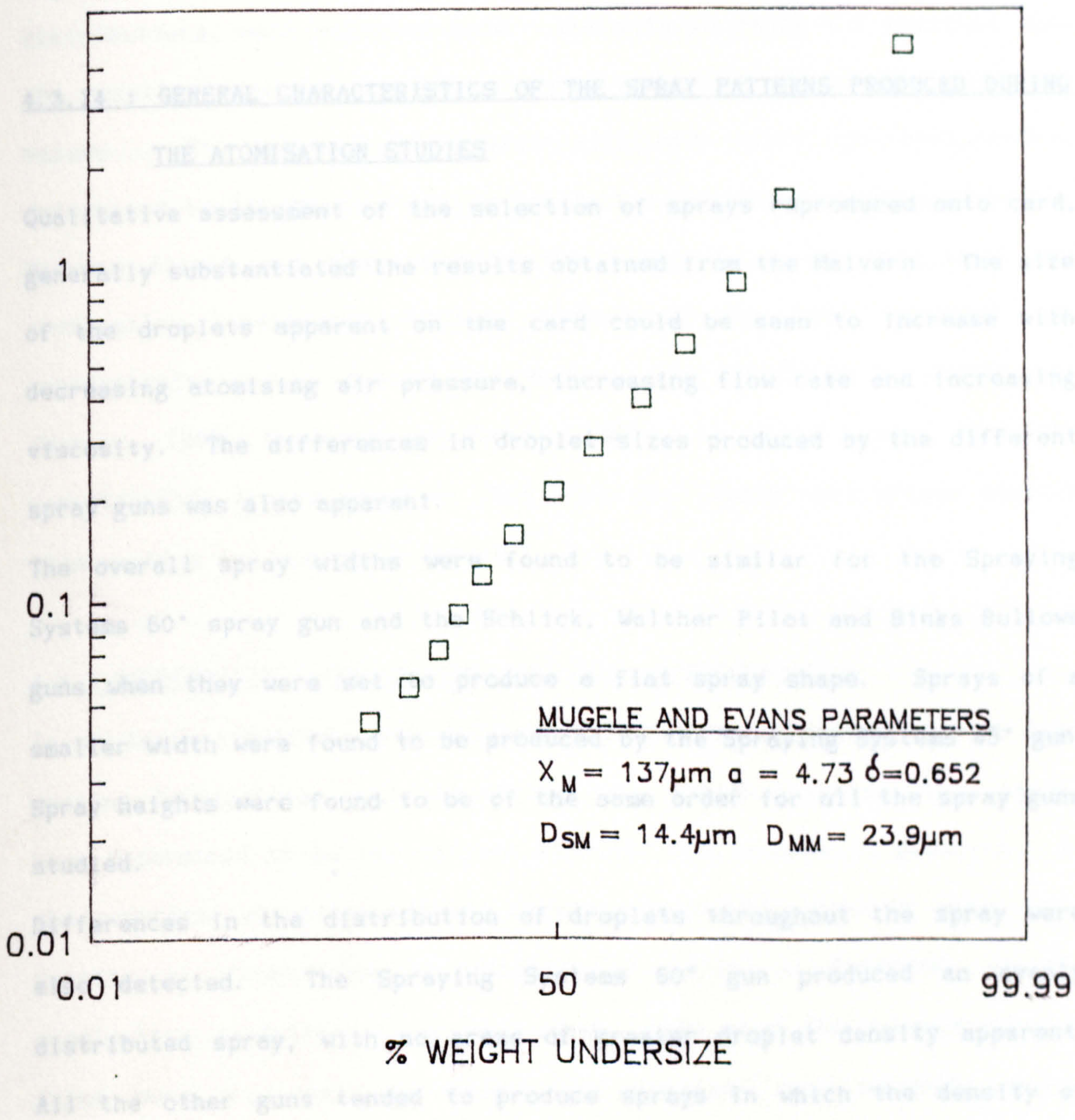

FIGURE 4.44

Values for the three sprays analysed are given in Figures 4.43, 4.44 and 4.45 and in Table 4.17. Table 4.17 also gives the comparative values calculated from the original data using the equations in section 4.1.5. The similarity in values is further evidence of the applicability of the Mugele and Evans function for defining the sprays.

4.3.14 : GENERAL CHARACTERISTICS OF THE SPRAY PATTERNS PRODUCED DURING THE ATOMISATION STUDIES

Qualitative assessment of the selection of sprays reproduced onto card, generally substantiated the results obtained from the Malvern. The size of the droplets apparent on the card could be seen to increase with decreasing atomising air pressure, increasing flow rate and increasing viscosity. The differences in droplet sizes produced by the different spray guns was also apparent.

The overall spray widths were found to be similar for the Spraying Systems 60° spray gun and the Schlick, Walther Pilot and Binks Bullows guns when they were set to produce a flat spray shape. Sprays of a smaller width were found to be produced by the Spraying Systems 45° gun. Spray heights were found to be of the same order for all the spray guns studied.

Differences in the distribution of droplets throughout the spray were also detected. The Spraying Systems 60° gun produced an evenly distributed spray, with no areas of greater droplet density apparent. All the other guns tended to produce sprays in which the density of droplets was greater in the central region. This effect was particularly noticeable with the Walther Pilot and Binks Bullows guns.

A more detailed account of the spray patterns, including a fuller description and actual spray dimensions, is detailed in Chapter 5.

4.4 DISCUSSION

The distribution of droplet sizes produced when atomising film coating solutions with a variety of spray guns and atomisation conditions has been determined using a Malvern droplet size analyser. This instrument allowed the generation of large amounts of data on atomised droplet distributions, with relative ease. The data in Table 4.4 indicate that the results presented are likely to be within in ±6% of the true mean values. The degree of repeatability and error in measurements determined by the Malvern will arise from two sources, those due to the Malvern itself and those due to the error in exactly producing the atomisation conditions required. Since it has been reported that repeatability errors due to the Malvern are likely to be within ±3% (Weiner, 1982; Hirleman and Dodge, 1985), it would appear that the repeatability errors found in this work are likely have arisen equally from machine and operation errors.

4.4.1 DROPLET SIZE DISTRIBUTIONS AND THEIR REPRESENTATION

In an ideal situation, the droplets produced on atomising aqueous film coating formulations would be of the same chosen diameter, this having been determined to be the optimum size for the process in question. In the practical situation however droplets have been shown to exist in a variety of sizes, the distribution of which is dependent on the atomisation conditions. In all cases, even when the largest droplet sizes were produced, the weight distributions were markedly skewed towards the smaller droplet sizes and did not follow a normal distribution (Figures 4.15, 4.33 and 4.37). In many of the droplet distributions there appeared to be evidence of a bi-modal distribution, as illustrated in Figures 4.15, 4.33 and 4.37. It is thought that this arises from the nature of the liquid delivery and is caused by the

pulsations in flow produced by the peristaltic pump system. The extent to which the apparent bi-modal distribution was observed appeared to be greater with the Binks Bullows spray gun and to be less apparent with the Spraying Systems gun combinations. Increasing the flow rate also appeared to reduce its occurrence. These latter observations would support the likely cause being due to the pump mechanism, since both the smaller liquid nozzle diameter (0.51mm and 0.71mm with Spraying Systems guns compared with 1.8mm on the Binks Bullows gun) and the increased spray rate tended to reduce the pulsation. The Schlick gun appeared to cause less pulsation than the Binks Bullows gun even when liquid nozzles of similar diameter were used. Differences in the way the liquid is delivered to the orifice may therefore also affect this phenomenon. Use of a liquid delivery system which does not produce a pulsed flow may lead to the production of sprays which do not exhibit a bi-modal distribution of droplet sizes. The type of distributions found in this work are however likely to be representative of many of the sprays used in coating work, including aqueous film coating, since peristaltic pumps are commonly used for these applications.

In an attempt to see if the spray could be described by any of the commonly used mathematical functions, data from selected runs covering a range of droplet size distributions were subjected to the appropriate mathematical and/or graphical analysis. Those studied included log normal (Figure 4.40), square root normal (Figure 4.41), Rosin-Rammler (Figure 4.42), and upper-limit log probability functions (Figures 4.43 to 4.45).

The log normal distribution, which has been reported to be applicable for the representation of sprays produced by rotary (vaned wheel) atomisers (Masters, 1976), was not found to adequately describe the three sprays examined in this work, since there was not a linear

relationship between the logarithm of the droplet diameter and the % weight oversize plotted on a probability scale.

The square root normal distribution has been shown to represent sprays from a centrifugal pressure nozzle (Masters, 1976). This distribution was found to be better than the log normal distribution in describing the sprays produced in this work, but the plots shown on Figure 4.41 indicate a sigmoidal rather than a linear relationship, with deviation appearing to occur at both low and high values of the % weight oversize. The empirical Rosin-Rammler function (Rosin and Rammler, 1933), was shown to more closely describe the sprays produced in this work (Figure 4.42). However there did appear to be a tendency for deviation to occur at the largest and smallest droplet sizes. A graphical plot of this function allows the Rosin-Rammler mean diameter (D_{RR}) and a dispersion coefficient (q) to be calculated. The value of q, which is determined from the slope of the plot, gives an indication of the uniformity of the distribution. The higher the value of q, the more uniform the distribution. The values of D_{RR} and q for the three representative sprays are shown in Figure 4.42. These, as would be expected from the general droplet distribution patterns, show the dispersion coefficient to increase with increasing D_{RR}.

The sprays subjected to the mathematical treatment described by Mugele and Evans (1951) showed this function to most closely describe their droplet distribution pattern (Figures 4.43 to 4.45). This occurred despite there being evidence of the droplet distribution having a bi-model distribution.

The usefulness of the upper-limit function in describing sprays and its superiority over other functions has been demonstrated for a variety of sprays by Masters (1976) and Bayvel (1985), as well as by Mugele and Evans (1951). The close association between the droplet distributions

produced from atomising the film coating solutions in this work and the distribution proposed by Mugele and Evans, means that the sprays may be described by defining the three factors in the Mugele and Evans equation; a distribution function (δ), a constant (a) and the maximum droplet size (X_m). Examples of these parameters are shown in Figures 4.43 to 4.45. The three parameters can be used to reconstruct the droplet distribution if the appropriate straight line is generated on probability paper. This technique is described by Mugele and Evans (1951). Further evidence for its applicability in describing these film coating sprays is demonstrated when the function is used to calculate values of D_{mm} and D_{sm}, which are seen to closely resemble those calculated from the original data (see Table 4.17).

The function however is not without its problems. The value of the maximum droplet diameter (X_m), needs to be estimated initially either from the data or by calculation. Estimating from the data may be difficult, especially if large droplets are present, since the Malvern droplet diameter band widths cover a wide range of droplet sizes. Calculation of the value mathematically requires the generation of values for $X_{0.1}$ and $X_{0.9}$ and may give significantly different X_m values to those estimated from the data. In practice some degree of trial and error is required to establish the appropriate value of X_m. Analysis of the data using the upper-limit function is also time consuming and is not conducive to computer generation of characteristic droplet sizes. Because of the excessive time required to subject all of the data sets generated in this work to the upper-limit analysis, the effects of atomisation conditions were generally explored by comparing mass median diameters (D_{mm}) and surface mean diameters (D_{sm}). Examination of cumulative weight percent undersize curves and the droplet distributions

showed these to be suitable representations of the spray for comparative purposes.

4.4.2 FACTORS INFLUENCING THE DROPLET SIZES OF SPRAYS PRODUCED DURING AQUEOUS FILM COATING

It was apparent from examination of the droplet distributions and characteristic droplet sizes that many factors will influence the size of the droplets impinging on a tablet surface during aqueous film coating. These factors include the atomising air pressure, spray rate, solution viscosity, spray gun type, distance from the spray gun, spray shape and the velocity and mass flow rate of the atomising air. These influencing factors in general cannot be examined in isolation since the effect of one variable is dependent to a varying extent on the one or more of the other variables.

Factors influencing droplet behaviour after leaving the spray gun

Before discussing the factors affecting droplet production, it is pertinent to examine the factors which may affect the droplets after they have left the spray gun, since these will contribute to the *actual* sizes measured by the Malvern droplet sizer.

Changes in droplet size which occur between leaving the spray gun and hitting the tablet surface may potentially arise from two sources; evaporation of volatile components from the droplets (Arai et al., 1982; Yoakam and Campbell, 1984; Meyer and Chigier, 1985; Tambour et al.,1985) or droplet coalescence (Wigg, 1964; Meyer and Chigier, 1985; Tambour et al., 1985). Their potential influence during aqueous film coating was investigated in this work by studying four factors. The changes in droplet size with increasing distance from the spray gun, the radial distribution of droplet sizes across the sprays, the effect of spray shape and the influence of atmospheric conditions into which spraying

took place.

When both 9%w/w and 12%w/w HPMC E5 solutions were atomised with the Schlick spray gun, it was found that as the distance from the gun at which the sprays were analysed increased, so did the mean droplet diameter at the centre of the spray. This type of behaviour has been reported by Wigg (1964), Prasad (1982), Arai et al. (1982) and Meyer and Chigier (1985), although not found to occur by Weiss and Worsham (1959). An increase in distance from 180mm to 350mm was found to give rise to an approximate doubling of the calculated mean droplet diameters (Figure 4.35 and 4.36). There are two possible explanations for these results. It may be that droplets are coalescing, which would reduce the number of the smaller droplets, increase the number of the larger droplets and increase the range of droplet sizes encountered. Alternatively, although evaporation would be expected to reduce the mean droplet size, it could be envisaged that evaporation may result in the smaller droplets effectively disappearing from the measuring range, thereby increasing the relative proportion of the larger droplet sizes and giving artificially high values for the droplet diameters (Arai et al., 1982). In this latter case an increase in the range of droplet diameters detected would not be expected. If evaporation was occurring, it might be expected to be potentiated by an increase in the temperature of the atmosphere into which evaporation was taking place. This would arise since there would be a decrease in the initial relative humidity of the air and an increase in the moisture carrying capacity. These would in turn increase the driving force for evaporation and allow a greater amount of water to be evaporated before the local saturation point was reached. A comparison of the results of experiments carried out with atomisation occurring either into a moving airstream created to simulate actual coating air conditions within a model 10 Accela-Cota, or

into still air at ambient temperature, is shown in Figures 4.38 and 4.39 and Table 4.14. Even though there were considerable differences in the air temperatures and thus their moisture carrying capacities and relative humidities, the results showed there to be no significant differences between droplet sizes measured in the two different environments. This was apparent over a range of distances from the spray gun and with a variety of atomisation conditions and mean droplet sizes. These results would appear to suggest that at the centre of the flat spray where the droplets were measured, little evaporation was taking place. The predominant cause of the increase in measured droplet sizes with increasing distance from the spray gun was therefore likely to have been due to droplet coalescence effects. A further indication of the occurrence of coalescence was given by an increase in the actual range of droplet sizes detected at distances of 280mm and 350mm. This effect was however small, probably due to the increased droplet size band range detected by the Malvern at the larger droplet sizes.

Droplet coalescence is likely to arise from the different momentum and velocities exhibited by droplets of differing sizes. The larger droplets are likely to be travelling at a greater speed (Meyer and Chigier, 1985) and thus may collide with the smaller droplets, resulting in coalescence. This will be aided by the natural turbulence created in the spray by the atomising air which tends to potentiate the speed and directional differences. Since the average droplet speed drops rapidly after leaving the spray gun, the time taken to travel a unit distance will increase as the distance from the gun increases. This, coupled with the greater differential between droplet velocities at increasing distances may tend to increase the amount of coalescence that occurs. Spray density (number of droplets per unit area) will however reduce as the distance from the spray gun increases, this occurring as a

consequence of the natural expansion of the spray. This reduction in spray density would tend to reduce the tendency for coalescence to occur, although its influence in this study would appear to have been small relative to the increase in size arising from droplet velocity effects.

Spray density, as well as changing with more obvious factors such as liquid flow rate, may also differ at different areas within the spray. The extent to which this occurs will depend on the type of spray gun and the relative proportions of atomising and spray shaping air. In order to determine whether variations in droplet density may produce radial differences in droplet sizes within a spray, sprays produced by the Schlick gun were analysed at various distances from the spray centre. The results of this study, which are detailed in Table 4.9, indicated that within the spray examined there were no obvious differences in droplet sizes at radial distances of up to 50mm from the centre of the spray. At a distance of 75mm however there was a suggestion that a decrease in droplet size occurred. Visual examination of the spray produced onto card indicated that there was a significantly greater spray density in the centre 130mm of the spray (65mm each side of the centre). Obscuration values from the Malvern also indicated a progressive lowering of spray density as the distance from the centre increased, especially between 50mm and 75mm from the spray centre. Droplet analysis could not be undertaken at distances greater than 75mm, since the density of droplets was insufficient for results to be obtained by the Malvern.

Three effects may potentially be occurring at increasing radial distances. Firstly, the reduction in spray density may reduce the tendency for droplet coalescence, this effect most likely to be occurring at distances greater than about 65mm from the spray centre.

Secondly, as the radial distance from the centre of the spray increases so does the actual distance travelled by the droplets before they are analysed. For example, if the droplets have to travel 180mm at the centre of the spray before being measured then they will have to travel 195mm when measured 75mm from the spray centre. This increased distance may potentiate coalescence as previously described. Thirdly, although evaporation from the droplets was thought likely to have been small at the spray centre, it may occur to a greater extent at increasing radial distances due to the reduced spray density and greater distance of droplet travel. For the sprays analysed, it would appear that at distances of up to 65mm from the spray centre the three effects described above tend to cancel each other out resulting in little change in droplet size. At greater distances it may be that the reduction in spray density has the predominant effect and therefore smaller droplets result.

Other factors which may influence the tendency for droplet coalescence to occur are the surface tension and viscosity of the droplets. The theoretical factors affecting the surface tension of droplets have been discussed in Chapter 3. If the concepts described are applied to the results generated from the Malvern, it is possible to estimate the droplet surface tension values. For a 9%w/w HPMC E5 solution it was calculated that droplets of greater than 137μm in diameter may have a surface tension (γ_d) of between 45.7mNm^{-1} and 55.4mNm^{-1}, whereas droplets below this diameter would have surface tension values above 55.4mNm^{-1}, the value of which can be calculated from the equation:

$$\gamma_d = 72.8 - 0.127D_d$$

where D_d is the droplet diameter below 137μm and 72.8 represents the surface tension of water in mNm^{-1}. Corresponding equations for 6%w/w and 12%w/w HPMC E5 solutions are given in Table 3.14.

If the data in Table 4.2 (which represents a spray produced using typical atomising parameters) is analysed using the above equation, it is apparent that within the spray, droplets of markedly different surface tension may potentially exist and that the surface tension of a significant weight proportion of droplets may approach that of water. For example the 21.8wt.% of droplets below 11.4μm can be calculated to have a surface tension above 71.4mNm^{-1}, the 49.4wt.% below 23.7μm a value above 69.9mNm^{-1}, the 74.8 wt.% below 39.0μm a value above 67.9mNm^{-1} and the 99.7wt.% below 112.8μm a value of greater than 58.5mNm^{-1}. It should be noted that these values are calculated on the basis that all the available HPMC E5 molecules have time to reach the droplet surface. If this is not the case, then droplet surface tension values may be even higher than those calculated. The high droplet surface tension values are calculated to occur despite the surface tension of the bulk unatomised solution being approximately 45mNm^{-1}. As well as potential consequences when the droplets contact the tablet surface, these differences in droplet surface tension may also influence the degree of droplet coalescence that occurs during passage to the tablet surface. Coalescence will be more likely to occur when surface tension and thus surface free energy values are high, since there is a greater tendency to try and reduce the surface area. The potential for coalescence is thus likely to increase as the droplet size decreases. This effect is more likely to occur with decreasing HPMC E5 solution concentrations, since both the droplet sizes generated after atomisation will be smaller (Figures 4.27 to 4.32) and there will be less molecules present to reduce the surface tension (see Chapter 3). Reducing the solution concentration will in addition reduce solution viscosity, which will also increase the likelihood of droplet coalescence.

Although the results indicate that at the centre of the spray the predominant effect that is occurring is coalescence, it is not suggested that evaporation does not take place. Indeed the occurrence of spray drying during aqueous film coating demonstrates that evaporation can occur. It is likely that evaporation will be most prevalent where the spray density is lowest, that is at the edges of the spray. This arises from reduced local relative humidity levels and is potentiated by the increased distances needed to be travelled and the associated increased time for evaporation to occur. An increased spray surface area arising from the production of smaller droplets will also increase the evaporation potential. Yoakam and Campbell (1984) reported that during the aqueous film coating process up to 30% of the solvent may be evaporated before the droplets contact the tablet bed, this value being determined from the temperature loss of the process air. However their methodology is questionable, few details of the coating process were reported and inlet air temperatures of up to 150°C were used.

A further factor which might be expected to influence evaporation is the temperature of the coating solution, with higher temperatures increasing the driving force for evaporation. Heating the coating solution however introduces a further complicating factor, since it will potentially also affect solution viscosity. This effect is discussed in more detail latter in this chapter.

Since the droplets contain dissolved polymer, it may be that a "crust" is formed on the droplet surface after a small amount of evaporation has taken place. This "crust" may then serve to maintain the diameter of the evaporating droplet despite further solvent loss. If this was occurring even considerable evaporation may only result in small decreases in the measured droplet size. This effect would be potentiated with HPMC E5 solutions due to the surface active nature of

the polymer.

The effect of the spray gun design on the atomisation process

Different spray guns were shown to produce different droplet size distributions, with different mean droplet sizes, when atomising solutions using otherwise identical conditions (Figures 4.11 to 4.14). At an air pressure of 414kPa (60psi) and spray rates of 50gmin^{-1} and below, the smallest droplets were produced by the Spraying Systems 60° gun, followed by the Spraying Systems 45° gun, Schlick gun, Walther Pilot gun and Binks Bullows gun. This was apparent at both of the solution concentrations investigated. This order was not maintained however at lower air pressures and higher flow rates, when the Spraying Systems guns were shown to produce relatively larger droplets. In each case however the droplets produced by the Schlick gun were smaller than those produced by the Walther Pilot gun, which in turn were smaller than those produced by the Binks Bullows gun which produced the largest droplets in every case studied.

The results could have potentially arisen from differences in:

1. The spray dimensions and the distribution of droplets throughout the spray
2. The liquid nozzle internal diameter
3. The area of the annulus between the liquid nozzle and the air cap and thus the volume flow rate, mass flow rate and velocity of the annulus atomising air
4. The total volume of air accompanying the spray to the point of analysis

One of these factors, the difference in liquid nozzle internal diameter between the spray guns, is unlikely to be a contributing factor in this work, since similar droplet sizes were produced with both the Schlick and Spraying Systems guns regardless of the liquid nozzles used (Table

4.10). This is in agreement with conclusions drawn by Weiss and Worsham (1959), Kim and Marshall (1971), Hukuo et al. (1976) and Shæffer and Worts (1977). Gretzinger and Marshall (1961) reported that increasing the liquid nozzle diameter may reduce the effective energy utilisation during atomisation which therefore may result in larger droplets being produced. The liquid nozzle diameters investigated in this latter study however ranged up to 5.51mm, which is significantly in excess of those used in this work or generally in aqueous film coating.

Liquid nozzle diameter differences could potentially influence the speed the liquid exits from the nozzle and thus both its speed relative to the atomising air and the shear forces it encounters. Increasing diameters would reduce the average liquid nozzle exit velocity and thus potentiate the velocity difference and reduce the shear forces exerted on the liquid. Liquid exit velocities can be calculated to range from an average 0.17ms^{-1} when spraying at a rate of 25gmin^{-1} through a 1.8mm nozzle, to 6.8ms^{-1} when spraying at 80gmin^{-1} through a 0.5mm nozzle. The atomising air velocity as it exits the air annulus is however likely to be greater than 150ms^{-1} (Table 4.16) and thus the relative difference in velocities will be affected minimally by changes in liquid nozzle diameter. Any effect of varying shear forces arising from different liquid velocities would not have been detected in this work, since the results in Table 4.10 were generated for Newtonian liquids.

It should be remembered that in this study changes in liquid nozzle internal diameter did not alter the air annulus area, since the external diameter remained constant. If this was not the case then changes in the liquid nozzle could potentially influence the atomisation process.

The spray dimensions and the distribution of droplets within the spray may affect the extent to which evaporation and coalescence effects occur and thus the droplet sizes measured by the Malvern. The likelihood of

coalescence occurring at the centre of the sprays (where they were analysed) becomes greater as the density of droplets increases. Examination of the spray patterns indicated that all spray guns except the Spraying Systems 60° gun produced sprays which had a central region in which the droplet density was greater than the rest of the spray. This effect was most noticeable with the Binks Bullows and Walther Pilot guns, probably due to the presence of either containing holes (Walther Pilot) or containing holes and angular converging holes (Binks Bullows) in the air cap as described in section 4.1.3. The central region of the sprays produced by the Schlick gun were less dense than either of the those from the above two guns, but more dense than those produced by the Spraying Systems 45° gun. These visual findings were confirmed by the obscuration values determined by the Malvern at the spray centres. Coalescence effects would therefore most likely to be occurring in the centre of sprays produced by the Binks Bullows and Walther Pilot guns, followed by the Schlick gun, Spraying Systems 45° gun and Spraying Systems 60° gun. As a result of this, radial differences in droplet sizes across the spray would also be most likely with the Walther Pilot and Binks Bullows guns and least likely with the Spraying Systems 60° gun. Droplet size distributions measured by the Malvern in the centre of the sprays may not therefore be truly representative of the actual overall droplet distribution. They will however reflect the majority of the spray, since this is contained within the more dense central region.

The overall degree of evaporation from the spray at any given distance from the spray gun may be expected to be highest in the case of the Spraying Systems 60° gun, due to its more even droplet distribution and greater proportion of droplets towards the spray periphery.

The annulus through which the atomising air exits can vary considerably, as evidenced by the data in Table 4.1. As a result of this, values for

volume flow rates, mass flow rates and velocity of the atomising air are different for each spray gun, as shown in Table 4.16. Since the energy used to atomise the droplets is derived from the kinetic energy of the atomising air, these differences may potentially influence droplet production. The air mass flow rate, calculated from the air density and volume flow rate, was shown to increase as the area of the annulus increased irrespective of the atomising air pressure used. There was no direct correlation however between the annulus area and atomising air velocity, although the trend was for the velocity to increase as the annulus area decreased.

Previous studies have demonstrated that the atomising air velocity is a major determinant of the droplet size produced by a spray gun, this arising from its influence on the relative air to liquid velocity at the nozzle exit, U_r (Nukiyama and Tanasawa, 1938; Mayer, 1961; Wigg, 1964; Kim and Marshall, 1971; Kumar and Prasad, 1971; Rizkalla and Lefebvre, 1975; Hukuo et al., 1976). Weiss and Worsham (1959) reported that D_{nn} was proportional to $U_r^{-1.33}$, Rizkalla and Lefebvre (1975) that D_{sm} was proportional to U_r and Hukuo et al. (1976) that D_{sm} was proportional to $U_r^{-0.61}$. Since it has been shown that in aqueous film coating the liquid exit velocity is negligible compared with the atomising air exit velocity, any changes in the value of U_r are likely to arise from changes in air velocity.

The mass flow rate of the atomising air has generally only been found to influence the droplet size if the ratio of air to liquid mass flow rates (M_a/M_L) drops below approximately 4, when a progressive increase in droplet size is seen (Gretzinger and Marshall, 1961; Rizkalla and Lefebvre, 1975). A similar trend has also been reported for air to liquid volume ratios (V_a/V_L) below approximately 4000 (Hukuo et al., 1976) and 5000 (Nukiyama and Tanasawa, 1938).

Figures 4.11 to 4.14 and Table 4.16 show that at an atomising air pressure of 414kPa (60psi), the higher the atomising air mass flow rate through the annulus of the spray gun, the greater is the size of the droplets produced. At this air pressure therefore it would seem that the air mass flow rate is not an important determinant of droplet size, despite the value of M_a/M_L being below 1.5 for both of the two Spraying Systems guns. At an air pressure of 414kPa, the smallest droplets were produced by the Spraying Systems 60° gun which exhibited the highest atomising air exit velocity and the largest droplets by the Binks Bullows gun which had the lowest air exit velocity. This suggests that at this atomising air pressure, the air velocity is the more important factor influencing atomisation. If this was the case, then it might be expected that of the other three guns the Walther Pilot would produce the smallest droplets, followed by the Spraying Systems 45° gun and the Schlick gun, although the difference would be expected to be small due to the similarity of the air exit velocities. The results however showed that the droplet sizes did not follow in the order given above, the smallest droplets of the three being produced by the Spraying Systems gun and the largest by the Walther Pilot gun. This discrepancy could well be explained however by the occurrence of droplet coalescence at the centre of the spray, which as previously described, would be greatest with Walther Pilot gun and least likely with the Spraying Systems 45° gun.

For each gun studied, the atomised droplet size increased as the atomising air pressure decreased, this effect tending to be particularly noticeable at air pressures of around 276kPa and below, and as the solution viscosity and spray rate increased. With the Schlick spray gun the atomising air velocity remained essentially constant irrespective of the air pressure used since the volume of air passing through the

annulus remained constant. The significant increases in droplet size seen with decreasing air pressure when using the Schlick gun are therefore not likely to be due to changes in air exit velocity, but to the reduction in air mass flow rate which occurs as the air pressure and thus air density decreases. It would appear that with the Schlick gun, the increase in droplet size with decreasing air pressure is relatively small until M_a/M_L decreases to a 'critical' value, below which the droplet size increases significantly. This critical value can be calculated to be approximately equal to 1.

With the other spray guns, reducing the atomising air pressure not only reduced the air mass flow rate but also the exit air velocity, this latter effect being especially noticeable in the case of the two Spraying Systems guns. The increase in droplet size with decreasing air pressure with these guns is therefore likely to be due to a combination of both a reduction in air velocity and air mass flow rate. This makes it difficult to determine the critical values of M_a/M_L.

The relative droplet sizes produced by the spray guns was also seen to alter as the air pressure was reduced. The Spraying Systems guns for example produced the smallest droplets at an air pressure of 414kPa, but at a pressure of 138kPa produced larger droplets than both the Schlick and Walther Pilot guns. This is thought to be due to the lower atomising air mass flow rates exhibited by the Spraying Systems guns and the reaching of the critical M_a/M_L values at higher atomising air pressures.

Another potentially important factor which has been shown to vary between different spray guns and at different air pressures, is the total volume of cool air (air consumption) which accompanies the spray after it has been produced (Table 4.5). This comprises a combination of the atomising and spray shaping air after they have expanded on leaving

the air cap of the spray gun. Although not a determinant of the atomised droplet size (this being dependent on the annulus air velocity and mass flow rate), the total volume of air may influence the behaviour of the droplets on the way to and on arriving at the tablet surface. The momentum of the droplets after leaving the spray gun will be obtained from the kinetic energy of the atomising and spray shaping air, and will thus be a function of the air mass flow rate and velocity. The momentum of the air/droplets at the point of reaching the tablet bed will therefore be dependent on both the air exit velocity from the annulus and the side-port holes, and the air density and total volume. Increases in atomising air pressure, which increase air consumption, and usage of spray guns with higher air consumption values, will both increase the momentum of the droplets and may therefore influence the spreading and penetration behaviour of droplets on the tablet surface.

Changes in air consumption will also influence the total volume of air passing through the coating pan and its temperature. This in turn may influence the tablet bed temperature, the evaporation from the droplets on the way to the tablet bed and the drying characteristics of the droplets on the tablet surface. The likely extent of these effects may be calculated if the drying air volume flow rate and temperature and the spray gun air consumption and air temperature are known.

<u>The influence of spray shape on the atomised droplet size</u>

The influence of spray shape on the droplet size measured by the Malvern was investigated for the Schlick and Walther Pilot guns, the results being shown in Table 4.8. The results indicated that the droplet size at the centre of sprays produced by the Walther Pilot gun was independent of the spray shape. The Schlick gun however appeared to produce larger droplets at the spray centre when set to form a narrow angle cone shape. These observations are thought to arise from

differences in the distribution of droplets within the sprays produced by the two guns. As previously described, when the Walther Pilot gun is set to produce a flat spray, the spray contains a dense region of droplets in the spray centre. The Schlick gun, although also producing a more dense central region, does so to a lesser extent than the Walther Pilot gun and consequently produces a more evenly distributed spray. The cone-shaped sprays produced by both guns cover a similar area (approximately one-third of that of the flat sprays) and have a similar droplet density. Thus when the spray is changed from flat shape to a cone, there is a greater increase in droplet density in the centre of sprays produced by the Schlick gun than the Walther Pilot gun and consequently a greater likelihood of the droplet size increasing due to increased coalescence. The reduction in total atomising air volume which accompanies the change to the cone-shaped spray is thought unlikely to have been a contributing factor, since this reduction was greater with the Walther Pilot gun than with the Schlick gun.

<u>The influence of liquid viscosity on the atomised droplet size</u>

The influence of liquid viscosity on the droplet size produced by the various spray guns is detailed in Figures 4.27 to 4.32 and Table 4.6. Increases in HPMC E5 solution concentration (and thus viscosity) increased the average size of the atomised droplets, this effect appearing to be more noticeable as the flow rate increased and the atomising air pressure decreased. The increase in droplet size is thought to have arisen mainly from the increased energy required to overcome the viscous forces resisting liquid acceleration and droplet formation. The tendency for more viscous liquids to exhibit reduced evaporation and resist coalescence may also have been contributing factors.

To gain an estimation of the mathematical relationship between viscosity

and droplet size, sets of data were analysed where the solution viscosity was the only parameter varied. This analysis took the form of a plot of the logarithm of the mean droplet size against the logarithm of the solution viscosity. The plots were generally of a linear form for both the surface mean diameter and mass median diameter, bearing in mind the inherent variation in determining the droplet sizes and the fact that only three data points were available for the majority of the plots. This linearity indicates that the relationship between the mean atomised droplet diameter and viscosity can be described in the form $D_a \alpha \mu^n$. Since there was no evidence to suggest that the values of n (gradient of the slope) were dependent on either the atomisation conditions, air pressure, liquid flow rate or spray gun type, an average value was calculated from the 17 sets of data (13 from the Schlick gun (data from Figures 4.27 to 4.32) and one each from the other four spray guns (data from Table 4.6)). For the mass median diameter n was found to be 0.185 ± 0.036 and for the surface mean diameter, 0.114 ± 0.033. The equations describing the relationship between droplet diameter and viscosity therefore are:

$$D_{mm} \alpha \mu^{0.19} \text{ or } D_{mm} = B\mu^{0.19} \qquad \text{and}$$

$$D_{sm} \alpha \mu^{0.11} \text{ or } D_{sm} = B\mu^{0.11}$$

where B is composite factor dependent on the other atomisation conditions.

These values of n are in good agreement with those of Masters (1976) and Shæffer and Wørts (1977) who suggested values of n for the mass median diameter of 0.17 to 0.20 and 0.17 respectively. They differ however from those of Weiss and Worsham (1959) and Wigg (1964) who reported values of 0.34 and 0.50 respectively.

The above equations were generated from HPMC E5 solutions which are Newtonian in character and can therefore be represented by a single

value of viscosity. When suspensions such as the Opadry formulations are atomised, the situation is more complex, since pseudoplastic properties are exhibited and the viscosity at the point of atomisation will be dependent on the shear forces encountered at that time. In addition, the droplet size may be influenced by the volume of the solid components present, as described by Sakai et al. (1985). Consideration of these effects may explain why the droplet sizes measured from atomised Opadry suspensions appear to be smaller than would be envisaged from their apparent Newtonian viscosity values.

Sakai et al. (1985) suggested that the diameter of droplets increases with addition of solid components by a factor of $\alpha^{-1/3}$, where α is the liquid volume fraction. This effect is however thought to have been of minimal importance with the suspensions examined in this work, since the maximum dispersed solids volume fraction (for a 25%w/w Opadry suspension) was of the order of about 0.04, which would have only increased the droplet size by a factor of approximately 1.01.

The Opadry suspensions may encounter considerable shear forces both during their passage through the liquid nozzle and from the high velocity atomising air as it leaves the annulus surrounding the liquid nozzle. Using methods suggested by Henderson et al. (1961), it can be calculated that the approximate shear rates encountered by the suspensions as they pass through a 0.8mm liquid nozzle, would be $8300s^{-1}$ for a flow rate of $50gmin^{-1}$ and $13,280s^{-1}$ for a flow rate of $80gmin^{-1}$.

An indication of the shear forces exerted by the atomising air at the point of exit from the air cap, can obtained from the equation for the rate of shear,

$$S = dv/dr$$

where v is the velocity at which the suspension is sheared (the difference between the air and liquid exit velocities) and r is the

thickness of the suspension layer. For a 0.8mm diameter liquid nozzle and a value of v of 200ms^{-1} (typical for an atomising air pressure of 414kPa, see Table 4.16), the shear rate can be calculated to be 5 x 10^{5}s^{-1}. Viscosity values at various shear rates can be calculated for each suspension using the power-law equation (Equation 3.8) and the data in Tables 3.6 and 3.7. Because of the nature of these relationships, the most noticeable reduction in viscosity with increasing shear rate occurs at low shear rates. As the shear rate increases, the viscosity tends to plateau out and at values over 10,000s^{-1}, little further reduction in viscosity is apparent. Since with each spray gun at each atomising air pressure the shear rate is likely to be considerably greater than 10,000s^{-1}, then it would appear that at the point of atomisation, the suspension viscosities will be of a similar order irrespective of the spray gun or atomising air pressure used. Estimated viscosity values were calculated as being 260mPa s and 730mPa s for 15%w/w and 20%w/w Opadry type OY suspensions respectively and 150mPa s and 360mPa s for 20%w/w and 25%w/w Opadry type OY-D suspensions. Substitution of these values for those of the apparent Newtonian viscosities in Table 4.7 supports the validity of the calculations, since the droplet sizes are then seen to increase in relation to viscosity.

<u>The effect of heating film coating solutions prior to atomisation</u>

Heating film coating solutions has been shown to cause a reduction in their viscosity (section 3.3.1 and Table 4.15). It was considered therefore that the heating of formulations prior to atomisation may be used as a method of reducing the atomised droplet size. This has been demonstrated previously by Garner and Henry (1953) and is also suggested in the manufacturers literature for Pharmacoat (a range of HPMC products of various grades). The results in Table 4.15 for solutions atomised by

the Schlick spray gun however indicate that heating the coating solutions up to temperatures of 37°C before they enter the spray gun has a minimal effect on the resultant atomised droplet size. Similar findings were reported by Shæffer and Worts (1977) for the pneumatic atomisation of fluidised-bed granulation solutions. There are two factors which may explain these results. Firstly, the reduction in droplet size arising from the lower solution viscosities is likely to be relatively small. For example heating a 9%w/w HPMC E5 solution from 20°C to 37°C, which produces a reduction in viscosity from 166mPa s to 83mPa s, can be estimated from previously described equations to cause the mass median droplet diameter to fall by 3.7µm for flow rates of 80gmin^{-1} and 2.7µm for flow rates of 40gmin^{-1} when using a Schlick gun and an atomising air pressure of 414kPa. The second possible explanation for the results is that at the point of droplet detachment, the viscosity has returned to its original (unheated) value. Since the coating solution travels relatively slowly through the liquid nozzle in comparison with the cool atomising air in the surrounding chamber of the spray gun, a type of heat exchanger system may exist within the gun which may cool the solution before it leaves the liquid nozzle. As the solution leaves the liquid nozzle in a the form of a small diameter cylinder, it is immediately surrounded by a large volume of high velocity expanding cool air. This again may provide a sufficiently good heat transfer system to cool the liquid before it is accelerated and broken up into droplets.

It would thus appear that attempts to reduce the droplet size produced by the Schlick gun by heating the coating solutions would prove unsuccessful. This is also likely to be the case with the Walther Pilot and Binks Bullows guns, since both the time taken for the coating solutions to pass through these guns and the volume of the atomising air

are greater. With the Spraying Systems guns studied there may be a reduced potential for the cooling effects to occur, since the air volumes through the gun are lower and there is shorter distance over which heat exchange can occur within the gun.

The effect of spray rate on the atomisation process

Increasing the spray rate between 25gmin^{-1} and 80gmin^{-1} was shown to cause an increase in the mean atomised droplet size. This effect occurred with each spray gun, atomising air pressure and solution viscosity studied. The actual increases in droplet size appeared to be greater as the air pressure decreased and solution viscosity increased and were particularly noticeable for the Spraying Systems 60° gun.

It was concluded from previous dicussions, that at a fixed liquid mass flow rate (spray rate), increases in the atomising air mass flow rate had only a small effect on droplet size providing the air:liquid mass ratio was above a critical value. Data in Figures 4.17 to 4.26 however demonstrate that at a fixed air pressure, increases in spray rate cause an increase in droplet size, this occurring despite the air:liquid critical ratio being exceeded. This indicates that the spray rate influences the droplet size independently of the other atomisation parameters, a finding also reported by Kim and Marshall (1971). This independent effect of the spray rate will act in addition to its influence on the air:liquid mass flow ratio, the latter effect tending to become important at low atomising air pressures.

To determine if there was a mathematical relationship between spray rate (SR) and mean droplet size, an approach similar to that described previously for solution viscosity effects was adopted. Plots of the logarithm of droplet size against the logarithm of spray rate indicated that for the Schlick gun the following relationships applied:

$$D_{nn} \alpha SR^{c}$$

$$D_{sn} \alpha SR^{D}$$

where C = 0.370 ± 0.084 (%CV = 22.7) and D = 0.288 ± 0.082 (%CV =.28.4). n = 14 in both cases.

The values of C and D appeared to be independent of solution viscosity or atomising air pressure.

There was insufficient data for meaningful equations to be generated for the other spray guns, although it did appear than the values of C and D were likely to be different from those of the Schlick gun.

4.4.3 CONCLUSIONS

The results detailed in this chapter have demonstrated that during the aqueous film coating process, many variables may potentially affect the properties of the droplets when they reach the tablet surface. The most important of these are the type of spray gun and its distance from the tablet bed and the atomising air pressure used. These will not only exert a considerable influence on the atomised droplet size, but also on the droplet momentum, spray density and the degree of evaporation and coalescence that occurs during travel to the tablet bed. Increasing coating solution concentration and thus viscosity will increase the atomised droplet size, although over the viscosity range used practically this effect is likely to be relatively small. Attempts to reduce droplet sizes by heating the solutions prior to atomisation were not successful. The liquid flow rate used during coating will influence the droplet size independently of the other atomisation parameters. During their passage to the tablet surface, the droplets in the centre of the spray are likely to increase in size since droplet coalescence effects predominate over solvent evaporation effects.

The surface tension of the droplets contacting the tablet surface may

potentially vary considerably between droplets of different size and solutions of different concentration. It is suggested that droplet surface tension values may be significantly higher than envisaged from measurement of the unatomised solution surface tension.

The effect of the atomisation stage on the aqueous film coating process and resultant film coat properties is examined in Chapter 5.

CHAPTER 5

THE INFLUENCE OF ATOMISATION AND PROCESS CONDITIONS ON THE PROPERTIES OF AQUEOUS FILM COATED TABLETS

5.1 INTRODUCTION AND LITERATURE REVIEW

The properties of aqueous film coated tablets will depend primarily on four factors; the constituents and properties of the tablet core, the coating formulation applied, the process conditions under which film coating takes place and the environment in which the tablets are consequently stored.

The following sections review the literature pertaining to the above factors which have relevance to this thesis.

5.1.1 THE TABLET CORE

During the film coating process tablets are subjected to abrasive and mechanical forces whilst tumbling in the coating pan. The tablet cores must therefore be sufficiently robust to withstand these forces in order that an elegant product containing the appropriate level of active ingredient is produced. The problems associated with preparing tablet cores with suitable mechanical properties and their subsequent evaluation has been discussed by Gamlen (1983). Seager et al. (1985) concluded that direct compression, precompression, wet massing, fluidised-bed granulation and spray drying techniques could all be used to prepare tablets for film coating, although the method of preparation could give rise to differences in biopharmaceutical characteristics.

Leaver et al. (1985) showed that when coating in a 24in Accela-Cota, the size of the tablet core influenced the duration at the bed surface and the time between surface appearances (circulation time). For tablets between 7.5mm and 11mm in diameter, it was found that the larger the tablet the longer was the average surface residence time and the

circulation time. This was attributed to changes in the balance of forces acting on the tablets, the smaller tablets being lifted further and forming a steeper bed surface angle.

Rowe and Forse (1974) showed that for 6.5mm, 8.5mm and 10mm biconvex tablets coated in a 24in Accela-Cota, the proportion of tablets failing a film continuity test increased as the tablet diameter increased. This was attributed to the greater momentum of the larger tablets as they struck the coating pan resulting in greater attrition forces.

The selection of intagliation shape was shown by Rowe (1981a) to be an important consideration in the preparation of tablets for film coating. It was demonstrated that tablets with larger/deeper intagliations were less susceptible to the defect of intagliation bridging. This was thought to be due to enhanced film to tablet adhesion arising from the greater intagliation surface area.

The initial porosity and surface roughness of tablets intended for film coating will be dependent on both the compaction pressure used in their preparation and their shape (Rowe, 1978a; Rowe, 1978b; Rowe, 1979). Fisher and Rowe (1976) showed a direct correlation between the arithmetic mean surface roughness of tablets and their porosity. For tablets with porosities of up to 20%, it was shown that a rise in porosity yielded film coats with a proportionately larger value of measured adhesion to the tablet substrate. These findings were attributed to differences in the penetration rate of the film coating solution.

Nadkarni et al. (1975) also demonstrated an increase in film adhesion with increasing tablet surface roughness. They however suggested that this was due to an increase in interfacial area between the tablet and solution rather than due to enhanced tablet coating solution penetration.

Zografi and Johnson (1984) suggested that the adhesion of film coats to rough surfaces may be facilitated by the tendency of droplets to exhibit receding contact angles approaching zero on these surfaces, this ensuring good coverage of the surface on evaporation of the coating solvent.

The increase in arithmetic mean roughness with increasing tablet porosity has also been shown to influence the surface roughness of the final coated product (Rowe, 1978b). Generally the higher the initial surface roughness, the greater was the surface roughness after the completion of the coating process. The surfaces of biconvex tablets were demonstrated to be rougher than those of flat tablets of the same diameter, composition and porosity. These differences were still found to be apparent after film coats had been applied.

The tablet core constituents will play an important role in achieving a successful coated product. Rowe (1977) examined the effect of some direct compression excipients and tablet lubricants on adhesion values of HPMC film coats. He found adhesion to be influenced by the polarity of tablet surface. Tablets prepared from microcrystalline cellulose were shown to exhibit high adhesion values, this being attributed to the presence of hydroxyl groups at the surface which were able to form hydrogen bonds with the HPMC. The effect of tablet lubricants was found to be dependent on their non-polar hydrocarbon content. Of the lubricants studied, stearic acid was found to be preferable as far as adhesion was concerned, a factor accredited to the presence of the free carboxyl group. When this carboxyl group was combined with either calcium (calcium stearate) or magnesium (magnesium stearate) the measured adhesion was markedly reduced.

The tablet surface free energy and polarity and interactions with the coating solution components have been shown by Costa and Baszkin (1985)

to influence the contact angle, spreading and penetration at the tablet surface. They showed that the contact angles made by a series of polyols on tablets of various formulations were dependent on the tablet surface free energy, and that the constituents played a part in modifying this surface energy. The authors also showed the tablet core constituents to influence tablet pore size and consequently penetration rates into the tablet.

Simpkin et al. (1983) illustrated the importance of considering the proportion and solubility of the active ingredient within the tablet core. Tablets where the active ingredient comprised the majority of the tablet, were shown to be particularly susceptible to coat defects such as poor adhesion and peeling, if the active ingredient was soluble in coating solvent. This applied whether the solvent was aqueous or organic. It was suggested that this effect was due to the formation of an intermediate surface layer between the tablet core and the film coat which interfered with the adhesive forces through physical or chemical means.

The role of the tablet constituents in the build up of stresses within the film coat and the incidence of coat defects has been discussed by Rowe in a series of papers (Rowe, 1980b; 1981b; 1981c; 1983b and 1986). Equations adapted from those of Croll (1979) and Sato (1980) illustrated the importance of the relative thermal expansion coefficients of components of the tablet core and film coat. It was illustrated that the inclusion of tablet components which have low coeffients of thermal expansion compared to the coating polymer HPMC (eg magnesium stearate and calcium stearate), produce film coats which are particularly prone to defects. This was proposed to be a result of the build up of stresses within the film, these arising from the differing degrees of expansion and contraction between the core and coat as the tablet warms

up and cools down during the coating process.

The importance of considering the melting point and purity of the tablet components has been illustrated by Rowe and Forse (1983b) in relationship to pitting, a defect where pits occur in the surface of the tablet core without any visible disruption of the film coating. Pitting was shown to occur when the tablet bed temperature exceeded the melting point of one or more of the constituents. This phenomenon was illustrated with reference to stearic acid, which has a melting point between 51°C and 69°C depending on its quality and PEG 6000 and vegetable stearin which have melting points of 60°C and 62°C respectively.

5.1.2 COATING FORMULATION

Hydroxypropyl methylcellulose (HPMC) is the most commonly used coating polymer for non-modified release coats. HPMC is available in a variety of grades, these being characterised by the apparent viscosity (mPa s) of a 2% aqueous solution at 20°C when measured under defined conditions. The viscosity grades used in aqueous film coating are predominantly those with viscosity designations between 3mPa s and 15mPa s. A particular polymer grade is made up of a wide variation of molecular weight fractions, as demonstrated by Rowe (1980a), Tufnell et al. (1983) and Davies (1985). These fractions are responsible for the viscosity of the polymer solution and the film properties. Rowe (1976a) showed that for HPMC grades having a nominal viscosity between 3mPa s and 50mPa s, the properties of films applied to tablets could be related to the polymer average molecular weight. Higher molecular weight polymers were shown to be harder, less elastic, more resistant to abrasion, to dissolve more slowly and to give rise to an increased tablet crushing strength.

The effect of polymer average molecular weight on the incidence of cracking and edge splitting of HPMC aqueous film coated tablets, was investigated by Rowe and Forse (1980) using a tablet substrate which was known to be prone to these defects. HPMC grades between 5mPa s and 15mPa s were utilised and the films plasticised with glycerol and pigmented with titanium dioxide. Increasing the molecular weight from 4.8×10^4 to 5.8×10^4 (equivalent to a change from a 5mPa s to a 8mPa s grade) was shown to produce a marked reduction in the incidence of film splitting, but a further increase to 7.8×10^4 (equivalent to a 15mPa s grade) produced much less of a reduction. These results were compared with data from Rowe (1980a) involving free films and it was demonstrated that there was an inverse relationship between the incidence of edge splitting and the free film tensile strength.

Further evidence of the influence of HPMC grade on film mechanical properties was shown by Fell et al. (1979) when measuring the mechanical strength of film coated tablets. For grades of nominal viscosity between 3mPa s and 60mPa s it was found that the maximum breaking load of the coated tablets progressively increased as the polymer average molecular weight increased.

The influence of polymer grade on the adhesion properties of film coats was investigated by Rowe (1976a) and Fisher and Rowe (1976). Lower molecular weight grades were shown to lead to higher adhesion values when applied from 2.5%w/v solutions in dichloromethane-methanol (70:30 %v/v). This was thought to be due to viscosity differences between the solutions, those containing low molecular weight grades being able to penetrate further into the pores of the tablet and thus enhance adhesion. In a later paper, Rowe (1978b) used the same solvent system and polymer concentration to determine the effect of polymer grade on film coat surface roughness. He demonstrated that arithmetic surface

roughness was greatest with the lowest molecular weight grades, decreasing to a minimum with the 15mPa s grade and subsequently increasing with further increases in the polymer grade. These findings were said to be due to viscosity differences between the solutions, which gave rise to differences in atomised droplet size, evaporation of solvent from the droplets and droplet spreading at the tablet surface. These same factors were also said to be responsible for the progressive increase in coat surface roughness observed when the concentration of a 6mPa s HPMC grade in an organic solvent system was increased from 1%w/v to 10%w/v.

The influence of polymer solution concentration on film coat surface roughness, was also investigated by Relland and Eber (1986), using aqueous gloss solutions prepared from a 5mPa s HPMC grade. Coats were applied in a specially designed spray box using solution concentrations of between 1%w/v and 8%w/v. It was found that when solution concentrations of less than 5%w/v were applied, there was no discernable difference in film surface roughness. Increasing the concentration between 5%w/v and 8%w/v however produced a doubling of the film roughness.

Plasticisers are often included in polymeric films in order to alter the physical properties and enhance the film-forming characteristics. The method by which they impart flexibility to the film is thought to be due to imposition of the plasticiser between the polymer chains and thus the disruption of the forces which hold the chains together. The most effective plasticisers are generally those having structures which closely resemble those of the polymer they are plasticising. Plasticisers used with HPMC in aqueous film coating are limited by toxicity and compatibility, to the water soluble polyols. These include glycerol, propylene glycol and the series of polyethylene glycols

(PEGs), these all having hydroxyl groups which enable suitable interaction with HPMC. The compatibility levels of these plasticisers with HPMC have been reported by Aulton et al. (1981), Okhamafe and York (1985) and Sakellariou et al. (1986).

Interactions between various plasticisers and HPMC and their effect on the properties of free films have been investigated by Entwistle and Rowe (1978 and 1979), Aulton et al. (1981), Okhamafe and York (1983 and 1985), Masilungan and Lordi (1984) and Sakellariou et al. (1986). Since some of the effects caused by adding plasticisers might be detrimental to the properties of the film when applied to tablets, Aulton et al. (1981) concluded that careful consideration should be given as to whether a plasticiser should be included and to its concentration. The authors also demonstrated the considerable plasticising action of water by comparing the properties of unplasticised HPMC films stored at relative humidities of 10% and 60%. This latter finding was also reported by Masilungan and Lordi (1984) who showed the softening temperature of unplasticised HPMC films to be reduced after storage at 79% RH for eight weeks.

Fisher and Rowe (1976) reported that the inclusion of glycerol and propylene glycol at concentrations of up to 20%w/w in HPMC films sprayed from organic solutions did not have a significant effect on the film/tablet adhesion properties. Films prepared from the same constituents were studied by Rowe (1976b) in respect to their hardness and elastic properties. Increasing the plasticiser concentration was found to produce a progressively softer more elastic film. The same paper showed that increasing the molecular weight grade of PEG, at a fixed plasticiser concentration of 20%w/w, was found to produce less elastic films, a fact that was attributed to the decrease in mole fraction of hydroxyl groups.

Porter (1980) investigated the properties of tablets coated with HPMC films plasticised with glycerol, propylene glycol, PEG 400 and PEG 4000 at concentrations of up to 40%w/w. The inclusion of all the plasticisers was found to produce tablets possessing a lower diametral crushing strength, the effect becoming greater as the plasticiser concentration increased. Little effect on film adhesion was however apparent.

The effect of plasticiser type and concentration on the incidence of bridging of the intagliations of film coated tablets was investigated by Rowe and Forse (1981) using PEG 200, propylene glycol and glycerol. At levels of 10%w/w and 20%w/w the rank order of plasticising efficiency, as measured by the lowering of the incidence of the coat defect, was found to be PEG 200 > propylene glycol > glycerol. These findings were explained in terms of plasticiser volatility and the ability to reduce the residual stresses built up in the film during solvent evaporation.

The volatility of a plasticiser is dependent both on its effective vapour pressure and its rate of diffusion through the polymer matrix. These in turn are dependent on polymer/plasticiser interactions. Pickard (1979) found that a considerable loss of the plasticiser propylene glycol occurred both during the coating process and on storage. This loss resulted in significant changes in film water vapour permeability, strength and elasticity. Loss of propylene glycol during coating was also reported by Skultety and Sims (1987).

Colorants and opaquant extenders are often added to coating formulations in order to improve appearance and facilitate product identification (Rowe, 1983c) and to reduce film tackiness (Lindberg and Jönsson, 1972). Colorants fall into three main categories; synthetic water-soluble organic dyes (eg tartrazine, sunset yellow and erythrosine), their insoluble aluminium lakes, and inorganic pigments (eg titanium dioxide,

talc, calcium carbonate and the iron oxides). The structures, particle size distribution and properties of these have been reviewed by Patton (1979) and Rowe (1984b), and the methods by which colorants impart appearance by Rowe (1983c and 1985b).

The influence of aluminium lakes and inorganic pigments (solid inclusions) on the properties of both free and applied films is generally opposite to that of plasticisers. Films are usually rendered harder with an increased modulus of elasticity and more brittle with a decreased elongation at break and tensile strength (Porter, 1980; Aulton et al., 1984).

The influence of solid inclusions on the cracking and edge splitting of HPMC films has been studied extensively by Rowe (1982a, 1982b, 1982c, 1984c, 1986a and 1986b) and by Gibson et al. (1988b and 1989). Iron oxides and titanium dioxide have been shown to increase the incidence of film defects. This was attributed to the increase in film modulus of elasticity caused by these additives which was thought to increase the build-up of internal stresses within the film during solvent evaporation and film formation. Talc and magnesium carbonate were however shown to reduce the incidence of the tablet defects studied. This latter effect was thought to be a consequence of the morphology of the additives, the particles existing as flakes which orientate themselves parallel to the surface resulting in a restraint in volume shrinkage of the film parallel to the plane of coating.

Studies by Gibson et al. (1988a) on the interactions between HPMC and solid inclusions using immersion calorimetry, showed only titanium dioxide to interact significantly with the polymer.

Film permeability to water vapour has been shown to be affected by the nature and concentration of solid inclusions (Parker et al., 1974; Porter, 1980; Okhamafe and York, 1984a). Generally, in the presence of

low concentrations there is a reduction in permeability, the particles serving as a barrier and thus causing an increased diffusional pathway. As the concentration increases however, a point known as the *critical pigment volume concentration* (CPVC) is reached where the polymer can no longer bind all the pigment particles together. Pores therefore appear in the film resulting in an increased permeability to water vapour.

Film adhesion was shown by Fisher and Rowe (1976) to be reduced by 45% by the addition of 10%w/w of titanium dioxide. Additional increases in titanium dioxide content to 50%w/w were however shown to have little further effect. This phenomenon was not found by Porter (1980) who, instead, showed both titanium dioxide and FD&C Yellow No.5 aluminium lake to have little effect on adhesion at concentrations of up to 40%w/w. This discrepancy may have arisen from either the use of different solvent systems (Porter using an aqueous system and Rowe an organic system) or to differences in the equipment used to measure the adhesion.

The influence of solid inclusion particle size on film surface roughness was examined by Rowe (1981a) using dolomites of known particle size distribution. The film surface roughness was shown to be dependent on the dolomite concentration and particle size distribution and the inherent roughness of the tablet substrate. For the largest particle size dolomite (mean size 18μm) there was a marked increase in surface roughness at low concentrations (16%w/v) and a fall in surface roughness as the concentration increased to 48%w/v. The opposite effects were noted for the smaller particle size grades used (mean particle sizes below 5μm).

Prillig (1969) showed that colorants may have a detrimental effect on the solubility characteristics of HPMC films. The inclusion of FD&C Red No.3, RD&C Red No.4 and RD&C Red No.22 dyes at a concentration of

3.3%w/w was shown to produce films which were insoluble in simulated gastric fluid. FD&C Red No.21 dye produced films which were insoluble in both simulated gastric fluid and de-ionised water. These solubility characteristics were reflected in the dissolution behaviour of coated tablets.

The importance of the refractive indices of solid inclusions has been discussed by Rowe and Forse (1983a) and Rowe (1983a). It was reported that some solid inclusions possess the property of optical anisotropy, that is the ability to have different refractive indices depending on the orientation of the particles. Calcium carbonate for example was illustrated to possess two refractive indices (1.510 and 1.645) and talc three (1.539, 1.589 and 1.589). HPMC was however said to be isotropic, possessing only one refractive index, 1.49. Since the opacity of HPMC film coats is dependent on the refractive indices of all the components, it was postulated that coats could potentially possess differing opacities depending on the nature of the particles and how they were orientated within the film. This phenomenon was proposed by Rowe (1983a) to explain the production of tablets with highlighted intagliations when calcium carbonate was used in the formulation. The pigment was said to orientate equivalent to its lowest refractive index (which is similar to HPMC) on the body of the tablet thus producing a clear film, and to orientate randomly or to its highest refractive index in the intagliation, thereby producing a degree of opacity. This effect was not found to be substrate dependent but attempts to reproduce highlighted intagliations on single tablets attached to the inside of a coating drum were unsuccessful.

3.3%w/w was shown to produce films which were insoluble in simulated gastric fluid. FD&C Red No.21 dye produced films which were insoluble in both simulated gastric fluid and de-ionised water. These solubility characteristics were reflected in the dissolution behaviour of coated tablets.

The importance of the refractive indices of solid inclusions has been discussed by Rowe and Forse (1983a) and Rowe (1983a). It was reported that some solid inclusions possess the property of optical anisotropy, that is the ability to have different refractive indices depending on the orientation of the particles. Calcium carbonate for example was illustrated to possess two refractive indices (1.510 and 1.645) and talc three (1.539, 1.589 and 1.589). HPMC was however said to be isotropic, possessing only one refractive index, 1.49. Since the opacity of HPMC film coats is dependent on the refractive indices of all the components, it was postulated that coats could potentially possess differing opacities depending on the nature of the particles and how they were orientated within the film. This phenomenon was proposed by Rowe (1983a) to explain the production of tablets with highlighted intagliations when calcium carbonate was used in the formulation. The pigment was said to orientate equivalent to its lowest refractive index (which is similar to HPMC) on the body of the tablet thus producing a clear film, and to orientate randomly or to its highest refractive index in the intagliation, thereby producing a degree of opacity. This effect was not found to be substrate dependent but attempts to reproduce highlighted intagliations on single tablets attached to the inside of a coating drum were unsuccessful.

5.1.3 PROCESS CONDITIONS

Although much research has been carried out into how the tablet formulation and constituents of the coating solution influence the film properties, there has been little published work involving extensive studies of the role of process conditions in determining the appearance and behaviour of the coated product.

The coating process is complex involving many interacting variables. These variables however can divided into three groups based upon: the coating equipment design, the physical properties of the coating solution/suspension and the conditions of application.

Coating equipment design

A variety of coating pans are commercially available for aqueous film coating. These have been reviewed by Pickard and Rees (1974) and Porter (1982). They range from those adapted from traditional sugar coating pans, to those specially designed for aqueous film coating. Early coating work utilising organic solvents was often carried out in pans essentially the same as those used for the sugar coating process. These pans had the disadvantages of poor operator protection, inadequate mixing and poor evaporation capabilities. The latter two factors made them particularly unsuitable for aqueous film coating, due to the large latent heat of evaporation of water and difficulty in achieving an even thin film. Steps taken to help ensure a more even coating included changes to the pan shape and the incorporation of baffles. Protection from solvents was achieved by using a totally enclosed system, as for example in the Pelligrini coating pan (Zanasi-Nigris, Italy). Improved contact between the drying air and tablet surface, with the associated increase in surface area for heat exchange, was achieved with the Strunk immersion tube (Strunk, West Germany) and Glatt immersion sword (Glatt, West Germany) processses. The Accela-Cota (Manesty Machines Ltd.,

Liverpool) took these improvements a step further by utilising a system which forced air to pass through the tablet bed before venting. This latter improvement was also included in the Hi-Coater (Freund, Japan) and Driacoater (Driam, West Germany), although the design of these pans and the techniques used to achieve the air flow were significantly different.

Tablets have also been coated in various types of fluidised bed equipment. These, although offering excellent drying efficiency, tend to subject the tablets to greater attrition forces. Their use appears to be mainly restricted to small scale development work since batch sizes as low as 1kg can be coated.

The most widely used coating pan within the pharmaceutical industry for aqueous film coating is the Accela-Cota. This has been the subject of the bulk of research work investigating the coating process. It is available in a range of different sizes, from the model 10 (24inch (600mm) pan diameter) which is capable of coating up to about 15kg of tablet cores and is used for development and small scale manufacture, to models capable of coating around 700kg of tablet cores.

The Accela-Cota consists of a perforated, cylindrical shaped drum rotating on a horizontal axis. A charge of tablets is held within the drum through which a current of heated air is continuously passed before being exhausted by means of a plenum at the back of the tablet bed. The perforated periphery allows an even distribution of the hot drying air with minimal disturbance of the spray pattern. As the pan rotates, the tablets are carried upwards starting a tumbling action which is dependent on the speed of rotation. To promote tablet mixing the sides of the pan have different angles and baffles are incorporated. One or more spray guns are mounted within the pan so that the coating solution is sprayed co-currently with the drying air onto the tablet bed surface.

The model 10 version of the Accela-Cota is illustrated diagramatically in Figure 5.1.

Leaver et al. (1985) demonstrated that increasing the pan rotation speed of a model 10 Accela-Cota, decreased both the average time interval that the tablet was exposed to the spray at each appearance at the bed surface (surface residence time) and the average time between surface appearances. Increases in pan rotation speed were reported by Kara et al. (1981) to lead a decrease in process efficiency within the model 10 Accela-Cota. This effect was however very small, an increase in rotation speed from 12rpm to 24rpm reducing the process efficiency from 98.2% to 97.8%.

It is envisaged that differences in coating pan design and consequently the way in which the films are formed, could lead to the production of coats which exhibit different properties. Little reference can however be found to this in the literature.

Stafford and Lenkeit (1982) demonstrated that although some coating formulations based on HPMC could be successfully coated using various models of the Accela-Cota, a Pellegrini sugar coating pan with a dip sword and a modified conventional sugar coating pan, others, although successful when applied in the Accela-Cota, needed modification before an adequate product could be produced in the alternative coating pans.

A comparison of the coating efficiency of a range of Hi-Coater and Accela-Cota models was performed by Alcorn et al. (1988). This took the form of a colorimetric assessment of the coated tablets, which showed little difference between coats obtained from both the two different types of coater and between different sizes of the same coater.

<u>The physical properties of the coating solution/suspension</u>

The physical properties of aqueous film coating solutions have been discussed in Chapter 3 of this thesis and by Abdul-Razzak (1982) and

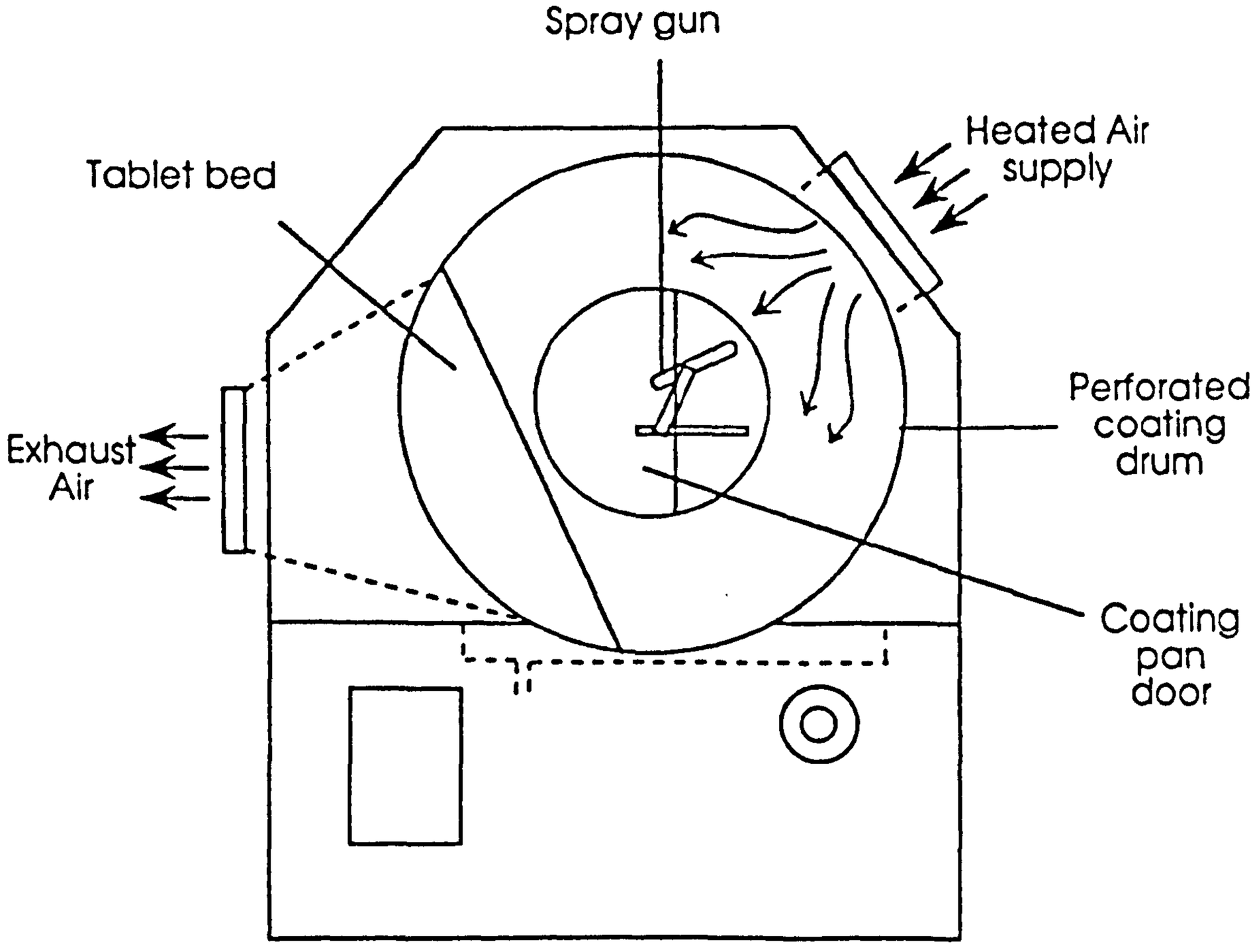

Figure 5.1: Diagramatic representation of a model 10 Accela-Cota

Prater (1982). Their influence on the atomised droplet size distribution produced during aqueous film coating is detailed in Chapter 4 of this thesis. Once atomised droplets have impinged on a tablet surface, their physical properties may influence the contact angle, degree of spreading and degree of penetration into the tablet surface.

The influence of HPMC solution concentration (and thus solution viscosity) on film coat surface roughness has been studied by Rowe (1978b) using organic solutions and Reiland and Eber (1986) using aqueous solutions in a model coating system. Both authors found an increase in the coat roughness with increasing solution concentration. With organic solutions the effect was pronounced at concentrations as low as 1%w/w, whereas with aqueous solutions it only became marked when the concentration rose above 5%w/w.

Down (1982) reported that the occurrence of foam in-filling of tablet intagliations during the aqueous coating process, may be overcome by the simultaneous reduction in surface tension and viscosity brought about by the inclusion of ethanol in the formulation.

Application conditions

Differences in film density, strength, hardness, moisture absorption and surface appearance have been demonstrated between cast and sprayed films (Banker et al., 1966; Zaro and Smith, 1972; Annan et al., 1974; Hawes, 1978; Pickard, 1979). Similarly films prepared using airless and pneumatic sprays have been shown to possess different properties (Bayer and Speiser, 1971; Spiteal and Kinget, 1977; Pickard, 1979). These papers illustrate the potential importance of the film coat application process in determining the properties of aqueous film coated products. Characterisation of aqueous film coating process variables and their effect on the properties of the resulting film coat has not been the subject of intensive study, although work has been carried out to try

and isolate some of the more fundamental parameters.

There are several aspects of the coating process which may be subject to variation and may therefore potentially influence film characteristics. These include the properties of the drying air, the type of spray gun used and its distance from the tablet bed, the atomising air pressure and the liquid feed rate (spray rate).

The volume, temperature and humidity of the drying air will govern its evaporative capacity and therefore influence the rate of solvent evaporation from the atomised droplets both whilst travelling to, and once impinged on the tablet surface. The drying air properties will therefore influence the rate at which the coating solution can be successfully applied. In the absence of other process changes, and providing the tablet bed is not overwetted, increasing either the drying air volume flow rate or temperature will serve to increase the tablet bed temperature. This in turn will increase the temperature differential between the tablet surface and the impinged droplets. Since heat transfer to the droplets occurs mainly by conduction (Franz and Doonan, 1983; Yoakam and Campbell, 1984), the evaporation rate will also be increased and therefore the time for molecular orientation before the film is formed reduced. Over zealous increases in the temperature and volume flow rate of the drying air may lead to droplet spray drying, thermal degradation of tablet ingredients and uneconomic coating processes. Conversely too low a tablet bed temperature may allow penetration into the tablet core and therefore the possibility of hydrolytic degradation.

Rowe and Forse (1982) assessed the influence of inlet air temperature on the incidence of intagliation bridging and film edge splitting for aqueous film coats applied in a model 10 Accela-Cota. Increasing the temperature was found to be beneficial in the case of intagliation

bridging but detrimental in the case of film edge splitting. This was thought to arise from an increase in evaporation rate at higher inlet air temperatures and a consequent reduction in the Young's modulus and tensile strength of the film. Cole et al. (1983) when examining the influence of process variables on the appearance of aqueous film coated tablets prepared in a model 10 Accela-cota, concluded that inlet temperature was not an important parameter as long as it was above 50°C for liquid flow rates of 20gmin^{-1} to 30gmin^{-1} and 60°C for flow rates of 30gmin^{-1} to 50gmin^{-1}. They found successful coats could be obtained with inlet air volume flow rates as low as 0.014m^{3}s^{-1} (30 cubic feet per minute (cfm)), although this was not reproducible. Unless the coating pan was sealed, the negative air pressure created inside the pan when using air volume flow rates of 0.014m^{3}s^{-1} tended to both draw cold air in from the room and displace the spray. Changing the drying air temperature from 40°C to 60°C was found by Reiland and Eber (1986) to have a significant effect on film surface roughness when aqueous coating solutions were applied in their model system.

The inlet air temperature and relative humidity will govern the wet bulb temperature of the air. This parameter was defined by Yoakam and Campbell (1984) to be equal to the temperature of the atomised droplets impinging on the tablet surface during aqueous film coating. Since the inlet air temperature during aqueous film coating is usually above 50°C, the inlet air relative humidity is consequently usually below 20% and has been suggested by Reiland et al. (1983) to be of little importance in the evaporation process.

The model of spray gun used to atomise film coating solutions has been shown in Chapter 4 to have a profound effect on the resultant droplet size distribution. In addition, it has been shown to influence the droplet velocity and the volume of atomising air accompanying the

droplets to the tablet surface. The importance of the spray gun and its influence on the process of film formation has however tended to be ignored, with many papers failing to fully define the exact nature of spray gun used. Cole et al. (1983) reported that a much wider spray angle could be achieved using a Schlick model 732/7-1 spray gun than with a Walther Pilot WA/WX spray gun, and that in a model 75 Accela-Cota one Schlick gun could replace two Walther Pilot guns. The Schlick gun was said to possess the additional advantage of being smaller than than the Walther Pilot gun, a factor especially useful in the model 10 Accela-Cota where space available for the spray gun is limited. Porter and Saracini (1989) reported that the use of two Binks model 605 spray guns instead of the customary one, could result not only in more uniformly applied films, but also in reduced processing times and material costs. Relland and Eber (1986) whilst carrying out a designed experiment into the aqueous coating process in a model system, indicated that the type of air cap used with a Spraying Systems spray gun (1/4J series) fitted with a number 2850 liquid nozzle could exert a significant effect on tablet film coat surface roughness. This was postulated to arise from differences in the atomised droplet size and the atomising air volume and velocity. No measurement of these parameters was however undertaken. The same authors showed that increasing the distance of the spray gun from the tablet surface from 6" (152mm) to 10" (254mm) resulted in significantly rougher surfaces when coating in the model system. This was attributed to increased spray drying.

Increasing the spray gun to bed distance, when spraying solutions of cellulose acetate in acetone in a model system, was found by Allen et al. (1972) to produce weaker films which were less dense, more permeable and more elastic.

The air pressure used to atomise coating solutions has been shown in Chapter 4 not only to influence the distribution of droplet sizes, but also the volume and velocity of the atomising air. Its role in the production of tablet film coats has however been the subject of little investigation. Horvath et al. (1978) reported that in a fluidised-bed system, increasing the atomising air pressure produced coats with a reduced release rate, a fact which was attributed to the increased homogeneity of the droplet size distribution. Cole et al. (1983) suggested that when using a Walther Pilot WA/WX spray gun in a model 10 Accela-Cota, atomising air pressures above 50psi (345kPa) were required for satisfactory spray patterns to be maintained and acceptable coats to be formed. Increasing the atomising air pressure from 20psi (138kPa) to 50psi (345kPa) when using a Spraying Systems 1/4J series spray gun fitted with a 2850 liquid nozzle and 67228-45 and 134255-45 air caps, was shown not to have a significant influence on the coat surface roughness when examined by Reiland and Eber (1986) in their model system.

The rate of fluid application (spray rate) has been shown to exert an influence on the coating process by several authors. The increase in evaporative cooling which accompanies an increase in spray rate, was shown by Franz and Doonan (1983) and Cole et al. (1983) to result in a reduction in tablet bed temperature.

Kara et al. (1982) reported that when applying organic film coating solutions in a model 10 Accela-Cota, an increase in the spray rate from 200gmin^{-1} to 315gmin^{-1} resulted in a decrease in process efficiency from 99.3% to 95.8%. In contrast, Horvath et al. (1978) when coating in a fluidised-bed apparatus found coating efficiency to increase with increasing spray rate.

Allen et al. (1972) when spraying solutions of cellulose acetate in

acetone in a model system, found that increasing the flow rate could result in films which were stronger and less elastic, as well as being more dense and less permeable to moisture. When applying aqueous film coats in a model 10 Accela-Cota, increasing the spray rate between 40gmin^{-1} and 60gmin^{-1} was found to decrease the exhaust air temperarature, reduce the incidence of film edge splitting and increase the incidence of intagliation bridging (Rowe and Forse, 1982). The latter two findings were postulated to be due to an increase in Young's modulus and tensile strength of the film.

Cole et al. (1983) concluded that in a model 10 Accela-Cota, satisfactory aqueous film coats could not be obtained with spray rates above 50gmin^{-1}.

Kim et al. (1986) found that in a model 10 Accela-Cota, by reducing the application rate of aqueous coating solutions from 60gmin^{-1} to 20gmin^{-1}, both the incidence of film bridging and the weight gain required for uniform and complete coating could be reduced. Nagai et al. (1989) suggested that for 5mPa s and 6mPa s grades of HPMC, the spray rate that can be used before coat "picking" occurs diminishes as the solution concentration increases.

Modelling of the aqueous film coating process

Modelling of the film coating process can take two forms. Either coating can be performed in a system which mimics that of the actual coating process, or the process can be modelled mathematically, so that the effect of changing process variables on a dependent process parameter can be predicted.

Use of a model system which mimics conditions in commercial coating equipment has obvious advantages for research work. Information on the coating process can be obtained without either the considerable capital cost, space or services required for commercial coating equipment or the

need for large amounts of tablets. Prater (1983) measured coating conditions experienced in a model 10 Accela-Cota and used this information to prepare a model system. The apparatus consisted of a timing belt to which the substrate was attached and a timed shutter mechanism which allowed the substrate to be exposed to the spray for a required interval. The apparatus was positioned in a modified fume cupboard and was capable of investigating the effect of the drying air flow rate and temperature, spray rate, atomising air pressure and nozzle to bed distance. Although the design of this apparatus was described in great detail, little work was carried out to elucidate the effect of the above mentioned variables on the properties of films prepared in the model system, or to confirm that it was a realistic model. A model system developed by Reiland and Eber (1986), constructed within a specially designed stainless steel spray box, was also intended to mimic coating in a model 10 Accela-Cota. The spray gun was mounted on a moveable track and the substrate on an assembly rotating at 30rpm. The apparatus gave a spray exposure time of 0.12 seconds with interdispersed drying cycles. Although the apparatus was used for an extensive study on the effect of process variables on the surface gloss and roughness of films prepared from aqueous gloss solutions, no attempt was made to demonstrate that the apparatus was an adequate simulation of practical coating conditions, and no information on drying air volumes or substrate temperatures was given. Neither of the two model systems described above simulated the tumbling action of tablets within the coating pan.

Mathematical modelling of the aqueous coating process has been undertaken in order to be able to predict the influence of coating variables on some aspect of the process and therefore aid in the prevention of potential coating problems.

Franz and Doonan (1983) when studying the tablet bed temperature in a 48" Accela-Cota using infrared thermometry, found the significant process parameters to be the inlet air temperature and volume flow rate and the spray rate. The relative importance of these parameters was ascertained and data developed which enabled the prediction of the tablet bed temperature over a range of coating conditions. Conditions which could potentially lead to damage of heat sensitive ingredients or to tablet bed overwetting were thus identified and could be avoided.

Vaporisation Efficiency (VE), defined as the ratio of the application rate to the theoretical maximum application rate under given drying conditions, was used by Reiland et al. (1983) in their mathematical model of the aqueous coating process. For HPMC based formulations coated in a model 10 Accela-Cota, it was found that if VE was below approximately 0.20 to 0.29, tablets of an acceptable quality were produced. Equations predicting operating conditions giving appropriate VE values were produced.

Ebey (1987) developed mathematical equations to predict evaporation rates of water from tablet surfaces during the aqueous film coating process. It was suggested that once conditions producing a suitable coat had been elucidated, these equations could determine how to successfully reproduce this coat when environmental or process conditions were changed.

Instrumentation and automation of the aqueous film coating process

Instrumentation and automation of the coating process enables both the validation of the coating process and a reduction in operator costs, whilst reducing variability between coating runs. Details of such systems have been given by Wheeler (1977), Cole et al. (1983), Yoakam and Campbell (1984) and Rosencranz (1984). Commercially available systems include the Pro-Coat film coating system (Profile Automation,

Bromley, England) and the Accelacomp system (Manesty Machines Ltd., Liverpool, England). Details of a relatively simple low cost automated system were reported by Message (1987).

Before automated systems can be used optimally however, a thorough understanding of the coating process is required in order to select the parameters which will produce acceptable coated products.

5.1.4 TABLET STORAGE

Rowe (1983b) reported that direct compression tablet formulations coated with HPMC could be susceptible to coating defects such as intagliation bridging when stored at high humidities. This was proposed to be due to the build up of internal stresses within the film as the tablets swell upon absorbing moisture.

Okhamafe and York (1986) showed that little or no change occurred in the Brinell hardness or Young's modulus of some film coatings based on HPMC, when applied to aspirin tablets and stored at 20°C for five months in sealed containers. However at 37°C / 75%RH, unplasticised HPMC films and unplasticised HPMC films with talc or titanium dioxide were shown to exhibit a reduced hardness and Young's modulus. Films plasticised with PEG 400 remained virtually unchanged. The authors attributed these findings to a reduction in crystallinity levels in the unplasticised films arising from the enhanced polymer chain mobility at 37°C / 75%RH. Salicylic acid sublimation into the film was also mentioned as a possible contributing factor.

Saarnivaara and Kahela (1985) investigated the stability of aspirin tablets coated with HPMC films and stored at room temperature (25°C) or 40°C. Glycerol or PEG 6000 was used as the coat plasticiser and titanium dioxide as the pigment. Tablets stored at room temperature were shown to exhibit little change in disintegration or dissolution

behaviour over a period of 48 months. Storage at 40°C however produced tablets with considerably increased disintegration times and slower dissolution rates, this effect being particularly noticable when glycerol was the coat plasticiser.

5.1.5 SCOPE OF THE CHAPTER

The preceding discussion has illustrated that although a significant amount of research has been undertaken to investigate the film coating process, much is left undetermined. Little information is available regarding the role of the atomisation stage of the process and the influence of the coating spray gun and atomising air pressure. This section of work therefore aimed to correlate the properties of the film coating solutions and the information obtained from the study of the atomisation process, with the properties of film coated tablets. It was intended that this, along with information from other workers in the field of film coating, would enable a greater understanding of the coating process and allow rational manipulation of the coating conditions to achieve coats possessing the desired properties.

5.2 COATING STUDIES

5.2.1 EXPERIMENTAL

Coating pan

All coating work was carried out in a model 10 Accela-Cota (Manesty Machines Ltd., Liverpool) fitted with eight standard baffles (see Figure 5.1, section 5.1.3). The pan rotation speed was kept constant at 10rpm throughout the studies. No attempt was made to eliminate the passage of air from the pan to the room or vice-versa by sealing the coating pan door.

Drying air

The inlet drying air was drawn from the surrounding air through a Uniglass air filter (Universal Filters Ltd., Woodford Green) and heated using a heater/fan unit (Skerman Fabrications Ltd., Sudbury-on-Thames). The temperature of the air was determined by adjusting the power input setting on the unit between 6kW, 9kW and 12kW, giving inlet air temperatures of approximately 57°C, 65°C and 83°C respectively. The volume flow rate of drying air entering the coating pan was controlled by adjusting a stainless steel opposed blade control damper system (Actionair Equipment Ltd., Whitstable). The air volume flow rate was calculated from air velocity measurements in the inlet conduit (internal diameter 226mm) using a Testovent 4000 vane anemometer (Testoterm Ltd., Emsworth). Inlet air volume flow rates from $0.06m^3s^{-1}$ to $0.14m^3s^{-1}$ (127cfm to 295cfm) could be achieved.

Inlet and exhaust air temperatures were measured constantly using Zeal probe thermometers (G.H. Zeal Ltd., Merton). These were positioned just prior to the pan inlet plenum and just after the air exit port respectively.

Drying air was passed through the tablet bed (with intermittent jogging) before coating was commenced so that the tablets were pre-warmed to approximately 40°C.

Inlet drying air relative humidity values were calculated from a psychrometric chart using the ambient air temperature and humidity in the vicinity of the heater unit (measured using a Humicap HM31 temperature and humidity probe (Vaisala (UK) Ltd., Cambridge)) and the inlet air temperature. Exhaust air relative humidity values were measured after the air had passed through the exhaust fan. These were not the true exhaust air values however since the air is heated during passage through the fan, this adding up to 4°C to the temperature. True

exhaust air relative humidity values were calculated from a psychrometric chart, using the exhaust air temperature just after exiting the coating pan and the temperature and relative humidity of the air on leaving the exhaust fan. This method of measurement was found to give exactly the same exhaust relative humidity values as when the probe was placed in the air-stream just after it had exited the pan, and enabled the measuring unit to be accessible during coating for measurement of ambient conditions.

Atomising air and liquid control assembly air supply

Atomising air pressure was controlled and measured using Spirax-Monnier IP2 filter/regulator unit fitted with a pressure gauge (Spirax-Sarco Ltd., Cheltenham). Nylon reinforced safety tubing of 16mm external and 9.5mm internal diameter was used to connect the regulator and the spray gun. Tubing length was kept as short as possible to minimise air pressure loss (see section 4.2.3). The atomising air volume flow rate was monitored using a Brooks model 1120 full view volume flow meter fitted with a type 10-RV-15 float (see section 4.3.2). This facilitated the exact reproduction of any required spray pattern for a given set of atomisation conditions. It also enabled any reduction in atomising air flow rate, due for example to blockage of the air cap air exit ports, to be quickly detected and remedial action taken. The temperature of the atomising air was measured by a thermocouple placed in the tubing just prior to the point that the air entered the spray gun.

If an air supply was required for the liquid control assembly, this was passed through a Watts miniature filter/regulator fitted with an automatic drain and pressure gauge (Watts Regulators (UK) Ltd.), before being fed to the spray gun.

Spray guns

The spray guns used were those manufactured by Walther Pilot, Binks Bullows, Spraying Systems and Schlick. Their design, functions and operating conditions are described in section 4.2.2. The characteristics of sprays produced by the guns are detailed in section 4.3.

The guns were positioned so that the spray contacted the tablets approximately one third of the way down the tumbling bed. Unless otherwise stated, the Binks Bullows, Schlick and Walther Pilot guns were adjusted to form a flat spray pattern giving as even a spray distribution as possible without spraying the sides of the pan or causing excessive disruption of the tablet bed.

Coating solutions

Coating solutions were prepared from the constituents detailed below. These constituents are described in Chapter 2. The methods of solution preparation and the solution properties are detailed in Chapter 3.

a. HPMC E5 (Methocel E5, Colorcon Ltd.)

HPMC E5 batch 2 (see Tables 3.2 and 3.3) was used in all coating runs except for runs 70 and 71. In these two cases batches 3 (run 71) and 5 (run 70) were used (see Table 3.3). These latter two batches were selected as being representative of batches exhibiting viscosities towards the top and bottom of the HPMC E5 viscosity specification respectively.

HPMC E5 solution concentrations of either 6%w/w, 9%w/w or 12%w/w were applied.

b. Opadry type OY (Colorcon Ltd.)

Opadry type OY batch 2 (see Table 3.6) was used in coating runs 48 to 53 and 65 to 68. Concentrations of 10%w/w, 15%w/w and 20%w/w were applied.

c. Polyethylene glycol 400

Polyethylene glycol 400 was used at a solution concentration of 1%w/w in coating runs 69, 72 and 73.

d. Calcium Carbonate

Calcium carbonate was used at a concentration of 3.5%w/w in coating runs 72 and 73.

Coating solution application

The coating solutions were fed to the spray gun via a Watson-Marlow model 501S peristaltic pump, using silicon tubing of internal bore 8mm and wall thickness 1mm. The rate of application and the total coat applied was monitored using a digital balance. The coating solution temperature at the point of entry into the spray gun was measured using a thermocouple placed in the liquid stream.

Tablet cores

The tablets which were to be analysed after the completion of the coating process were made from a direct compression blend consisting of:

Microcrystalline cellulose NF	79.25%w/w
Starch 1500 (Pregelatinised starch NF)	20.00%w/w
Stearic acid BPC 1973	0.75%w/w

Details of these materials are given in Chapter 2.

Three different tablet types were compressed from one blend of these excipients using a Manesty B3B rotary tablet press (Manesty Machines Ltd., Liverpool). The properties of these tablets are detailed below.

	Tablet type 1	Tablet type 2	Tablet type 3
Shape	normal convex with central score	flat	flat
Diameter (mm)	10	10	15
Weight range (mg)	299-313	286-300	636-683
Average weight (mg)	306	293	655
% CV	1.4	1.6	2.1
Thickness (mm)	5.00±0.13	3.40±0.13	3.16±0.13
Disintegration time (s)	<10	<10	<20
Friability* (%)	0.13	0.13	0.06
Crushing force⊙ (kg)	5.30±0.33	9.74±0.66	20.60±1.38
True density (gcm^{-3})▽	1.459	1.459	1.459
Porosity (%)		24.9	19.5

* Roche friabulator, 30rpm for 15 minutes (20 tablets)

⊙ CT40 tablet breaking strength tester, 1mm/minute crushing rate (20 tablets)

▽ Beckmann air comparison pycnometer

Coating runs

For each coating run, one hundred 10mm flat, one hundred 15mm flat and two hundred 10mm scored convex tablets were used. These were added to 8mm unscored normal convex placebo tablets to give a total weight of 12kg.

Each load of tablets was coated with 270g of coating constiuents, equivalent to a theoretical weight gain of 2.25%w/w.

Each batch of 8mm placebo tablets was used for approximately 10 coating runs before being replaced.

Details of the coating solutions and process conditions used for each of the coating runs performed are given in Appendix 1.

Coating runs 1 to 56, 58 to 68 and 74 and 77 were undertaken in order to investigate the influence of spray gun type, atomising air pressure, spray rate, solution type and concentration, spray gun to bed distance, spray shape and liquid nozzle diameter on the coating process. Runs 57 and 79 investigated the effect of changing the drying (inlet) air temperature and run 76 the effect of reducing its volume flow rate. The potential for HPMC E5 batch variation to influence the coating process was investigated in runs 70 and 71, the model system suggested by Prater (1982) in run 75 and the effect of heating the coating solution prior to spraying in run 78. Runs 72 and 73 were undertaken to investigate the phenomenon reported by Rowe (1983a) where the inclusion of calcium carbonate in the coating formulation was shown to produce tablets with highlighted intagliations when applied onto previously coated coloured tablets. In order to do this, fifty of the 10mm scored convex uncoated tablets were replaced with fifty coated 10mm scored convex tablets taken from run 67.

During each coating run the inlet and exhaust temperature, inlet and exhaust humidity and inlet solution and atomising air temperatures were monitored. The spray guns nozzles were examined for signs of fouling and blockage and the coating pan scrutinised for any evidence of tablet adhesion to the baffles or perforated periphery.

5.2.2 RESULTS

5.2.2.1 INFLUENCE OF THE PROCESS CONDITIONS ON THE MONITORED PARAMETERS AND COATING PROCESS

Details of the monitored process parameters for each of the coating runs are given in Tables 5.1 and 5.2. These are summarised below, along with parameters not detailed in the tables.

Ambient relative humidity and temperature

Ambient temperature ranged from 22°C to 28°C and ambient relative humidity from 27% to 54%.

Atomising air temperature

Atomising air temperature, as monitored at the point of entry into the spray gun, was generally found to be within ±2°C of the ambient air temperature. A temperature range from 23°C to 28°C was encountered.

Inlet air temperature

The majority of the coating runs were carried out using a heater/fan setting of 9kW. With this setting the inlet air temperature was found to range from 64°C to 68°C. The two coating runs using a setting of 6kW were found to have inlet air temperatures of 56°C and 58°C, and that using a setting of 12kW, a temperature of 83°C.

Exhaust air temperature

Changes in the spray rate, inlet air temperature and inlet air volume flow rate were found to alter the outlet air temperature, as shown in Table 5.3. An exhaust air temperature range from 37°C to 49°C was encountered. Changes in atomising air pressure, solution concentration, gun type, gun-to-bed distance, spray shape or coating solution temperature had no discernable influence on the exhaust air temperature.

TABLE 5.1: COATING PROCESS PARAMETERS

RUN NO.	INLET AIR TEMP (°C)	EXHAUST AIR TEMP (°C)	EXHAUST AIR RELATIVE HUMIDITY (%)	SOLN TEMP ENTERING GUN (°C)	AIR CAP / LIQUID CAP BLOCKAGE	TABLET STICKAGE TO PAN	RUN COMPLETED OR ABORTED	RUN TIME (MIN.)
1	65	47	20	36	0	0	COMPLETED	100
2	65	42	34	29	0	1	COMPLETED	60
3	66	43	32	29	0	1	COMPLETED	60
4	67	44	30	29	0	0	COMPLETED	61
5	65	42	33	29	0	1	COMPLETED	59
6	65	42	31	29	0	1	COMPLETED	60
7	67	47	22	33	0	1	COMPLETED	74
8	65	45	23	33	0	0	COMPLETED	75
9	65	46	23	33	0	0	COMPLETED	75
10	65	45	23	30	0	1	COMPLETED	74
11	65	46	22	30	0	2	COMPLETED	76
12	65	46	21	29	0	1.5	COMPLETED	75
13	65	45	21	29	0	0	COMPLETED	75
14	65	45	20	31	1	0	COMPLETED	75
15	65	46	20	30	0	2	COMPLETED	75
16	65	46	20	31	0	1	COMPLETED	75
17	66	46	22	30	0	1	COMPLETED	74
18	66	47	25	33	0	0	COMPLETED	75
19	65	47	26	33	0	0	COMPLETED	75
20	65	46	26	33	0	1	COMPLETED	74
21	66	45	26	33	0	0	COMPLETED	75
22	66	46	25	34	0	0	COMPLETED	75
23	65	46	26	32	0	0	COMPLETED	75
24	65	43	26	33	0	1	COMPLETED	76
25	65	43	24	33	1	0	COMPLETED	75
26	66	43	23	32	0	0	COMPLETED	75
27	66	44	26	33	0	1	COMPLETED	74
28	67	45	23	33	1	1	COMPLETED	75
29	66	44	25	32	1	1	COMPLETED	76
30	66	42	27	32	0	0	COMPLETED	64
31	65	43	26	31	0	2	COMPLETED	75
32	66	44	23	33	0	0	COMPLETED	75
33	67	43	26	29	0	1	COMPLETED	64
34	66	44	24	33	0	0	COMPLETED	56
35	67	45	24	32	0	0	COMPLETED	56
36	67	42	29	30	0	1	COMPLETED	45
37	65	44	23	33	1	0	COMPLETED	56
38	65	44	23	32	0	1	COMPLETED	56
39	66	46	22	33	1	1	COMPLETED	56
40	66	46	21	31	3	0	ABORTED	35

The extent of both air cap/liquid cap blockage and tablet stickage to the coating pan were quantified on a scale between 0 and 3 (see text for details).

Full details of the coating runs are given in Appendix 1.

TABLE 5.2: COATING PROCESS PARAMETERS

RUN NO.	INLET AIR TEMP (°C)	EXHAUST AIR TEMP (°C)	EXHAUST AIR RELATIVE HUMIDITY (%)	SOLUTION TEMP (°C)	AIR CAP / LIQUID CAP BLOCKAGE	TABLET STICKAGE TO PAN	RUN COMPLETED OR ABORTED	RUN TIME (MIN.)
41	68	46	22	34	2	0	COMPLETED	56
42	66	40	32	30	0	0	COMPLETED	57
43	66	44	25	28	0	1	COMPLETED	57
44	65	42	22	28	3	1	ABORTED	51
45	64	42	26	27	2	3	COMPLETED	57
46	66	43	24	31	0	3	COMPLETED	113
47	67	45	22	30	0	0	COMPLETED	114
48	66	42	25	30	0	0	COMPLETED	35
49	67	43	25	30	2	1	COMPLETED	36
50	65	42	26	29	0	2	COMPLETED	36
51	65	42	26	29	3	0	ABORTED	12
52	66	42	26	26	2	1	COMPLETED	36
53	67	43	25	29	1	2	COMPLETED	35
54	67	43	26	32	0	0	COMPLETED	36
55	67	45	24	32	0	0	COMPLETED	75
56	67	45	25	32	0	1	COMPLETED	75
57	58	38	32	29	0	3	COMPLETED	75
58	67	48	22	36	0	0	COMPLETED	74
59	68	47	24	34	0	1	COMPLETED	57
60	67	47	24	34	3	1	ABORTED	54
61	68	44	28	33	0	1	COMPLETED	45
62	68	46	24	33	3	0	COMPLETED	113
63	68	46	24	29	0	2,5	COMPLETED	116
64	68	44	27	26	0	3	COMPLETED	60
65	68	43	29	28	0	1	COMPLETED	54
66	68	49	22	36	0	0	COMPLETED	41
67	68	46	25	32	0	0	COMPLETED	45
68	68	48	22	36	0	0	COMPLETED	60
69	68	46	28	34	0	0	COMPLETED	75
70	68	47	27	35	1	1	COMPLETED	57
71	68	46	28	34	2	1	COMPLETED	58
72	68	42	35	31	0	3	COMPLETED	40
73	68	49	22	37	0	0	COMPLETED	60
74	68	47	24	34	3	3	ABORTED	63
75	83	51	18	33	0	3	COMPLETED	160
76	67	42	31	33	0	1	COMPLETED	74
77	67	46	24	34	0	3	COMPLETED	76
78	68	46	23	43	0	0	COMPLETED	75
79	56	36	29	29	0	3	COMPLETED	75

The extent of both air cap/liquid cap blockage and tablet stickage to the coating pan were quantified on a scale between 0 and 3 (see text for details).

Full details of the coating runs are given in Appendix 1.

TABLE 5.3: EFFECT OF PROCESS CONDITIONS ON EXHAUST AIR TEMPERATURE

HEATER/FAN SETTING (kW)	INLET AIR TEMP RANGE (°C)	SPRAY RATE ($gmin^{-1}$)	AIR VOLUME FLOW RATE (m^3s^{-1})	EXHAUST AIR TEMP RANGE (°C)
9	64-68	30	0.129	47-49
9	64-68	40	0.129	42-46
9	64-68	50	0.129	40-44
9	68	40	0.088	42
6	56-58	40	0.129	37-38

Inlet and exhaust air relative humidity

The inlet air relative humidity was calculated to be less than 10% for all coating runs. These low values arose since it was ambient air from the coating room which was heated and drawn through the coating pan. Examination of a psychrometric chart indicates that for the inlet temperatures studied, the inlet humidity is unlikely to ever be above 15% if the drying air is obtained in this way.

Exhaust air relative humidity values were found to range between 18% and 35%, as shown in Tables 5.1 and 5.2. The factors influencing the exhaust air relative humidity were inlet air temperature, spray rate and drying air volume flow rate, as illustrated in Table 5.4. The range of humidities encountered for a particular set of coating conditions resulted from variations in the inlet air temperature and relative humidity of the ambient air.

Coating solution temperature

The results in Table 5.5 show that the temperature of the coating solution as it enters the spray gun may be considerably greater than that envisaged from measurements of the ambient air temperature or ambient coating solution temperature. Values ranging from 26°C to 37°C

were detected for solutions which had not been heated prior to being fed to the spray gun. The extent of the increase in coating solution temperature during passage through the silicon tubing to the spray gun was found to be dependent on the spray rate, inlet air temperature and spray gun type.

TABLE 5.4: EFFECT OF PROCESS CONDITIONS ON EXHAUST AIR RELATIVE HUMIDITY

HEATER/FAN SETTING (kW)	INLET AIR TEMP RANGE (°C)	SPRAY RATE ($gmin^{-1}$)	AIR VOLUME FLOW RATE (m^3s^{-1})	EXHAUST AIR RELATIVE HUMIDITY RANGE (%)
9	64-68	30	0.129	20-22
9	64-68	40	0.129	20-26
9	64-68	50	0.129	25-35
9	68	40	0.088	31
6	56-58	40	0.129	29-32

TABLE 5.5: EFFECT OF PROCESS CONDITIONS ON COATING SOLUTION TEMPERATURE

HEATER/FAN SETTING (kW)	INLET AIR TEMP RANGE (°C)	SPRAY RATE ($gmin^{-1}$)	SPRAY GUN	SOLUTION TEMP RANGE (°C)
9	64-68	30	SCHLICK	36-37
9	64-68	40	SCHLICK	31-34
9	64-68	50	SCHLICK	29-32
9	65-68	40	SPRAYING SYSTEMS	31-34
9	65	50	SPRAYING SYSTEMS	29
9	65-68	40	WALTHER PILOT	28-31
9	67-68	50	WALTHER PILOT	26-29
9	64-66	40	BINKS BULLOWS	27-31
9	66	50	BINKS BULLOWS	26
6	56-58	40	SCHLICK	29

Air cap/liquid cap blockage

The extent of air cap/liquid cap blockage during the coating runs is detailed in Tables 5.1 and 5.2. This was subjectively assessed and a value assigned from zero, indicating minimal fouling, to three, indicating a blockage sufficient to warrent a temporary interruption of the coating process. The Spraying Systems 60° spray gun was found to be particularly prone to fouling and blockage, this occurring with the Opadry suspension and all HPMC E5 solution concentrations. The same gun fitted with the 45° air cap was only found to exhibit fouling when spraying a 12%w/w HPMC E5 solution with an atomising air pressure of 207kPa, or when a smaller bore liquid nozzle (0.51mm) was fitted. With the Schlick and Walther Pilot guns the only significant problems were encountered when a 12%w/w HPMC E5 solution was sprayed with an atomising air pressure of 276kPa or below.

Stickage of tablets to the coating pan

This was subjectively assessed and values between zero (no stickage) and three (significant stickage) assigned (see Tables 5.1 and 5.2). The majority of the stickage encountered arose as a result of the 15mm tablets adhering to the perforated periphery of the pan, although sticking did occur to a lesser extent with the 10mm flat tablets and the 8mm bulking tablets. Only a few tablets were found to adhere to the baffles or other parts of the pan. Sticking was particularly noticeable when the Binks Bullows and Walther Pilot guns were used. Conditions of reduced drying capacity, caused for example by a reduction in the inlet temperature or inlet air volume flow rate, were also found to exacerbate the problem. The greatest amount of stickage was found when using coating conditions similar to those of the model system suggested by Prater (1982).

Aborted coating runs

Coating runs which were aborted before the required coat level had been applied are detailed in Tables 5.1 and 5.2. In each case the stoppage was due to a blockage at the liquid nozzle exit, the run being abandoned either because of repeated blockages or because the blockage had resulted in a deflection of the spray which had consequently caused excessive tablet sticking. In most cases the blockages were a result of a gradual build up of solids at the liquid nozzle exit, and most of the solids were applied before the run was aborted (see Tables 5.1 and 5.2). The main exception to this was run 51 where blockage repeatedly re-occurred within minutes of the nozzle being cleared.

Reproducibility

Several of the coating runs were repeated to check the reproducibility of the coating process. The matching runs were: 2, 5 and 6; 8 and 32; 10 and 31; and 57 and 79. Examination of the coating conditions and monitored parameters in Tables 5.1 and 5.2 shows there to be good reproducibility between these runs.

5.2.2.2 THE INFLUENCE OF PROCESS CONDITIONS ON THE INCIDENCE OF FILM COAT DEFECTS

General comments

The incidence of the main coat defects, namely tablet sticking, coat picking, film edge splitting and the presence of spray drying are shown in Appendix 2. The occurrence of sticking, picking and edge splitting was expressed as a percentage of the tablets of a particular type coated. The extent of spray drying was subjectively quantified by examining the score mark of the 10mm convex tablets. Values were assigned ranging from 0, where no spray drying was apparent, to 3, indicating the worst case.

Coat defects were assessed for all coating runs except for run 51, which was aborted at an early stage. Defect values are quoted for the four other aborted coating runs (40, 44, 60 and 74) although these should be viewed with some caution since the full coat level was not applied.

No evidence of either sticking or score bridging was detected with the 10mm scored convex tablets after any of the coating runs.

The occurrence of sticking with the flat faced tablets was found to be more prevalent with the 15mm diameter tablets than the 10mm diameter tablets.

The effect of spray gun type and coating solution formulation on the incidence of film coat defects

The effect of the spray gun type and coating solution formulation and concentration on the incidence of film coat defects is illustrated in Table 5.6. It is clear from these results that the use of different spray guns can markedly affect the occurrence of film coat defects, despite otherwise identical process conditions. Coating with the Binks Bullows, Walther Pilot and Spraying Systems 45° spray guns was shown to produce significantly more tablet sticking and film picking than coating with either the Schlick or Spraying Systems 60° spray guns. This effect was apparent when using a variety of different atomising air pressures and coating solution formulations, and occurred with all three tablet shapes. The influence of the spray gun on the incidence of film edge splitting appeared to be dependent on the coating solution applied. The Walther Pilot and Binks Bullows guns produced the highest incidence with the 9%w/w HPMC E5 solution, whereas the Schlick and Spraying Systems 45° guns produced the highest incidence with the 6%w/w solution. No difference was apparent with either the 12%w/w HPMC E5 solution or the

TABLE 5.6: THE EFFECT OF SPRAY GUN TYPE AND COATING SOLUTION FORMULATION ON THE INCIDENCE OF FILM COAT DEFECTS

RUN No.	GUN TYPE	AIR CAP	SOLUTION TYPE	SOLUTION CONC %w/w	AIR PRESS kPa	SPRAY RATE gmin⁻¹	INCIDENCE OF FILM COAT DEFECTS							
							10mm CONVEX TABLETS		15mm FLAT TABLETS			10mm FLAT TABLETS		
							PI	SD	ST	PI	ES	ST	PI	ES
63	WP	STD	HPMC E5	6	414	40	51	0	12	9	8	10	26	2
47	SCH	STD	HPMC E5	6	414	40	2	0,5	0	0	50	0	0	38
46	SS	45°	HPMC E5	6	414	40	25	0,5	10	8	18	3	20	11
62	SS	60°	HPMC E5	6	414	40	4	0	1	0	3	1	2	0
12	WP	STD	HPMC E5	9	276	40	44	0	43	42	1	16	61	0
15	BB	63PB	HPMC E5	9	276	40	45	0	26	57	0	23	58	0
7	SCH	STD	HPMC E5	9	276	40	43	0,5	2	31	1	7	36	0
29	SS	60°	HPMC E5	9	276	40	6	1,5	18	9	3	12	14	0
10	WP	STD	HPMC E5	9	414	40	44	0	20	22	10	8	50	6
31	WP	STD	HPMC E5	9	414	40	40	0	21	21	16	12	47	9
16	BB	63PB	HPMC E5	9	414	40	19	0	28	47	6	8	54	4
9	SCH	STD	HPMC E5	9	414	40	3	0,5	9	2	0	3	5	0
13	SS	45°	HPMC E5	9	414	40	27	0,5	10	6	2	5	9	2
14	SS	60°	HPMC E5	9	414	40	3	1,5	6	2	2	6	3	1
11	WP	STD	HPMC E5	9	552	40	35	0	10	30	44	10	29	46
17	BB	63PB	HPMC E5	9	552	40	18	0	22	27	14	10	44	7
8	SCH	STD	HPMC E5	9	552	40	3	1	3	3	6	1	11	0
32	SCH	STD	HPMC E5	9	552	40	1	1	0	2	8	1	0	1
24	SS	45°	HPMC E5	9	552	40	23	0	0	12	7	2	19	7
25	SS	60°	HPMC E5	9	552	40	1	1,5	3	2	3	1	1	3
43	WP	STD	HPMC E5	12	414	40	6	0	12	19	0	7	36	0
45	BB	63PB	HPMC E5	12	414	40	39	0	30	40	0	12	61	1
34	SCH	STD	HPMC E5	12	414	40	0	0,5	4	1	0	4	2	0
38	SS	45°	HPMC E5	12	414	40	26	0,5	17	22	0	6	26	0
37	SS	60°	HPMC E5	12	414	40	2	1,5	18	3	0	4	1	0
53	WP	STD	OPADRY	15	414	50	9	0	21	35	4	3	31	0
52	BB	63PB	OPADRY	15	414	50	10	0	26	20	0	6	28	0
48	SCH	STD	OPADRY	15	414	50	1	0,5	16	5	5	5	11	3
65	SCH	STD	OPADRY	10	414	50	9	0	0	0	30	0	3	4
50	SS	45°	OPADRY	15	414	50	9	0	52	23	0	27	31	0

Key: PI = picking SD = spray drying ST = sticking ES = edge splitting

Defect values are expressed as percentages, except for spray drying which is quantified on a scale between 0 and 3 (see text).

Full details of the coating runs are given in Appendix 1.

15%w/w Opadry formulation. The greatest incidence of spray drying occurred when the tablets were coated with the Spraying Systems 60° spray gun. Minimal spray drying was apparent with the Schlick and Spraying Systems 45° spray guns and none detected with either the Binks Bullows or Walther Pilot spray guns.

The HPMC E5 solution concentration applied to the tablets had no consistent influence on either the extent of picking of the 10mm convex tablets, or the sticking and picking of the two types of flat tablets. It did however influence the degree of edge splitting, there being a trend towards a reduction in edge splitting with increasing solution concentration. Edge splitting was virtually eliminated when the coat was applied as a 12%w/w solution. Increasing the Opadry concentration from 10%w/w to 15%w/w was also found to significantly reduce edge splitting. The only anomalous result appeared to be with the Walther Pilot gun, which exhibited fewer tablets with edge splitting when coated with a 6%w/w HPMC E5 solution than with a 9%w/w solution.

Spray drying was not markedly affected by the solution concentration applied.

<u>The effect of atomising air pressure on the incidence of film coat defects</u>

The effect of atomising air pressure on the occurrence of film coat defects is shown in Table 5.7. The data demonstrate that the incidence of film coat picking and tablet sticking can be markedly affected by the atomising air pressure, with these defects being reduced in the majority of cases as the atomising air pressure increased. This was especially noticeable as the atomising air pressure was increased above 276kPa. The effect was seen with each of the spray guns studied and at different HPMC E5 concentrations, spray rates and spray gun-to-bed distances. It

TABLE 5.7: THE EFFECT OF ATOMISING AIR PRESSURE ON THE INCIDENCE OF FILM COAT DEFECTS

RUN No.	GUN TYPE	AIR CAP	HPMC E5 SOLUTION CONC %w/w	AIR PRESS KPa	SPRAY RATE $gmin^{-1}$	SPRAY SHAPE	GUN TO BED DIST, mm	INCIDENCE OF FILM COAT DEFECTS							
								10mm CONVEX TABLETS		15mm FLAT TABLETS			10mm FLAT TABLETS		
								PI	SD	ST	PI	ES	ST	PI	ES
7	SCH	STD	9	276	40	FLAT	180	43	0,5	2	31	1	7	36	0
9	SCH	STD	9	414	40	FLAT	180	3	0,5	9	2	0	3	5	0
8	SCH	STD	9	552	40	FLAT	180	3	1	3	3	6	1	11	0
32	SCH	STD	9	552	40	FLAT	180	1	1	0	2	8	1	0	1
23	SCH	STD	9	276	40	FLAT	250	0	1,5	11	9	1	8	1	4
22	SCH	STD	9	414	40	FLAT	250	0	2	0	3	5	0	0	1
21	SCH	STD	9	552	40	FLAT	250	0	2	0	1	15	0	0	0
20	SCH	STD	9	276	40	CONE	180	28	0	52	6	28	33	11	14
19	SCH	STD	9	414	40	CONE	180	43	0	56	3	27	35	18	17
18	SCH	STD	9	552	40	CONE	180	39	0	63	1	22	46	5	10
60	SCH	STD	12	207	40	FLAT	180	12	0,5	36	17	0	15	26	0
41	SCH	STD	12	276	40	FLAT	180	0	1	1	1	0	1	0	0
34	SCH	STD	12	414	40	FLAT	180	0	0,5	4	1	0	4	2	0
40	SCH	STD	12	207	40	FLAT	250	1	1	12	3	0	0	5	0
35	SCH	STD	12	414	40	FLAT	250	1	1	2	0	0	0	0	0
3	SCH	STD	9	276	50	FLAT	180	99	0	93	4	0	80	18	0
2	SCH	STD	9	414	50	FLAT	180	27	0	37	29	0	39	32	0
5	SCH	STD	9	414	50	FLAT	180	31	0	38	38	0	32	45	0
6	SCH	STD	9	414	50	FLAT	180	33	0	22	42	0	10	55	0
4	SCH	STD	9	552	50	FLAT	180	12	0	62	7	0	36	8	0
12	WP	STD	9	276	40	FLAT	180	44	0	43	42	1	16	61	0
10	WP	STD	9	414	40	FLAT	180	44	0	20	22	10	8	50	6
31	WP	STD	9	414	40	FLAT	180	40	0	21	21	16	12	47	9
11	WP	STD	9	552	40	FLAT	180	35	0	10	30	44	10	29	46
44	WP	STD	12	207	40	FLAT	180	1	0,5	13	24	0	5	21	0
43	WP	STD	12	414	40	FLAT	180	6	0	12	19	0	7	36	0
15	BB	63PB	9	276	40	FLAT	180	45	0	26	57	0	23	58	0
16	BB	63PB	9	414	40	FLAT	180	19	0	28	47	6	8	54	4
17	BB	63PB	9	552	40	FLAT	180	18	0	22	27	14	10	44	7
28	SS	60°	9	138	40	FLAT	180	18	1	54	18	0	23	21	0
29	SS	60°	9	276	40	FLAT	180	6	1,5	18	9	3	12	14	0
14	SS	60°	9	414	40	FLAT	180	3	1,5	6	2	2	6	3	1
25	SS	60°	9	552	40	FLAT	180	1	1,5	3	2	3	1	1	3
13	SS	45°	9	414	40	FLAT	180	27	0,5	10	6	2	5	9	2
24	SS	45°	9	552	40	FLAT	180	23	0	0	12	7	2	19	7
39	SS	45°	12	207	40	FLAT	180	49	1	63	28	0	25	49	0
38	SS	45°	12	414	40	FLAT	180	26	0,5	17	22	0	6	26	0

Key: PI = picking SD = spray drying ST = sticking ES = edge splitting

Defect values are expressed as percentages, except for spray drying which is quantified on a scale between 0 and 3,
Full details of the coating runs are given in Appendix I,

was not noticeable however with the Schlick gun when coating with a cone spray shape.

The incidence of edge splitting, where it occurred, appeared to increase with increasing atomising air pressure, this being particularly noticeable with the 15mm flat tablets. Again with the coating runs using the cone spray shape no trend was apparent.

Only small differences in the extent of spray drying were apparent at different atomising air pressures. With the Schlick gun, there was a general trend for a greater degree of spray drying to occur as the atomising air pressure increased, although no spray drying was apparent at any air pressure when a cone shape spray was employed or a spray rate of 50gmin^{-1} was used. No spray drying was observed with either the Walther Pilot and Binks Bullows guns at air pressures between 276kPa and 552kPa. There was some evidence to suggest that, with the Walther Pilot and Spraying Systems 45° spray guns, decreasing the air pressure below 276kPa may increase the incidence of spray drying.

<u>The effect of spray gun-to-bed distance and liquid nozzle diameter on the incidence of film coat defects</u>

With the Spraying Systems and Schlick spray guns it was possible to achieve spray gun to tablet bed distances of up to 300mm in the model 10 Accela-Cota. The size and design of the Walther Pilot and Binks Bullows spray guns however limited the maximum gun-to-bed distance easily achieved within the model 10 Accela-Cota to approximately 180mm. Increasing the gun-to-bed distance when using the Schlick and Spraying Systems guns was shown to decrease the incidence of tablet sticking and coat picking at all conditions studied (Table 5.8).

The incidence of edge splitting appeared to increase with increasing gun-to-bed distance when the Schlick gun applied a 9%w/w HPMC E5

TABLE 5.8 : THE EFFECT OF GUN-TO-BED DISTANCE AND LIQUID NOZZLE DIAMETER ON THE INCIDENCE OF FILM COAT DEFECTS

RUN No.	GUN TYPE	AIR CAP	LIQUID NOZZLE DIAM mm	HPMC E5 SOLUTION CONC %w/w	AIR PRESS kPa	SPRAY RATE $gmin^{-1}$	GUN TO BED DIST. mm	INCIDENCE OF FILM COAT DEFECTS							
								10mm CONVEX TABLETS		15mm FLAT TABLETS			10mm FLAT TABLETS		
								PI	SD	ST	PI	ES	ST	PI	ES
7	SCH	STD	0,80	9	276	40	180	43	0,5	2	31	1	7	36	0
23	SCH	STD	0,80	9	276	40	250	0	1,5	11	9	1	8	1	4
9	SCH	STD	0,80	9	414	40	180	3	0,5	9	2	0	3	5	0
22	SCH	STD	0,80	9	414	40	250	0	2	0	3	5	0	0	1
8	SCH	STD	0,80	9	552	40	180	3	1	3	3	6	1	11	0
32	SCH	STD	0,80	9	552	40	180	1	1	0	2	8	1	0	1
21	SCH	STD	0,80	9	552	40	250	0	2	0	1	15	0	0	0
2	SCH	STD	0,80	9	414	50	180	27	0	37	29	0	39	32	0
5	SCH	STD	0,80	9	414	50	180	31	0	38	38	0	32	45	0
6	SCH	STD	0,80	9	414	50	180	33	0	22	42	0	10	55	0
33	SCH	STD	0,80	9	414	50	250	0	1	0	3	1	0	1	0
34	SCH	STD	0,80	12	414	40	180	0	0,5	4	1	0	4	2	0
35	SCH	STD	0,80	12	414	40	250	1	1	2	0	0	0	0	0
61	SCH	STD	0,80	12	414	50	180	3	0,5	12	9	0	6	16	0
36	SCH	STD	0,80	12	414	50	250	0	1	11	3	0	3	1	0
42	SCH	STD	0,80	12	414	50	300	0	1,5	6	0	0	1	0	0
24	SS	45°	0,71	9	552	40	180	23	0	0	12	7	2	19	7
27	SS	45°	0,71	9	552	40	250	1	0,5	1	1	2	3	1	0
25	SS	60°	0,71	9	552	40	180	1	1,5	3	2	3	1	1	3
26	SS	60°	0,71	9	552	40	250	3	2	2	3	0	0	2	0
9	SCH	STD	0,80	9	414	40	180	3	0,5	9	2	0	3	5	0
55	SCH	STD	1,20	9	414	40	180	0	0,5	8	2	1	2	4	1
56	SCH	STD	1,80	9	414	40	180	0	0,5	5	3	0	1	3	0
74	SS	45°	0,51	9	414	40	180	22	0	6	12	7	5	14	0
13	SS	45°	0,71	9	414	40	180	27	0,5	10	6	2	5	9	2

Key: PI = picking SD = spray drying ST = sticking ES = edge splitting

Defect values are expressed as percentages, except for spray drying which is quantified on a scale between 0 and 3.

Full details of the coating runs are given in Appendix 1.

TABLE 5.9 : THE EFFECT OF SPRAY RATE AND SPRAY SHAPE ON THE INCIDENCE OF FILM COAT DEFECTS

RUN No.	GUN TYPE	AIR CAP	SOLN TYPE	SOLN CONC %w/w	AIR PRESS kPa	SPRAY RATE gmin⁻¹	SPRAY SHAPE	GUN TO BED DIST. mm	INCIDENCE OF FILM COAT DEFECTS								
									10mm CONVEX TABLETS		15mm FLAT TABLETS			10mm FLAT TABLETS			
									PI	SD	ST	PI	ES	ST	PI	ES
1	SCH	STD	HPMC E5	9	414	30	FLAT	180	0	1.5	10	0	0	4	4	0
9	SCH	STD	HPMC E5	9	414	40	FLAT	180	3	0.5	9	2	0	3	5	0
2	SCH	STD	HPMC E5	9	414	50	FLAT	180	22	0	37	29	0	39	32	0
5	SCH	STD	HPMC E5	9	414	50	FLAT	180	31	0	38	38	0	32	45	0
6	SCH	STD	HPMC E5	9	414	50	FLAT	180	33	0	22	42	0	10	55	0
22	SCH	STD	HPMC E5	9	414	40	FLAT	250	0	2	0	3	5	0	0	1
33	SCH	STD	HPMC E5	9	414	50	FLAT	250	0	1	0	3	1	0	1	0
26	SS	60°	HPMC E5	9	552	40	FLAT	250	3	2	2	3	0	0	2	0
30	SS	60°	HPMC E5	9	552	50	FLAT	250	3	2	15	3	0	5	3	0
10	WP	STD	HPMC E5	9	414	40	FLAT	180	44	0	20	22	10	8	50	6
31	WP	STD	HPMC E5	9	414	40	FLAT	180	40	0	21	21	16	12	47	9
64	WP	STD	HPMC E5	9	414	50	FLAT	180	45	0	22	42	0	8	44	0
58	SCH	STD	HPMC E5	12	414	30	FLAT	180	0	0.5	0	0	0	0	0	0
34	SCH	STD	HPMC E5	12	414	40	FLAT	180	0	0.5	4	1	0	4	2	0
61	SCH	STD	HPMC E5	12	414	50	FLAT	180	3	0.5	12	9	0	6	16	0
35	SCH	STD	HPMC E5	12	414	40	FLAT	250	1	1	2	0	0	0	0	0
36	SCH	STD	HPMC E5	12	414	50	FLAT	250	0	1	11	3	0	3	1	0
68	SCH	STD	OPADRY	15	414	30	FLAT	180	3	1	0	0	26	0	0	10
67	SCH	STD	OPADRY	15	414	40	FLAT	180	3	0.5	4	2	16	1	2	6
48	SCH	STD	OPADRY	15	414	50	FLAT	180	1	0.5	16	5	5	5	11	3
9	SCH	STD	HPMC E5	9	414	40	FLAT	180	3	0.5	9	2	0	3	5	0
77	SCH	STD	HPMC E5	9	414	40	MID	180	0	0	20	0	0	6	0	0
19	SCH	STD	HPMC E5	9	414	40	CONE	180	63	0	56	3	27	35	18	17
7	SCH	STD	HPMC E5	9	276	40	FLAT	180	43	0.5	2	31	1	7	36	0
20	SCH	STD	HPMC E5	9	276	40	CONE	180	28	0	52	6	28	33	11	14
8	SCH	STD	HPMC E5	9	552	40	FLAT	180	3	1	3	3	6	1	11	0
32	SCH	STD	HPMC E5	9	552	40	FLAT	180	1	1	0	2	8	0	1	0
18	SCH	STD	HPMC E5	9	552	40	CONE	180	39	0	63	1	22	46	5	10
34	SCH	STD	HPMC E5	12	414	40	FLAT	180	0	0.5	4	1	0	4	2	0
59	SCH	STD	HPMC E5	12	414	40	CONE	180	19	0	2	8	4	2	15	0

Key: PI = picking SD = spray drying ST = sticking ES = edge splitting

Defect values are expressed as percentages, except for spray drying which is quantified on a scale between 0 and 3.

Full details of the coating runs are given in Appendix 1.

solution at a rate of 40gmin^{-1}. This trend however appeared to be reversed with the two Spraying Systems guns.

Spray drying was seen to increase with increasing gun-to-bed distance.

Changing the liquid nozzle diameter when using the Schlick and Spraying Systems guns did not appear to influence the extent of any of the film coat defects monitored.

The effect of spray rate and spray shape on the incidence of film coat defects

Table 5.9 demonstrates that increasing the spray rate results in an increase in coat picking and tablet sticking, but that this may be potentially beneficial in decreasing the incidence of edge splitting, especially when applying Opadry suspensions.

The extent of spray drying was generally reduced as the spray rate increased.

Table 5.9 also illustrates that changing the spray shape, so that the area covered by the spray is reduced, results in an increase in the incidence of film picking, tablet sticking and film edge splitting. Spray drying was however reduced.

The effect of inlet air temperature and volume flow rate on the incidence of film coat defects

The effect of both the inlet air temperature and volume flow rate on the incidence of film coat defects is shown in Table 5.10. All four coating runs used the Schlick gun positioned 180mm from the tablet bed. A flat spray shape was produced and a 9%w/w HPMC E5 solution atomised at a rate of 40gmin^{-1} using an atomising air pressure of 414kPa.

It is apparent from the data in Table 5.10 that the reduction in the air volume flow rate from 0.129m^{3}s^{-1} to 0.088m^{3}s^{-1} produced no discernable

difference in the incidence of sticking and picking, whereas a reduction in the inlet air temperature of approximately 10°C led to a large increase. In the former case the reduction in tablet bed temperature was approximately 4°C, whereas in the latter it was approximately 6°C (see Tables 5.1 and 5.2).

A reduction in spray drying was seen to accompany both a decrease in inlet air temperature and air volume flow rate.

TABLE 5.10: THE EFFECT OF INLET TEMPERATURE AND VOLUME FLOW RATE ON THE INCIDENCE OF FILM COAT DEFECTS

RUN NO.	INLET AIR TEMP (°C)	AIR VOLUME FLOW RATE (m^3s^{-1})	INCIDENCE OF FILM COAT DEFECTS							
			10mm CONVEX TABLETS		15mm FLAT TABLETS			10mm FLAT TABLETS		
			PI	SD	ST	PI	ES	ST	PI	ES
9	65	0.129	3	0.5	9	2	0	3	5	0
76	67	0.088	4	0	2	3	1	4	1	2
57	58	0.129	24	0	27	51	0	19	49	0
79	56	0.129	17	0	15	36	2	1	42	0

Key: PI = picking SD = spray drying ST = sticking ES = edge splitting

Defect values are expressed as percentages, except for spray drying which is quantified on a scale between 0 and 3.

Full details of the coating runs are given in Appendix 1

The effect of other process variables on the incidence of film coat defects

The effect of some other process variables on the incidence of film coat defects is shown in Table 5.11.

Inclusion of 1%w/w PEG 400 in the formulation or heating the coating solution so that it entered the spray gun at 43°C, appeared (from these results) to have a minimal effect on the incidence of the defects reported.

The use of coating conditions similar to those developed by Prater (1982) for a model coating system was found to produce many coat defects. Of particular note was the incidence of edge splitting, which was the highest of all the runs reported. This coating run was also the only one which produced film edge splitting on the 10mm convex tablets, the incidence of this defect being 6%.

Coating runs 70 and 71 were carried out in order to investigate the potential for HPMC E5 batch variation to influence the coat properties. The results in Table 5.11 indicate the HPMC E5 batch with a measured viscosity towards the top of the specification range (batch 3) caused a significant increase in the incidence of film defects compared to the batch used for the majority of the coating runs (batch 2), whose measured viscosity was near the middle of the viscosity specification range. Use of the batch with a measured viscosity towards the bottom of the viscosity specification (batch 5) was found to give an incidence of coat defects similar to that of batch 2.

TABLE 5.11: THE EFFECT OF SOME PROCESS VARIABLES ON THE INCIDENCE OF FILM COAT DEFECTS

RUN NO.	MAJOR VARIABLE	INCIDENCE OF FILM COAT DEFECTS							
		10mm CONVEX TABLETS		15mm FLAT TABLETS			10mm FLAT TABLETS		
		PI	SD	ST	PI	ES	ST	PI	ES
9	REFERENCE COATING RUN FOR RUNS 69 AND 78	3	0.5	9	2	0	3	5	0
69	INCLUSION OF 1%w/w PEG 400	0	0.5	7	0	0	3	1	0
78	SOLUTION ENTERING SPRAY GUN AT 43°C	0	0.5	6	12	0	3	7	0
75	MODEL SYSTEM DETAILED BY PRATER (1982)	57	0	0	13	65	4	12	66
34	12%w/w HPMC E5 SOLUTION (BATCH 2)	0	0.5	4	1	0	4	2	0
70	12%w/w HPMC E5 SOLUTION (BATCH 5)	4	0.5	6	3	0	2	6	0
71	12%w/w HPMC E5 SOLUTION (BATCH 3)	12	1.5	28	20	0	21	20	0

Note: Twelve 10mm convex tablets from run 75 exhibited edge splitting.

Key: PI = picking SD = spray drying ST = sticking ES = edge splitting

Defect values are expressed as percentages, except for spray drying which is quantified on a scale between 0 and 3.

Full details of the coating runs are given in Appendix 1.

5.3 THE INFLUENCE OF PROCESS CONDITIONS ON THE MECHANICAL STRENGTH OF AQUEOUS FILM COATED TABLETS

5.3.1 EXPERIMENTAL

The mechanical strength of the uncoated test tablets (see section 5.2.1) and tablets from selected coating runs, was assessed using a CT40 tablet breaking strength tester (I. Holland Ltd.) at a compression rate of $0.0167 mms^{-1}$. All the tablets tested had been stored at a temperature of 20°C and a relative humidity of 58% for at least four weeks prior to testing. The 10mm scored convex tablets were tested with the compression force applied at 90° to the tablet score. Traces of the applied load versus the crosshead vertical movement were obtained. At least five of each of the three different shapes of coated tablet from any run were tested, along with twenty of each of the uncoated tablets. No part of the coat was removed prior to compression.

Coating parameters investigated were spray gun type, HPMC E5 solution concentration/viscosity and atomising air pressure.

5.3.2 RESULTS

Traces of the increase in applied force with the top platen vertical movement of the CT40, showed that irrespective of the tablet type or the coating conditions, the initial peak always corresponded to the highest applied force. Any subsequent peaks if present, occurred at lower recorded applied forces. This indicates that in each case the coating and substrate fail at the same time and at the same breaking load. Multiple peaks, with the highest applied force corresponding to a peak other than the initial peak (as reported by Fell et al. (1979)) were not observed in these studies.

Mechanical strength values (with the corresponding standard deviations) for the three types of uncoated test tablets used in these studies were;

208.9N ± 14.9N for the 15mm flat tablets, 97.4N ± 6.8N for the 10mm flat tablets and 53.0N ± 5.9N for the 10mm scored convex tablets. The tablet constituents and other properties are detailed in section 5.2.1.

The influence of the viscosity of the applied solution and the spray gun used in its application on the mechanical properties of the three types of coated tablets are detailed in Table 5.12. Full details of the coating runs can be found in Appendix 1.

TABLE 5.12: THE EFFECT OF SPRAY GUN TYPE AND COATING SOLUTION VISCOSITY ON THE MECHANICAL STRENGTH OF AQUEOUS FILM COATED TABLETS

RUN NO.	GUN TYPE	SOLUTION VISCOSITY (mPa s)	BREAKING LOAD (N) ± s.d. (% CHANGE FROM UNCOATED TABLET)		
			10mm flat	15mm flat	10mm convex
47	SCH	46	93.0 ± 10.8 (-4.7%)	199.7 ± 11.0 (-4.4%)	62.6 ± 7.8 (+18.1%)
9	SCH	166	100.1 ± 5.9 (+2.8%)	193.1 ± 9.8 (-7.6%)	67.1 ± 3.7 (+26.6%)
70	SCH	359	100.3 ± 7.1 (+3.0%)	201.8 ± 13.3 (-3.6%)	76.9 ± 9.9 (+45.1%)
34	SCH	520	89.9 ± 7.3 (-7.7%)	197.5 ± 10.8 (-5.5%)	60.3 ± 4.6 (+13.8%)
71	SCH	840	91.1 ± 5.4 (-6.5%)	198.4 ± 9.2 (-5.0%)	58.9 ± 4.7 (+11.1%)
63	WP	46	95.6 ± 11.3 (-1.8%)	201.7 ± 4.5 (-3.4%)	65.4 ± 9.0 (+23.4%)
31	WP	166	103.6 ± 7.6 (+6.4%)	191.1 ± 6.7 (-8.5%)	74.5 ± 2.7 (+40.6%)
43	WP	520	92.2 ± 4.5 (-5.3%)	205.8 ± 15.7 (-1.5%)	65.7 ± 5.8 (+25.4%)
16	BB	166	107.2 ± 14.0 (+10.1%)	209.0 ± 12.7 (±0.0%)	88.6 ± 4.9 (+67.2%)
45	BB	520	97.0 ± 6.3 (-0.4%)	202.9 ± 10.4 (-2.9%)	67.3 ± 4.2 (+27.0%)
62	SS 60°	46	114.3 ± 8.5 (+17.4%)	223.7 ± 10.2 (+7.1%)	60.9 ± 4.4 (+14.9%)
14	SS 60°	166	99.7 ± 11.1 (+2.4%)	197.1 ± 10.6 (-5.6%)	72.3 ± 8.6 (+36.4%)
37	SS 60°	520	86.7 ± 5.1 (-11.0%)	206.4 ± 5.5 (-1.2%)	60.7 ± 5.6 (+14.5%)
46	SS 45°	46	109.0 ± 5.4 (+11.9%)	194.4 ± 13.2 (-6.9%)	59.9 ± 5.8 (+13.0%)
13	SS 45°	166	92.6 ± 8.8 (-4.9%)	182.4 ± 8.1 (-12.7%)	65.6 ± 6.2 (+23.8%)
38	SS 45°	520	96.1 ± 8.5 (-1.3%)	198.4 ± 8.8 (-5.0%)	59.3 ± 7.1 (+11.9%)

In each of the above cases the atomising air pressure was 414kPa, the spray rate 40gmin^{-1} and the spray gun placed 180mm from the tablet bed.

Full details of the coating runs are given in Appendix 1.

The results in Table 5.12 show that the application of a film coat of approximately 2.25%w/w, increased the mechanical strength of the 10mm convex tablets irrespective of the viscosity of the applied solution. This increase ranged from 11.1% to 67.2%. It can be seen that for each spray gun studied, the mechanical strength of the 10mm convex tablets coated with the 46mPa s (6%w/w) and 520mPa s (12%w/w) solutions are very similar. In each case however when the 166mPa s solution was applied, the resulting tablets were stronger.

When the Schlick gun was used, the largest value of the breaking load was seen when the 359mPa s solution was applied, this corresponding to a 12%w/w solution of the low viscosity batch of HPMC E5 (designated batch 5, see Table 3.3). This suggests that for the 10mm convex tablets coated using the conditions detailed, an increase in mechanical strength occurs with an increase in the applied solution viscosity up to a certain value, whereafter further increases in solution viscosity result in a reduction in the coated tablet mechanical strength.

With the 10mm flat tablets, the difference between the mechanical strength of the coated and uncoated tablets was smaller, with some coating runs resulting in an increase in mechanical strength and some a decrease. With the Schlick and Walther Pilot guns, the trend seen with the 10mm convex tablets was apparent, whereby maximum strength tablets were produced when the intermediate viscosity solutions were applied. The two Spraying Systems guns however produced the strongest 10mm flat tablets when the lowest viscosity solution (46mPa s) was applied. A coating run with a 46mPa s solution using the Binks Bullows gun was not performed.

The mechanical strength of the 15mm flat tablets, was, with one exception, found to be reduced after coating. Only tablets from run 62

where the Spraying Systems 60° spray gun was used to apply a 46mPa s solution was an increase in mechanical strength apparent.

The effect of atomising air pressure on the mechanical strength of the three types of coated test tablets is detailed in Table 5.13.
The results show that for both the 166mPa s and 520mPa s solutions, a reduction in the atomising air pressure resulted in an increase in the mechanical strength of the tablets. This was most noticeable with the 10mm convex tablets, the effect on the 10mm flat and 15mm flat tablets being relatively small.

TABLE 5.13: THE EFFECT OF ATOMISING AIR PRESSURE ON THE MECHANICAL STRENGTH OF AQUEOUS FILM COATED TABLETS

RUN NO	GUN TYPE	SOLUTION VISCOSITY (mPa s)	AIR PRESSURE (kPa)	BREAKING LOAD (N) ± s.d. (% CHANGE FROM UNCOATED TABLET)		
				10mm flat	15mm flat	10mm convex
32	SCH	166	552	99.7 ± 6.3 (+2.4%)	193.2 ± 8.6 (-7.5%)	63.3 ± 4.2 (+19.4%)
9	SCH	166	414	101.1 ± 5.9 (+2.8%)	193.1 ± 9.8 (-7.6%)	67.1 ± 3.7 (+26.6%)
7	SCH	166	276	98.4 ± 3.6 (+1.0%)	195.6 ± 18.3 (-6.4%)	77.1 ± 6.1 (+45.5%)
25	SS,60°	166	552	92.4 ± 6.7 (-5.1%)	192.8 ± 8.9 (-7.7%)	66.8 ± 8.1 (+26.0%)
14	SS 60°	166	414	99.7 ± 11.1 (+2.4%)	197.1 ± 10.6 (-5.6%)	72.3 ± 8.6 (+36.4%)
28	SS 60°	166	138	122.9 ± 9.0 (+26.2%)	203.6 ± 14.0 (-2.5%)	82.1 ± 9.9 (+54.9%)
31	WP	166	414	103.6 ± 7.6 (+6.4%)	191.1 ± 6.7 (-8.5%)	74.5 ± 2.7 (+40.6%)
12	WP	166	276	106.2 ± 7.4 (+9.0%)	193.4 ± 11.3 (-7.4%)	79.3 ± 3.6 (+49.6%)
34	SCH	520	414	89.9 ± 7.3 (-7.7%)	197.5 ± 10.8 (-5.5%)	60.3 ± 4.6 (+13.8%)
60	SCH	520	207	96.9 ± 9.8 (-0.5%)	204.7 ± 10.4 (-2.0%)	74.3 ± 4.5 (+40.2%)
43	WP	520	414	92.2 ± 4.5 (-5.3%)	205.8 ± 15.7 (-1.5%)	65.7 ± 5.8 (+25.4%)
44	WP	520	207	95.8 ± 5.1 (-1.6%)	213.8 ± 19.7 (+2.3%)	71.3 ± 2.3 (+34.5%)

In each case a spray rate of $40g^{-1}$ was used and the spray gun placed 180mm from the tablet bed.

Full details of the coating runs are given in Appendix 1.

5.4 ASSESSMENT OF THE THICKNESS AND SURFACE ROUGHNESS OF AQUEOUS FILM COATED TABLETS USING A LIGHT SECTION MICROSCOPE

5.4.1 THE LIGHT SECTION MICROSCOPE

The thickness of polymer films applied to tablets is usually determined either by using a micrometer to measure the film thickness after its removal from the tablet, or by extrapolation from knowledge of the amount of polymer/coat applied. The former method is destructive and only measures the thickest parts of the applied film. Adhesion of substrate particles may also lead to artificially high thickness values being obtained. With the latter method, accurate values for film density and coating efficiency are required for a meaningful thickness determination to be made. Both methods yield a single value for film thickness and give no indication of the thickness variation.

The Light Section Microscope (Carl Zeiss, Oberkochen, West Germany) non-destructively measures the thickness of transparent coatings, allowing the determination of tablet film coat thickness at selected regions on the tablet surface and analysis of the film thickness variation. Assessment of surface roughness can also be made without contacting the tablet surface.

The Light Section Microscope operates on the light-section principle as shown diagramatically in Figure 5.2. An incandescent lamp of variable brightness, illuminates a slit which projects a narrow band of light through an objective (O_1) at an angle of 45° to the surface being measured. This band of light is then observed as a series of peaks and troughs through a microscope at the opposite 45° angle after it has been reflected/refracted from the sample. The microscope objective O_2 has the same magnification as the objective O_1 and can be set at either x200 or x400. A cross-line reticle in the eye-piece can be shifted within the field of view by means of a graduated measuring drum. The required

Figure 5.2 Schematic representation of the light section microscope

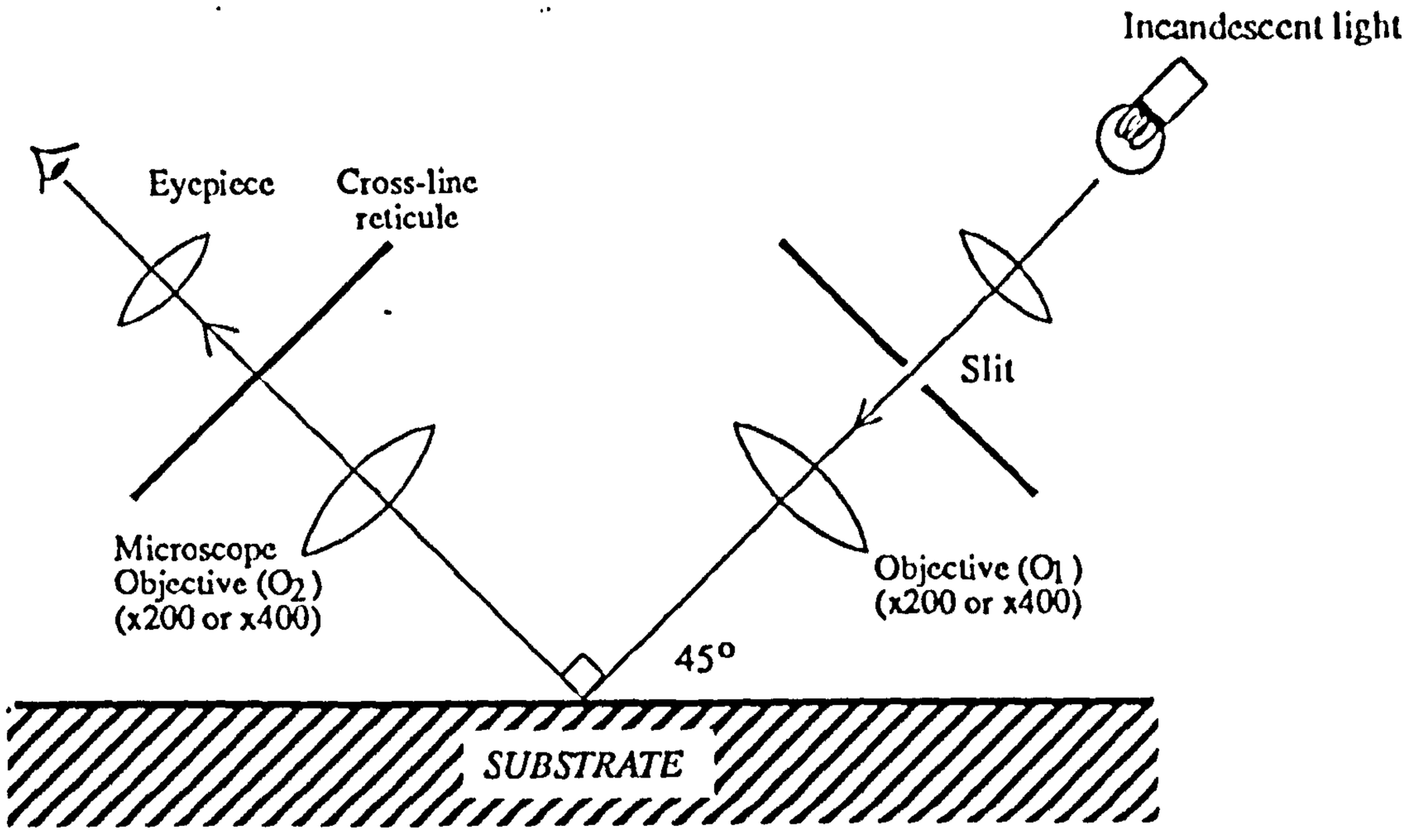

Figure 5.3 Light path through a coated substrate

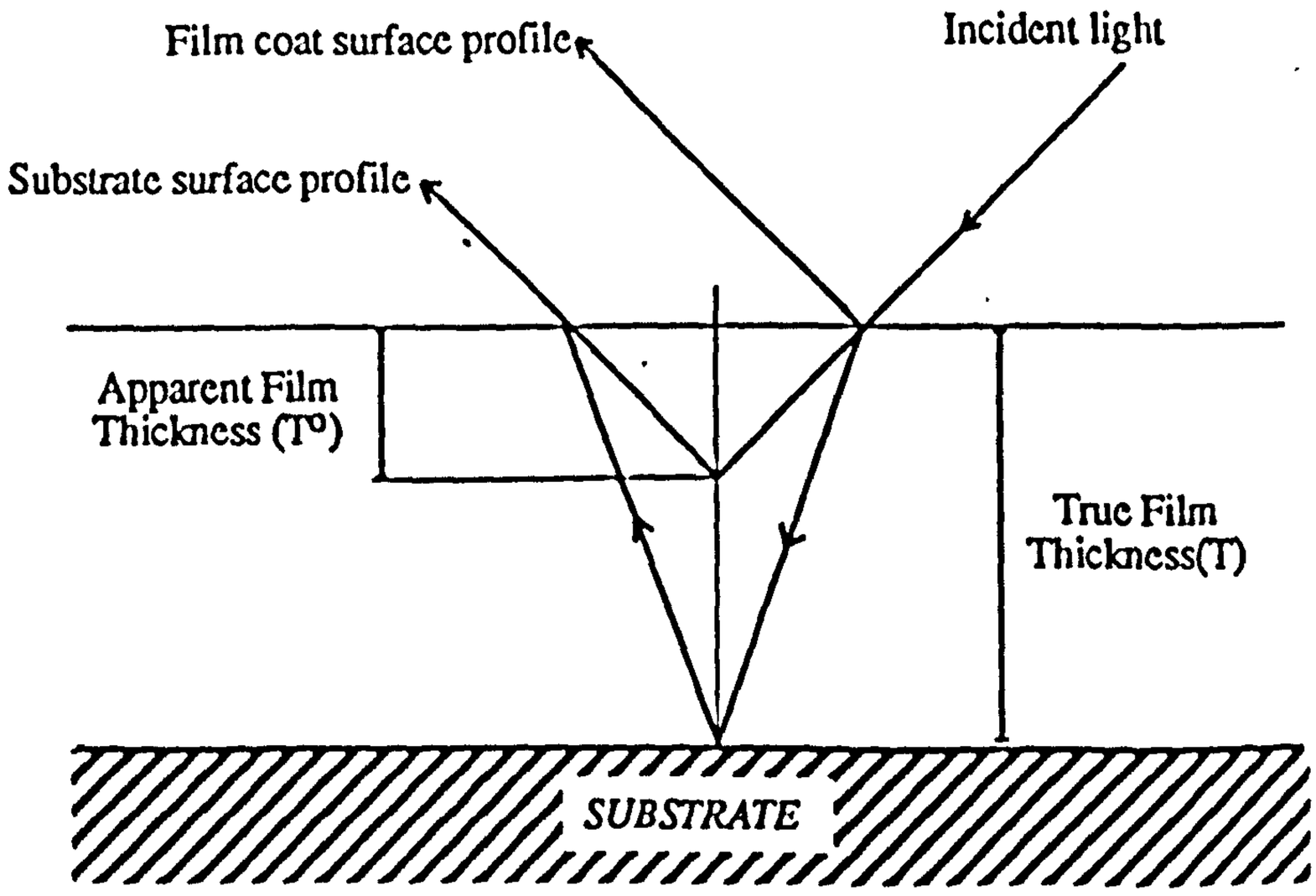

distance values can then be read off the drum with a sensitivity of 0.1μm. The image appears inverted in the eye-piece. A mechanical stage allows longitudinal or transversal movement of the sample by up to 25mm by means of micrometers.

Surface roughness parameters which can be obtained using the Light Section Microscope include; R_T, the distance between the highest peak and deepest valley, R_{TM}, the average of five peak to valley distances and R_w, the average distance between peaks or troughs. Calculation of Ra, the arithmetic mean roughness can only be undertaken after a photographic record has been obtained.

If a transparent film is being analysed, then two light bands are seen in the eye-piece, one corresponding to the film surface and the other to the surface of the substrate. Due to the refraction of the light as it penetrates the transparent layer, the distance between the light bands as measured through the eye-piece does not represent the true thickness of the coating (see Figure 5.3). The relationship between the actual thickness of the coat (T) and the apparent thickness (T°) can be calculated from the formula:

$$T = T^{\circ} \ (2n^2 - 1)^{0.5}$$

where n is the refractive index of the transparent layer. For the HPMC coatings studied in this work, the value of n was taken to be 1.49 (Rowe and Forse, 1983a) and thus $T = 1.85T^{\circ}$.

5.4.2 EXPERIMENTAL

Values of R_{TM}, R_w and coat thickness for 10mm flat, 15mm flat and 10mm scored convex tablets taken from various coating runs, were assessed using the Light Section Microscope. Measurements were taken from different sections on the tablet surface and on at least five different tablets from each coating run studied. For the two types of flat

tablets, measurements were taken on the main tablet body and over the edge 0.5mm. With the convex tablets, measurements were taken over the tablet crown, on the main tablet body and within the score. Due to the instrument design, it was only possible to make measurements over approximately the central two thirds of the score area and not possible to investigate the edge of the convex tablets. Film thicknesses were calculated both from the coat peak to the substrate (designated T1) and the coat trough to the substrate (designated T2) for five consecutive peaks/troughs from each measured section. Values of R_u were calculated from ten consecutive peaks and troughs.

5.4.3 RESULTS

In view of both the considerable time needed to manually carry out measurements using the Light Section Microscope and its limited availabilty, it was only possible to determine values for a limited number of coating runs. The results from those tablets examined are detailed in Table 5.14, full details of the coating conditions being given in Appendix 1. The ratio of T1 to T2 is included in Table 5.14 to give an indication of how evenly the coat was applied.

Film roughness and thickness values were found not to be significantly different when taken at different regions on the main body of the flat tablets and the results were therefore grouped together. Differences were noted however when the edges of the tablets were examined and these results are reported separately. With the 10mm convex tablets, differences in both the roughness and thickness characteristics were noted when measurements were taken on the crown of the tablet, on the normal body of the tablet and within the score.

The results in Table 5.14 indicate that the film coat surface roughness, as measured by R_{TM}, can vary considerably, this being dependent on the

TABLE 5.14: FILM COAT THICKNESS AND SURFACE ROUGHNESS VALUES MEASURED USING A LIGHT SECTION MICROSCOPE

COATING RUN	TABLET TYPE (REGION)	R_{TM} ± s.d. (μm)	R_w ± s.d. (μm)	COATING THICKNESS ± s.d. T1 (μm)	T2 (μm)	T2/T1
UNCOATED	15mm flat	10.5±0.9				
UNCOATED	10mm flat	17.1±1.6				
UNCOATED	10mm convex	18.3±1.8				
UNCOATED	10mm convex (crown)	30.3±3.7				
UNCOATED	10mm convex (intagliation)	4.1±2.6				
7	15mm flat	11.6±3.1	123.8±6.4	55.1±5.1	43.6±6.6	0.791
7	15mm flat (edge)	4.3±1.2		41.8±8.3	36.7±7.4	0.878
11	15mm flat	10.4±2.3	155.7±19.3	44.1±9.1	22.2±8.0	0.503
11	15mm flat (edge)	9.0±2.8		29.0±8.4	17.0±5.7	0.586
11	10mm flat	9.9±2.5	175.5±5.7	42.4±7.2	28.7±5.9	0.677
11	10mm flat (edge)	7.0±2.0		32.5±4.0	19.0±6.2	0.585
11	10mm convex	10.5±2.6		50.2±5.6	35.4±3.2	0.705
11	10mm convex (intagliation)	3.6±1.9		41.4±6.9	38.5±7.9	0.930
12	15mm flat	12.4±4.5	187.3±6.6	56.2±9.0	42.0±4.3	0.747
12	15mm flat (edge)	2.5±1.9		47.0±5.1	38.6±4.7	0.821
16	15mm flat	10.1±2.4	151.2±5.2	52.6±4.5	41.9±6.9	0.797
16	15mm flat (edge)	1.7±2.2		37.4±4.6		
17	15mm flat	10.7±2.6	239.5±27.3	46.7±5.1	35.6±6.4	0.762
17	15mm flat (edge)	6.8±1.9		40.5±5.3	30.6±5.6	0.756
17	10mm flat	10.7±2.7	251.7±2.2	58.7±6.4	45.1±5.0	0.768
17	10mm flat (edge)	8.1±2.2		45.2±8.2	31.9±2.4	0.706
17	10mm convex	10.5±3.1		58.8±6.8	48.9±7.9	0.832
17	10mm convex (intagliation)	1.3±1.7		53.1±4.4	51.5±3.4	0.970
18	15mm flat	6.2±2.5	278.1±21.0	42.4±4.3	22.6±2.9	0.533
18	10mm flat	7.2±2.4		45.1±3.9	25.7±3.2	0.569
18	10mm convex			46.2±5.6	25.4±4.2	0.550
18	10mm convex (crown)			56.3±8.1	12.3±3.2	0.218
18	10mm convex (intagliation)			38.0±3.5	34.4±2.9	0.905
20	15mm flat	1.1±2.3	193.2±16.8	56.6±5.7	50.2±8.2	0.886
20	15mm flat (edge)	2.2±1.9		37.9±5.6	32.1±5.7	0.847
21	15mm flat	15.4±3.8	132.5±14.5	52.6±6.0	43.9±6.8	0.835
21	10mm convex	12.5±2.4		51.0±4.7	45.1±6.7	0.884
21	10mm convex (intagliation)	6.0±1.1		51.2±4.7	49.2±2.6	0.961
23	15mm flat	14.9±3.4	127.8±10.1	53.1±4.7	42.9±5.3	0.808
23	10mm flat	15.3±3.1	120.1±1.8	51.0±7.4	37.1±6.1	0.727
23	10mm convex	12.1±1.9		55.2±6.7	47.0±6.7	0.851
23	10mm convex (intagliation)	6.5±0.9		55.4±9.1	49.0±9.6	0.884

Full details of the coating runs are given in Appendix 1.

coating process conditions. Of the samples studied, the highest values of R_{TM} were encountered on the main body of tablets from coating runs 21 and 23 where the main process variation was an increased gun-to-bed distance, and the lowest in runs 18 and 20 where a solid cone spray pattern was employed (see Appendix 1 for coating run details). Other process variations, such as the use of different spray guns, spray rates and atomising air pressures, produced intermediate R_{TM} values.

The roughness values determined over the edge 0.5mm of the flat tablets were found to be considerably lower than on the main body of the tablet. This was more noticeable with the 15mm flat tablets than with the 10mm flat tablets. With the 10mm convex tablets, the roughness values appeared greater on the crown of the tablet than on the main tablet body and least rough within the score. Roughness measurements at the edge of the 10mm convex tablets were not possible due to the geometry of the tablets and the measuring capabilities of the Light Section Microscope.

Values of R_{TM} were generally similar on the main body of each of the three types of tablets studied. Arithmetic mean roughness (Ra) values for the samples in Table 5.14 are given in section 5.5.

Rw, the average distance between coat peaks/troughs was also shown to vary considerably between coating runs. Smaller values were generally associated with the greater values of R_{TM} and the larger values with the smoother surfaces. The main exceptions to this were the values from run 17. Thus it would appear that generally those coats which have greater vertical average distances between the peaks and troughs also have a greater frequency of peaks/troughs across the tablet surface. Values measured on both the 10mm and 15mm flat tablets were of the same order.

The film thickness readings show there to be considerable differences between tablets from different coating runs, both in terms of the distance from the coat peak to the tablet surface (T1) and the coat

trough to the tablet surface (T2). Similarly differences between the ratio of the two measurements were demonstrated. In every case the value of T1 was found to be greater than T2, indicating that the average distance from the coat peak to the tablet surface was greater than that from the coat trough.

Lower film thickness values appeared to be associated with smoother film surfaces, with these films also possessing relatively larger variations in film thickness (as evidenced by the low ratios of T2:T1). The main exception to this was run 20 which was found to possess relatively thick films despite exhibiting low roughness values. Examination of the coating conditions in Appendix 1 reveals that lower film thickness values are associated with an atomising air pressure of 552kPa. Of the coating runs examined, the only instance where this air pressure did not produce relatively thin coats was run 21, which utilised the greater spray gun-to-bed distance of 250mm.

When the film coats exhibiting the relatively thin coats and small T2:T1 ratios were viewed through the Light Section Microscope, it was apparent that they did not follow the contours of the substrate, that is peaks in the coat profile did not occur at the point that peaks in the substrate profile occurred. The converse was generally true for the remainder of the coated tablets examined, with contours of the film tending to correspond to those of the tablet.

The coat thicknesses on the main body of the three types of test tablets were found not to be significantly different. Film thicknesses at the edge (0.5mm) of the flat tablets were however found to be less than those on the main tablet body. There was a greater variation in film thickness on the crown of the 10mm convex tablets than on the main tablet body. Within the tablet score, little difference between two thickness values was apparent, resulting in large values of T2:T1.

5.5 THE SURFACE ROUGHNESS OF AQUEOUS FILM COATED TABLETS

The surface roughness values of tablets coated in this study were assessed by determining their arithmetic mean surface roughness (Ra). This may be defined as the arithmetic mean value of the departure of the roughness profile above and below a central reference line and is illustrated in Figure 5.4.

Figure 5.4 Arithmetic mean roughness (Ra)

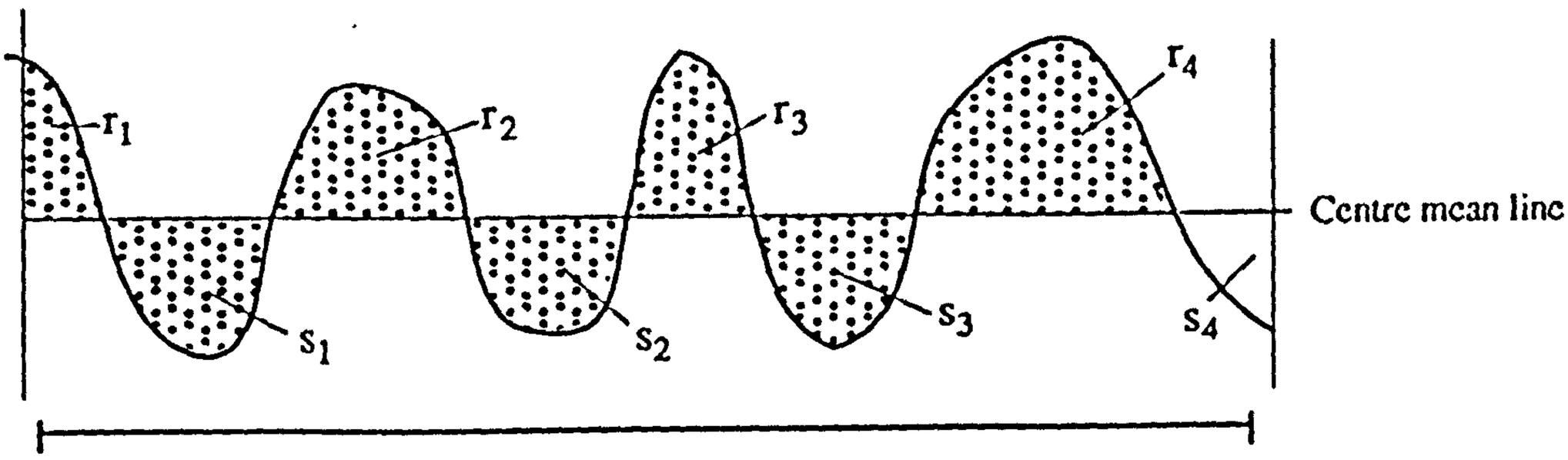

$$Ra = \frac{\text{sum of areas (r)} + \text{sum of areas (s)}}{L}$$

5.5.1 EXPERIMENTAL

Surface roughness measurements were determined from both sides of at least five individual 15mm flat coated tablets, using a Talysurf 10 surface measuring instrument (Rank Taylor Hobson, Leicester). This instrument assesses surface roughness from the vertical movement of a stylus traversed across the surface of the tablet. The vertical movement is converted into an electrical signal which is amplified and processed to give an Ra value. Ra values up to 5µm can be obtained. The standard skid nosepiece was used on the pick-up arm for all readings. A hard copy trace was also produced. The machine accuracy was checked both prior to testing and periodically during the study using a calibration standard and was found to be within specification.

Individual coat surface roughness measurements were averaged over a 5mm traverse length using an 0.8mm cut off (sampling) length (see British Standard 1134 Parts 1 and 2 (1972)). All tablets were stored at 20°C and 58% RH for at least two weeks prior to testing. Measurements were taken at ambient temperatures (21°C to 25°C). To ensure that the skid nosepiece and stylus were not damaging the surface during the test process (and therefore producing erroneous readings), five repeat Ra values were determined over the same sample length on tablets taken from five different coating runs.

5.5.2 RESULTS

Repeated determinations of Ra values over the same sampling area were found to give identical results for all five different coated tablets tested. This indicates that the skid nosepiece and stylus were not damaging the film surface during measurement.

The Ra values for tablets from all the coating runs studied are shown in Appendix 3. Each value and its associated standard deviation was derived from at least ten measurements. The Ra value of the uncoated 15mm flat tablets was found to be 2.21 ± 0.26. Data indicating the influence of various process conditions on film surface roughness have been abstracted from Appendix 3 and are reported below.

5.5.2.1 THE EFFECT OF SPRAY GUN TYPE AND FORMULATION CONCENTRATION ON FILM COAT SURFACE ROUGHNESS

The roles of the spray gun and coating formulation in determining the surface characteristics of aqueous film coated tablets are illustrated in Table 5.15. It is apparent that both these process variables may potentially exert a marked influence on product coat surface roughness.

TABLE 5.15: EFFECT OF SPRAY GUN TYPE AND SOLUTION CONCENTRATION ON FILM COAT SURFACE ROUGHNESS

RUN NUMBER	SPRAY GUN TYPE	LIQUID NOZZLE DIAMETER (mm)	AIR CAP	SOLUTION TYPE	SOLUTION CONCENTRATION (%w/w)	ATOMISING AIR PRESSURE (kPa)	SPRAY RATE ($gmin^{-1}$)	TABLET FILM COAT SURFACE ROUGHNESS (Ra) (µm)
63	WP	1.0	STD	HPMC E5	6	414	40	1.75
47	SCH	0.8	STD	HPMC E5	6	414	40	1.83
46	SS	0.71	45°	HPMC E5	6	414	40	1.90
62	SS	0.71	60°	HPMC E5	6	414	40	2.00
12	WP	1.0	STD	HPMC E5	9	276	40	2.54
15	BB	1.8	63PB	HPMC E5	9	276	40	2.41
7	SCH	0.8	STD	HPMC E5	9	276	40	2.72
29	SS	0.71	60°	HPMC E5	9	276	40	3.75
31	WP	1.0	STD	HPMC E5	9	414	40	1.94
10	WP	1.0	STD	HPMC E5	9	414	40	2.16
16	BB	1.8	63PB	HPMC E5	9	414	40	2.10
13	SS	0.71	45°	HPMC E5	9	414	40	2.30
9	SCH	0.8	STD	HPMC E5	9	414	40	2.53
14	SS	0.71	60°	HPMC E5	9	414	40	3.40
11	WP	1.0	STD	HPMC E5	9	552	40	1.90
17	BB	1.8	63PB	HPMC E5	9	552	40	2.03
24	SS	0.71	45°	HPMC E5	9	552	40	2.08
32	SCH	0.8	STD	HPMC E5	9	552	40	2.23
8	SCH	0.8	STD	HPMC E5	9	552	40	2.29
25	SS	0.71	60°	HPMC E5	9	552	40	3.09
43	WP	1.0	STD	HPMC E5	12	414	40	2.86
45	BB	1.8	63PB	HPMC E5	12	414	40	2.86
38	SS	0.71	45°	HPMC E5	12	414	40	3.26
34	SCH	0.8	STD	HPMC E5	12	414	40	3.51
37	SS	0.71	60°	HPMC E5	12	414	40	>5.00
53	WP	1.0	STD	OPADRY	15	414	50	2.28
52	BB	1.8	STD	OPADRY	15	414	50	3.99
48	SCH	0.8	STD	OPADRY	15	414	50	2.98
65	SCH	0.8	STD	OPADRY	10	414	50	2.20
50	SS	0.71	45°	OPADRY	15	414	50	2.85
68	SCH	0.8	STD	OPADRY	15	414	30	2.61
66	SCH	0.8	STD	OPADRY	20	414	30	4.24

FULL DETAILS OF ALL THE COATING RUNS ARE GIVEN IN APPENDIX 1

Increasing both the HPMC E5 and Opadry concentration (and thus viscosity) was found to produce increasingly rougher coats irrespective of the other process conditions used. This effect was particularly apparent with the change from a 9%w/w to a 12%w/w HPMC E5 solution and when the 20%w/w Opadry suspension was applied. The 6%w/w HPMC E5 solution produced coats which were smoother than the original substrate. Conversely each coating run using either a 12%w/w HPMC E5 solution or a 15%w/w Opadry suspension produced coats which were rougher than the original substrate. With the 9%w/w solution the roughness of the coat in relation to substrate was dependent on the process conditions used. Further results illustrating the effect of coating formulation and viscosity are detailed in section 5.5.2.6.

The choice of spray gun used to apply the 6%w/w HPMC E5 solution appeared to have a relatively small influence on the resultant film coat roughness. With other coating formulations however, there were significant differences in roughness when different spray guns were used. The smoothest coats were produced by the Walther Pilot and Binks Bullows guns, the roughness values for these coats being for all practical purposes identical. The next smoothest coats were produced by the Spraying Systems, 45°gun followed by the Schlick gun. The roughest coat surfaces were found on tablets coated with the Spraying Systems 60° gun, which with the exception of when the 6%w/w solution was applied, produced coats which were far rougher than from any of the other guns.

5.5.2.2 THE EFFECT OF ATOMISING AIR PRESSURE ON FILM COAT SURFACE ROUGHNESS

The effect of changes in the atomising air pressure on the roughness of the resultant film coat is demonstrated in Table 5.16. It can be seen that an increase in atomising air pressure resulted in a decrease in

TABLE 5.16: THE EFFECT OF ATOMISING AIR PRESSURE ON FILM COAT SURFACE ROUGHNESS

RUN NUMBER	SPRAY GUN TYPE	LIQUID NOZZLE DIAMETER (mm)	AIR CAP TYPE	HPMC E5 SOLUTION CONCENTRATION (%w/w)	ATOMISING AIR PRESSURE (kPa)	SPRAY RATE ($gmin^{-1}$)	GUN TO BED DISTANCE (mm)	SPRAY SHAPE	TABLET FILM COAT SURFACE ROUGHNESS (Ra) (μm)
7	SCH	0.8	STD	9	276	40	180	FLAT	2.72
9	SCH	0.8	STD	9	414	40	180	FLAT	2.53
32	SCH	0.8	STD	9	552	40	180	FLAT	2.23
8	SCH	0.8	STD	9	552	40	180	FLAT	2.29
23	SCH	0.8	STD	9	276	40	250	FLAT	3.20
22	SCH	0.8	STD	9	414	40	250	FLAT	2.71
21	SCH	0.8	STD	9	552	40	250	FLAT	2.60
20	SCH	0.8	STD	9	276	40	180	10°CONE	1.68
19	SCH	0.8	STD	9	414	40	180	10°CONE	1.44
18	SCH	0.8	STD	9	552	40	180	10°CONE	1.29
60	SCH	0.8	STD	12	207	40	180	FLAT	4.06
41	SCH	0.8	STD	12	276	40	180	FLAT	3.98
34	SCH	0.8	STD	12	552	40	180	FLAT	3.51
40	SCH	0.8	STD	12	207	40	250	FLAT	4.67
35	SCH	0.8	STD	12	414	40	250	FLAT	4.09
6	SCH	0.8	STD	9	414	50	180	FLAT	1.90
2	SCH	0.8	STD	9	414	50	180	FLAT	2.00
4	SCH	0.8	STD	9	552	50	180	FLAT	1.60
12	WP	1.0	STD	9	276	40	180	FLAT	2.54
31	WP	1.0	STD	9	414	40	180	FLAT	1.94
10	WP	1.0	STD	9	414	40	180	FLAT	2.16
11	WP	1.0	STD	9	552	40	180	FLAT	1.90
44	WP	1.0	STD	12	207	40	180	FLAT	3.20
43	WP	1.0	STD	12	414	40	180	FLAT	2.86
15	BB	1.8	63PB	9	276	40	180	FLAT	2.41
16	BB	1.8	63PB	9	414	40	180	FLAT	2.10
17	BB	1.8	63PB	9	552	40	180	FLAT	2.03
28	SS	0.71	60°	9	138	40	180	FLAT	4.08
29	SS	0.71	60°	9	276	40	180	FLAT	3.75
14	SS	0.71	60°	9	414	40	180	FLAT	3.40
25	SS	0.71	60°	9	552	40	180	FLAT	3.09
13	SS	0.71	45°	9	414	40	180	FLAT	2.30
24	SS	0.71	45°	9	552	40	180	FLAT	2.08
39	SS	0.71	45°	12	207	40	180	FLAT	4.16
38	SS	0.71	45°	12	414	40	180	FLAT	3.26

FULL DETAILS OF ALL THE COATING RUNS ARE GIVEN IN APPENDIX 1

film surface roughness. This occurred at different solution concentrations, spray rates, spray shapes, spray gun to tablet bed distances and for each gun type studied. The extent of the reduction in roughness with increasing air pressure, although varying depending on the other coating conditions was generally of the same order.

5.5.2.3 THE EFFECT OF SPRAY GUN TO BED DISTANCE AND LIQUID NOZZLE DIAMETER ON FILM COAT SURFACE ROUGHNESS

The effect on film coat surface roughness of changing the distance that the spray gun was positioned from the tablet bed, and the internal diameter of the liquid nozzle, are illustrated in Table 5.17. With both the Schlick and Spraying Systems guns, an increase in the gun-to-bed distance resulted in coats exhibiting rougher surfaces, this occurring irrespective of the other coating conditions used. The design of the Binks Bullows and Walther Pilot spray guns meant that it was not possible to perform coating runs where the gun-to-bed distance exceeded approximately 180mm. The results of the coating runs using the Schlick gun to apply a 9%w/w HPMC E5 solution suggest that the effect of increasing the gun to bed distance may become greater as the atomising air pressure is reduced.

Data in Table 5.17 from the coating runs investigating the role of the liquid nozzle orifice diameter, did not provide any evidence to suggest that this process variable influenced the film coat surface roughness.

5.5.2.4 THE EFFECT OF SPRAY RATE AND SPRAY SHAPE ON FILM COAT SURFACE ROUGHNESS

The effect of changes in coating solution application rate and spray shape on film coat surface roughness is shown in Table 5.18. The results do not indicate a clear relationship between spray rate and surface

TABLE 5.17: THE EFFECT OF GUN TO BED DISTANCE AND LIQUID NOZZLE DIAMETER ON FILM COAT ROUGHNESS

RUN NUMBER	SPRAY GUN TYPE	LIQUID NOZZLE DIAMETER (mm)	AIR CAP	HPMC E5 SOLUTION CONCENTRATION (%w/w)	ATOMISING AIR PRESSURE (kPa)	SPRAY RATE ($gmin^{-1}$)	GUN TO BED DISTANCE (mm)	SPRAY SHAPE	TABLET FILM COAT SURFACE ROUGHNESS (Ra) (µm)
7	SCH	0.8	STD	9	276	40	180	FLAT	2.72
23	SCH	0.8	STD	9	276	40	250	FLAT	3.20
9	SCH	0.8	STD	9	414	40	180	FLAT	2.53
22	SCH	0.8	STD	9	414	40	250	FLAT	2.71
32	SCH	0.8	STD	9	552	40	180	FLAT	2.23
8	SCH	0.8	STD	9	552	40	180	FLAT	2.29
21	SCH	0.8	STD	9	552	40	250	FLAT	2.60
2	SCH	0.8	STD	9	414	50	180	FLAT	1.90
6	SCH	0.8	STD	9	414	50	180	FLAT	2.00
33	SCH	0.8	STD	9	414	50	250	FLAT	2.27
34	SCH	0.8	STD	12	414	40	180	FLAT	3.51
35	SCH	0.8	STD	12	414	40	250	FLAT	4.09
61	SCH	0.8	STD	12	414	50	180	FLAT	3.56
36	SCH	0.8	STD	12	414	50	250	FLAT	4.06
42	SCH	0.8	STD	12	414	50	300	FLAT	4.24
24	SS	0.71	45°	9	552	40	180	FLAT	2.08
27	SS	0.71	45°	9	552	40	250	FLAT	2.31
25	SS	0.71	60°	9	552	40	180	FLAT	3.09
26	SS	0.71	60°	9	552	40	250	FLAT	3.26
9	SCH	0.8	STD	9	414	40	180	FLAT	2.53
55	SCH	1.2	STD	9	414	40	180	FLAT	2.31
56	SCH	1.8	STD	9	414	40	180	FLAT	2.38
13	SS	0.71	45°	9	414	40	180	FLAT	2.30
74	SS	0.51	45°	9	414	40	180	FLAT	2.15

FULL DETAILS OF ALL THE COATING RUNS ARE GIVEN IN APPENDIX 1

TABLE 5.18: THE EFFECT OF SPRAY RATE AND SPRAY SHAPE ON FILM COAT SURFACE ROUGHNESS

RUN NUMBER	SPRAY GUN TYPE	LIQUID NOZZLE DIAMETER (mm)	AIR CAP	SOLUTION TYPE AND CONCENTRATION (%w/w)	ATOMISING AIR PRESSURE (kPa)	SPRAY RATE ($gmin^{-1}$)	GUN TO BED DISTANCE (mm)	SPRAY SHAPE	TABLET FILM COAT SURFACE ROUGHNESS (Ra) (µm)
1	SCH	0,8	STD	9%w/w HPMC E5	414	30	180	FLAT	3,90
9	SCH	0,8	STD	9%w/w HPMC E5	414	40	180	FLAT	2,53
6	SCH	0,8	STD	9%w/w HPMC E5	414	50	180	FLAT	1,90
2	SCH	0,8	STD	9%w/w HPMC E5	414	50	180	FLAT	2,00
22	SCH	0,8	STD	9%w/w HPMC E5	414	40	250	FLAT	2,71
33	SCH	0,8	STD	9%w/w HPMC E5	414	50	250	FLAT	2,27
26	SS	0,71	60°	9%w/w HPMC E5	552	40	250	FLAT	3,26
30	SS	0,71	60°	9%w/w HPMC E5	552	50	250	FLAT	4,17
31	WP	1,0	STD	9%w/w HPMC E5	414	40	180	FLAT	1,94
10	WP	1,0	STD	9%w/w HPMC E5	414	40	180	FLAT	2,16
64	WP	1,0	STD	9%w/w HPMC E5	414	50	180	FLAT	1,94
58	SCH	0,8	STD	12%w/w HPMC E5	414	30	180	FLAT	2,54
34	SCH	0,8	STD	12%w/w HPMC E5	414	40	180	FLAT	3,51
61	SCH	0,8	STD	12%w/w HPMC E5	414	50	180	FLAT	3,56
35	SCH	0,8	STD	12%w/w HPMC E5	414	40	250	FLAT	4,09
36	SCH	0,8	STD	12%w/w HPMC E5	414	50	250	FLAT	4,06
68	SCH	0,8	STD	15%w/w OPADRY	414	30	180	FLAT	2,61
67	SCH	0,8	STD	15%w/w OPADRY	414	40	180	FLAT	3,11
48	SCH	0,8	STD	15%w/w OPADRY	414	50	180	FLAT	2,98
9	SCH	0,8	STD	9%w/w HPMC E5	414	40	180	FLAT	2,53
77	SCH	0,8	STD	9%w/w HPMC E5	414	40	180	ELIPSE	2,19
19	SCH	0,8	STD	9%w/w HPMC E5	414	40	180	10°CONE	1,44
7	SCH	0,8	STD	9%w/w HPMC E5	276	40	180	FLAT	2,72
20	SCH	0,8	STD	9%w/w HPMC E5	276	40	180	10°CONE	1,68
8	SCH	0,8	STD	9%w/w HPMC E5	552	40	180	FLAT	2,29
32	SCH	0,8	STD	9%w/w HPMC E5	552	40	180	FLAT	2,23
18	SCH	0,8	STD	9%w/w HPMC E5	552	40	180	10°CONE	1,29
34	SCH	0,8	STD	12%w/w HPMC E5	414	40	180	FLAT	3,51
59	SCH	0,8	STD	12%w/w HPMC E5	414	40	180	10°CONE	2,07

FULL DETAILS OF ALL THE COATING RUNS ARE GIVEN IN APPENDIX 1

roughness, the effect of changes in spray rate appearing to be dependent on the nature of the coating solution applied and possibly the spray gun used. For the 9%w/w HPMC E5 solutions applied with the Schlick and Walther Pilot guns, it would appear that increases in the spray rate result in smoother films. The opposite however appeared to be true when the Spraying Systems 60° gun was used. When 12%w/w HPMC E5 solutions were applied with the Schlick gun, it appeared that an increase in spray rate from $30gmin^{-1}$ to $40gmin^{-1}$ resulted in a rougher surface, but further spray rate increases to $50gmin^{-1}$ caused no further roughness increase. A similar effect was seen when the 15%w/w Opadry suspensions were applied.

A change in spray shape from the standard flat spray shape to a narrow angle cone, produced a marked reduction in surface roughness for each set of conditions studied. Run number 77, which used a spray shape exhibiting dimensions approximately midway between the flat and cone shapes (see section 5.8), produced a coat exhibiting an intermediate roughness value.

5.5.2.5 THE EFFECT OF DRYING AIR TEMPERATURE AND VOLUME FLOW RATE ON FILM COAT SURFACE ROUGHNESS

Results in Table 5.19 indicate that the reduction in the drying air volume flow rate from $0.129m^3hr^{-1}$ to $0.088m^3hr^{-1}$, or the reduction in its temperature from 65°C to 58°C had only a small effect on coat surface roughness, the reduction in both parameters producing coats which were slightly smoother.

TABLE 5.19: THE EFFECT OF DRYING AIR TEMPERATURE AND VOLUME FLOW RATE ON FILM COAT SURFACE ROUGHNESS

RUN NUMBER	DRYING AIR TEMPERATURE (°C)	DRYING AIR VOLUME FLOW RATE (m^3s^{-1})	FILM COAT SURFACE ROUGHNESS (Ra) (μm)
9	65	0.129	2.53
76	67	0.088	2.39
57	58	0.129	2.43
79	59	0.129	2.47

Full details of these coating runs are given in Appendix 1.

5.5.2.6 THE EFFECT OF OTHER PROCESS VARIABLES ON FILM COAT SURFACE ROUGHNESS

The effect on the tablet film coat surface roughness of the other process variables investigated, which have not been previously described, are shown in Table 5.20. The inclusion of 1%w/w PEG 400 in the coating formulation (run 69) and the heating of the solution so that it entered the spray gun at 43°C (run 78) both appeared to cause a small increase in the coat surface roughness, the Ra value rising from 2.53μm to 2.93μm and 2.88μm respectively. The coating run using conditions similar to those described by Prater (1982) for a model coating system, produced film coats with an Ra value of 1.45μm. The only two runs which yielded smoother coats than this were runs 18 and 19, which used the Schlick gun

TABLE 5.20: THE EFFECT OF SOME PROCESS VARIABLES ON FILM COAT SURFACE ROUGHNESS

RUN NUMBER	COATING PROCESS VARIABLE INVESTIGATED	FILM COAT SURFACE ROUGHNESS (Ra) (μm)
9		2.53
69	INCLUSION OF 1%w/w PEG 400	2.93
75	MODEL SYSTEM DETAILED BY PRATER (1982)	1.45
78	COATING SOLUTION ENTERING GUN AT 43°C	2.88
70	12%w/w HPMC E5 SOLUTION FROM BATCH 5	2.88
34	12%w/w HPMC E5 SOLUTION FROM BATCH 2	3.51
71	12%w/w HPMC E5 SOLUTION FROM BATCH 3	3.99

Full details of the coating runs are given in Appendix 1. Information on the different batches of HPMC E5 are given in Table 3.3.

with a narrow angle cone spray shape.

The application of 12%w/w HPMC E5 solutions prepared from powder batches selected to yield widely varying solution viscosities (see Table 3.3), was shown to produce film coats exhibiting different roughness values. The solution prepared from batch 3 (apparent Newtonian viscosity 840mPa s, coefficient of non-Newtonian behaviour 0.975) produced a rougher coat than that prepared from batch 2 (viscosity 520mPa s) which in turn produced a rougher coat than when using the solution prepared from batch 5 (viscosity 389mPa s). The roughness of the applied film

coat was thus shown to increase as the viscosity of the applied solution increased and to be potentially dependent upon the batch of polymer used.

Data taken from Table 5.15 and Table 5.20 are plotted in Figure 5.5 to demonstrate the effect of coating formulation viscosity on film coat surface roughness. In each case all other coating conditions were similar. Two points are plotted on the viscosity scale for coating runs 48 (15%w/w Opadry type OY suspension applied), 65 (10%w/w Opadry type OY suspension applied) and 71 (12%w/w HPMC E5 solution using batch 3), since in these cases the coating formulations exhibited pseudoplastic behaviour. The higher viscosity value represents the apparent Newtonian viscosity (viscosity at a shear rate of $1s^{-1}$, see Equation 3.8) and the lower value the likely viscosity at the point of atomisation (minimum potential viscosity), as discussed in section 4.3. Figure 5.5 indicates that the relationship between film coat roughness and formulation viscosity is of a linear form over the viscosity range studied, with both the HPMC E5 and Opadry coated tablets fitting into the same general pattern. The data appear to suggest that for pseudoplastic formulations, estimation of the potential surface roughness from values of the minimum potential viscosity may yield values which are too low and estimation from the apparent Newtonian viscosity values may give values which are too high.

THE EFFECT OF COATING SOLUTION VISCOSITY ON FILM COAT SURFACE ROUGHNESS

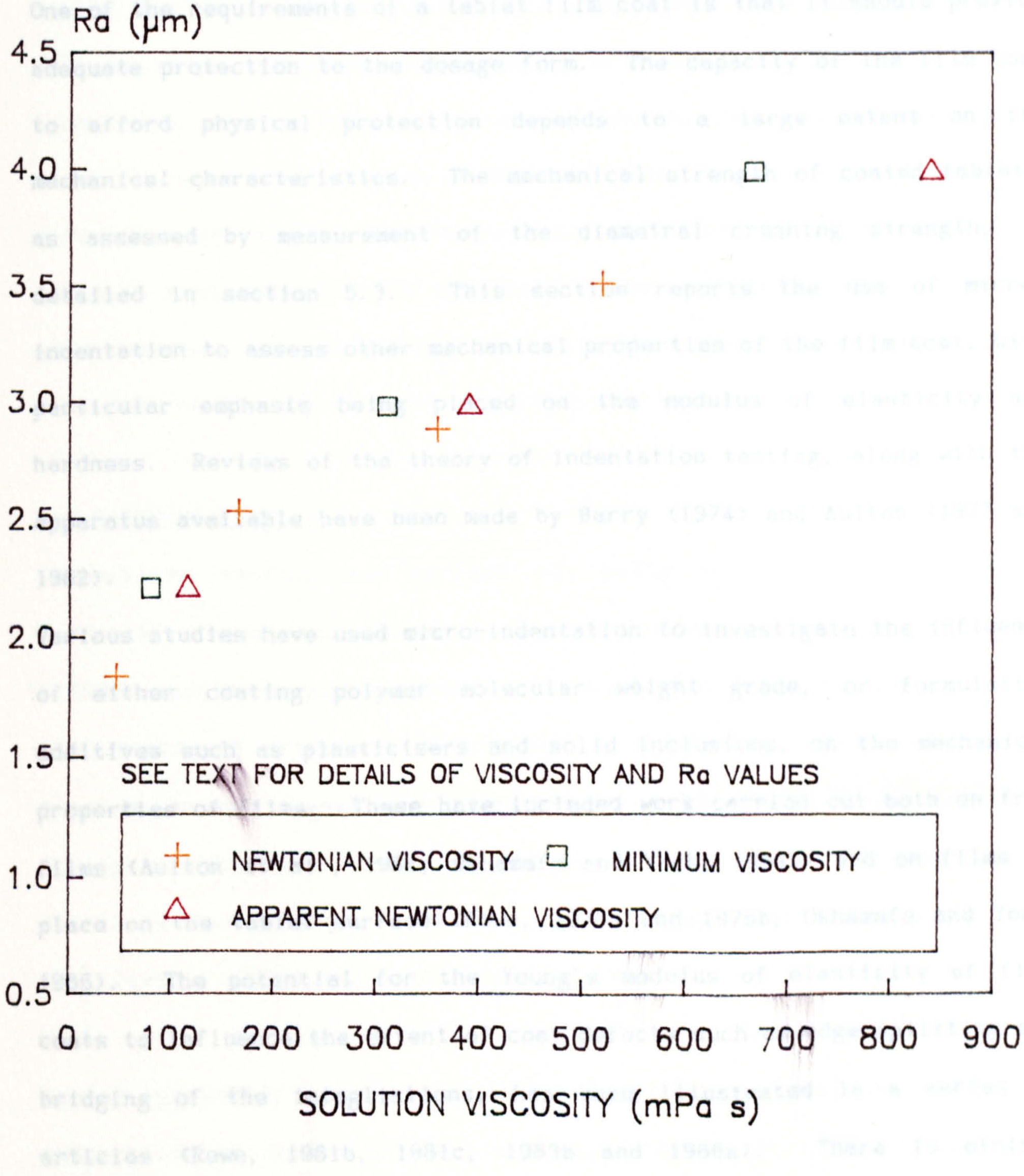

FIGURE 5.5

5.6 THE ASSESSMENT OF THE MECHANICAL PROPERTIES OF AQUEOUS FILM COATED TABLETS USING MICRO-INDENTATION

5.6.1 INTRODUCTION

One of the requirements of a tablet film coat is that it should provide adequate protection to the dosage form. The capacity of the film coat to afford physical protection depends to a large extent on its mechanical characteristics. The mechanical strength of coated tablets, as assessed by measurement of the diametral crushing strength, is detailed in section 5.3. This section reports the use of micro-indentation to assess other mechanical properties of the film coat, with particular emphasis being placed on the modulus of elasticity and hardness. Reviews of the theory of indentation testing, along with the apparatus available have been made by Barry (1974) and Aulton (1977 and 1982).

Various studies have used micro-indentation to investigate the influence of either coating polymer molecular weight grade, or formulation additives such as plasticisers and solid inclusions, on the mechanical properties of films. These have included work carried out both on free films (Aulton et al., 1984; Okhamafe and York, 1984b) and on films in place on the tablet surface (Rowe, 1976a and 1976b; Okhamafe and York, 1986). The potential for the Young's modulus of elasticity of film coats to influence the extent of coat defects such as edge splitting and bridging of the intagliations, has been illustrated in a series of articles (Rowe, 1981b, 1981c, 1983b and 1986a). There is minimal information available however on the effect of the conditions of film production on the resulting film mechanical properties. Rowe (1976b) found no significant difference between films cast onto a glass substrate and those applied to tablets from dilute organic solutions. Okhamafe and York (1986) however reported Young's modulus values for

cast films to be about two to five times greater than equivalent films applied to aspirin tablets.

The intention of this work was to use micro-indentation testing to assess the visco-elastic mechanical properties of films "in-situ" on tablets which had been coated using a variety of different process conditions. It was hoped this information may then aid the explanation of differences in the degree of edge splitting between tablets coated in different ways and enable the process conditions to be manipulated to minimise coat defects. In addition it was considered that information as to whether the fundamental visco-elastic parameters of the coat are dependent on the way in which the films are formed may be elucidated.

5.6.2 EXPERIMENTAL

Indentation testing was carried out using an ICI pneumatic micro-indentation apparatus (Research Equipment (London) Ltd.) fitted with a 1.55mm sapphire indenter sphere. The equipment was modified to include a displacement transducer to determine indentation depth, the output from which was logged and processed by a BBC Model B microcomputer (Acorn Electronics). The complete indentation system is described in detail by Aulton et al. (1986). All readings were performed on 15mm flat tablets which had been stored at 20°C and 58% RH for at least two weeks prior to testing. The indentation apparatus was housed in a sealed glove-box which enabled testing to be carried out at a temperature of 20°C ± 2°C and a relative humidity of 58% ± 3%. This eliminated the potential for different degrees of film plasticisation to arise from variable film moisture contents, as reported by Aulton et al. (1981).

Measurements of indentation depth are usually performed by lowering the indenter sphere until it just touches the surface to be indented, adding

an appropriate weight and monitoring the penetration. When this technique was employed on the film coated tablets produced in this work however, it was found that the results were often very erratic, with coefficients of variation of up to 100% being encountered and indentations of greater than 6µm being observed with only a 1g indentation load. These effects were particularly noticeable with the roughest film coats. It was considered that this may have been due to slippage of the indenter sphere into the "troughs" of the coat and/or movement of poorly adhering spray dried portions of the coat and/or the indentation of air trapped within the coat. The indentation method was therefore slightly modified. The indenter tip was lowered until it just touched the tablet surface (detected as a negative voltage output from the transducer). The indenter beam assembly was then further lowered (with no load present) until the indenter had been displaced upwards by 6µm, the load applied and depth of penetration monitored. This action had the effect of causing a small pre-load to be applied to the film. This overcame the problem of high coefficients of variation and unrealistic indentation rheological profiles.

An indentation load of 5g was used for each analysis and the depth of indentation logged by the computer every 0.1 second for the first three seconds and then every second for a further 250 seconds. Indentations were carried out on at least five tablets from each coating run tested.

The indentation profile was analysed by the computer to give the instantaneous elastic compliance (J_o), the overall creep compliance of the time-dependent elastic deformations (J_R), the instantaneous elastic modulus ($1/J_o$), creep compliance of the non-recoverable viscous deformation (J_N) and the Newtonian viscosity (t/J_N). These values were calculated from a plot of $J_c(t)$ versus time (t) - see Figure 5.6, with $J_c(t)$ being derived from Equation 5.1 (see Lee and Radok, 1960):

$$J_c(t) = \frac{16\sqrt{R}}{3} \cdot \frac{1}{F} \cdot h(t)^{3/2}$$ Equation 5.1

where $J_c(t)$ = creep compliance at time t (Pa^{-1}), R = radius of the indenting sphere (m), F = indentation load (kg) and h(t) = depth of indentation at time t (m).

For the load and indenter sphere used in this work this equation simplifies to:

$$J_c(t) = 42\ h(t)^{3/2}$$

The Brinell hardness was calculated from the initial instantaneous penetration depth using Equation 5.2:

$$\text{Brinell hardness (Pa)} = \frac{F}{\pi D h}$$ Equation 5.2

where F = the load applied, h = the depth of penetration and D = the indenter sphere diameter. For this work this simplifies to:

$$\text{Brinell hardness (Pa)} = \frac{1.027}{h}$$

FIGURE 5.6 : A PLOT OF CREEP COMPLIANCE VERSUS TIME

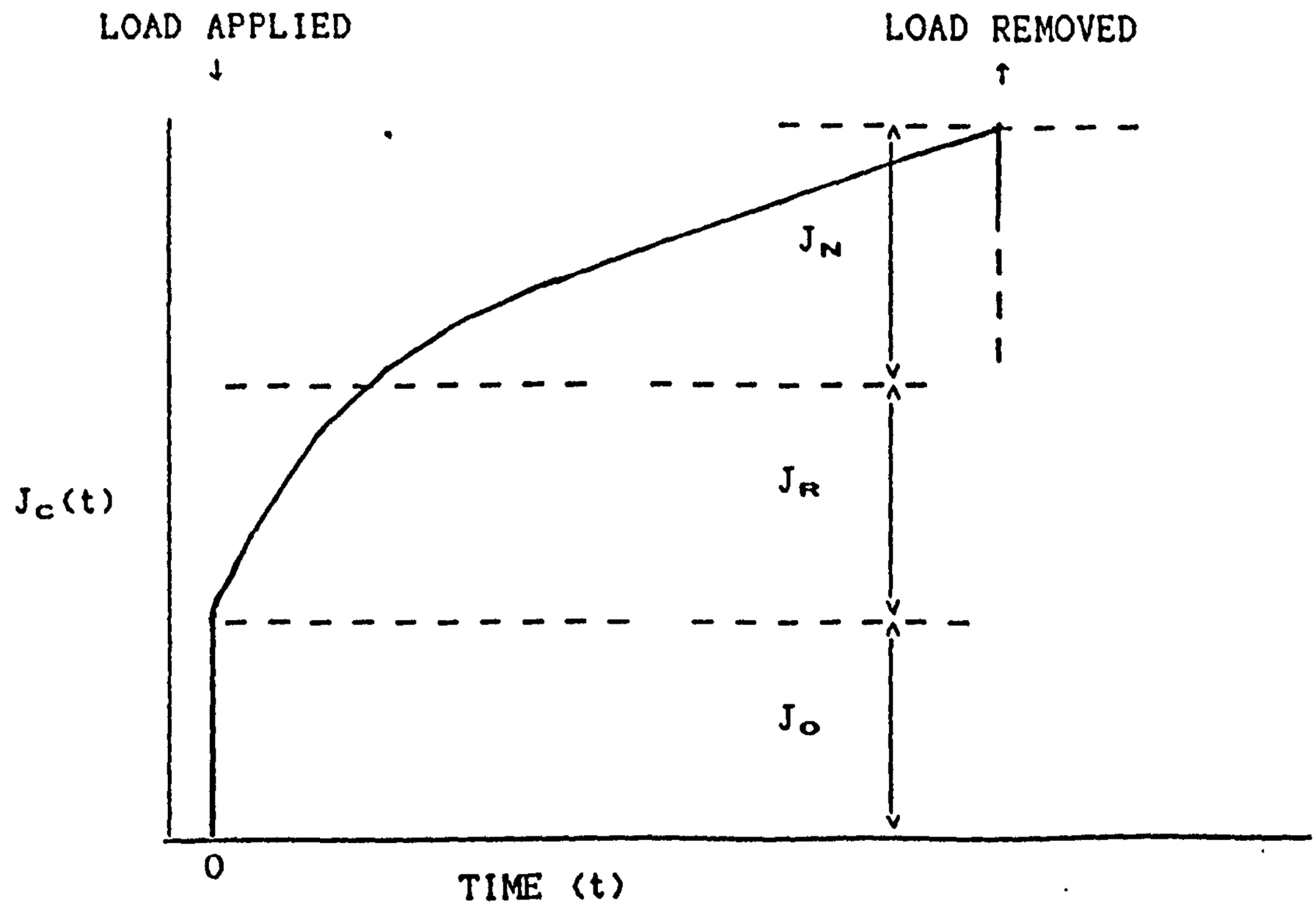

5.6.3 RESULTS

Examination of the indentation profiles showed them to be typically represented by Figure 5.7. Little in the way of film viscoelastic behaviour was apparent for any of the coated tablets tested and the viscous response was small in each case. This behaviour is typical of a material which is glassy in nature, and is similar to that reported by Aulton et al. (1981) for unplasticised HPMC films.

The viscoelastic response that did occur tended to be complete within 20 seconds, with typical values of J_R being about 2×10^{-9} $(Pa)^{-1}$. Coefficients of variation for the five tablets tested from any particular run were between 20% and 40%. There were no discernable relationships between either the conditions used to apply the film and the degree of viscoelastic behaviour, or between other film properties and the viscoelastic behaviour.

FIGURE 5.7 : REPRESENTATIVE FILM COAT INDENTATION PROFILE

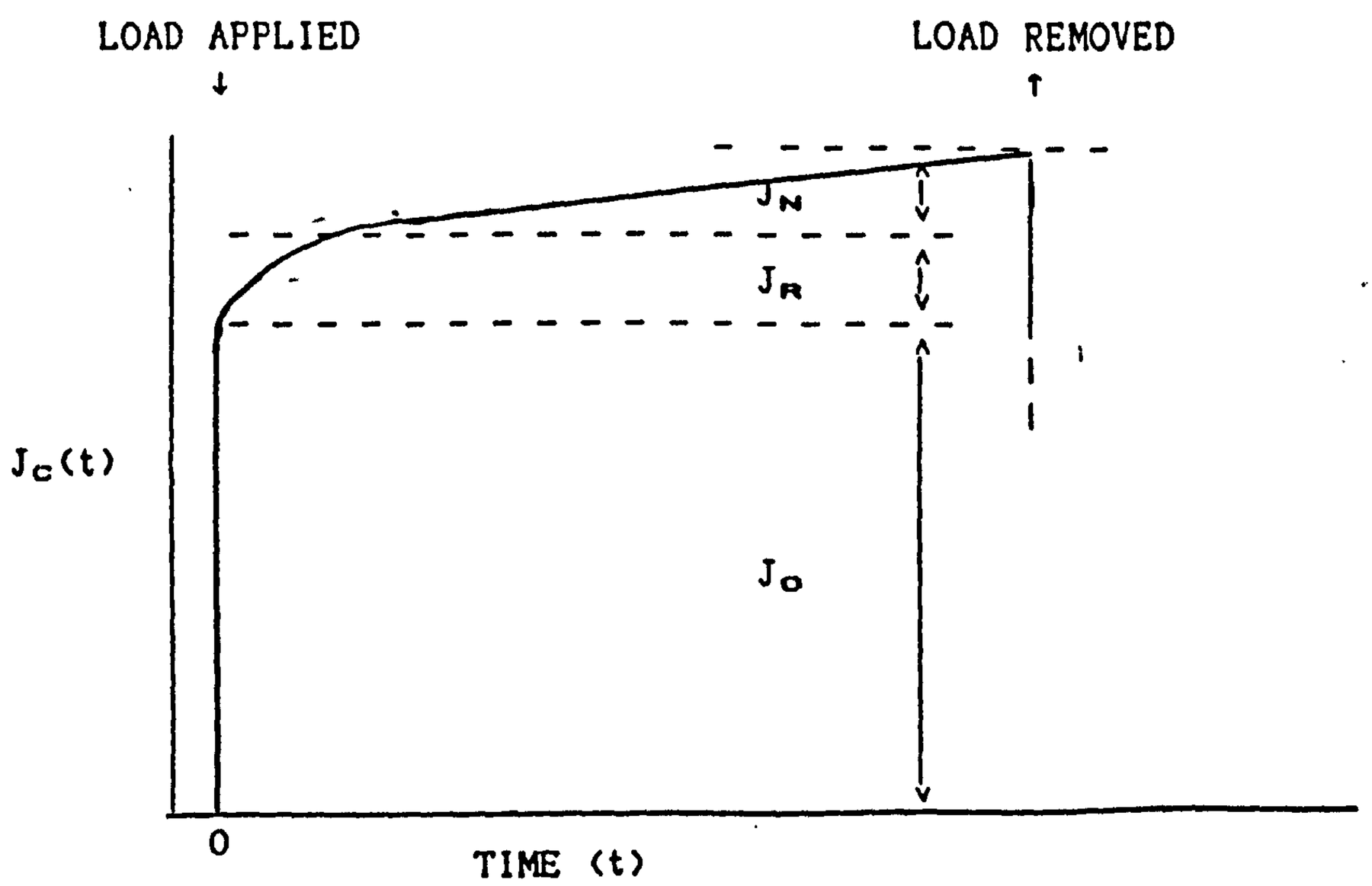

As illustrated in Figure 5.7, there was little viscous deformation occurring over the time of the test. Values calculated for the Newtonian viscosity of the samples ranged from about 0.5 x 10^{11} to 4 x 10^{11}Pa s. Since the viscous response was small, these values tended to be prone to measurement errors when interpreting the traces. Coefficients of variation of up to 65% were found. No relationship was detected between the extent of the viscous response and either the method of film preparation or other film properties.

The predominant difference between the film coats tested was in the extent of the initial instantaneous elastic deformation. Values calculated for the instantaneous elastic modulus and Brinell hardness of the applied films are shown in Table 5.21, along with the film arithmetic mean surface roughness (Ra) values (see section 5.5.2). Details of the coating conditions with which the films were applied are given in Appendix 1.

It would appear from the results in Table 5.21 that the film elastic modulus and hardness are dependent on the way in which the film was generated. With some, values were up to five times greater than others in the case of the instantaneous elastic modulus and up three times greater in the case of the Brinell hardness. The highest values of each of these two parameters are similar to the Brinell hardness value of 3.53MPa and Young's modulus value of 135.7MPa reported by Rowe (1976b) for films applied to flat faced tablets in a Wurster column.

Values of the instantaneous elastic modulus and Brinell hardness plotted against the arithmetic mean surface roughness (Ra), are shown in Figure 5.8. This Figure illustrates that there is a statistically significant linear relationship ($p<0.01$) between both the film elastic modulus and hardness values and the film arithmetic surface roughness.

TABLE 5.21 : BRINELL HARDNESS AND INSTANTANEOUS ELASTIC MODULUS VALUES OF SOME APPLIED FILM COATS

COATING RUN NUMBER	FILM BRINELL HARDNESS (MPa)	FILM INSTANTANEOUS ELASTIC MODULUS (MPa)	FILM ARITHMETIC MEAN SURFACE ROUGHNESS (Ra) (μm)
1	1.49 ± 0.13	41.9 ± 5.4	3.90
6	2.92 ± 0.48	115.3 ± 28.3	1.90
7	1.98 ± 0.43	64.1 ± 20.7	2.72
17	2.68 ± 0.51	101.6 ± 26.3	2.03
19	3.21 ± 0.31	132.5 ± 19.7	1.44
20	2.85 ± 0.26	111.3 ± 14.0	1.68
24	1.88 ± 0.25	59.4 ± 11.9	2.08
25	1.24 ± 0.26	31.8 ± 6.3	3.09
31	2.32 ± 0.45	82.1 ± 22.3	1.94
34	1.14 ± 0.25	28.1 ± 9.2	3.51
35	1.11 ± 0.26	27.6 ± 7.7	4.09
37	1.07 ± 0.23	25.6 ± 7.8	>5.00
38	1.88 ± 0.52	59.7 ± 25.6	3.26
43	1.64 ± 0.22	48.5 ± 9.4	2.86
44	2.18 ± 0.38	74.4 ± 18.8	3.20
45	2.91 ± 0.17	115.1 ± 9.2	2.86
46	3.11 ± 0.11	125.9 ± 6.8	1.90
47	2.29 ± 0.30	80.8 ± 17.3	1.83
49	1.71 ± 0.27	51.6 ± 11.9	3.37

Full details of the coating runs are given in Appendix 1.

Arithmetic mean surface roughness values are taken from Appendix 3

RELATIONSHIP BETWEEN FILM SURFACE ROUGHNESS AND ITS INSTANTANEOUS ELASTIC MODULUS AND BRINELL HARDNESS

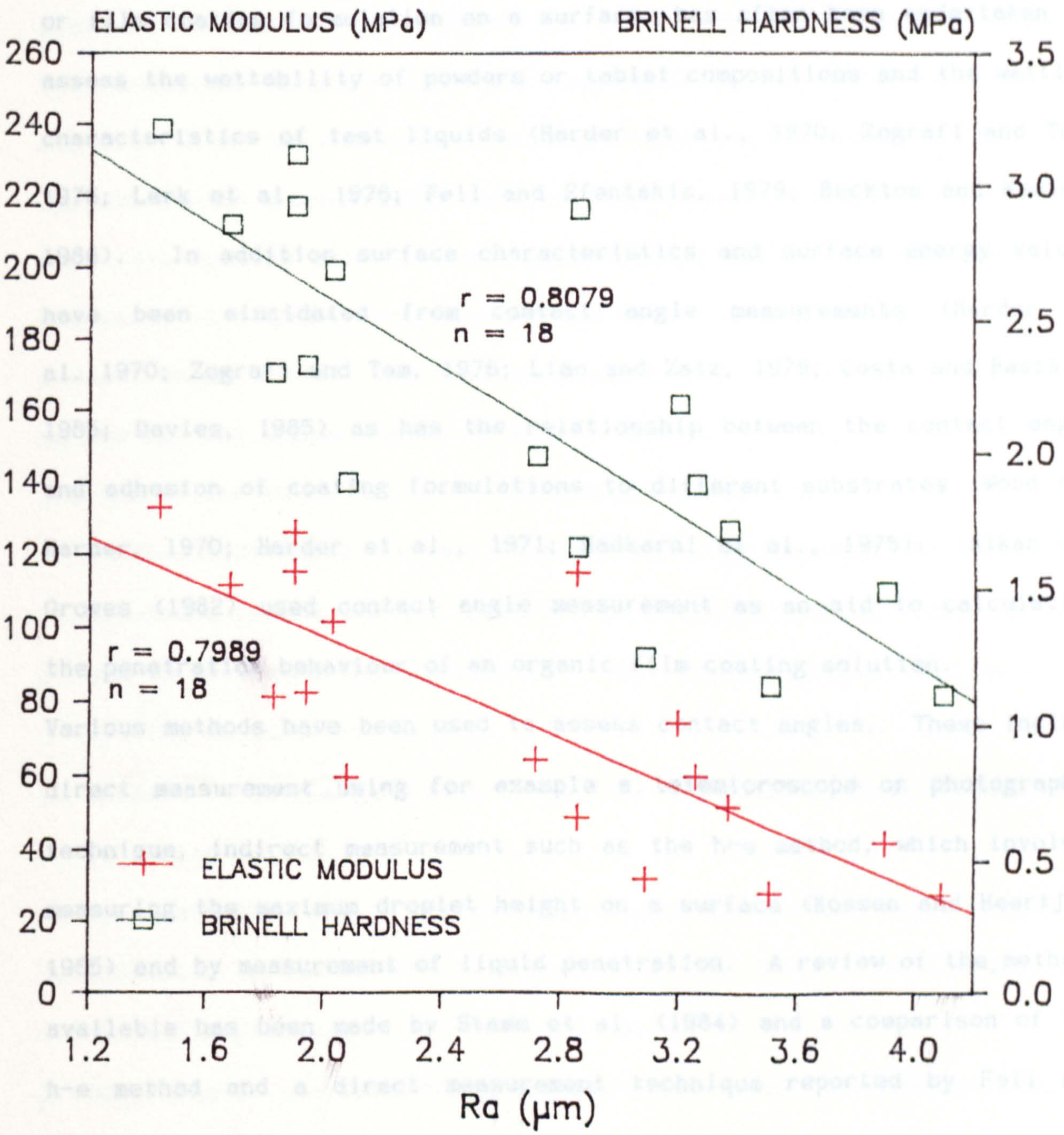

FIGURE 5.8

5.7 THE CONTACT ANGLE OF FILM COATING SOLUTIONS ON COATED AND UNCOATED TABLETS

5.7.1 INTRODUCTION

Measurement of the contact angle made by a liquid, solution, suspension or film coating formulation on a surface, has often been undertaken to assess the wettability of powders or tablet compositions and the wetting characteristics of test liquids (Harder et al., 1970; Zografi and Tam, 1976; Lerk et al., 1976; Fell and Efentakis, 1979; Buckton and Newton, 1986). In addition surface characteristics and surface energy values have been elucidated from contact angle measurements (Harder et al.,1970; Zografi and Tam, 1976; Liao and Zatz, 1979; Costa and Baszkin, 1985; Davies, 1985) as has the relationship between the contact angle and adhesion of coating formulations to different substrates (Wood and Harder, 1970; Harder et al., 1971; Nadkarni et al., 1975). Alkan and Groves (1982) used contact angle measurement as an aid to calculating the penetration behaviour of an organic film coating solution.

Various methods have been used to assess contact angles. These include direct measurement using for example a telemicroscope or photographic technique, indirect measurement such as the h-e method, which involves measuring the maximum droplet height on a surface (Kossen and Heertjes, 1965) and by measurement of liquid penetration. A review of the methods available has been made by Stamm et al. (1984) and a comparison of the h-e method and a direct measurement technique reported by Fell and Efentakis (1979).

As far as aqueous film coating is concerned, measurement of contact angles may provide useful information on film adhesion, droplet spreading and penetration tendencies, and interactions between the constituents of the coating formulation and those of the tablet substrate. To date, work done on the wetting of pharmaceutical

materials utilising contact angle measurement has concentrated on measuring the angles of drops which have been carefully placed on a substrate surface. In addition, the substrates have tended to be specially prepared, for example by using either a high compaction pressure to minimise penetration and reduce surface roughness or using test solutions saturated with the components of the tablet to avoid any dissolution of the substrate. Although these latter techniques may give information of a fundamental nature, they do not reflect what may happen when film coating solutions are applied practically. No information is available at present regarding the influence of droplet momentum on the contact angle formed, the role of changes in film coating formulations, or the contact angles formed on coated tablets.

The aim of the work reported in this section was to:

1. Assess stationary contact angles made by aqueous film coating solutions on the tablets used in the coating studies (section 5.2) and to determine the dependency of the contact angle on the film coating formulation used.
2. Measure contact angles made by various different coating formulations on coated tablets.
3. Elucidate the role of droplet momentum on the contact angle formed.
4. Determine if the surface roughness of coated tablets influences the contact angle.
5. Determine if the substrate temperature influences the contact angle.
6. Assess the time-dependent nature of the contact angle on uncoated and coated tablets.

5.7.2 EXPERIMENTAL

Choice of method of contact angle measurement

In order to reflect the practical situation, the method chosen to measure the contact angle should involve no alterations in either the substrate or coating formulation from those used in the coating studies. In addition, because of the great affinity between the substrate and the water in the coating formulation and the desire to examine the time-dependent nature of the contact angle, the method should be as rapid as possible. For both these reasons a photographic means of assessment was chosen. This method also has the advantage that a permanent copy is produced.

Method of contact angle measurement

All measurements were taken on the 15mm flat tablets. The uncoated tablets were those detailed in section 5.2.1 and the coated tablets taken from coating runs 21, 37 and 63 (see Appendix 1 for full coating details), these having arithmetic mean surface roughness values (Ra) of 2.60μm, >5.00μm and 1.75μm respectively (see section 5.5). All tablets were lightly brushed before testing. The tablets were stored either at room temperature (20°C ± 2°C) or had been equilibrated at 40°C for at least 24 hours. The test coating formulations were all at room temperature. Droplets of approximately 30μl were either placed gently on the tablet surface using a micropipette, or allowed to fall under gravity from a height of 50mm, 100mm or 200mm, the micropipette being held in position in a clamp-stand. Buckton and Newton (1986) reported that droplet volumes between 10μl and 50μl were not found to influence the contact angle. Photographs were taken approximately one second after the droplets had contacted the tablet surface and at intervals thereafter. A magnification factor of 7.2 was achieved using a x6 close-up lens attached to a 50mm lens and extension tubes of length

61mm. Photographic records from at least five separate droplets were obtained for the initial contact angles (time = 1 second) measured, and at least three photographs taken for all other time intervals thereafter. Contact angles from both sides of the droplet were measured and averaged.

The coating formulations tested were:

1. HPMC E5 solutions of 6%w/w, 9%w/w, 11%w/w, 12%w/w and 15%w/w prepared using HPMC E5 batch 2 (see Table 3.2)
2. Opadry type OY suspensions of 7%w/w, 11%w/w, and 16%w/w prepared from batch 1 (see Table 3.6))
3. A 9%w/w HPMC E5 solution (using batch 2) including 1%w/w PEG 400.

Contact angles of droplets of double distilled water and dilute HPMC E5 solutions (5×10^{-6}%w/w to 2×10^{-5}%w/w) of different surface tension values (see section 3.3.2), could not be measured since the liquids penetrated the surface completely within a few seconds.

5.7.3 RESULTS

The contact angles of droplets allowed to fall from various distances onto the uncoated 15mm flat tablets are shown in Table 5.22. The maximum % coefficient of variation for the contact angles presented both in Table 5.22 and in subsequent tables was found to be 4.6%.

It is apparent from the results that the contact angle is dependent on both the viscosity of the formulation and the kinetic energy possessed by the droplet. When the droplets were carefully placed on the tablet surface, increasing the HPMC E5 concentration from 6%w/w to 15%w/w, with the resultant viscosity increase from 45mPa s to 1417mPa s (see Table 3.2), gave rise to an increase in the contact angle both initially and after a period of 30 seconds. In all cases the contact angle measured after 30 seconds was lower than the initial value, the difference

ranging from 14° to 27°. Opadry suspensions and HPMC E5 solutions with similar viscosity values were found to produce comparable contact angles. It should be remembered in the case of the Opadry suspensions, the viscosity value quoted is the apparent Newtonian viscosity. Any shear forces exerted on the Opadry suspensions, as for example when they impinge on the tablet, may produce a reduction in the viscosity, this being dependent on the extent of the shear forces encountered. The inclusion of PEG 400 in the HPMC E5 formulation appeared to have a minimal effect on the contact angle formed. These latter two observations indicate that when droplets are placed on a tablet surface,

TABLE 5.22: THE INFLUENCE OF DROPLET FORMULATION AND KINETIC ENERGY ON THE CONTACT ANGLE FORMED ON UNCOATED TABLETS

COATING FORMULATION TYPE	COMPONENT CONCENTRATION (%w/w)	VISCOSITY (mPa s)	CONTACT ANGLE (°) DISTANCE OF DROPLET FALL		
			0mm	100mm	200mm
HPMC E5	6	45	39 (25)		29 (23)
HPMC E5	9	166	62 (39)	50 (40)	46 (38)
HPMC E5	11	350	72 (45)		58 (43)
HPMC E5	12	520	73 (57)	71 (56)	67 (54)
HPMC E5	15	1417*	82 (62)		82 (61)
HPMC E5 WITH PEG 400	9 1	171	57 (39)		45 (36)
OPADRY-OY	7	51*	42 (24)	33 (24)	27 (22)
OPADRY-OY	11	161*	63 (39)		48 (38)
OPADRY-OY	16	514*	70 (58)		65 (53)

* Apparent Newtonian viscosity values.

The figures in brackets refer to the contact angle 30 seconds after impingement onto the tablet surface.

All tests were performed at room temperature.

it is viscosity rather than the components of the formulation which has the major influence on the contact angle formed.

Droplets that were allowed to fall from a height of either 100mm or 200mm were shown, with the exception of the 15%w/w HPMC E5 solution, to produce smaller contact angles than droplets placed on the surface. Again, the contact angle formed by the droplets was dependent primarily on the viscosity of the formulation and was found to decrease with time. The 12%w/w HPMC E5 solution showed only a small reduction in contact angle (6°) when allowed to fall from 200mm and the 15w/w solution no change at all.

Contact angles formed by various coating formulations on coated tablets of differing surface roughness are shown in Tables 5.23 to 5.25. For each of the three coated tablet types tested, there was a trend for the contact angle of droplets gently placed on the surface to increase with increasing droplet viscosity. This effect was however considerably smaller than that seen on the uncoated tablets. There were minimal differences between the results obtained on the coated tablets taken from coating runs 21 and 63 (Ra values 2.60μm and 1.75μm), but angles formed on tablets from coating run 37 (Ra value >5μm) were found to be consistently higher.. After a period of thirty seconds on the coated tablet surface, all formulations exhibited reduced contact angles, although these were still considerably higher than those formed on the uncoated tablets after an equivalent time.

When the droplets were allowed to fall onto the coated tablets from different heights, the contact angle formed was found to be dependent on both the droplet kinetic energy and viscosity, but not the coat surface roughness. The effect of droplet kinetic energy was found to become more pronounced at lower values (shorter droplet fall distances) as the droplet viscosity was reduced.

Table 5.23: THE INFLUENCE OF DROPLET FORMULATION AND KINETIC ENERGY ON THE CONTACT ANGLE FORMED ON TABLETS FROM COATING RUN 63

COATING FORMULATION TYPE	COMPONENT CONC (%w/w)	VISCOSITY (mPa s)	CONTACT ANGLE (°) DISTANCE OF DROPLET FALL 0mm	50mm	100mm	200mm
HPMC E5	6	45	98 (85)	46	39	33 (27)
HPMC E5	9	166	99 (88)	70	55	47 (42)
HPMC E5	12	520	105 (97)	--	90	80 (76)
HPMC E5 AND PEG 400	9 1	171	102 (92)	--	--	48 (44)
OPADRY	11	161*	98 (89)	--	--	46 (42)

TABLE 5.24: THE INFLUENCE OF DROPLET FORMULATION AND KINETIC ENERGY ON THE CONTACT ANGLE FORMED ON TABLETS FROM COATING RUN 21

COATING FORMULATION TYPE	COMPONENT CONC (%w/w)	VISCOSITY (mPa s)	CONTACT ANGLE (°) DISTANCE OF DROPLET FALL 0mm	50mm	100mm	200mm
HPMC E5	6	45	96 (84)	52	36	34 (30)
HPMC E5	9	166	98 (88)	69	55	47 (42)
HPMC E5	12	520	106 (93)	99	93	80 (77)
HPMC E5	15	1417*	109 (99)	--	--	98 (93)
HPMC E5 AND PEG 400	9 1	171	103 (92)	--	--	49 (44)
OPADRY	11	161*	97 (89)	--	--	50 (44)

* Apparent Newtonian viscosity values.

Ra values of tablets: Run 63 = 1.75μm Run 21 = 2.60μm. See Appendix 1 for details of the coating runs. The figures in brackets refer to the contact angle 30 seconds after impingement onto the tablet surface. All tests were performed at room temperature.

TABLE 5.25: THE INFLUENCE OF DROPLET FORMULATION AND KINETIC ENERGY ON THE CONTACT ANGLE FORMED ON TABLETS FROM COATING RUN 37

COATING FORMULATION TYPE	COMPONENT CONC (%w/w)	VISCOSITY (mPa s)	CONTACT ANGLE (°) DISTANCE OF DROPLET FALL 0mm	50mm	100mm	200mm
HPMC E5	6	45	102 (88)	53	39	31 (29)
HPMC E5	9	166	106 (90)	71	56	47 (42)
HPMC E5	12	520	108 (96)	--	--	81 (79)
HPMC E5 AND PEG 400	9 1	171	111 (99)	--	--	47 (42)
OPADRY	11	161*	107 (93)	--	--	49 (45)

* Apparent Newtonian viscosity values.

Ra value of tablets = >5.00µm. See Appendix 1 for coating run details. The figures in brackets refer to the contact angle 30 seconds after impingement onto the tablet surface. All tests were performed at room temperature.

Comparison of the results in Tables 5.23 to 5.25 with those in Table 5.22, shows that for droplet viscosities of 171mPa s and below, there was little difference between the angles formed on coated and uncoated tablets when the droplets were allowed to fall from 200mm. Higher droplet viscosities were however found to produce consistently higher contact angles on the coated tablets.

The effect of heating the tablets to 40°C prior to determining the contact angle is shown in Table 5.26. With tablets from coating run 37 (Ra value >5µm), heating the tablets to 40°C had no discernable effect on the contact angles formed by a variety of coating formulations. On tablets from run 63 (Ra value 1.75µm), the same pretreatment appeared to

cause a small but consistent increase in the initial contact angle, but did not affect the angles formed after 30 seconds. A similar small increase in the initial contact angle was seen on the heated uncoated tablets, but in this latter case the angles formed 30 seconds after contacting the substrate were considerably greater than those seen on the unheated tablets (see Table 5.22).

Results presented in Tables 5.22 to 5.26 have included near instantaneous contact angle values and those formed after 30 seconds. Studies examining the course of the change in contact angle with time, indicated that in every case the majority of the reduction in contact angle occurred within the first 10 seconds and that any reduction thereafter was relatively small or non-existent.

TABLE 5.26: CONTACT ANGLES FORMED ON TABLETS HEATED TO 40°C

COATING FORMULATION TYPE	COMPONENT CONC (%w/w)	VISCOSITY (mPa s)	CONTACT ANGLE (°) UNCOATED TABLETS	COATED TABLETS RUN 37	COATED TABLETS RUN 63
HPMC E5	6	45	42 (32)	96 (84)	99 (86)
HPMC E5	9	166	68 (61)	104 (84)	106 (86)
HPMC E5	12	520	81 (77)	108 (97)	111 (98)
HPMC E5	15	1417*	91 (80)	108 (99)	109 (99)
OPADRY	11	161*	66 (60)	105 (94)	107 (88)

* Apparent Newtonian viscosity values.

Ra values of tablets: Run 63 = 1.75μm Run 37 = >5.0μm. See Appendix 1 for details of the coating runs. The figures in brackets refer to the contact angle 30 seconds after impingement onto the tablet surface.

All readings were taken fron droplets gently placed on the tablet surface.

5.8 THE PENETRATION BEHAVIOUR OF AQUEOUS FILM COATING SOLUTIONS INTO TABLETS

The penetration behaviour of some aqueous film coating solutions into the tablets used in the coating studies (section 5.2) was investigated, in order to more fully understand the role of the coating formulation in governing the film properties and the incidence of film coat defects.

5.8.1 EXPERIMENTAL

An autopipette was used to deliver 10µl droplets of various HPMC E5 solutions onto the surface of uncoated 15mm flat tablets identical to those used in the coating studies. The composition and properties of these tablets are given in section 5.2.1. HPMC E5 from batch 2 was used (see Table 3.2 for solution viscosity values). The mean time taken for the droplets to penetrate into the tablets (ie to completely disappear from the tablet surface) was calculated from 10 determinations. Both the tablets and the droplets were at room temperature (20°C ± 2°C).

5.8.2 RESULTS

Mean penetration times and corresponding standard deviation values for the HPMC E5 solutions investigated are shown in Table 5.27. These data demonstrate that the penetration rate is markedly dependent on the coating solution viscosity. It can be seen that over the range of solution concentrations likely to be used practically (6%w/w to 12%w/w), there is the potential for an eighteen-fold difference in penetration rate.

The role of the penetration behaviour in influencing droplet contact angles, film properties and the extent of film defects is discussed in section 5.11.

TABLE 5.27: PENETRATION BEHAVIOUR OF AQUEOUS HPMC E5 SOLUTIONS INTO TABLETS

HPMC E5 SOLUTION CONCENTRATION (%w/w)	SOLUTION VISCOSITY (mPa s)	PENETRATION TIME ± s.d. (n = 10) (s)
0	1.0	0.86 ± 0.14
6	45	52 ± 5
9	166	379 ± 54
11	350	468 ± 68
12	520	939 ± 89
15	1287*	1374 ± 115

* Apparent Newtonian viscosity value.

Details of the 15mm flat tablets used are given in section 5.2.1.

Tablets and penetrating droplets were both at room temperature (20°C ± 2°C).

5.9 CHARACTERISATION OF THE SPRAY PATTERNS PRODUCED DURING AQUEOUS FILM COATING

5.9.1 INTRODUCTION

In order to understand more fully the influence of coating conditions on the properties of a resultant film coat, a knowledge of the influence of these conditions on the spray patterns produced during coating is required. Some information on the spray patterns has been reported earlier (see sections 4.2.9 and 4.3.14), however no information was given on spray dimensions. Thus, the aim of this section of work was to assess quantitatively the dimensions of sprays produced during the coating runs and to obtain a qualitative indication of the distribution of droplets within the spray. It was hoped this would then aid in explaining the differences in film coat properties observed when different process conditions were used.

5.9.2 EXPERIMENTAL

All spray pattern determinations were carried out within a model 10 Accela-Cota. Drying air of inlet temperature between 64°C and 66°C at a volume flow rate of 0.129m^3s^{-1} was used and 5kg of 8mm normal convex placebo tablets were present. The spray patterns used in the actual coating runs were reproduced by adjustment of the atomising air pressure, and, in the case of the Schlick, Walther Pilot and Binks Bullows guns, the volume flow rate of the spray shaping air. The latter parameter was adjusted so that the total atomising air volume flow rates matched those measured during the coating runs. In order that the spray patterns could be clearly seen, suspensions of Opadry type OY (batch 1, see Table 3.6) were atomised. The suspension concentrations were calculated so that at the point of atomisation they were of approximately the same viscosity as the HPMC E5 solutions used in the

coating runs. The concentrations used and their respective apparent Newtonian viscosities were: 7%w/w (51mPa s), 11%w/w (161mPa s) and 16%w/w (514mPa s). To detect the spray patterns, a piece of absorbant white card of dimensions 350mm by 300mm, protected by a futher piece of card, was placed within the coater at the position occupied by the tablet bed during coating. The Opadry suspensions were then sprayed onto the protecting card for about 15 seconds using the desired conditions. The protecting card was quickly removed to allow spraying onto the evaluating card for about three seconds and then replaced. The position of the spray gun was adjusted to achieve the appropriate gun-to-card distances.

Each spray record was examined visually. Firstly, to gain a qualitative assessment of the colour depth across the spray and thus an indication of the droplet distribution within the spray, and secondly to see if differences in droplet sizes detected by the Malvern droplet size analyser could be observed. Measurements of the maximum spray width and maximum spray height were also obtained. The spray patterns generated represented those used in the coating runs and examined the effect of spray gun type, atomising air pressure, viscosity, spray rate, liquid nozzle diameter, atomising air volume flow rate and spray gun to bed distance.

5.9.3 RESULTS

The maximum width and maximum height of sprays produced by the five spray guns, when atomising solutions of differing viscosity at various atomising air pressures, are shown in Table 5.28. Details of the spray guns are given in section 4.2.2 and the atomising air volume flow rates used in Table 4.5. Unless otherwise stated a type 2850 liquid nozzle was used with the Spraying Systems guns. It can be seen that the

TABLE 5.28: THE INFLUENCE OF VISCOSITY, SPRAY GUN TYPE AND ATOMISING AIR PRESSURE ON THE SPRAY DIMENSIONS OF ATOMISED FILM COATING SOLUTIONS

SPRAY GUN TYPE	ATOMISING AIR PRESSURE (kPa)	* OPADRY VISCOSITY (mPa s)	MAXIMUM SPRAY WIDTH (mm)	MAXIMUM SPRAY HEIGHT (mm)
Schlick 930/7-1	276	51	195	125
Schlick 930/7-1	414	51	200	110
Schlick 930/7-1	552	51	200	125
Schlick 930/7-1	276	161	200	105
Schlick 930/7-1	414	161	205	110
Schlick 930/7-1	552	161	205	110
Schlick 930/7-1	276	514	185	100
Schlick 930/7-1	414	514	195	100
Schlick 930/7-1	552	514	195	100
Walther Pilot	276	51	170	85
Walther Pilot	414	51	185	85
Walther Pilot	552	51	170	90
Walther Pilot	276	161	185	90
Walther Pilot	414	161	200	100
Walther Pilot	552	161	180	90
Walther Pilot	276	514	190	85
Walther Pilot	414	514	185	80
Walther Pilot	552	514	185	95
Binks Bullows	276	51	180	85
Binks Bullows	414	51	180	85
Binks Bullows	516	51	185	90
Binks Bullows	276	161	190	90
Binks Bullows	414	161	210	90
Binks Bullows	516	161	210	105
Binks Bullows	276	514	180	80
Binks Bullows	414	514	210	75
Binks Bullows	516	514	180	75
Spraying Sys. 45°	276	51	135	80
Spraying Sys. 45°	414	51	145	105
Spraying Sys. 45°	552	51	155	105
Spraying Sys. 45°	276	161	145	85
Spraying Sys. 45°	414	161	150	90
Spraying Sys. 45°	552	161	145	85
Spraying Sys. 45°	276	514	135	80
Spraying Sys. 45°	414	514	145	90
Spraying Sys. 45°	552	514	145	90
Spraying Sys. 60°	276	51	240	105
Spraying Sys. 60°	414	51	200	100
Spraying Sys. 60°	552	51	185	110
Spraying Sys. 60°	276	161	250	90
Spraying Sys. 60°	414	161	220	80
Spraying Sys. 60°	552	161	205	100
Spraying Sys. 60°	276	514	250	85
Spraying Sys. 60°	414	514	215	75
Spraying Sys. 60°	552	514	185	90

* Apparent Newtonian viscosity values. In all cases a spray rate of 40gmin^{-1} and a gun-to-card distance of 180mm was used.

influence of atomising air pressure on the spray dimensions produced by the Spraying Systems guns is dependent on which of the two air caps is present. With the Spraying Systems 45° gun, the spray patterns are of the same shape irrespective of the air pressure used. Increasing the atomising air pressure when using the Spraying Systems 60° gun however caused a reduction in the spray width but had minimal effect on spray height. The Spraying Systems 60° gun was found to produce wider sprays than the Spraying Systems 45° gun, this arising from differences in the air cap geometry. The dimensions of sprays produced by the Spraying Systems 60° gun were found to be approximately the same as those produced by the Schlick, Walther Pilot and Binks Bullows guns, whereas the Spraying Systems 45° gun produced sprays which were consistently narrower. Over the range of viscosities studied, which covers those likely to used practically, there was no discernable effect of viscosity on the spray dimensions produced by any of the spray guns.

It can be seen from Table 5.28, that the aim of producing sprays of approximately equal widths by alteration of the total atomising air volume when using the Schlick, Walther Pilot and Binks Bullows guns was achieved. The spray heights produced by the Schlick gun however appeared to be greater than those from the Walther Pilot and Binks Bullows guns. This latter observation probably arose from differences in air cap design (see Table 4.1). Within the air cap, the Walther Pilot gun has a pair of containment holes and the Binks Bullows gun a pair of containment holes and a series of angular converging holes. These extra holes, which are not present in the Schlick gun air cap, serve to contain the spray and restrict the spray height.

Table 5.29 illustrates the influence of spray rate on spray dimensions 180mm from the spray gun, when using an atomising air pressure of 414kPa. It is apparent that if all other parameters are kept constant,

TABLE 5.29: THE EFFECT OF SPRAY RATE ON THE SPRAY DIMENSIONS OF ATOMISED FILM COATING SOLUTIONS

SPRAY GUN TYPE	SPRAY RATE ($gmin^{-1}$)	* OPADRY VISCOSITY (mPa s)	MAXIMUM SPRAY WIDTH (mm)	MAXIMUM SPRAY HEIGHT (mm)
Schlick 930/7-1	30	51	205	105
Schlick 930/7-1	40	51	210	110
Schlick 930/7-1	50	51	220	125
Schlick 930/7-1	30	161	185	100
Schlick 930/7-1	40	161	205	110
Schlick 930/7-1	50	161	215	120
Schlick 930/7-1	30	514	180	90
Schlick 930/7-1	40	514	195	100
Schlick 930/7-1	50	514	210	110
Walther Pilot	30	51	145	90
Walther Pilot	40	51	185	85
Walther Pilot	50	51	195	95
Walther Pilot	30	161	175	100
Walther Pilot	40	161	200	100
Walther Pilot	50	161	200	90
Walther Pilot	30	514	160	70
Walther Pilot	40	514	185	80
Walther Pilot	50	514	195	80
Binks Bullows	30	51	165	90
Binks Bullows	40	51	180	85
Binks Bullows	50	51	190	100
Binks Bullows	30	161	190	80
Binks Bullows	40	161	210	90
Binks Bullows	50	161	230	100
Binks Bullows	30	514	165	70
Binks Bullows	40	514	210	75
Binks Bullows	50	514	245	80
Spraying Sys. 45°	30	51	135	100
Spraying Sys. 45°	40	51	145	100
Spraying Sys. 45°	50	51	150	120
Spraying Sys. 45°	30	161	140	90
Spraying Sys. 45°	40	161	150	90
Spraying Sys. 45°	50	161	170	110
Spraying Sys. 60°	30	51	170	85
Spraying Sys. 60°	40	51	200	100
Spraying Sys. 60°	50	51	225	130
Spraying Sys. 60°	30	161	180	95
Spraying Sys. 60°	40	161	220	80
Spraying Sys. 60°	50	161	225	100
Spraying Sys. 60°	30	514	185	95
Spraying Sys. 60°	40	514	215	75
Spraying Sys. 60°	50	514	250	75

* Apparent Newtonian viscosity values. In all cases an atomising air pressure of 414kPa and a gun-to-card distance of 180mm was used.

an increase in the spray rate causes an increase in the width of the spray and to a lesser extent the height of the spray. The influence of the spray rate appeared particularly pronounced with the Binks Bullows gun and the Spraying Systems 60° gun.

Since the spray guns used in this thesis utilised liquid inserts of differing internal diameter (see Table 4.1), a series of spray patterns were produced to determine if the liquid insert diameter influenced the spray dimensions. The results of this study are detailed in Table 5.30. The data appear to indicate that increasing the liquid insert diameter may cause a decrease in the spray width and spray height, although this effect is relatively small, and unlikely to be practically significant.

TABLE 5.30 : THE INFLUENCE OF LIQUID NOZZLE DIAMETER ON THE SPRAY DIMENSIONS OF ATOMISED FILM COATING SOLUTIONS

SPRAY GUN TYPE	LIQUID NOZZLE REFERENCE	LIQUID NOZZLE DIAMETER mm	SPRAY RATE $gmin^{-1}$	MAXIMUM SPRAY WIDTH mm	MAXIMUM SPRAY HEIGHT mm
Spraying Sys. 45°	2050	0.51	40	160	100
Spraying Sys. 45°	2850	0.71	40	150	90
Spraying Sys. 60°	2050	0.51	40	220	100
Spraying Sys. 60°	2850	0.71	40	220	90
Schlick 930/7-1	-	0.80	40	205	110
Schlick 931/7-1	-	1.20	40	200	110
Schlick 932/7-2	-	1.80	40	195	105
Schlick 930/7-1	-	0.80	50	215	120
Schlick 932/7-1	-	1.80	50	205	110

A suspension of apparent Newtonian viscosity 161mPa s and an atomising air pressure of 414kPa were used for all sprays.
Spray dimensions were determined 180mm from the spray gun.

Within the model 10 Accela-Cota, the potential for varying the spray gun to tablet bed distance is small, particularly with the Binks Bullows and Walther Pilot guns where the geometry of the guns and associated tubing limits the maximum gun-to-bed distance to approximately 200mm. The Spraying Systems and Schlick guns are smaller and designed so that both the atomising air and liquid input tubing enters at the side of the gun. This allows more scope for varying the gun to tablet bed distance, values of up to 300mm being attainable. Table 5.31 shows how the spray shape produced by these latter two guns alters with an increasing gun-to-card distance. As might be expected, both the width and the height of the spray increased as the distance from the spray gun increased. If the sprays had kept expanding at the same rate from 180mm to 250mm as they had from 0mm to 180mm, then from trigonometric considerations it might be expected that the spray dimensions would have increased by a factor of 1.39. Similarly increasing the distance from 180mm to 300mm would have been expected to increase the spray dimensions by a factor of 1.67. Generally however the increase in spray dimensions was smaller that might have been envisaged from trigonometric considerations, indicating that it is not possible to extrapolate dimensions measured at 180mm to give estimated dimensions at other distances. The only exception to this was when the cone shaped sprays were produced, where the diameter of the circular spray pattern did increase in the manner expected from the geometry of the system at 180mm.

The Schlick, Walther Pilot and Binks Bullows guns can be made to produce a variety of spray shapes by altering the amount of air entering the side port holes of the air cap, and thus the total atomising air volume flow rate. This is illustrated in Table 5.32. It can be seen that with the minimum atomising air volume flow rates (marked *) where the supply

TABLE 5.31 : THE SPRAY DIMENSIONS OF ATOMISED FILM COATING SOLUTIONS AT VARYING DISTANCES FROM THE SPRAY GUN

SPRAY GUN TYPE	SPRAY RATE $gmin^{-1}$	GUN DISTANCE mm	*OPADRY VISCOSITY mPa s	MAXIMUM SPRAY WIDTH mm	MAXIMUM SPRAY HEIGHT mm
Schlick 930/7-1	40	180	51	210	160
Schlick 930/7-1	40	250	51	220	160
Schlick 930/7-1	30	180	161	185	100
Schlick 930/7-1	30	250	161	210	135
Schlick 930/7-1	40	180	161	205	110
Schlick 930/7-1	40	250	161	230	120
Schlick 930/7-1	40	300	161	280	125
Schlick 930/7-1	50	180	161	215	120
Schlick 930/7-1	50	250	161	240	120
Schlick 930/7-1	50	180	514	210	110
Schlick 930/7-1	50	250	514	260	120
Schlick 930/7-1	40	180	514	195	100
Schlick 930/7-1	40	250	514	230	120
Schlick 930/7-1	30	180	514	180	90
Schlick 930/7-1	30	250	514	215	140
▼Schlick 930/7-1	40	180	161	80	80
▼Schlick 930/7-1	40	250	161	115	115
▼Schlick 930/7-1	40	300	161	130	130
Spraying Sys. 45°	40	180	51	135	105
Spraying Sys. 45°	40	250	51	155	110
Spraying Sys. 45°	40	180	161	150	90
Spraying Sys. 45°	40	250	161	175	105
Spraying Sys. 45°	40	300	161	230	125
Spraying Sys. 45°	40	180	514	174	85
Spraying Sys. 45°	40	250	514	195	90
Spraying Sys. 60°	40	180	161	220	80
Spraying Sys. 60°	40	250	161	240	105
Spraying Sys. 60°	40	300	161	270	130
Spraying Sys. 60°	40	180	514	215	75
Spraying Sys. 60°	40	250	514	230	90

All measurements were taken using an atomising air pressure of 414kPa.

Standard flat spray shapes were used except where indicated ▼, where a cone shaped spray was utilised.

* Apparent Newtonian viscosity values

TABLE 5.32 : THE INFLUENCE OF ATOMISING AIR VOLUME FLOW RATE ON THE SPRAY DIMENSIONS ATOMISED FILM COATING SOLUTIONS

SPRAY GUN TYPE	ATOMISING AIR PRESSURE kPa	ATOMISING AIR VOLUME FLOW RATE m^3hr^{-1}	SPRAY RATE $gmin^{-1}$	*OPADRY VISCOSITY mPa s	MAXIMUM SPRAY WIDTH mm	MAXIMUM SPRAY HEIGHT mm
Schlick 930/7-1	276	5,46 ◊	40	161	90	90
Schlick 930/7-1	276	11,23	40	161	200	105
Schlick 930/7-1	414	7,42 ◊	40	161	80	80
Schlick 930/7-1	414	12,17	40	161	160	100
Schlick 930/7-1	414	15,44 ●	40	161	205	110
Schlick 930/7-1	414	18,18 ■	40	161	250	110
Schlick 930/7-1	552	9,83 ◊	40	161	85	85
Schlick 930/7-1	552	19,98 ●	40	161	205	110
Schlick 930/7-1	414	7,42 ◊	50	161	90	90
Schlick 930/7-1	414	15,44 ●	50	161	210	110
Schlick 930/7-1	414	12,17	40	514	165	80
Schlick 930/7-1	414	15,44 ●	40	514	195	110
Schlick 930/7-1	414	18,18 ■	40	514	245	90
Schlick 930/7-1	414	7,42 ◊	50	514	80	80
Schlick 930/7-1	414	15,44 ●	50	514	210	110
Walther Pilot	414	11,74 ◊	40	51	75	75
Walther Pilot	414	20,00 ●	40	51	185	95
Walther Pilot	414	23,37 ■	40	51	245	90
Walther Pilot	414	11,74 ◊	40	161	80	80
Walther Pilot	414	15,65	40	161	120	85
Walther Pilot	414	20,00 ●	40	161	200	100
Walther Pilot	414	23,37 ■	40	161	240	90
Walther Pilot	414	11,74 ◊	50	161	85	85
Walther Pilot	414	20,00 ●	50	161	210	90
Walther Pilot	414	15,65	40	514	125	75
Walther Pilot	414	20,00 ●	40	514	185	80
Walther Pilot	414	23,37 ■	40	514	245	105
Binks Bullows	414	15,22 ◊	40	51	90	85
Binks Bullows	414	19,57	40	51	140	80
Binks Bullows	414	22,61 ●	40	51	180	85
Binks Bullows	414	15,22 ◊	40	161	105	105
Binks Bullows	414	19,57	40	161	140	105
Binks Bullows	414	22,61 ●	40	161	210	90
Binks Bullows	414	23,91 ■	40	161	225	80
Binks Bullows	414	15,22 ◊	50	161	110	110
Binks Bullows	414	22,61 ●	50	161	230	110
Binks Bullows	414	15,22 ◊	40	514	115	110
Binks Bullows	414	20,87	40	514	140	85
Binks Bullows	414	22,61 ●	40	514	210	75
Binks Bullows	414	23,91 ■	40	514	230	90

Key: ◊ minimum possible atomising air volume flow rate
● standard atomising air volume flow rates for flat spray shapes used in coating runs
■ maximum possible atomising air volume flow rates

Sprays measured 180mm from the spray gun. * Apparent Newtonian viscosity values

to the air cap side ports is closed, the spray patterns produced by all the guns were circular. Despite the large differences in atomising air volume flow rates and the differences in air cap designs, the spray dimensions were very similar. As the air allowed to enter the side ports of the air caps was increased, the spray widths were also seen to progressively increase. At a distance of 180mm from the spray gun, the Walther Pilot and Schlick guns were demonstrated to produce maximum spray widths (marked ■) of approximately 250mm and the Binks Bullows a maximum width of approximately 230mm. Large increases in the atomising air volume flow rate were found to have little effect on the spray height.

Under normal operating conditions within the model 10 Accela-Cota, these three spray guns would appear to utilise atomising air volume flow rates approaching the maximum available.

In addition to the measurement of the dimensions of the spray, the spray patterns were scrutinised to determine how evenly the spray was distributed across its width, how well the spray was contained within defined borders and to see if the differences in droplet sizes detailed in section 4.3 could be detected.

The Schlick gun was found to generally produce well contained sprays, that is the borders of the sprays were clearly indentifiable. At a distance of 180mm from the gun, there was a central region, extending to approximately half the width and height of the spray, where there appeared to be a greater density of droplets. When the distance was extended to 250mm, this region became far less noticeable and it was not detectable at a distance of 300mm. When atomising solution viscosities of 51mPa s and 161mPa s, there was little sign of any large droplets being produced or any detectable differences in droplet sizes when using

the different atomising air pressures. With a solution viscosity of 514Pa s, however, the spray appeared slightly less well contained and there was evidence of some larger droplets being formed, especially at 276kPa (the lowest air pressure studied). The phenomemon reported in section 4.3, whereby the droplet sizes measured by the Malvern droplet size analyser appeared to increase as the distance from the spray increased could not be observed.

The Walther Pilot gun also generally produced well contained sprays with a greater density of droplets in the central region. This central region appeared to contain a greater percentage of the spray than that of the Schlick gun. A few larger droplets not contained within the general spray border were observed when the 161mPa s solutions were atomised, this being especially apparent with an atomising air pressure of 276kPa. A similar but more noticeable effect was seen with the 514mPa s solutions. When sprays were produced using the maximum possible atomising air volume flow rate, deviation from the normal spray shape was apparent. The spray became less eliptical and tended to have the central section reduced in height, causing the spray pattern to appear like an infinity symbol.

Sprays produced by the Binks Bullows gun were found to have the same central more dense region as the Walther Pilot gun. The droplets were found however to be less well contained than those of the Schlick and Walther Pilot guns. At the edges of the spray, rather than there being a defined boundary, there tended to be a region where the droplet density gradually reduced, this being particularly noticeable at the widest points of the spray. This effect was potentiated by the use of higher viscosity solutions and lower atomising air pressures. When atomising the 161mPa s solution there was evidence of numerous large droplets, especially when using an atomising air pressure of 276kPa.

With the 514mPa s solution, the sprays were very poorly contained and evidence of large droplets was apparent even at the highest air pressure of 516kPa.

The Spraying Systems 45° gun produced fairly well contained sprays, although the presence of some droplets outside the confines of the main spray was detected. The central area of greater droplet density was similar to that produced by the Schlick gun. No evidence of the production of large droplets was apparent when the 51mPa s and 161mPa s solutions were atomised using air pressures greater than 138kPa. With the 514mPa s solution, there was evidence of the presence of larger droplets especially at 276kPa.

The Spraying Systems 60° gun produced spray patterns which were markedly different from any of the other guns. The distribution of droplets throughout the spray was far more even, there being little evidence of an area of greater droplet density in the centre of the spray. The only evidence of the presence of large droplets was seen when the 514mPa s solution was atomised at 276kPa. The central region of spray patterns produced using atomising air pressures of 414kPa and above tended to be reduced in height causing the spray shape to appear like an infinity symbol.

Generally the qualitative visual assessment of the spray traces agreed with the findings of the Malvern droplet size analyser reported in section 4.3. Evidence of the largest droplets was seen on the traces from the Binks Bullows gun and the smallest on the traces from the Spraying Systems 60° gun. Increases in droplet sizes were seen mainly to occur when the atomising air pressure dropped to 276kPa or the viscosity increased to 514mPa s. Any differences in droplet size due to changes in flow rate between 30gmin^{-1} and 50gmin^{-1} were difficult to detect.

5.10 SCANNING ELECTRON MICROGRAPHS OF AQUEOUS FILM COATED TABLETS

Scanning electron micrographs (SEMs) were obtained of the surface of film coated tablets taken from selected coating runs. These are illustrated in Figures 5.9 to 5.12. The degree of magnification used was either x100, x300 or x1000. All SEMs were taken from the 15mm flat coated tablets. The main process variable(s) illustrated by the SEMs is given with each figure. Full details of the coating runs referred to are given in Appendix 1.

The SEMs in Figure 5.9 (magnification x300) and Figure 5.10 (magnification x1000) illustrate how the nature of the film surface is influenced by coating solution viscosity. In each case the coat was applied using a Schlick model 930/7-1 spray gun set to produce a flat spray shape. An atomising air pressure of 414kPa and a spray rate of 40gmin^{-1} were used and the gun-to-bed distance was 180mm. Figures 5.9a and 5.10a represent the surface of tablets from coating run 47, which used a 6%w/w HPMC E5 solution (viscosity 45mPa s). The arithmetic mean surface roughness (Ra) of the coated 15mm flat tablets from run 47 is 1.83µm. Figures 5.9b and 5.10b are of coating run 9 which used a 9%w/w HPMC E5 solution (viscosity 166mPa s) and Figures 5.9c and 5.10c of coating run 34 which used a 12%w/w HPMC E5 solution (520mPa s). The Ra values are 2.53µm and 3.51µm for runs 9 and 34 respectively. It can be seen clearly from these figures that the extent of droplet spreading and coalescence on the tablet surface is dependent on the viscosity of the solution applied. Droplets produced from the 6%w/w HPMC E5 solution are seen to generally have spread well. All except the smallest droplets appear to have coalesced to some degree with other droplets on the surface. Droplets produced from the 12%w/w solution however are seen as more discrete units which have a far more rounded appearance, this indicating a lack of spreading and droplet coalescence on the surface.

FIGURE 5.9a

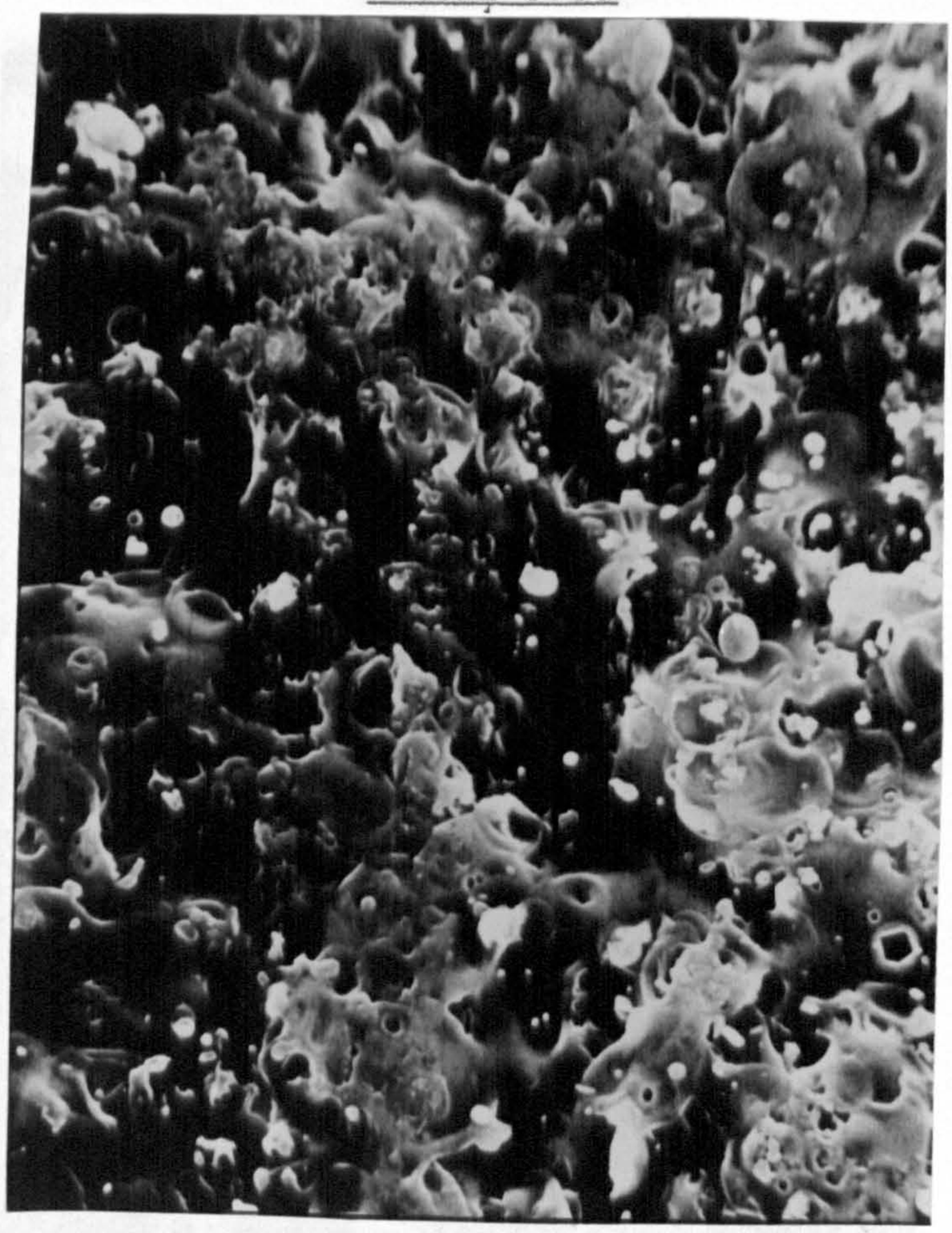

FIGURE 5.9b

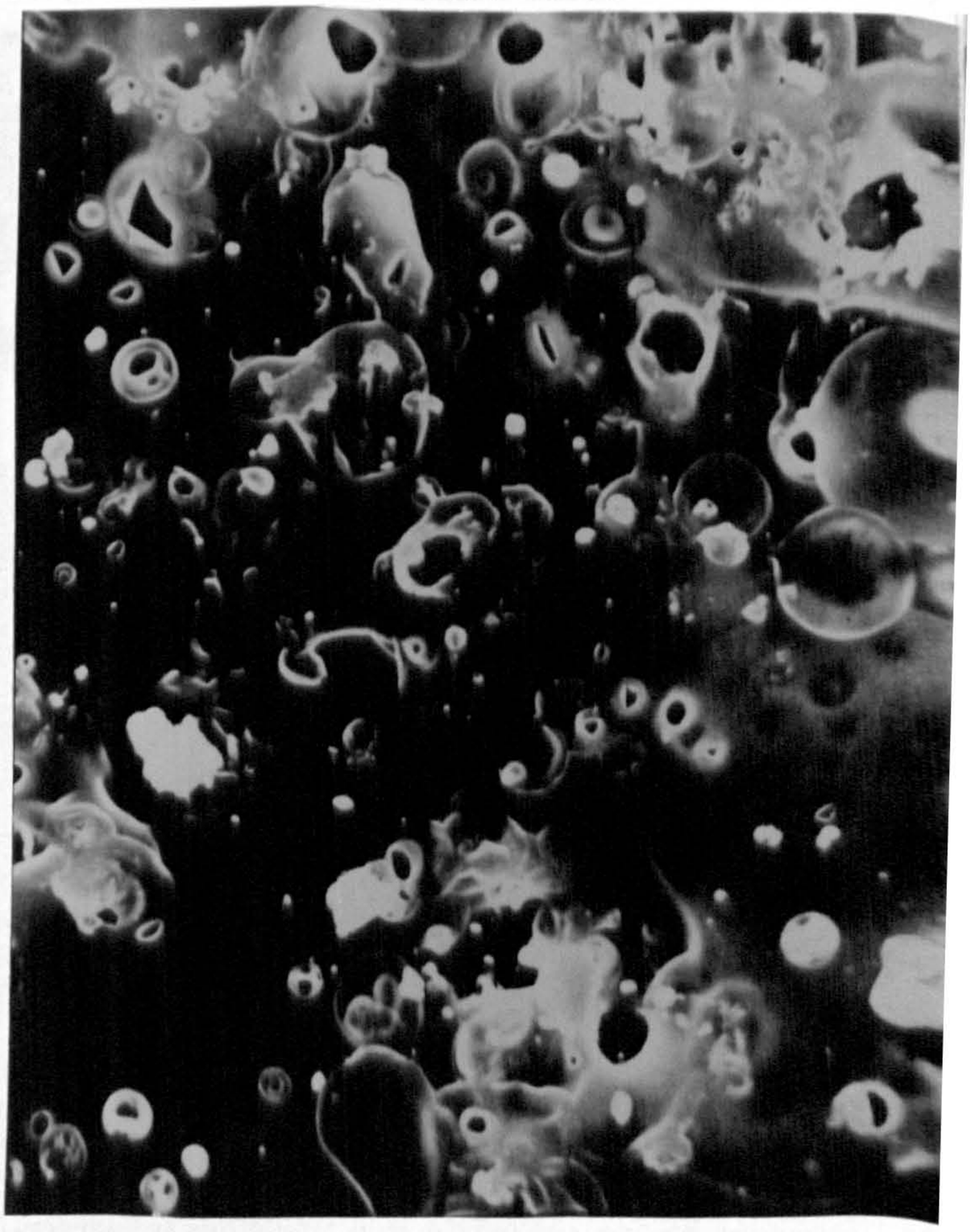

KEY

FIGURE 5.9a

Coating run 47, 6%w/w HPMC E5 solution, magnification x300, Ra = 1.83µm

FIGURE 5.9b

Coating run 9, 9%w/w HPMC E5 solution, magnification x300, Ra = 2.53µm

FIGURE 5.9c

Coating run 34, 12%w/w HPMC E5 solution, magnification x300, Ra = 3.51µm

See Appendix 1 for coating run details.

FIGURE 5.9c

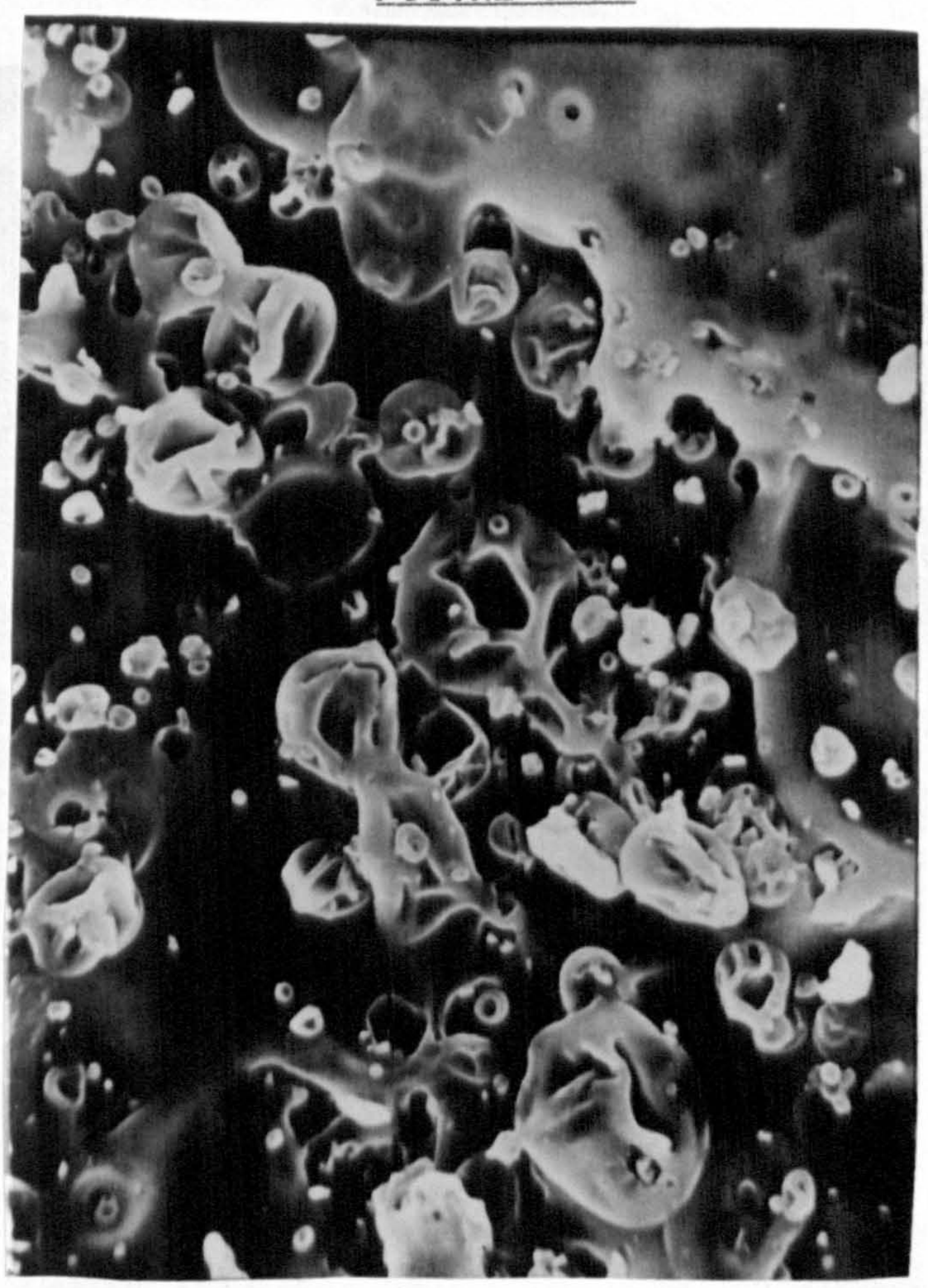

FIGURE 5.10a

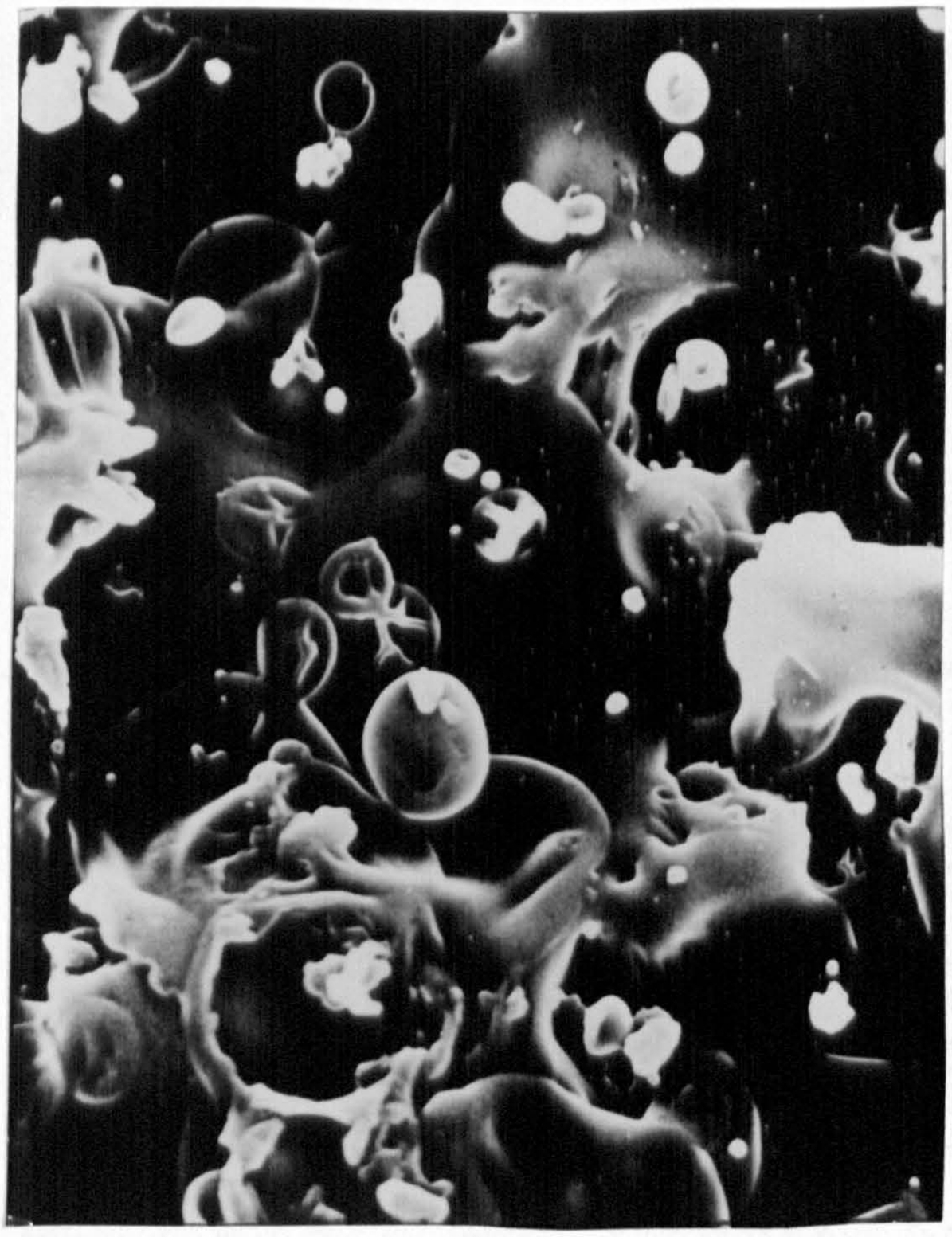

FIGURE 5.10b

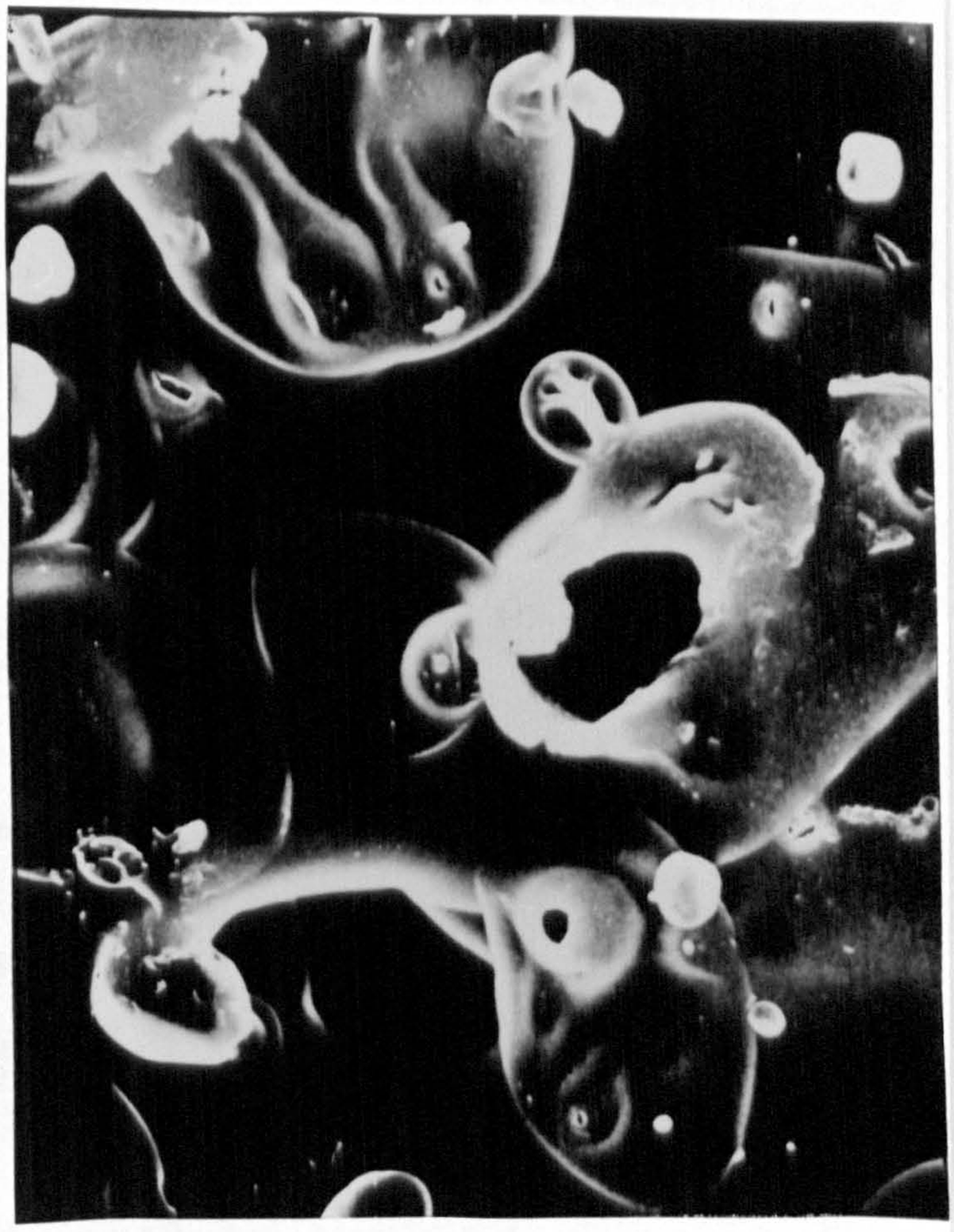

FIGURE 5.10c

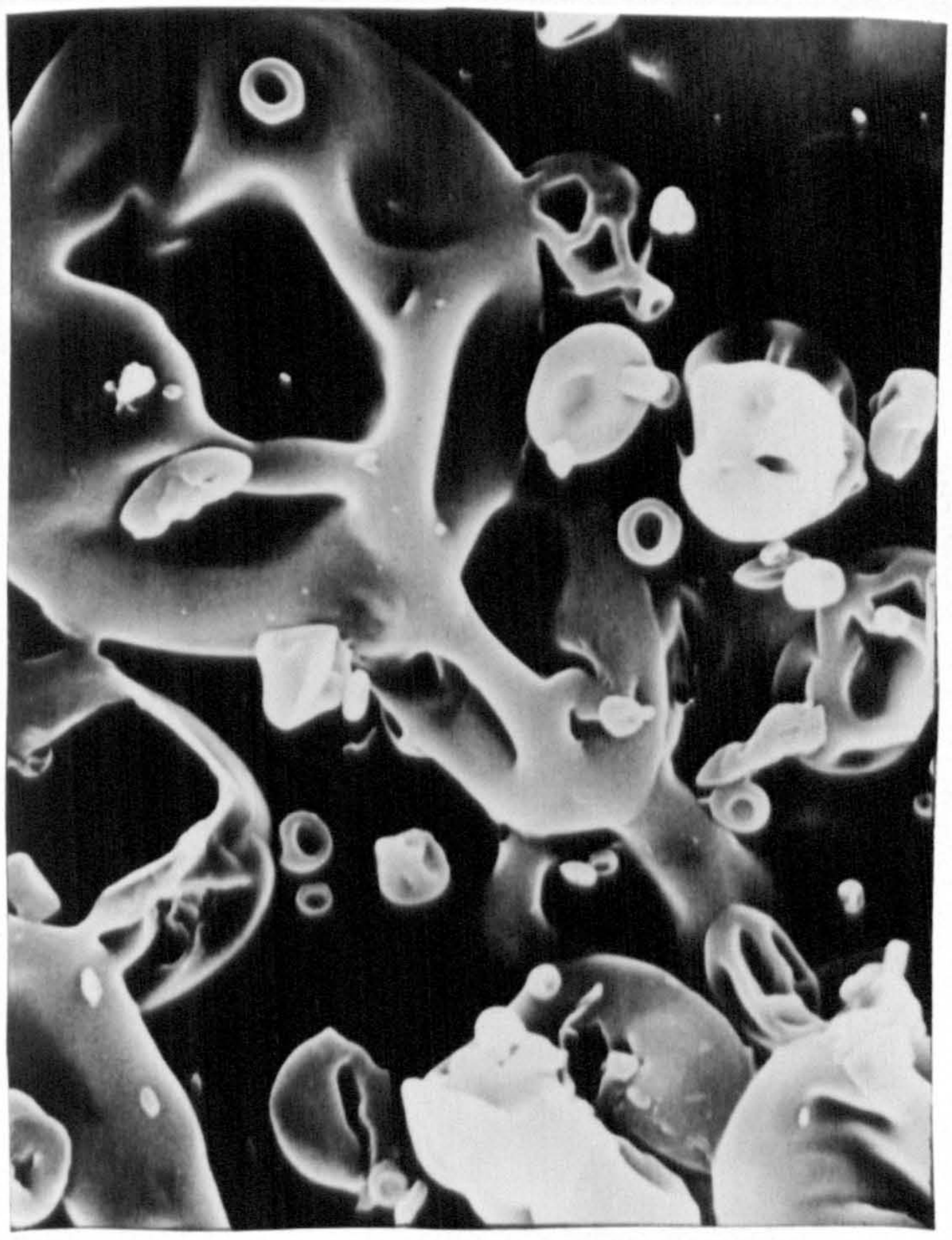

KEY

FIGURE 5.10a

Coating run 47, 6%w/w HPMC E5 solution, magnification x1000, Ra = 1.83µm

FIGURE 5.10b

Coating run 9, 9%w/w HPMC E5 solution, magnification x1000, Ra = 2.53µm

FIGURE 5.10c

Coating run 34, 12%w/w HPMC E5 solution, magnification x1000, Ra = 3.51µm

See Appendix 1 for coating run details.

The figures also illustrate the range of droplet sizes produced during the atomisation process and the heterogeneous nature of the film. Some of the smaller droplets appear opaque, suggesting that spray drying has occurred in these cases. Generally the smaller droplets are seen to spread less well than the larger droplets. Holes or craters are apparent in the centre of some of the dried droplets. This is particularly noticeable in Figures 5.9c and 5.10c where the 12%w/w solution was applied. These holes are thought to be due to the solvent bursting through the dried crust of the droplet surface. The reduction in spreading, coalescence and evaporation on the tablet surface arising as a consequence of increased droplet viscosity, are likely to have potentiated this phenomenon.

Figure 5.11 shows a SEM of the surface of a 15mm flat tablet taken from coating run 19. The conditions used to apply this coat were the same as those for Figures 5.9b and 5.10b, except that instead of a flat spray shape, a narrow cone spray shape was used. Tablets from this run had an Ra value of 1.44μm (only coating run 18 had a lower surface roughness value). The droplets appear to be have spread well on the surface and the appearance suggests that mutual rubbing between tablets may have been responsible for some of this spreading.

Figure 5.12 illustrates the surface appearance of tablets from coating runs 31 (Figure 5.12a), 37 (Figure 5.12b) and 47 (Figure 5.12c) at a magnification of x100. These coats were applied using a spray rate of 40gmin^{-1}, an atomising air pressure of 414kPa and a gun-to-bed distance of 180mm. Run 31 used a Walther Pilot gun to apply a 9%w/w HPMC E5 solution, run 37 a Spraying Systems 60° gun to apply a 12%w/w solution and run 47 a Schlick gun to apply a 6%w/w solution. The film Ra values were 1.94μm, >5.00μm and 1.83μm respectively. The SEMs from runs 31 and 47 (Figures 5.11a and 5.11c) indicate that comparatively good spreading

FIGURE 5.11

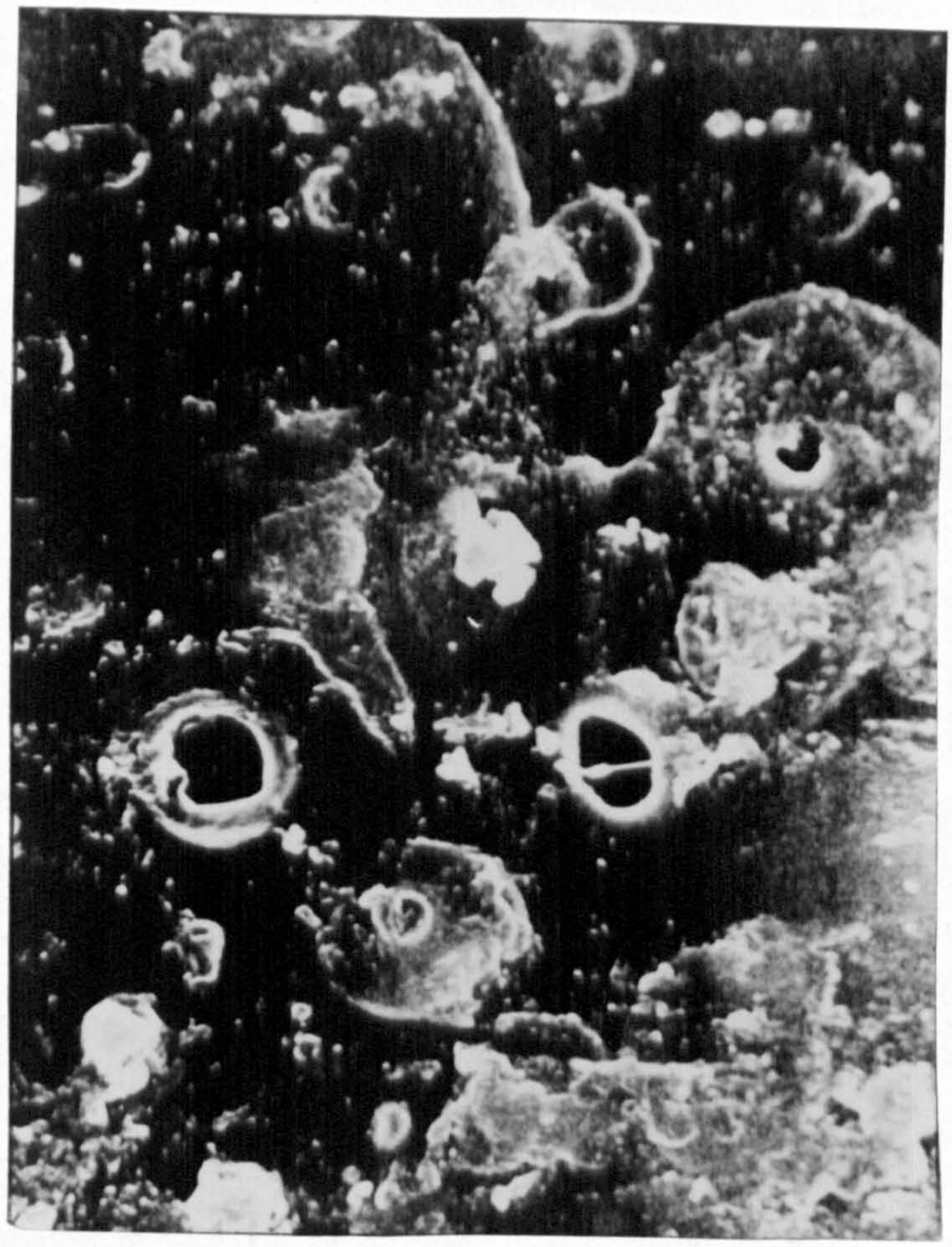

Coating run 19, 9%w/w HPMC E5 solution, Schlick gun set to produce a narrow cone spray shape, magnification x1000, Ra = 1.44μm

See Appendix 1 for coating run details.

FIGURE 5.12a

FIGURE 5.12b

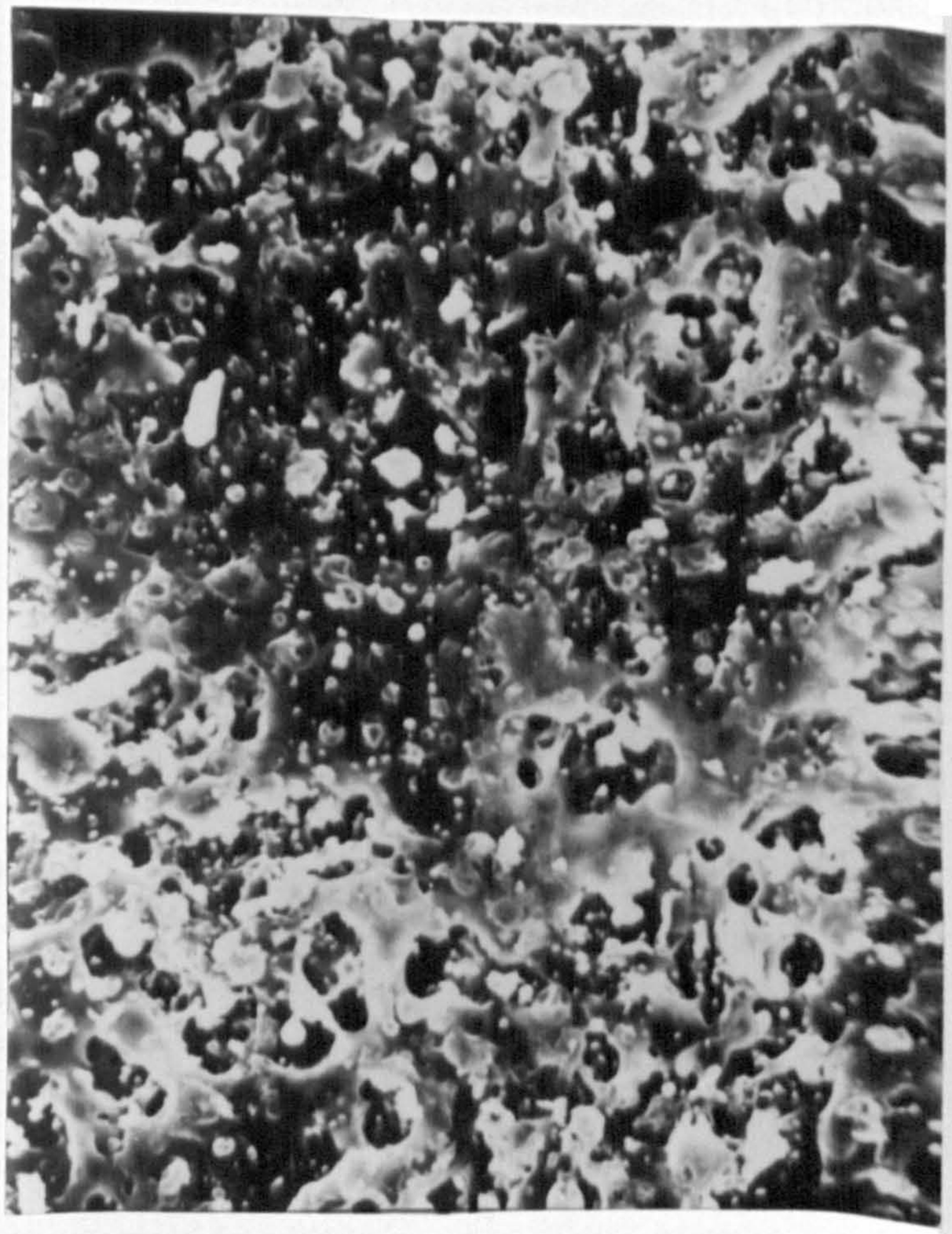

FIGURE 5.12c

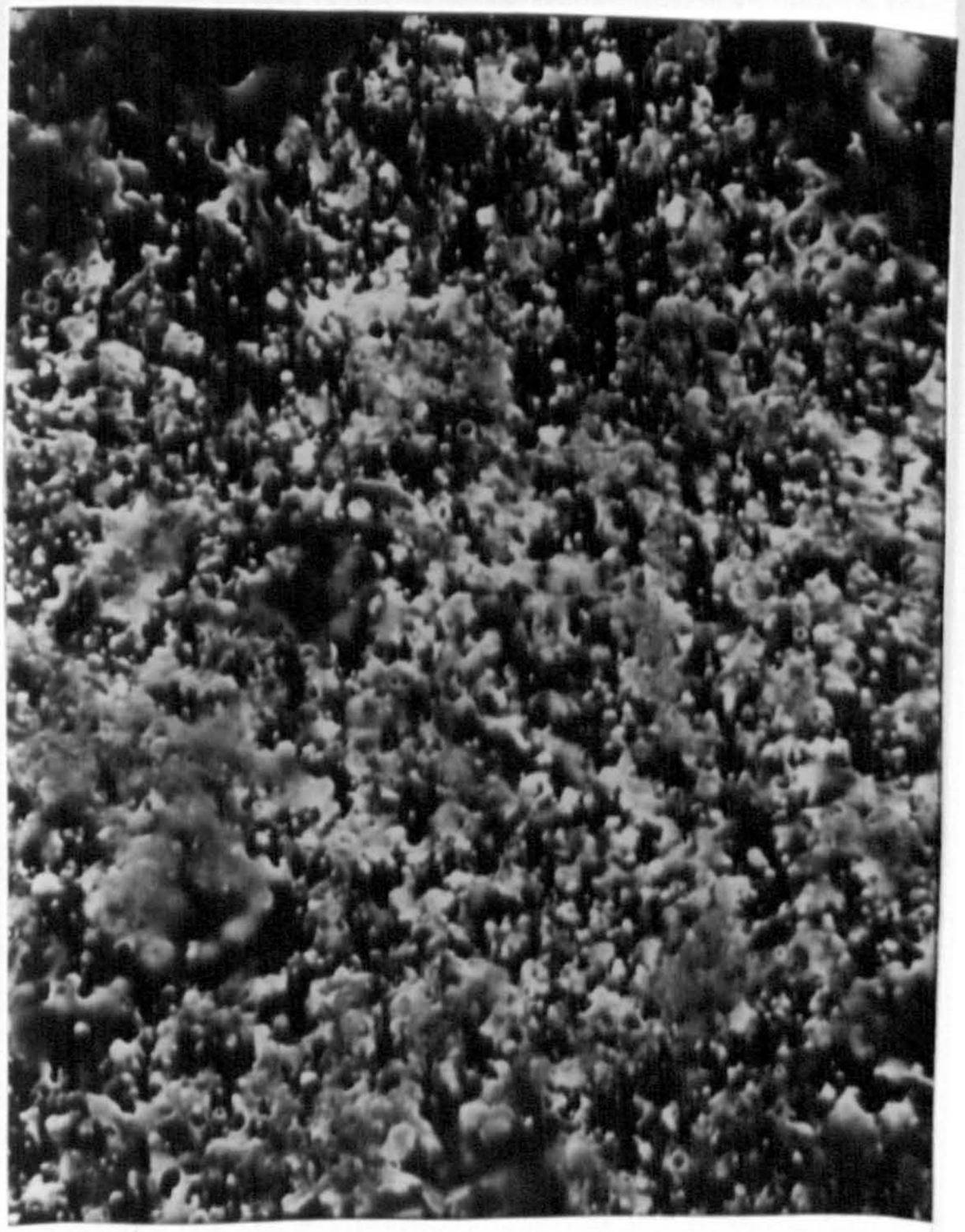

KEY

FIGURE 5.12a

Coating run 31, 9%w/w HPMC E5 solution, Walther Pilot gun, magnification x100, Ra = 1.94μm

FIGURE 5.12b

Coating run 37, 12%w/w HPMC E5 solution, Spraying Systems 60° gun, magnification x100, Ra = >5.00μm

FIGURE 5.12c

Coating run 47, 6%w/w HPMC E5 solution, Schlick gun, magnification x100, Ra = 1.83μm

See Appendix 1 for coating run details.

occurs when the 6%w/w solution is applied and when the Walther Pilot gun is used to apply a 9%w/w solution. Coalescence between droplets appears to be particularly good in Figure 5.12a and the occurence of spray dried droplets comparatively low. Figure 5.12b shows the very rough surfaces produced during coating run 37. There are many "craters" present, a lack of spreading and a greater extent of spray drying. This coat was the roughest of all the tablets studied.

5.11 DISCUSSION

The aim of commercial film coating processes is to produce efficiently and reproducibly a dosage form possessing the desired characteristics. These characteristics may include taste masking, improved product appearance, physical protection, reduction of dust formation during packaging and transport, or the modification of drug release eg by providing a controlled release or enteric membrane. In the latter two cases it is especially important that the coat does not possess defects which may compromise the coat, since undesirable pharmacological effects may result.

Film coats may be applied in a variety of ways using different coating equipment, process conditions and coating formulations. The intention of the work in this chapter was to examine the effects of the application conditions on the coating process and resultant film properties, in order to facilitate a more rational choice of application conditions and help minimise product development time and costs.

In this discussion section, initially the behaviour of the droplets upon impingement on the tablet surface is discussed, and this, together with information obtained from examination of the coat physical properties is used to interpret the occurrence of film defects.

5.11.1 THE CONTACT ANGLE OF FILM COATING SOLUTIONS ON UNCOATED AND COATED TABLETS

The contact angles formed by droplets on a substrate during aqueous film coating may potentially influence the roughness and appearance of the coated product. They may also affect the rate of solvent removal and thus the degree of penetration into the substrate and consequently coat adhesion. Young's equation (equation 3.3 in section 3.1.3) equates the forces acting on a drop of liquid on a solid surface. This equation implies that the contact angle is dependent upon the surface tension of the liquid, the solid/liquid interfacial tension and the surface tension of the solid. Low contact angles are favoured by high solid and liquid surface tensions and a low solid/liquid interfacial tension. Since (i) the coating formulations in this work exhibited minimal differences in surface tension, (ii) the uncoated tablets were the same for each coating run and (iii) the solid/liquid interfacial tensions were likely to have been the same, it might be expected from theoretical considerations that the contact angles of droplets on the tablets during the coating process would be of the same order, irrespective of the coating conditions. This indeed may be the case if (i) the substrate has zero porosity, (ii) the droplets have time to reach equilibrium on the substrate, (iii) the droplets are saturated with components of the substrate so that dissolution does not occur and (iv) no other external forces are acting on the spreading process. In the practical situation however the above conditions do not exist and there is therefore the potential for the droplet contact angles to be dependent upon the application conditions.

During the initial stages of the aqueous film coating process, the droplets will impinge onto an uncoated tablet surface and simultaneously penetrate into and spread onto the surface. The degree of penetration

will be governed by the degree of interaction between the components of the substrate and those of the coating formulation, the pore structure of the substrate and the coating solution physical properties (Alkan and Groves, 1982). The degree of spreading will be dependent on the droplet properties and the interaction between the components of the tablet and those of the droplet.

The test tablets used in this study consisted of microcrystalline cellulose, pregelatinised starch and stearic acid (see section 5.2.1). The former two components can both be used as tablet disintegrants and allow water to penetrate quickly into the tablet surface (Table 5.27), resulting in the disruption of tablet bonds and rapid tablet disintegration. This, coupled with the relatively high porosity of the test tablets would facilitate the formation of low aqueous coating solution contact angles. Counteracting those factors which aid penetration are droplet viscous forces. The wide range of penetration times detailed in Table 5.27 demonstrates the potential importance of HPMC solution concentration/viscosity in governing the degree of atomised droplet penetration into a substrate. The extremely slow penetration rates found for the higher solution concentrations (despite the favourable substrate properties described above), suggests that problems associated with poor adhesion eg intagliation bridging, may occur with these solutions, especially if applied to low porosity or hydrophobic substrates.

The potential influence of the energy possessed by coating solution droplets when they impinge on an uncoated substrate in determining the degree of "forced" spreading and the contact angle was demonstrated in section 5.7. The results indicate that only a small amount of energy would need to be imparted to droplets atomised from low HPMC E5 solution concentrations (6%w/w and below) in order for them to spread well. The

fact that these concentrations are applied to produce smooth high gloss coats (Reiland and Eber, 1986) suggests that sufficient energy to spread the droplets is imparted during typical coating processes. With higher HPMC E5 solution concentrations however it was demonstrated that the contact angle was dependent on the kinetic energy and viscosity of the droplets. The data indicated that considerably greater amounts of energy need to be imparted to highly viscous droplets in order to force them to spread on a tablet surface after contact. The extent of spreading will therefore be dependent on the droplet viscosity and the atomisation conditions.

The reduction in droplet contact angle which occurred after 30 seconds contact on the uncoated tablet will have arisen from a combination of droplet penetration into the tablet surface and "flowing out" of the droplet under surface tension and gravitational forces. The former is most likely to have occurred with the lower viscosity solutions which can penetrate relatively easily and have a low initial contact angle. With the higher viscosity solutions, penetration effects would have been much smaller and the latter effect thought to predominate. Since "flowing out" or levelling of droplets on the surface is resisted by the droplet viscosity (Rowe, 1988), there may be insufficient time during the coating process for highly viscous droplets to level to any great extent. The initial contact angle may therefore be the most important determinant of surface roughness.

The contact angles formed on uncoated tablet surfaces during coating are therefore likely to depend on the droplet viscosity and kinetic energy and the degree of penetration into the tablet surface.

The results in section 5.7 indicate that the contact angles formed by HPMC-based formulations on coated tablets can be different from those formed on uncoated tablets. Droplets placed gently on the surface of

coated tablets showed greater initial contact angles than those on uncoated tablets, this being especially apparent with the low viscosity solutions. Droplet viscosity appeared to have minimal influence on the contact angles formed by droplets placed gently on coated tablet surfaces. These latter two findings are due to a reduction in droplet penetration into the coated tablet surface compared with the uncoated tablet surface. This would also explain the smaller decrease in contact angle which occurred within 30 seconds of the droplets contacting the coated tablet surfaces. The potential for very rough coated surfaces to increase the contact angle of droplets placed gently on the surface was also demonstrated. This is likely to have arisen from a tendency for the rougher surface to resist movement across the surface, thereby reducing the advancement of the droplet.

An estimation of the *work of adhesion* (W_A) (see Equation 3.6, section 3.1.5) for HPMC coating solution droplets on an HPMC coated tablet surface can be calculated from the equilibrium contact angles (contact angles after 30 seconds) of the droplets placed gently on the coated tablet surfaces (see Tables 5.23 to 5.25). Using an average contact angle (θ) of 92° and an average droplet surface tension value (γ_{LV}) of 45.5mNm^{-1} (Table 3.10), W_A can be estimated to be 43.9mNm^{-1}.

When the droplets were given kinetic energy during the contact angle measurements, droplet viscosity was found to be important in determining the contact angle formed on coated tablets and differences in contact angles formed on the coated and uncoated tablets became much smaller. The reduction in contact angle found with increasing droplet kinetic energy was in contrast to results reported by Zografi (1985), which suggested that if droplets were forced to move at greater velocities across a surface a greater contact angle may result.

Coated surfaces of different roughness were not found to exhibit

different contact angles when the droplets were given kinetic energy, the resistance to droplet advancement presumably being overcome by the momentum of the droplet. This latter finding may not necessarily occur however during practical film coating, since the droplets hitting the tablet are much smaller and their size relative to the undulations in the surface is also much smaller.

On coated tablets therefore the spreading behaviour and contact angle formed by atomised coating solution droplets are likely to be dependent mainly on the droplet viscosity and kinetic energy. If however the droplets are so viscous that the kinetic energy gained from the atomising air causes minimal forced spreading on the surface, or the substrate is sufficiently hydrophobic, surface tension and interfacial tension forces may play a more dominant role. In these circumstances, the behaviour discussed in Chapter 3 whereby the droplet surface tension could be potentially dependent upon droplet size, may also be a contributing factor.

It should be noted that the determination of contact angles in this work can only give an indication of the likely effects in practice and serve to offer explanations for subsequent coat properties. In the practical situation, the time taken for droplet penetration and spreading to occur is very small (<1 second) and the droplet is continuously and rapidly being evaporated and its viscosity therefore continually changing. The droplets will also impinge on the tablets at various angles, with the momentum of the tablet itself making a contribution to the forced spreading process. The results do however demonstrate that formulation viscosity and droplet kinetic energy are likely to play an important role in governing the degree of penetration and spreading on uncoated tablets, and the spreading behaviour on partially coated and coated tablets.

5.11.2 COATED TABLET SURFACE ROUGHNESS

The appearance of a coated tablet is governed to a large extent by the surface roughness. Coats which have smooth surfaces tend to have a glossy appearance, whilst those with a rough surface appear more matt and may exhibit a surface like that of an orange skin. The surface properties of a coated tablet may therefore be important for aesthetic reasons. Because of the difficulties in achieving glossy film surfaces, gloss solutions are often added after the main coating process (Relland and Eber, 1986). This inevitably increases batch process time and expense. Knowledge of the factors which would negate use of gloss solutions whilst still producing an acceptable product in an acceptable time would therefore be beneficial. The measurement of surface roughness may provide information on the behaviour of atomised film coating droplets on the tablet surface and thus aid in optimising the coating process. It may also be used as a quality control tool to monitor film coating at the production scale (Trudelle et al., 1988).

Coat surface roughness will be dependent upon the roughness of the substrate, the properties of the coating formulation applied and the coat application conditions. The composition and properties of each of the three test tablet types remained constant throughout all of the coating runs and therefore any differences in roughness found in this study for a paticular tablet type, could be attributed to the formulation or the application conditions. Hansen (1972), King and Thomas (1978) and Rowe (1981a) suggested that the inherent roughness of original substrate is the most important determinant of the roughness of a coated surface. The results in section 5.5 show the coat arithmatic mean surface roughness values (Ra) in this study to range from 1.3µm to >5µm, despite being applied to the same substrate. Rowe (1979) however showed that even using a large range of compaction pressures and tablet

porosities, the tablet Ra was only found to be between 0.55µm and 1.88µm. This indicates that with aqueous film coating, the application conditions and coating solution formulation can have at least as great, if not a greater effect than the original substrate roughness.

Film surface roughness values determined using a stylus instrument (Ra values, section 5.5) provided similar information on the effect of formulation and application conditions as those values determined using a Light Section Microscope optical method (Rtm values, section 5.4). The ratio of Rtm values to Ra values (see Tables 5.14 and 5.16) was calculated to be 4.86 ± 0.35 (n=9, range 4.26-5.49). This value is similar to that of 5.4 reported by Rowe (1979) for film coats applied from organic solutions.

The effect of coating formulation viscosity on film coat surface roughness

The viscosity of the coating formulation was shown to influence both the visual appearance of the tablet and the surface roughness parameters, with increases in solution viscosity from 46mPa s to 840mPa s producing tablets which had progressively rougher, more matt surfaces. Similar behaviour was reported by Rowe (1979) for organic film coating solutions and Relland and Eber (1986) for aqueous film coating in a model system. Unlike at higher concentrations, the application of 6%w/w HPMC E5 solutions (viscosity 46mPa s) using different spray guns produced tablets with very similar Ra values and surfaces which were much smoother than the original uncoated tablet. These results reflect the relatively small amount of kinetic energy required to force droplets generated from low viscosity solutions to spread and coalesce on the tablet surface and illustrate why they are used to impart a gloss finish to coated tablets. Any initial penetration that may have occurred as a result of the low viscosity (see Table 5.27) would have potentiated the

formation of a low contact angle and contributed to low initial surface roughness values. The ease of droplet spreading of low viscosity coating solutions would also explain why Relland and Eber (1986) found HPMC E5 solutions of between 1%w/v and 6%w/v to produce very similar surface roughness values when applied using their model coating system.

As the coating solution viscosity increases, there is a greater resistance to spreading on the tablet surface and a reduced tendency to coalesce, both of which increase surface roughness. This is illustrated by the SEMs in Figures 5.9 and 5.10. The greater incidence of holes or craters in the centre of the dried droplets, caused by the reduced spreading, coalescence and drying rate, is likely to have contributed to the increased roughness. Other factors arising from an increase in solution viscosity which may potentiate surface roughness, include the larger mean droplet size produced on atomisation and the reduced penetration into the uncoated tablet surface. The rougher nature of the partially coated tablet may itself also contribute to a reduction in spreading, by reducing the advancing contact angle, as discussed by Zografi and Johnson (1984). Any levelling of the droplets on the tablet surface that may occur due to gravitational and surface tension forces (Rowe, 1988) would also be expected to be less significant with higher viscosity solutions.

The potential for the coated product surface roughness to be affected by HPMC E5 batch variation is illustrated in Table 5.20. This effect would be expected to be greater with increasing polymer concentration and not to be significant at solution concentrations of around 6%w/w or below.

The effect on surface roughness of any changes in HPMC moisture content that may occur during storage, would be expected to be related to changes in the coating solution viscosity.

When coating formulations containing dispersed solids are applied, the

surface roughness may be dependent not only upon the viscosity but also on the nature of the dispersed solids. Rowe (1981a) using dolomites of various sizes, showed that the dispersed solid particle size and concentration could influence film coat Ra values. He did not however detail the viscosity values of the coating formulations or consider the changes in viscosity that may have accompanied the inclusion of the different sized dolomites. The mean particle size of the aluminium lakes in the Opadry formulations used in this work were likely to have been below 5μm (manufacturers data) and their concentration was approximately 50%w/w (based on HPMC content). Data from Rowe (1981a) indicates that the effect on surface roughness of the dispersed solid particle size and concentration in the Opadry formulations was likely to have been small. The viscosity of the Opadry formulations was therefore likely to have been the main determinant of the surface roughness. Opadry formulations are psuedoplastic and therefore have different viscosities when subjected to different shear stresses. The data in Figure 5.5 indicate that during film formation the Opadry formulations behave as if their viscosity is between the apparent Newtonian viscosity value and that calculated for an infinite shear rate.

It has been suggested that the shear forces generated from mutual rubbing between tablets during the coating process, are sufficient to smooth out even the most viscous partially gelled coating formulations (Rowe, 1988). The large differences in surface roughness reported in Table 5.15 for tablets coated with different solution viscosities, suggests that in this work mutual rubbing did not generally play a significant role. This is probably due to the fact that the droplets had generally dried sufficiently to form part of the viscoelastic film, before they entered the tablet bulk where mutual surface rubbing effects mainly occur. There was however evidence of surface rubbing when a

narrow cone shaped spray was used to apply the coating solution (see Figure 5.11). In this latter case, the concentration of the spray over a small area tends to cause overwetting of the tablets (as evidenced by the high incidence of picking and sticking reported in Table 5.9). A proportion of the tablets may therefore subsequently enter the tablet bulk within the coater before the coat has dried and there is therefore the potential for the shear forces generated from mutual rubbing between tablets to effect thr partially dried droplets/film..

Any smoothing of the dry film surface arising from attrition forces between the tablets as they tumble in the coating pan would have been expected to be greater when applying the lower viscosity solutions and when using lower spray rates, since the total coating time would have been proportionately longer.

<u>The effect of spray shape on film coat surface roughness</u>

Changing the shape of the spray pattern generated by the Schlick gun from the typically used flat shape, to a narrow angle solid cone, was found to produce smoother more glossy surfaces. Even the 12%w/w HPMC E5 solutions applied using a cone shaped spray produced relatively smooth surfaces, these being less rough than those produced by a 9%w/w solution applied using a typical flat spray shape. These effects are thought to be due to differences in average droplet velocity and the extent of spray drying. With the narrow spray cone, because the droplets are concentrated in the centre of the spray, the average distance of droplet travel is reduced and the droplets are propelled by the faster moving central air stream. Both these factors serve to increase the kinetic energy of the droplet on impingement on the tablet surface, and this coupled with the reduced incidence of spray drying in the centre of the spray (as evidenced by data in Table 5.9) will increase the extent of droplet spreading. The increased density of droplets in the central

region of the narrow cone spray may also lead to an increase in both the coalescence of droplets on the tablet surface and the likelihood of droplets hitting partially dried droplets and causing further spreading. Smoothing of the surface due to mutual rubbing between tablets within the coater may also have been a contributing factor as previously described. Any factors which increase the proportion of droplets within the central region of the spray are therefore likely to reduce coat surface roughness.

The results also illustrate the danger of using model systems such as those described by Prater (1982) and Relland and Eber (1986) to investigate the coating process, since these systems tend to expose the stationary test tablets only to the central area of the spray.

The effect of atomising air pressure on film coat surface roughness

In each case where the atomising air pressure was increased and all other parameters remained constant, there was a reduction in surface roughness. Several factors may have been responsible for these observations. Increasing the air pressure will in some cases have increased the exit velocity of the atomising air as it left the annulus surrounding the liquid nozzle and in all cases increased the mass of the atomising and spray shaping air. These in turn would have increased the energy and momentum of the atomising air. Since the droplets are propelled by and carried with the atomising air their momentum and kinetic energy would also have been increased. Droplets which possess greater momentum are more likely to undergo forced spreading at the tablet surface. Increased atomising air pressures also produced droplets of smaller mean diameter and reduced the incidence of large droplets, especially at pressures above 276kPa. This may also have contributed to the reduction in surface roughness, especially with the more viscous formulations.

The effect of atomising air pressure on surface roughness when applying 6%w/w HPMC E5 solutions was not studied. It is expected however that this would have been relatively small over the range of air pressures used practically, since the droplets are likely to spread well even when their kinetic energy is relatively low. The work of Relland and Eber (1986) supports this, since atomising air pressure was not found to exert a significant effect on surface roughness when applying low viscosity gloss solutions in a model system.

With the Schlick, Walther Pilot, Binks Bullows and Spraying Systems 45° spray guns, the general spray shape characteristics were similar at all atomising air pressures. With the Spraying Systems 60° spray gun however the spray dimensions were found to be reduced on increasing the atomising air pressure (Table 5.28). This reduction in spray dimensions may have contributed to the lower surface roughness for reasons previously described.

The role of the spray gun in governing film coat surface roughness

The spray gun chosen to apply a film coating solution was shown to potentially cause significant differences in the roughness and appearance of the coated product (Table 5.15). This could have arisen from differences in droplet size distribution, spray shape and droplet distribution within the spray, or the volume and velocity of the atomising and spray shaping air.

The formation of relatively smooth surfaces when using the Binks Bullows and Walther Pilot guns is considered to be due to the greater total air consumption (especially through the face of the air cap), the high proportion of droplets within the central section of the spray and the low incidence of spray drying. The Schlick gun, although having a higher annulus atomising air velocity, had a lower total atomising air mass flow rate and a more evenly distributed spray than both the Walther

Pilot and Binks Bullows guns. More of the droplets existed towards the edge of the spray, which coupled with the reduced atomising air mass flow rate, reduced the average droplet kinetic energy. This and the increased incidence of spray drying would explain why the Schlick gun produced rougher films than either the Walther Pilot or Binks Bullows guns. The Spraying Systems 45° spray gun produced films with similar surface roughness values to those of the Schlick gun despite its low atomising air mass (approximately one-third of the Walther Pilot and Binks Bullows guns and half of the Schlick gun). It is likely that this effect was due to both the smaller surface area covered by the spray, which led to the droplets and atomising air being concentrated over a smaller area, and the low incidence of spray drying. The Spraying Systems 60° spray gun produced sprays covering the largest surface area, had the lowest atomising air mass flow rate and produced the smallest droplets. These three factors led to an increase in spray drying (Table 5.6) and reduced the average droplet momentum. This in turn would have reduced the extent of spreading of the droplets on the tablet surfaces (as evidenced by Figure 5.12) and hence led to high roughness values.

It is considered that the predominant cause of the differences in surface roughness apparent when using different spray guns arose from differences in the average droplet kinetic energy on hitting the tablet surface and the associated degree of spreading. Smoother surfaces are likely to be formed by spray guns which tend to produce sprays which have a high density of droplets in the central region and which have high atomising air mass flow rates.

<u>The effect of spray rate on film coat surface roughness</u>

When using the Schlick spray gun, increasing the spray rate appeared to cause a reduction in surface roughness when a 9%w/w HPMC E5 solution (viscosity 166mPa s) was applied. An increase in surface roughness was

however observed for both 15%w/w Opadry and 12%w/w HPMC E5 solutions on increasing the flow rate from 30gmin^{-1} to 40gmin^{-1}, but little further effect with a flow rate increase to 50gmin^{-1}. It is probable that with the 9%w/w HPMC E5 solution, spreading is enhanced by the increased density of droplets within the spray, the accompanying reduction in spray drying (Table 5.9) and the lower tablet bed temperature (Table 5.3). However with higher viscosity formulations, where the tendency for the droplets to spread and coalesce on the tablet surface is reduced, any effects arising from the increased density of droplets and reduced tablet temperature are likely to be much smaller. The increase in roughness with increasing flow rate seen when the 12%w/w HPMC E5 solution and 15%w/w Opadry formulation were applied may have arisen from the production of larger droplets, which, if they did not spread well or coalesce with other droplets, would produce a rougher surface.

The effect of spray gun to tablet bed distance on film coat surface roughness

Increasing the distance of the spray gun from the tablet bed results in a reduced droplet momentum at the point of impingement on the tablet surface, a more even distribution of droplets within the spray (section 3.9), and an increase in spray drying (Table 5.8). These three factors will tend to reduce spreading and coalescence on the tablet surface and therefore contribute to the consistent increase in surface roughness values which accompanied increasing the distance of the spray gun from the tablet bed.

The effect of drying air temperature and volume flow rate on film coat surface roughness

Reducing the drying air temperature and volume flow rate over the ranges studied caused a small decrease in film surface roughness (Table 5.10). This may have been due to the overall reduction in heat input into the

system, which reduced the tablet bed temperature and evaporation from the droplets during travel to the tablet bed, both of which aid the spreading process.

The effect of liquid nozzle diameter on film coat surface roughness

Changes in the liquid nozzle diameter were found to have a minimal effect on film surface roughness values. This is perhaps not surprising, since with both guns where this was studied the atomising air characteristics and droplet size distributions were unchanged. Any effects arising from differences in the speed of liquid exit from the nozzle or the diameter of the "column" of liquid emitting from the nozzle would appear not to have influenced the droplet properties. It should be noted however that if changing the liquid nozzle diameter also changes the area of the annulus surrounding the liquid nozzle, differences in the atomising air characteristics and film surface roughness may result.

Film coat surface roughness values on different areas of the tablet surface

The film coat at the edges of the flat tablets was shown to be considerably smoother than on the main tablet body (Table 5.14). This arisis since the predominant point of contact between the flat tablets during the coating process is at the tablet edge and thus the attrition forces at the tablet edge are greater. This would have been potentiated by any enhanced droplet spreading that may have occurred at the tablet edge due to increased shear forces.

Rowe (1988) reported that when applying coats from both aqueous and organic systems, the film coat surface roughness within a tablet intagliation could be 2-3 times higher than on the tablet body. He suggested that on the exposed surface of the tablet the shear stresses induced by mutual rubbing were high enough to both smooth out even the

most viscous partially gelled coating formulations and to cause alignment of pigment particles if present. Within the intagliations however it was suggested that only small surface tension forces existed and that little levelling, smoothing or particle alignment occurred. The Light Section Microscope data reported in this thesis did not support the above theory, since in each case studied, the roughness in the tablet score mark of the 10mm convex tablets was considerably lower than on the main body of the tablet (see Table 5.14). One factor which is likely to have contributed to this effect was the very low initial roughness within the score compared with the main body or crown of the tablet, although this was also the case in the study reported by Rowe (1988). Data in Table 5.14 indicate that differences in film roughness between the score and the tablet body are unlikely to have arisen from differences in film thickness. The reasons for the discrepancy between the results of this study and that reported by Rowe (1988) are difficult to determine due to the lack of coating process details reported in the latter case. It could be that fundamental differences in the way films are formed within tablet intagliations and score marks may be responsible. Alternatively, differences in the methods of determining the surface roughness may have contributed. The Light Section Microscope used in this study measured the surface roughness of the film itself, whereas the stylus instrument used by Rowe (1988) could not discriminate between the film and any surface debris and may therefore have calculated artificially high values of Ra.

From the preceding discussion it can be concluded that the actions which can be taken in order to produce a smoother, more glossy tablet appearance include; a reduction in coating formulation viscosity, an increase in atomising air pressure, a reduction in spray dimensions, a

reduction in spray gun to tablet bed distance and the use of a spray gun which has a relatively high atomising air mass flow rate and tends to produce sprays where the droplets are concentrated in the central region.

5.11.3 FACTORS AFFECTING THE THICKNESS OF AQUEOUS FILM COATS

If after the completion of the coating process all the test tablets had received the theoretical coat level of 2.25%w/w and the film density is assumed to be 1.2gcm^{-3} (see Parker et al., 1974), then the theoretical film thickness on the 15mm flat tablets (specific surface area 0.77mm^{2}mg^{-1}, see section 5.2.1) can be calculated to be 24.4µm and on the 10mm flat tablets (specific surface area 0.90mm^{2}mg^{-1}) 20.8µm. Data in Table 5.14 suggest however that there is minimal difference in the average film thickness between the three test tablet types taken from a particular coating run. Thus it would appear that in practice the smaller specific surface area of the 15mm flat tablets did not lead to a thicker coat being applied. It is likely that the increase in specific surface area is counteracted by the faster speed of fall through the spray zone and the consequent reduction in coat applied on each pass through the spray.

The average film thickness values determined using the Light-Section Microscope (Table 5.14) were generally considerably greater than the theoretically calculated values and varied markedly between tablets from different coating runs. The similarity in film thickness of the three test tablet types from any particular coating run suggests that the effect of size differences between the test tablets and the bulking tablets was likely to have been small. Similarly differences in coating efficiency (ratio of the mean weight of coating found on the tablet to the mean weight of solids applied per tablet from the coating solution)

were thought to have had little effect, since those coating runs where efficiency was likely to have been lower (eg runs 21 and 23 (see Appendix 1) which utilised an increased gun-to-bed distance) did not produce thinner coats. The observed differences in film thicknesses both from the theoretical values and between tablets from different coating runs are thought to have arisen predominantly from variations in film density caused by the use of different application conditions. The potential for spray application conditions to influence film density has also been reported by Allen et al. (1972) when investigating free films generated from solutions of cellulose acetate in acetone. Coated tablet film density will be dependent upon the degree of air entrapment within the film. This air may be trapped either within spray dried droplets or between film layers due to insufficient droplet spreading and coalescence on the tablet surface. Thus, factors which enhance spreading (see 5.11.2) or reduce the tendency to cause spray drying (see section 5.5.2) would be expected to produce thinner, more dense films. This is substantiated by the results in Table 5.14.

Theoretical film thickness values are only likely to be produced if the application conditions produce films which have a similar density to cast films. This may occur with low viscosity solutions applied using conditions which maximise droplet spreading and coalescense and minimise spray drying.

For any particular tablet type, it was demonstrated that the film thickness could vary markedly at different points on the tablet surface. This was particularly apparent with tablets coated using conditions which produced smoother, more dense, thinner films. Since these conditions enhance droplet spreading, the droplets may preferentially "fill in" irregularities in the substrate surface, as suggested by Prater (1982). This was supported by the visual image seen through the

Light Section Microscope, which showed the thinnest areas of coat to exist at the peaks of the uncoated tablet surface and the thickest areas at the troughs of the uncoated tablet surface. Application conditions which produced relatively thick coats, tended to form films with a much more even thickness, the films tending to more closely follow the contours of the uncoated tablet surface.

The large variation in film thickness seen with the 10mm convex scored tablets will have arisen from the differences in uncoated tablet surface roughness at different points on the tablet surface. Within the tablet score where the tablet was very smooth, there were few irregularities to fill in and therefore the potential for film thickness variation was low. On the tablet crown however where the surface was very rough, a large proportion of the coat may be used in the filling of the irregularities before the coat can be built up over the peaks of the uncoated tablet surface. There is therefore a considerably greater likelihood of the existance of differences in film thickness.

The average film thickness at the edge of the flat tablets was also found to be considerably lower than on the tablet body. In this case however this was probably due to the greater attrition forces at the tablet edge experienced during tumbling in the coating pan.

The variations in film thickness at different points on the tablet surface may have important implications if the coat is to be used to confer controlled release or enteric properties. In these cases, the properties of the coat may depend not upon the average film thickness, but on the thinnest parts of the film coat. In these circumstances it may be possible to reduce the coat level required to achieve the desired effect by producing a coat of even thickness. This may be done by ensuring that the substrate has a low surface roughness and the application conditions produce a smooth coat. The widest variation in

film thickness is likely to occur with rough substrates and coating conditions which produce a low surface roughness

The occurrence of variations in film thickness across the tablet face also highlights the potential inaccuracy of determining film thickness values using a micrometer, since this instrument is likely to only measure the thickest part of the film. Similarly calculation of theoretical thickness values from cast film density measurements may only be applicable if the coating conditions produce films with a density similar to that of the cast film.

5.11.4 MICRO-INDENTATION BEHAVIOUR OF AQUEOUS FILM COATED TABLETS

The use of micro-indentation testing in the assessment of the hardness and elastic/viscoelastic properties both of film coating materials and film coated tablets has been reported by several authors. The results from these studies have been used to assess such factors as the effect of plasticisers and colorants/fillers (Rowe, (1976b; Aulton et al., 1981; Aulton et al., 1984; Okhamafe and York, 1986), stability behaviour (Okhamafe and York, 1986) and the potential for film defects such as edge splitting and intagliation bridging (Rowe, 1982a).

The coated tablets tested in this work did not have plasticisers or other additives present in the film and consisted solely of HPMC E5 and water. The films were found to be glassy in nature (typical of unplasticised HPMC films (Aulton et al., 1981)) and although they did exhibit both a small degree of visco-elastic behaviour and a small viscous response, the difference between the coated tablets was small and could not be correlated with any of the application conditions. Since the components of the coat were the same in each case, it might have been expected that the film elastic/hardness properties would have been very similar. This was not the case however, with large

differences in the instantaneous elastic modulus and Brinell hardness values being apparent between tablets coated using different application conditions (Table 5.21). The highest of the values reported in Table 5.21 are similar to those reported by Rowe (1976b) for unplasticised HPMC films sprayed from organic solutions using a Wurster column. However Okhamafe and York (1986) when applying an aqueous 10%w/w HPMC solution (Pharmacoat 606) in a Wurster column found a Brinell hardness value of approximately 1.9MPa (range in Table 5.21, 1.08 to 3.23MPa). They reported that the Young's moduli of the sprayed films (determined using indentation tests) were about 2 to 5 times lower than those of equivalent cast films (values determined from tensile tests). Pickard (1979) also reported that with organic based coating formulations, the use of a spray gun resulted in films which were weaker and had a lower modulus of elasticity when compared with poured films. The differences in hardness/elasticity found in this study and between results from other studies could have potentially arisen from either fundamental differences in the properties of the polymer, or from the way in which the film was formed. It has been suggested by Okhamafe and York (1986), that the film morphology and molecular features (such as crystallinity and glass transition temperature) can be influenced by the film drying rate. If this was the case, then coating conditions which allow a greater time for film formation and molecular orientation would be expected to produce harder less elastic films. These coating conditions could include; low atomising air pressures, narrow spray cones, spray guns which tend to concentrate the droplets within the centre of the spray, high spray rates or low drying air temperatures and volume flow rates. The results in Table 5.21 indicate that some of these conditions do tend to cause harder/more elastic films eg use of a narrow spray cone and guns with more dense central region of droplets. Others however

have the opposite effect, eg low atomising air pressures. Differences in film morphology and molecular features alone are therefore not thought likely to explain the elastic/hardness properties of applied films.

The formation of aqueous film coats on tablets is a gradual process which may take several hours to complete. The film is made up from a series of droplets which impinge initially on the uncoated substrate and subsequently on a partly produced film coat. In order for the film hardness to approach a maximum, it is considered that the film should be continuous with no entrapment of air, as occurs when films are cast from solutions. This is only likely to occur when there is no significant spray drying and when each droplet hitting the surface is able to flow and spread sufficiently to exclude air from within the film. In the practical situation the above criteria are unlikely to exist during the aqueous film coating process, since evaporation may occur from the droplets during their passage to the substrate and the formulation and coating conditions may be such that droplet spreading is restricted. Film coats applied using organic solvent systems are thought more likely to have higher hardness values, since they utilise considerably higher spray rates (typically around 5 times higher) and lower solution viscosities. This may explain why Rowe (1976b) found little difference in indentation behaviour between films cast onto glass substrates and those coated onto flat faced tablets when using organic coating solutions.

<u>The effect of process conditions on micro-indentation behaviour</u>

Results in section 5.4 indicate that the application conditions influence the thickness and density of the film and the spreading behaviour of droplets at the substrate/film surface. Conditions which were found to increase droplet spreading and film density (higher

atomising air pressure, areas of greater droplet density within the spray, low solution viscosity, reduced gun-to-bed distances and in some instances increased spray rate) and thus reduce the amount of entrapped air, were those which were found to produce the harder less elastic films. This would explain why there was a significant correlation between the film arithmetic surface roughness and both the film Brinell hardness and modulus of elasticity (Figure 5.8). The increased internal stress of these films (see section 5.11.6) may also have contributed to the higher hardness values.

The results of this work illustrate the dangers of using data from free films to predict the properties of films sprayed onto tablets, especially those using aqueous systems, since when producing the free films it is extremely difficult to adequately reproduce those conditions experienced within a film coating pan. The results also illustrate that care should be taken when investigating the effect of formulation variables on film properties using indentation testing. If changes in the formulation also affect solution viscosity or the atomisation process, the results may be a reflection of process changes rather than those of the formulation variable intended.

It has been postulated by Rowe (1986a), that in the absence of other changes, if the film modulus of elasticity is decreased, then the incidence of edge splitting and bridging of the intagliations should be reduced. Unfortunately with the aqueous film coating process, one factor can never be changed in isolation. Conditions which influence the modulus of elasticity may also influence droplet spreading, penetration and adhesion, coat roughness, film strength and coat thickness and density. The hardess and elasticity values are therefore likely to be just two of several factors contributing to the nature of film defects.

5.11.5 THE MECHANICAL STRENGTH OF AQUEOUS FILM COATED TABLETS

One of the reasons why tablets may be film coated is to increase their overall tablet strength and thus their resistance to attrition and mechanical damage. Knowledge of how various coating process factors influence the mechanical properties may not only aid in the selection of appropriate process conditions, but also give an insight into the behaviour of droplets at the substrate surface and thus aid in understanding how the film is formed. Results of diametral compression tests carried out on three different tablet types, each coated using a variety of application conditions, are presented in section 5.3. For the tablets tested in this study, it was found that the initial peak in the compression traces was always at a point corresponding to the highest applied force. This indicates that the tablet and the coat were failing at the same time and that the film did not have enough intrinsic strength and elasticity to hold the core together once the core had broken. Similar behaviour was reported by Fell et al. (1979) for tablets coated with organic solutions of HPMC E3 (Pharmacoat 603) and HPMC E6 (Pharmacoat 606), providing in the latter case the films were not thicker than 35μm. Fell et al. (1979) however found that with higher molecular weight grades of HPMC, additional peaks which were greater than the intial peak were seen in the compression profile. This was attributed to the ability of the coat to remain intact after the core had ruptured. Stanley et al. (1981) pointed out that the substrate and coat tended to fail together when there was a high substrate/coating adhesion and/or a thin coat (17μm in the case when Pharmacoat 606 was applied). No explanation was offered as to how the high adhesion caused this effect, but it was suggested that if the film was too thin, then it was unlikely to provide an envelope of sufficient strength to carry the load once substrate fracture had occurred. The average coat

thickness values in this study were found to be around 25µm to 50µm, depending upon the application conditions, substrate properties and the position on the tablet surface (Table 5.14). Although no adhesion values were determined, it is thought likely that they would have been relatively high, due to the presence of microcrystalline cellulose, pregelatinised starch and stearic acid in the tablet core, these all having hydroxyl groups for interaction with those of the HPMC molecule (see Rowe, 1977). This was borne out by the extreme difficulty in removing the film from the tablet without removing part of the tablet in addition. The extent of the adhesion between the coat and substrate was thought to have been sufficient for them to act as a single unit during diametral compression, with the coat failing at the same time as the substrate. It should be noted that when higher molecular weight polymers are applied, the coat may remain intact after the core has failed and therefore the film strength may be dependent on the thinnest area of the film. This in turn has been shown to be markedly affected by the substrate properties and coat application conditions (see section 5.9.3).

<u>The effect of process conditions on coated tablet mechanical strength</u>

The results in section 5.3 demonstrate that the application of an aqueous film coat can either result in an increase or a decrease in the tablet mechanical strength, depending on the initial tablet properties and the application conditions. Reports in the literature have generally demonstrated that the application of a film coat causes a significant increase in mechanical strength, eg Stern (1976), Rowe (1976a) and Fell et al. (1979) for organic solutions and Porter (1980) for aqueous solutions. In this latter study it was also pointed out that the actual rotation of the cores in the coating drum during the coating process could reduce the core strength. This may therefore have

been a factor contributing to the reduced mechanical strength values reported in Table 5.12. Porter (1980) reported that the application of HPMC E5 solutions at a concentration of 10%w/w to placebo tablets of unspecified composition, resulted in an increase in diametral crushing force from approximately 90N to approximately 350N. The large differences between the results of Porter (1980) and those in Table 5.12 may have been due to differences in placebo tablet formulation, application conditions or the coat level applied (Porter (1980) applied a 2.75%w/w coat compared to a 2.25% coat in this study). It is difficult however to ascertain the relative effect of these since Porter (1980) did not give the constituents of the placebo tablets and used a modifed sugar coating pan. The results do however demonstrate the potential for the application of the same coating solution to have considerably different effects on mechanical strength depending on process conditions used.

When a tablet is subjected to diametral compression, failure will occur due to the tensile stresses set up within the film. Failure will commence at a suitably orientated flaw, which could be in the body of the tablet or at its surface. Fell et al. (1979) reported that the application of a film coating may influence a tablet strength in three ways:

1. The coat may act as an envelope which has enough intrinsic strength to resist breakage even after the core itself has broken.

2. The coat may act as a padding material and increase the breaking load by changing the stress distributions within the tablet.

3. The film may fill in irregularities in the core surface reducing the possibility of fracture commencing at surface flaws.

The preceding discussion has indicated that the first of these is unlikely to have occurred in this work, since the coat and substrate

were shown to fail together. The production of a more elastic film by for example either using lower atomising air pressures, applying higher viscosity solutions or using the Spraying Systems 60° spray gun, did not necessarily increase the crushing strength (see section 5.6). This indicates that padding effects alone were not responsible for the effects seen. The ability of the film to fill in the surface irregularities in the core, will be enhanced by those factors promoting droplet spreading at the tablet surface. Thus it might have been expected that increasing the atomising air pressure would have increased the crushing strength, as would the use of spray guns producing smoother surfaces and the application of lower viscosity solutions. Examination of data in Table 5.12 however indicates that increased spreading does not necessarily increase the tablet strength, with increases in atomising air pressure being shown to consistently reduce the crushing strength and increases in viscosity in some instances increasing the crushing strength. It would therefore appear that the application conditions may affect the tablet strength by some other mechanisms than those reported by Fell et al. (1979). These mechanisms may include differences in the degree of penetration of the coating solution into the substrate surface (and thus the disruption of particulate bonding) and differences in film internal stress.

Results in Table 5.12 indicated that when coating the 10mm convex tablets, there was an optimum coating solution viscosity for achieving tablets of maximum strength. With low viscosity coating solutions (46mPa s) the coated tablet strength is likely to have been enhanced by the filling in of irregularities in the core surface and high film substrate adhesion values. Disruption of core particulate bonds arising from greater penetration, higher internal film stress (as evidenced by greater tendency for edge splitting) and the increased stresses arising

from extended process times are however likely to have acted to reduce the coated tablet strength. With medium viscosity solutions (166mPa s to 359mPa s), the reduced disruption of core particulate bonds and the decrease in film and tablet internal stresses appear to more than compensate for any reduction in adhesion or filling in of core surface irregularities. With further increases in viscosity (to over 520mPa s), the reduction in surface irregularity filling and film adhesion appear to be greater than any further increase in strength arising from the decrease in both bond disruption and film/tablet internal stress, and thus the tablet strength begins to fall. The effect of solution viscosity was much less clear on the 10mm and 15mm flat tablets. This was thought to be due to the decreased core porosity, increased core initial strength and reduction in the extent of surface irregularities. These factors, coupled with the higher tablet stresses generated during coating due to the increased tablet weight and/or tablet shape are also thought to explain why the increase in mechanical strength after coating was much smaller than with the 10mm convex tablets.

The potential effect of solution viscosity should be borne in mind when examining the effect of formulation variables on the tablet strength. For example, Porter (1980) when investigating the role of plasticisers and pigments on tablet strength did so by replacing the polymer in the coating solution (HPMC E5) with the additive being investigated. Thus the addition of 40%w/w plasticiser (based on dry film weight) meant that the polymer concentration was reduced from 10%w/w to 6%w/w and thus the coating solution viscosity significantly reduced. Part of the effect attributed to the inclusion of plasticisers and pigments may therefore have arisen from the reduction in solution viscosity.

In all cases studied, when the atomising air pressure was reduced the film mechanical strength was increased. A reduction in atomising air

pressure will decrease droplet spreading (as evidenced by increased surface roughness) and therefore the film will be less likely to fill in surface irregularities. However reduced spreading will also lead to a reduction in the evaporation rate from the droplets and this coupled with the larger average droplet sizes, may serve to increase the penetration into the tablet surface and improve film adhesion. The decrease in film internal stress and increase in film elasticity which accompanies the use of a decreased air pressure may also contribute to the increased coated tablet strength. It would seem that in the cases in Table 5.13, the effect of increased film adhesion, increased film elasticity and decreased film internal stress had a greater effect than the reduction in surface irregularity infilling. Reducing the atomising air pressure may not necessarily however be beneficial in increasing tablet strength in all cases. For example with low viscosity solutions, the increased penetration and bond disruption may be sufficient to cause an overall reduction in coated tablet strength.

5.11.6 THE EFFECT OF PROCESS CONDITIONS ON THE INCIDENCE OF FILM COAT DEFECTS

Tablet sticking and film picking

Tablet sticking will occur when the cohesive and adhesive forces acting at the tablet-tablet interface are greater than the forces tending to separate the tablets, ie forces arising from the tumbling action in the coating pan. The related defect of film picking arises when tablets that have become stuck together break apart on subsequent tumbling and film fragments from one tablet are removed and stuck to another. The incidence of tablet sticking and film picking and their dependence on the coating process conditions is illustrated in section 5.2. Tablet sticking is obviously unacceptable, but can be easily detected and the

tablets rejected. A small degree of picking may be acceptable if the coat is applied for taste masking or reducing dust during packaging etc. However since film picking will cause an area of reduced coat thickness on one tablet and increased thickness on another, enteric or sustained released coats may be compromised.

Due to their surface curvature, the 10mm convex tablets can only have a relatively small area of surface in contact with another tablet at any particular time. Under normal coating conditions, and in all those coating runs carried out in this study, the cohesive and adhesive forces acting over this small area are not sufficient to resist the forces tending to separate the tablets and thus sticking does not occur. The flat tablets however have the potential for the cohesive and adhesive forces to act across the whole of the tablet face and therefore have a greater likelihood of exhibiting sticking, as demonstrated in Appendix 2. Examination of the tables in Appendix 2 shows that sticking is greater with the 15mm flat tablets than with the 10mm flat tablets. This could be due to the greater contact area with the 15mm flat tablets, although sticking would be opposed by their greater weight. Calculation of the single face surface area to weight ratio for the two flat tablet types (data from section 5.2.1) showed them to be identical at $0.27 mm^2 mg^{-1}$. The heavier 15mm tablets will tend to fall through the spray zone at a greater velocity and will therefore be exposed both to the spray and drying air for a shorter period of time before they enter the tablet bulk in the coating pan. As a consequence, less droplets may impinge on the 15mm flat tablets during a single passage through the spray and then may not dry sufficiently before they enter the tablet bulk, where the forces acting to separate the tablets are much less. It is thought that it is this increased failure to adequately dry which is mainly responsible for the greater incidence of sticking seen with the

15mm flat tablets. Studies by Chopra and Tawashi (1982) on the tack behaviour of coating solutions indicated that resistance to splitting increases with an increased rate of separation. This may be a further factor contributing to the greater sticking which occurs with the 15mm flat tablets, since the rate of separation would be higher due to the greater tablet weight.

The increased tendency for flat tablets to stick together is the main reason they are not often coated practically. However the results in section 5.2 indicate that if coating conditions are chosen carefully flat tablets may be coated successfully.

Film picking will occur when the cohesive forces between the droplets/film and/or film/film of two tablets in contact with each other are greater than the adhesive/cohesive forces between the film layers or between the film/substrate. This defect was found to occur on all the test tablet types and as with sticking, the extent of the defect was dependent upon the coating process conditions. Conditions which reduced sticking also reduced picking. The three spray guns which produced the greatest incidence of sticking and picking were those which produced sprays with either areas of greater droplet density in the centre of the spray (Walther Pilot and Binks Bullows guns) or a reduced spray coverage area (Spraying Systems 45° gun). Use of these guns would have led to tablets passing through certain areas of the spray being hit by a relatively larger number of droplets. In these areas there would be an increase in the surface area and time over which the cohesive and adhesive forces betweeen partially dried droplets and the film/core could act. The increase in drying time will lead to a greater likelihood of the tablets entering the tablet bulk within the coater in a wetter state. Once in the tablet bulk, the increased proximity of the tablets and the reduction in forces tending to separate the tablets,

coupled with the greater area over which the adhesive and cohesive forces can act will increase the tendency for picking and sticking. In the case of the Binks Bullows gun, the larger mean atomised droplet size produced and the presence of some very large droplets may have exacerbated the situation. A similar argument to that described above can be used to explain the increased sticking and picking which occurred with increasing spray rates, changing from a flat spray to a narrow cone shape and when the Spraying Systems gun with the type 120 air cap was used (coating run 75). In the former case the effect is likely to have been potentiated by the accompanying reduction in tablet bed temperature and corresponding increase in drying time.

Increasing the spray gun to tablet bed distance was found to increase the overall spray dimensions of sprays produced by the Spraying Systems 60° gun, and to produce a more evenly distributed spray with a less dense central region when using the Schlick gun. These factors coupled with the increased potential for evaporation from the droplets before hitting the tablet surface and the reduction in spreading, would explain the reduced sticking and picking seen when the gun-to-bed distance was increased.

The effects of atomising air pressure and droplet viscosity on the incidence of sticking and picking are more complex. Decreasing the atomising air pressure and increasing the solution viscosity will both cause larger droplets to be formed and decrease the tendency of the droplets to spread on the tablet surface. The production of larger droplets is likely to increase the potential for picking and sticking due to both an increase in drying time and a greater area over which the adhesive and cohesive forces can act. A decreased spreading could either reduce picking and sticking by virtue of the decrease in droplet surface area on the tablet, or increase it by decreasing the drying

rate. Since increasing the solution viscosity from 46mPa s to 520mPa s had little influence on the incidence of picking and sticking, it is thought that the main effect of the reduction in spreading was to reduce the cohesive and adhesive forces between the tablets and that this effect was roughly cancelled by the increase in droplet size. Evidence from the SEMs in section 5.9 and surface roughness data in section 5.4, suggests that the spreading of droplets produced from the 520mPa s HPMC E5 solution is small. There is therefore little potential for further decreases in cohesive and adhesive forces due to further reduced spreading when the solution viscosity is increased above 520mPa s. The droplet size will however increase with increasing solution viscosity above 520mPa s. This would explain why there was a greater extent of picking and sticking when the 840mPa s HPMC E5 solution was applied (run 71). It might also account for the results reported by Nagai et al. (1989), which suggested that the maximum spray rate which could be used before picking occurred decreased with increasing solution viscosity.

As the atomising air pressure decreased there was a greater tendency for picking and sticking to occur. In this case it is thought that the larger droplets and the reduced evaporation rate had a greater effect than the reduction in cohesive and adhesive forces arising from reduced droplet spreading.

The presence of titanium dioxide and an aluminium lake in the Opadry formulations reduced the extent to which picking and sticking occurred. This is thought to have arisen from a reduction in the cohesive forces between droplets on the tablet surface. This is supported by data reported by Chopra and Tawashi (1985) which showed both titanium dioxide and FD&C Blue No.2 aluminium lake to reduce tack values (after their effect on viscosity had been taken into account).

Film edge splitting and bridging

Edge splitting/peeling and intagliation/score bridging are two defects which may result in the rejection of a batch of film coated tablets. Bridging, where the film pulls out from an intagliation or score mark, although not necessarily influencing the pharmacological properties of the dosage form may be aesthetically unacceptable, since the identifying monogram may be obscured. Edge splitting and peeling, where the film cracks or splits at the edges and subsequently peels back, as well as being unsightly, may also cause dose dumping if it occurs on controlled release or enteric coated tablets.

The two film defects described above are thought to arise from the build up of stresses within the film, both due to film shrinkage on evaporation of the solvent and to differences in thermal expansion of the coating and the tablet substrate (Rowe, 1986a). As the solvent evaporates, the polymer concentration increases until a gel of the solvent in an open polymer network is formed. This gel contracts with further solvent loss until a viscoelastic film is produced. As the film solidifies only the thickness of the film can contract, movement in the other dimensions being constrained by the adhesion of the film to the substrate, thus producing an internal stress within the film. If the coefficients of thermal expansion of the tablet and film are markedly different then further stresses may be built up as the tablets heat and cool during the coating cycle. Since the stresses are built up in the plane of the coating, failure will occur at the film/tablet interface (bridging) or within the film itself (edge splitting/cracking).

The theoretical aspects of the stress build up and the effect of tablet and coating formulations on the defects of bridging and edge splitting have been extensively covered by Rowe and Forse (1980 and 1981) and Rowe (1981b, 1982a, 1982b, 1982d, 1983b, 1983d, 1984c and 1986a). Data

available indicating the effect of process conditions is however limited to studies by Rowe and Forse (1982) and Kim et al. (1986). In the former study it was shown that decreases in spray rate and increases in inlet air temperature could increase the incidence of edge splitting and reduce bridging. In the latter study the authors also reported that the incidence of bridging could be reduced by decreasing the spray rate.

The data generated in this thesis indicates that the incidence of edge splitting as well as being dependent on coat and core formulations could also be markedly affected by the process conditions. No bridging of the score mark was however seen on any of the 10mm convex tablets coated. This latter finding suggests that the inherent adhesion between the coat and substrate was high. This is supported by data generated by Rowe (1977), which indicated that both microcrystalline cellulose and stearic acid (two components of the direct compression placebo test tablets used in this work) tended to produce high adhesion values due to the presence of hydroxyl groups which formed hydrogen bonds with corresponding groups of the HPMC. It would be expected that the presence of pregelatinised starch in the formulation would have similarly acted to enhance film adhesion. The relatively rough, porous surfaces would also have been expected to aid adhesion properties, due to the tendency to allow an increased rate and depth of polymer solution penetration (Fisher and Rowe, 1976).

Rowe (1986a) suggested that film cracking will occur when the tensile strength of the film (σ) is less than the total internal film stress (P), where P is made up of the internal stress due to shrinkage (P_s) and that due to thermal expansion effects (P_T). This is represented by Equation 5.1.

$$\frac{\sigma}{E} < \frac{1}{3(1-\upsilon)} \left[\frac{\phi_s - \phi_R}{1 - \phi_R} + \Delta\alpha\Delta T \right] \qquad \text{Equation 5.1}$$

where E is the Young's modulus of the film coating, υ is the Poisson's ratio of the film coating, ϕ_s is the volume fraction of the solvent in the film at its solidification point (i.e. when the coating solution first behaves as a solid rather than a viscous liquid), ϕ_R is the volume fraction of the solvent remaining in the dry film at ambient conditions, $\Delta\alpha$ is the difference between the cubical thermal expansion coefficient of the tablet substrate and the film coating and ΔT is the difference between the glass transition temperature of the film coating and the equilibrium coating temperature.

For process conditions using the same polymer, solvent, spray rate, inlet air temperature and inlet air volume flow rate, the variables on the right hand side of the above equation are likely to remain unchanged. Thus when investigating changes in atomising air pressure, spray gun type, spray shape and solution viscosity, any changes in the extent of edge splitting would be expected to arise from changes in the ratio σ/E, edge splitting occurring if the ratio dropped below a certain value.

In this work edge splitting was found to occur to a greater extent when the atomising air pressure was increased, the solution viscosity was decreased and spray shapes producing a greater concentration of droplets in the centre of the spray were used. These were the same conditions which were shown to cause a decrease in surface roughness and film thickness and an increase in film hardness/instantaneous elastic modulus. The effect of these process variables on the film tensile strength could not be determined from the tablet diametral crushing strength studies, since other factors such as film adhesion, surface irregularity infilling and tablet bond disruption complicate the situation. It would appear however from the edge splitting data that the relative effect in increasing the elastic modulus was greater than

any effect in increasing film strength and thus the increase in edge splitting occurred.

In each case where edge splitting was prevalent, the films had low surface roughness values indicating that the droplets had spread well on the surface. Work on receding contact angles on solids of various roughness carried out by Zografi and Johnson (1984), suggested that after the initial droplet spreading has occurred, the droplet base in contact with a tablet surface does not recede on the evaporation of solvent but remains stationary, so that the contact angle gradually approaches zero. The SEMs and surface roughness values indicate that a similar effect is likely to have occurred during these coating studies. Droplets which had spread to a greater extent would therefore cover a larger surface area as the solvent evaporates. This would in turn produce a greater internal stress as the film resists the tendency to shrink with solvent loss. The film is in effect being "stretched" to a greater extent on the tablet surface. Factors which increase the tendency for droplets to coalesce may also increase internal stress since each evaporating unit on the tablet surface is larger. Similarly any spreading arising from tablet mutual rubbing effects on the surface would be expected to increase film internal stress and thus potentiate edge splitting.

The lack of edge splitting accompanying the application of a 12%w/w HPMC E5 solution is likely to have arisen from the lack of droplet spreading and coalescence (the droplets tending to act more as individual units on the tablet surface) and the reduced film elastic modulus. If edge splitting is a problem on a particular substrate, increasing the solution viscosity may be a simple method of overcoming the problem.

Increasing the spray rate was shown to decrease the incidence of edge splitting (Table 5.9) despite in some instances the surface roughness

being decreased. This finding is similar to that of Rowe and Forse (1982). The accompanying reduction in tablet bed temperature may have served to reduce the internal stress by reducing the evaporation rate and film temperature (see Equation 5.1).

The application of 15%w/w Opadry suspensions was found to give rise to a greater incidence of edge splitting than when 9%w/w HPMC E5 solutions were applied, despite the higher viscosity of Opadry suspensions. This is likely to have been due to the inclusion of titanium dioxide and aluminium lakes in the Opadry formulation, these decreasing the σ/E ratio (Rowe, 1986a).

Droplet spray drying

The occurrence of droplet spray drying during the aqueous film coating process may cause infilling of a tablet intagliation or score mark. Although unlikely to lead to the rejection of the coated tablet batch, this may be detrimental to the tablet appearance. The occurrence of spray drying may also result in an inefficient coating process, since spray dried material may either not adhere to the tablet surface or may be easily abraded off during tablet tumbling in the coating pan. Incorporation of air within the film due to the presence of spray dried droplets may also influence the mechanical properties of the film as previously discussed.

The results in Chapter 4 indicated that evaporation from droplets during travel to the tablet bed was unlikely to occur at the centre of the spray, due to their greater speed, shorter distance of travel and the local high relative humidity. Data on the incidence of spray dried material in the score mark of the 10mm convex tablets (section 5.2) supports this, since little or no spray drying was apparent when the majority of the droplets were concentrated in the centre of the spray ie when the Binks Bullows and Walther Pilot guns were used or the Schlick

gun when used to produce a narrow cone spray shape. A small amount of spray drying generally occurred when the Schlick gun was used to produce a typical flat spray shape or the Spraying Systems 45° gun was used. In the former case this is thought to be due to the relatively greater number of droplets towards the spray periphery. These move at a slower speed, have further to travel before hitting the tablet bed and are probably exposed to air which is not saturated with water vapour. In the latter case, although the spray dimensions are relatively small, the droplets are thought to be travelling at a relatively slow speed compared to the other guns, allowing an increased time for evaporation to occur. The significantly greater extent of spray drying which accompanied the use of the Spraying Systems 60° gun was likely to have arisen from the greater spray dimensions and more even distribution of droplets throughout the spray, and the relatively small size and low velocity of the droplets produced.

The lack of any significant effect of atomising air pressure on the extent of droplet spray drying, indicates that any increased spray drying which might accompany the production of smaller droplets on increasing the air pressure, is compensated for by the reduction in evaporation due to the increased droplet velocity.

The factor which had the greatest effect on increasing the extent of spray drying was the increasing of the distance of the spray gun from the tablet surface. This occurred due to the greater proportion of droplets towards the spray periphery, the reduced average droplet velocity and the greater distance of droplet travel, all of which led to a greater average time before the droplets hit the surface and thus an increase in the time for evaporation to occur.

The reduction in spray drying which accompanied an increase in the spray rate was likely to have been due to the increased average droplet size

and increased concentration of droplets within the spray. The latter factor would have increased the local relative humidity and therefore reduced the driving force for evaporation.

5.11.7 THE PRODUCTION OF TABLETS WITH HIGHLIGHTED INTAGLIATIONS

Rowe (1983a) and Rowe and Forse (1983a) reported that optically anisotropic materials (those which possess more than one refractive index (RI)) eg talc, calcium carbonate and magnesium carbonate, could be used to produce coated tablets with highlighted intagliations. On the main body of the tablet these three materials were said to orientate themselves equivalent to their state of lowest RI and since in each case this RI was very similar to the RI of HPMC, then the film appeared essentially transparent. Within the intagliation however they were said to be randomly orientated or orientated equivalent to their state of highest RI, resulting in the formation of a white opaque film. Examination of commercially produced coated tablets with highlighted intagliations (Tenormin, Stuart Pharmaceuticals) using a microscope, indicated however that within the intagliation, rather than the presence of a white opaque film, there appeared to be spray dried particles/agglomerates of various sizes. This suggests that the production of tablets with highlighted intagliations may be dependent upon the film coat application conditions. In order to test this theory, scored 10mm convex tablets which had previously been coated with a green Opadry formulation (coating run 67) were further coated with a formulation including calcium carbonate (coating runs 72 and 73, see Appendix 1). Coating run 72 was carried out using conditions which were known to produce minimal spray drying, whilst coating run 73 used application conditions which would produce a significant amount of spray drying. Examination of tablets at the end of these coating runs

revealed that with run 72 there was no evidence of a highlighted score mark or spray drying, the tablets essentially appearing the same as at the start of the coating run. Tablets from run 73 however did possess some highlighting of the score mark, which on examination under the microscope appeared to be due to the presence of spray dried material. The film on the body of these tablets also had a degree of opacity. These observations indicate that the production of highlighted intagliations may indeed be dependent upon the application conditions and that if certain application conditions are used there may be no highlighting at all. This may explain why Rowe (1983a) could not produce tablets with highlighted intagliations by applying a coating solution to single tablets attached to the inside of a coating drum. In this latter case the tablet was likely to have been exposed only to the centre of the spray, which results from this thesis have shown are less likely to contain any significant amounts of spray dried droplets. The formation of highlighted intagliations when calcium carbonate, magnesium carbonate or talc are used in the coating formulation is therefore thought to be due to the random orientation of these materials in spray dried material within the intagliation, rather than random orientation within the film in the intagliation. On the tablet body highlighting is probably not generally apparent since the spray dried material will be removed by tablet-tablet contact.

CHAPTER 6

SUMMARY OF THE ATOMISATION AND FILM FORMATION PROCESSES

6.1 THE FILM COATING PROCESS

The first stage of the aqueous film coating process is the preparation of the coating solution or suspension, the components of which will determine its physical properties. Only the solution rheological properties are likely to vary to any great extent between different coating formulations based on HPMC. Providing the components are accurately weighed, the coating formulation properties should be the same irrespective of the preparation method used. There is however the potential for the rheological properties to vary when different batches of raw materials are used, especially the coating polymer HPMC. Similarly, incorrect storage may give rise to differences in rheological behaviour. As the coating formulation is fed to the spray gun, it may be heated up as it passes through the feed tubing in the coating pan. The extent to which this occurs will be dependent on the tubing material, tubing length, spray rate and inlet drying air temperature and volume flow rate. On entering the spray gun, the liquid may be cooled down by the high velocity atomising air in the chamber surrounding the liquid nozzle. Pseudoplastic formulations may undergo changes in viscosity as they pass through the liquid nozzle, the extent of which will depend on the shear rates encountered. On leaving the liquid nozzle, the coating formulation is immediately surrounded by high velocity atomising air. This accelerates the liquid stream above a speed at which it is stable and supplies energy to overcome the viscous and surface tension forces, thereby producing droplets. Pseudoplastic formulations may undergo further changes in viscosity at this atomisation stage due to the shear forces exerted by the atomising air. The droplet size distribution produced will depend on the viscosity and

surface tension of the formulation, atomising air pressure, spray rate and the spray gun used. In the latter case it is the design of the spray gun air cap which is most important since this determines the velocity of the air as it exits the annulus around the liquid nozzle. The air cap design will also determine the spray shape and the mass flow rate of the atomising air which accompanies the droplets to the tablet surface. The latter factor is important in governing the droplet velocity. On leaving the spray gun, the droplets rapidly decelerate but still travel at a velocity which is considerably faster than the accompanying drying air. The droplet velocity will vary at different points within the spray. There may be insufficient HPMC molecules within the small atomised droplets to reduce the surface tension to that of the bulk solution and there may insufficient time for those molecules that are present in the droplet to reach the droplet surface before the droplet contacts the substrate. Droplets of different surface tension may therefore result. During passage to the tablet bed, a certain amount of water will evaporate from the droplets. This is most likely to be significant towards the spray periphery where the density of droplets is less, the droplet velocity is lower and the time taken to reach the surface is greater. Any evaporation that does occur will increase the droplet viscosity. At the centre of the spray, droplet coalescence may occur, the extent of which will depend on the spray shape, spray gun used and spray rate. Droplets hitting the tablet surface will therefore exist in a wide range of sizes which are travelling at different velocities and may have different surface tension and viscosity values.

The formation of a film coat on a pharmaceutical dosage form by the application of an atomised coating formulation is a gradual and intermittant process. As the substrate passes the spray zone, it will

be hit by coating formulation droplets possessing different properties, as described above. The number of droplets hitting the substrate during one pass through the spray will depend on the substrate velocity through the spray zone, the position of the substrate in relation to the spray gun and the spray shape and droplet distribution throughout the spray. The way in which the film is formed and the film properties will depend on the behaviour of the droplets on hitting the substrate surface. In order to form a continuous, smooth film of maximum density and hardness, each droplet hitting the substrate surface should wet, spread, adhere and interact with the substrate or underlying film in such a way that the droplet layers coalesce completely to form a continuous film with no entrapped air. Due to the differences in droplet properties described above, this is unlikely to occur practically. The extent to which droplets spread on a substrate surface may depend on the substrate properties and the droplet physical properties and kinetic energy. With droplets of low viscosity, the droplet kinetic energy is generally sufficient to force the droplet to spread on the surface. With high viscosity droplets the extent of spreading due to the droplet kinetic energy is considerably reduced and the spreading behaviour will become dependent upon the droplet surface tension, interactions with the substrate and the drying time. Droplets may dry on the substrate either as separate entities or as part of a collection of coalesced droplets. The extent to which droplet coalescence occurs will depend primarily on the distribution of droplets within the spray, the position the tablet passes through the spray and the droplet viscosity. Droplets are less likely to coalesce as their viscosity increases. On the uncoated substrate, droplets may penetrate into the surface this being governed by the properties of the substrate (porosity and surface composition), the viscosity of the droplets and the drying rate. The extent of

penetration may be important in determining the degree of film adhesion and coated tablet mechanical strength. As soon as the droplets hit the substrate, water will start to be evaporated and the droplet concentration and viscosity will increase until a gel of the water in an open polymer network is formed. This gel then contracts with further water loss until a viscoelastic film is produced. The extent of interaction and adhesion with the underlying film layers will be dependent on the degree of spreading, the droplet viscosity and the drying rate. As the water is evaporated and the polymer gel contracts to form a viscoelastic film, stresses are built up within the film. These are dependent on the the extent of spreading on the tablet surface, the speed of drying and the components of the formulation. If these internal stresses are sufficiently high, film edge splitting or intagliation bridging may occur.

6.2 SUMMARY OF THE ROLE OF SOME COATING PROCESS VARIABLES

Changing any individual coating process parameter will generally have multiple effects on the coating process. Some of these effects may be beneficial for certain aspects of the process or product properties, whilst others may be detrimental.

The following paragraphs summarise the effect on the coating process of changes in various coating process parameters, based on the data generated in this study. It should be borne in mind that the relative effect of any one variable may depend on the other coating conditions used.

Coating solutiuon viscosity

Increasing the viscosity of the coating formulation will lead to the formation of larger droplets and an increased likelihood of problems with spray gun nozzle blockage. On impingement on the substrate, the

more viscous droplets will exhibit a reduced tendency to spread and coalesce. They will penetrate less well into the substrate surface which may lead to problems associated with coat adhesion. The surfaces produced by more viscous droplets will be rougher and more matt in appearance and the films less dense with a greater degree of air entrapment. The films will also tend to have a lower elastic modulus and Brinell hardness. The effect on coated tablet mechanical strength will depend on the degree of penetration into the tablet surface and therefore the relative effects of changes in adhesion and in the disruption of bonds within the tablet surface. Using coating formulations of increased viscosity will tend to reduce the internal stresses generated within the film during its formation and therefore reduce the tendency for edge splitting to occur. There is unlikely to be any significant effect on the incidence of picking and spray drying with changes in formulation viscosity.

Atomising air pressure

If the atomising air pressure is insufficient, spray gun nozzle blockage may occur, especially with more viscous solutions. Increasing the atomising air pressure will decrease the mean atomised droplet size and the droplets formed will travel to the substrate surface with a greater velocity. These droplets will therefore tend to spread to a greater extent, causing a reduction in surface roughness and a more glossy appearance. The enhanced spreading will also increase the drying rate of the droplets on the surface and therefore decrease the incidence of film picking. Film density and hardness are likely to increase with increasing atomising air pressure due to a reduction in air entrapped within the film. Coated tablet mechanical strength may be reduced. The enhanced spreading caused by increasing the atomising air pressure may lead to an increased film internal stress and therefore a greater

incidence of film edge splitting. The incidence of spray drying is unlikely to be markedly affected by changes in air pressure.

Spray gun design

The design of the spray gun and most importantly the design of the air cap, will affect the droplet size distribution, spray shape and distribution of droplets within the spray, and the kinetic energy of the droplets hitting the tablet surface. Smaller droplets will tend to be produced by sprays guns where the air velocity exiting the annulus is higher. Sprays guns exhibiting higher total atomising air mass flow rates will tend to impart more kinetic energy to the droplets and thus produce effects similar to those described above for increases in atomising air pressure. Spray guns where there are extra holes (angular converging holes and/or containing holes) in the face of the air cap, exhibit higher atomising air mass flow rates and tend to concentrate the droplets within the central region of the spray. This in turn leads to the production of smoother more glossy film coat surfaces. The films also tend to be harder and more dense. Film defects such as picking and edge splitting may be increased, but spray drying is reduced.

The maximum spray rate which can be successfully applied with a particular spray gun is essentially limited by the area of greatest droplet density within the spray. Thus spray guns which produce sprays of reduced dimensions or where there are areas where the droplets are concentrated, will tend to have reduced maximum application rates. In these cases the use of a greater number of guns within the coater, each utilising a reduced spray rate, may give a more even distribution of droplets and allow an increase in the overall total spray rate.

Increasing gun-to-bed distance

Increasing the gun-to-bed distance results in a greater degree of drying from the droplets before they reach the substrate and a reduction in the

areas of high droplet density within the spray. The increased distance also results in a reduction in the kinetic energy of the droplets on reaching the substrate. These factors all lead to the production of softer, rougher films which have a greater tendency to exhibit spray drying. Film picking is however reduced.

Spray rate

Increasing the spray rate will increase the mean atomised droplet size and reduce the incidence of spray drying. There will however be an increased tendency for picking to occur. The effect on film surface roughness appears to depend on the viscosity of the solution applied. The maximum spray rate which can be successfully applied is generally limited by the spray gun used and the temperature and volume flow rate of the drying air.

REFERENCES

Abdul-Razzak, M.H. (1982) M.Phil Thesis, CNAA

Alcorn, G.J., Closs, G.H., Timko, R.J., Rosenburg, H.A., Hall, J. and Shatwell, J. (1988) Drug Dev. and Ind. Pharm., 14, 1699-1711

Alkan, M.H. and Groves, M.J. (1982) Pharm. Tech., 6, 56-67

Allen, D.J., DeMarco, J.D. and Kwan, K.C. (1972) J. Pharm. Sci., 61, 106-109

Anderson, R.J. and Johnson, E. (1983) Department of Energy (USA). Report No.DE83 017039

Annan, A.H., Lindstrom, R.E. and Swarbrick, J. (1974) J. Pharm. Sci., 63, 931-933

Arai, M., Kishi, T. and Hiroyasu, H (1982) ICLASS Proceedings, 11-4

Aulton, M.E. (May 1977) Manuf. Chem. and Aerosol News, 48, 28-36

Aulton, M.E. (1982) Int. J. Pharm. Tech. & Prod. Mfr., 3, 9-16

Aulton, M.E., Abdul-Razzak, M.H. and Hogan, J.E. (1981) Drug. Dev. and Ind. Pharm., 6, 649-668

Aulton, M.E., Abdul-Razzak, M.H. and Hogan, J.E. (1984) Drug. Dev. and Ind. Pharm., 10, 541-561

Aulton, M.E., Houghton, R.J. and Wells, J.I. (1986) Proc. 5th Pharm. Tech. Conf., Solid Dosage Research Unit, Harrowgate, II, 399

Banker, G.S., Gore, A.Y. and Swarbrick, J.J. (1966) J. Pharm. Pharmacol., 18, 457-466

Banker, G., Peck, G., Williams, E., Taylor, D. and Pirakitikulr, P. (1982) Drug Dev. and Ind. Pharm., 8, 41-51

Banks, M. (1981) Ph.D Thesis, CNAA

Barry, B.W. (1974) In: Advances in Pharmaceutical Sciences (vol. 4) Ed: Bean, H.S., Beckett, A.H. and Carless, J.E.. London: Academic Press

Batdorf, J.B. and Francis, P.S. (1963) J. Soc. of Cosmet. Chem., 14, 117-122

Bayvel, L.P. (1985) Atomisation and Spray Technology, 1, 3-20

Bayvel, L.P., Knight, J. and Robertson, G (1987) Part. Charact., 4, 49-53

Bayer, K. and Speiser, P. (1971) A.P.V., 17, 151-158

Bikerman, J.J. (1970) In: Physical Surfaces. Ed: Bikerman, J.J.. London: Academic Press

Bitron, M.D. (1955) Ind. Eng. Chem., 47, 23-28

British Standard 118 (1977). British Standard Institute, London

British Standard 1134 Parts 1 and 2 (1972). British Standard Institute, London

Buckton, G. and Newton, J.M. (1986) Powder Tech., 46, 210-208

Callahan, J.C., Cleary, G.W., Elefant, M., Kaplan, G., Kensler, T. and Nash, R.A. (1982) Drug Dev. and Ind. Pharm., 8, 355-369

Chigier, N. (1982) ICLASS Proceedings, 29-47

Chopra, S.K. and Tawashi, R. (1982) J. Pharm. Sci., 71, 907-913

Chopra, S.K. and Tawashi, R. (1984) J. Pharm. Sci., 73, 477-481

Chopra, S.K. and Tawashi, R. (1985) J. Pharm. Sci., 74, 746-749

Cole, G.C., May, G., Neale, P.J. and Olver, M.C. (1983) Drug Dev. and Ind. Pharm., 9, 909-944

Cole, G.C., Neale, P.J. and Wilde, J.S. (1980) J. Pharm. Pharmacol., 32, 92P

Costa, M.D.L. and Baszkin, A. (1985) J. Pharm. Pharmacol., 37, 455-460

Croll, S.G. (1979) J. Appl. Polm. Sci., 23, 847-858

Davies, M.C. (1985) Ph.D Thesis, University of London

Delporte, J.P. (1980) J. Pharm Belg., 35, 417-426

Down, G.R.B. (1982) J. Pharm. Pharmacol., 34, 281-282

Ebey, G.C. (1987) Pharm. Tech., 11, 40-50

Entwistle, C.A. and Rowe, R.C. (1978) J. Pharm. Pharmacol., 30, 27P

Entwistle, C.A. and Rowe, R.C. (1979) J. Pharm. Pharmacol., 31, 269-272

Fair, J.R. (1974) In: Chemical Engineers' Handbook, 5th Edn, 18.58-18.67. Ed: Perry, R.H. and Chilton, C.H., New York: McGraw-Hill.

Fell, J.T. and Efentakis, E. (1979) Int. J. Pharm., 4, 153-157

Fell, J.T., Rowe, R.C. and Newton, J.M. (1979) J. Pharm. Pharmacol., 31, 69-72

Felton, P.G., Hamidi, A.A. and Aigal, A.K. (1985) ICLASS Proceedings, IVA/4

Filkova, I. and Pavel, C. (1984) Advances In Drying, 3, 181-215

Fisher, D.G. and Rowe, R.C. (1976) J. Pharm. Pharmacol., 28, 886-889

Franz, R.M. and Doonan, G.W. (1983) Pharm. Tech., 7, 54-67

Frazer, R.P. and Eisenklam, E.P. (1956) Trans. Instit. Chem. Eng., 34, 294-307

Gamlen, M.J. (April 1983) Manuf. Chem., 54, 38-41

Garner, F.H. and Henry, V.E. (1953) Fuel, 32, 151-156

Gibson, S.H.M., Rowe, R.C. and White, E.F.T. (1988a) Int. J. Pharm., 47, 205-208

Gibson, S.H.M., Rowe, R.C. and White, E.F.T. (1988b) Int. J. Pharm., 48, 113-117

Gibson, S.H.M., Rowe, R.C. and White, E.F.T. (1989) Int. J. Pharm., 50, 163-173

Gretzinger, J. and Marshall, W.R. (1961) AIChE Journal, 7, 312-318

Hansen, C.M. (1972) J. Paint Technol., 44, 61-66

Harder, S.W., Zuck, D.A. and Wood, J.A. (1970) J. Pharm. Sci., 59, 1787-1792

Harkins, W.D. and Jordan, H.F. (1930) J. Am. Chem. Soc., 52, 1751-1772

Hawes, M.R. (1978) R. P. Shearer Award, Royal Pharmaceutical Society of Great Britain

Henderson, N.L., Meer, P.M. and Kostenbauder, H.B. (1961) J. Pharm. Sci., 50, 788-791

Hirleman, E.D. and Dodge, L.G. (1985) ICLASS Proceedings, IVA/3

Hogan, J.E. (1982) Int. J. Pharm. Tech. & Prod. Mfr., 3, 17-20

Horvath, E., Pataki, K. and Ormos, Z. (1978) Hung. J. Ind. Chem., 6, 225-242

Hukuo, K., Hikichi, Y. and Okado, K. (1976) Proceedings of the 19th Japan Congress on Materials Research, 244-248

Jones, A.R. (1977) Prog. Energy Combust. Sci., 3, 225-234

Kara, M.A.K., Leaver, T.M. and Rowe, R.C. (1982) J. Pharm. Pharmacol., 34, 469-470

Kim, S., Mankad, A. and Sheen, P. (1986) Drug Dev. and Ind. Pharm., 12, 801-809

Kim, K.Y. and Marshall, W.R. (1971) AIChE Journal, 17, 575-584

King, M.J. and Thomas, T.R. (1978) J. Coating Technol., 50, 56-61

Kossen, N.W.F and Heertjes, P.M. (1965) Chem. Eng. Sci., 20, 593-599

Kumar, R. and Prasad, K.S.L. (1971) Ind. Eng. Chem. Des. Develop, 10, 357-365

Lange, H. (1971) In: Non-Ionic Surfactants. Ed: Schick, M. London: Wiley-Interscience

Leaver, T.M., Shannon, H.D. and Rowe, R.C. (1985) J. Pharm. Pharmacol., 37, 17-21

Lee, E.H. and Radok, J.R.M. (1960) J. Appl. Mech., 27, 438-444

Levy, G. and Schwarz, T.W. (1958) Journal Of The American Pharmaceutical Association, 47, 44-46

Liao, W. and Zatz, J.L. (1979) J. Pharm. Sci., 68, 488-494

Lindburg, N.O. and Jönsson, E. (1972) Acta. Pharm. Suecica, 9, 589-594

Masters, K. (1976) In: Spray Drying. Ed: Masters, K., London: George Goodwin.

Masilungan, F.C. and Lordi, N.G. (1984) Int. J. Pharm., 20, 295-305

Matsumoto, S. and Takashima, Y. (1971) J. Chem. Eng. Japan, 4, 257-263

Mayer, P.L. and Chigier, N. (1985) ICLASS Proceedings, IVB(b)/1

Message, S.R. (May 1987), Manuf. Chem., 58, 85-87

Moore, W.R. (1971) In: Cellulose and Cellulose Derivatives.
Ed: Bikales, N.M., London: Wiley-Interscience

Mugele, R.A. and Evans, H.D. (1951) Ind. Eng. Chem., 43, 1317-1324

Nadkarni, P.D., Kildsig, D.A., Kramer, P.A. and Banker, G.S. (1975)
J. Pharm. Sci., 64, 1554-1557

Nagai, T., Sekigawa, F. and Hoshi, N (1989) In: Aqueous Polymeric Coatings
for Pharmaceutical Dosage Forms. Ed: McGinity, J.W., New York: Marcel
Dekker

Naining, W. and Hongjian, Z. (1986) Particulate Science and Technology, 4,
403-408

Neely, W.B. (1963) J. Polymer Sci (Part A), 1, 311-320

Negus, C. and Azzopardi, B.J. (1978) AERE Report No. 9075

Nukiyama, S. and Tanasawa, Y. (1939) Trans. Soc. Mech. Eng. (Japan), 5,
68-75

Nyqvist, H. (1983) Int. J. Pharm. Tech. & Prod. Mfr., 4, 47-48

Okhamafe, A.O. and York, P. (1983) Proc. 3rd A.G.P.I. Int. Conf. on Pharm.
Tech., Paris, V , 136-144

Okhamafe, A.O. and York, P. (1984a) Int. J. Pharm., 22, 265-272

Okhamafe, A.O. and York, P. (1984b) Int. J. Pharm., 22, 273-281

Okhamafe, A.O. and York, P. (1985) J. Pharm. Pharmacol., 37, 385-390

Okhamafe, A.O. and York, P. (1986) J. Pharm. Pharmacol., 38, 414-419

Parker, J.W., Peck, G.E. and Banker, G.S. (1974) J. Pharm. Sci., 63,
119-125

Patton, T.C. (1979) In: Paint Flow and Pigment Dispersion 2nd Edn.
Ed: Patton, T.C. New York: John Wiley & Sons

Philippoff, P. (1936) Cellulose Chem., 17, 57-77

Pickard, J.F. and Rees, J.F. (April 1974), Manuf. Chem. and Aerosol News, 45, 19-22

Pickard, J.F. (1979) Ph.D Thesis, CNAA

Pickett, J.M. (1977) In: Bentley's Textbook Of Pharmaceutics. Ed:Rawlins, E.A. London: Bailliere Tindall

Porter, S.C. (1980) Pharm Tech., 4, 67-75

Porter, S.C. (1982) Int. J. Pharm. Tech. & Prod. Mfr., 3, 27-32

Porter, S.C. and Saraceni, K. (1989) Pharm. Tech. Int., 1, 20-28

Prasad, K.S.L. (1982) ICLASS Proceedings, 4-3

Prater, D.H. (1982) Ph.D Thesis, University of Bath

Prillig, E.B. (1969) J. Pharm. Sci., 58, 1245-1249

Relland, T.L., Seitz, J.A., Yeager, J.L. and Brusenback, R.A. (1983) Drug Dev. and Ind. Pharm., 9, 945-958

Relland, T.L. and Eber, A.C. (1986) Drug Dev. and Ind. Pharm., 12, 231-245

Rizkalla, A.A. and Lefebvre, A.H. (1975) Trans. ASME, J. Fluids Eng., 97, 316-320

Rosencranz, R. (1984) Pharm. Tech., 8, 24-36

Rosin, P. and Rammler, E. (1933) J. Inst. Fuel., 7, 29-36

Rowe, R.C. (1974) J. Pharm. Pharmacol., 26, 61P

Rowe, R.C. (1976a) Pharm. Acta Helv., 51, 330-334

Rowe, R.C. (1976b) J. Pharm. Pharmacol., 28, 310-311

Rowe, R.C. (1977) J. Pharm. Pharmacol., 29, 723-726

Rowe, R.C. (1978a) J. Pharm. Pharmacol., 30, 343-346

Rowe, R.C. (1978b) J. Pharm. Pharmacol., 30, 669-672

Rowe, R.C. (1979) J. Pharm. Pharmacol., 31, 473-474

Rowe, R.C. (1980a) J. Pharm. Pharmacol., 32, 116-119

Rowe, R.C. (1980b) J. Pharm. Pharmacol., 32, 851

Rowe, R.C. (1981a) J. Pharm. Pharmacol., 33, 1-4

Rowe, R.C. (1981b) J. Pharm. Pharmacol., 33, 423-426

Rowe, R.C. (1981c) J. Pharm. Pharmacol., 33, 610-612

Rowe, R.C. (1982a) Pharm. Acta Helv., 57, 221-225

Rowe, R.C. (1982b) Int. J. Pharm. Tech. & Prod. Mfr., 3, 67-68

Rowe, R.C. (1982c) Int. J. Pharm., 12, 175-179

Rowe, R.C. (1982d) Int. J. Pharm. Tech. & Prod. Mfr, 3, 3-8

Rowe, R.C. (1983a) J. Pharm. Pharmacol., 35, 43-44

Rowe, R.C. (1983b) J. Pharm. Pharmacol., 35, 112-113

Rowe, R.C. (1983c) Pharm. Int., 4, 173-175

Rowe, R.C. (1983d) Acta Pharm. Technol., 29, 205-207

Rowe, R.C. (1984a) J. Pharm. Pharmacol., 36, 569-572

Rowe, R.C. (1984b) In: Materials Used In Pharmaceutical Formulation.
Ed: Florence, A.T., London: Blackwell Scientific Publications

Rowe, R.C. (1984c) Acta Pharm. Technol., 30, 235-238

Rowe, R.C. (1985a) J. Pharm. Pharmacol., 37, 761-765

Rowe, R.C. (1985b) Pharm. Int., 6, 225-230

Rowe, R.C. (1986a) S.T.P. Pharma., 2, 416-421

Rowe, R.C. (1986b) J. Pharm. Pharmacol., 38, 529-530

Rowe, R.C. (1988) Int. J. Pharm., 43, 155-159

Rowe, R.C. and Forse, S.F. (1980) J. Pharm. Pharmacol., 32, 583

Rowe, R.C. and Forse, S.F. (1981) J. Pharm. Pharmacol., 33, 174-175

Rowe, R.C. and Forse, S.F. (1982) Acta Pharm. Tech., 28, 207-210

Rowe, R.C. and Forse, S.F. (1983a) J. Pharm. Pharmacol., 35, 205-207

Rowe, R.C. and Forse, S.F. (1983b) Int. J. Pharm., 17, 347-349

Saarnivaara, K. and Kahela, P. (1985) Drug Devel. and Ind. Pharm., 11, 481-492

Sakai, T., Sadakata, M. and Saito, M. (1985) Atomisation and Spray Technology, 1, 147-164

Sakellariou, P., Rowe, R.C. and White, E.F.T. (1986) Int. J. Pharm., 31, 55-64

Sato, K. (1980) Prog. Org. Coatings, 8, 143-160

Schæfer, T. and Wørts, O. (1977) Arch. Pharm. Chemi. Sci. Ed., 5, 178-193

Schwartz, J.B. and Alvino, T.P. (1976) J. Pharm. Sci., 65, 572-575

Seager, H., Rue, P.J., Burt, I., Ryder, J., Warrack, J.K. and Gamlen, M.J. (1985) Int. J. Pharm. Tech. & Prod, Mfr., 6, 1-20

Simpkin, G.T., Johnson, M.C.R. and Bell, J.H. (1983) Proc. 3rd A.G.P.I. Int. Conf. on Pharm. Tech., Paris, V , 163-169

Skultety, P.F. and Sims, S.M. (1987) Drug Devel. and Ind. Pharm., 13, 2209-2219

Spitael, J. and Kingket, R. (1977) Acta. Pharm. Technol., 23, 267-277

Stafford, J.W. and Lenkeit, D. (1984) Pharm. Ind., 46, 1062-1067

Stamm, A., Gissinger, D. and Boymond, C. (1984) Drug Dev. and Ind. Pharm., 10, 381-408

Stanley, P., Rowe, R.C. and Newton, J.M. (1981) J. Pharm. Pharmacol., 33, 557-560

Swithenbank, J., Beer, J.M., Taylor, D.S., Abbot, D. and McCreath, G.C. (1976) AIAA 14th Aerospace Sciences Meeting, Washington, Paper No. 76-69

Tambour, Y., Greenburg, J.B. and Albagli, D. (1985) ICLASS Proceedings, VIA/2

Trudelle, F., Rowe, R.C. and Witkowski, A.R. (1988) S.T.P. Pharma, 4, 28-30

Tufnell, K.F., May, G. and Meakin, B.J. (1983) Proc. 3rd A.G.P.I. Int. Conf. on Pharm. Tech., Paris, V , 111-118

Wan, L.S.C. and Lee, P.F.S (1974) J. Pharm. Sci., 63, 136-137

Washburn, W.E. (1921) Physiol. Rev., 17, 273

Weiner, B.B. (1982) In: Particle Sizing. Ed: Chigier, N., New York: Wiley

Weiss, M.A. and Worsham, C.H. (1959) ARS Journal, 29, 252-259

Weast, R.C. (1988) In: Handbook of Chemistry and Physics 69th Edn.. Ed: Weast, R.C., Florida: CRC Press

Wheeler, V. (1977) Drug and Cosmet. Ind., 121, 48-51

Winters, P.J. (1989) ASME Publ. Fed., 79, 113-119

Wood, J.A. and Harder, S.W. (1970) Can. J. Pharm. Sci., 5, 18-23

Yoakam, D.A. and Campbell, R.J. (1984) Pharm Tech., 8, 38-44

Zaro, J.J. and Smith, W.E. (1972) J. Pharm. Sci., 61, 814-815

Zografi, G. (1985). Presented to the Institute of Applied Pharmaceutical Sciences, Centre for Professional Advancement, Amsterdam.

Zografi, G. and Johnson, B.A. (1984) Int. J. Pharm., 22, 159-176

Zografi, G and Tam, S.S. (1976) J. Pharm. Sci., 65, 1145-1149

APPENDIX 1

DETAILS OF MODEL 10 ACCELA-COTA COATING RUNS

RUN No.	GUN TYPE	LIQUID NOZZLE DIAM. (mm)	AIR CAP TYPE	SOLUTION TYPE	SOLUTION CONC (%w/w)	AIR PRESS (kPa)	SPRAY RATE ($gmin^{-1}$)	GUN TO BED DIST (mm)	SPRAY SHAPE
1	SCH	0.8	STD	HPMC E5	9	414	30	180	FLAT
2	SCH	0.8	STD	HPMC E5	9	414	50	180	FLAT
3	SCH	0.8	STD	HPMC E5	9	276	50	180	FLAT
4	SCH	0.8	STD	HPMC E5	9	552	50	180	FLAT
5	SCH	0.8	STD	HPMC E5	9	414	50	180	FLAT
6	SCH	0.8	STD	HPMC E5	9	414	50	180	FLAT
7	SCH	0.8	STD	HPMC E5	9	276	40	180	FLAT
8	SCH	0.8	STD	HPMC E5	9	552	40	180	FLAT
9	SCH	0.8	STD	HPMC E5	9	414	40	180	FLAT
10	WP	1.0	STD	HPMC E5	9	414	40	180	FLAT
11	WP	1.0	STD	HMPC E5	9	552	40	180	FLAT
12	WP	1.0	STD	HPMC E5	9	276	40	180	FLAT
13	SS	0.71	45°	HPMC E5	9	414	40	180	FLAT
14	SS	0.71	60°	HPMC E5	9	414	40	180	FLAT
15	BB	1.8	STD	HPMC E5	9	276	40	180	FLAT
16	BB	1.8	STD	HPMC E5	9	414	40	180	FLAT
17	BB	1.8	STD	HPMC E5	9	552	40	180	FLAT
18	SCH	0.8	STD	HPMC E5	9	552	40	180	10°CONE
19	SCH	0.8	STD	HPMC E5	9	414	40	180	10°CONE
20	SCH	0.8	STD	HPMC E5	9	276	40	180	10°CONE
21	SCH	0.8	STD	HPMC E5	9	552	40	250	FLAT
22	SCH	0.8	STD	HPMC E5	9	414	40	250	FLAT
23	SCH	0.8	STD	HPMC E5	9	276	40	250	FLAT
24	SS	0.71	45°	HPMC E5	9	552	40	180	FLAT
25	SS	0.71	60°	HPMC E5	9	552	40	180	FLAT
26	SS	0.71	60°	HPMC E5	9	552	40	250	FLAT
27	SS	0.71	45°	HPMC E5	9	552	40	250	FLAT
28	SS	0.71	60°	HPMC E5	9	138	40	180	FLAT
29	SS	0.71	60°	HPMC E5	9	276	40	180	FLAT
30	SS	0.71	60°	HPMC E5	9	552	50	250	FLAT
31	WP	1.0	STD	HPMC E5	9	414	40	180	FLAT
32	SCH	0.8	STD	HPMC E5	9	552	40	180	FLAT
33	SCH	0.8	STD	HPMC E5	9	414	50	250	FLAT
34	SCH	0.8	STD	HPMC E5	12	414	40	180	FLAT
35	SCH	0.8	STD	HPMC E5	12	414	40	250	FLAT
36	SCH	0.8	STD	HPMC E5	12	414	50	250	FLAT
37	SS	0.71	60°	HPMC E5	12	414	40	180	FLAT
38	SS	0.71	45°	HPMC E5	12	414	40	180	FLAT
39	SS	0.71	45°	HPMC E5	12	207	40	180	FLAT
40	SCH	0.8	STD	HPMC E5	12	207	40	250	FLAT

An inlet air temperature between 65°C and 69°C and an inlet air volume flow rate of $0.129 m^3 s^{-1}$ were used for all runs in the above table.

APPENDIX 1 (CONT)

DETAILS OF MODEL 10 ACCELA-COTA COATING RUNS

RUN No.	GUN TYPE	LIQUID NOZZLE DIAM. mm	AIR CAP TYPE	SOLUTION TYPE	SOLUTION CONC %w/w	AIR PRESS kPa	SPRAY RATE $gmin^{-1}$	GUN TO BED DIST mm	SPRAY SHAPE	ADDITIONAL PROCESS PARAMETERS
41	SCH	0.8	STD	HPMC E5	12	276	40	180	FLAT	
42	SCH	0.8	STD	HPMC E5	12	414	50	300	FLAT	
43	WP	1.0	STD	HPMC E5	12	414	40	180	FLAT	
44	WP	1.0	STD	HPMC E5	12	207	40	180	FLAT	
45	BB	1.8	STD	HPMC E5	12	414	40	180	FLAT	
46	SS	0.71	45°	HPMC E5	6	414	40	180	FLAT	
47	SCH	0.8	STD	HPMC E5	6	414	40	180	FLAT	
48	SCH	0.8	STD	OPADRY	15	414	50	180	FLAT	
49	SCH	0.8	STD	OPADRY	15	207	50	180	FLAT	
50	SS	0.71	45°	OPADRY	15	414	50	180	FLAT	
51	SS	0.71	60°	OPADRY	15	414	50	180	FLAT	
52	BB	1.8	STD	OPADRY	15	414	50	180	FLAT	
53	WP	1.0	STD	OPADRY	15	414	50	180	FLAT	
54	SCH	0.8	STD	OPADRY	15	414	50	250	FLAT	
55	SCH	1.2	STD	HPMC E5	9	414	40	180	FLAT	
56	SCH	1.8	STD	HPMC E5	9	414	40	180	FLAT	
57	SCH	0.8	STD	HPMC E5	9	414	40	180	FLAT	INLET AIR TEMP 57°C
58	SCH	0.8	STD	HPMC E5	12	414	30	180	FLAT	
59	SCH	0.8	STD	HPMC E5	12	414	40	180	10°CONE	
60	SCH	0.8	STD	HPMC E5	12	207	40	180	FLAT	
61	SCH	0.8	STD	HPMC E5	12	414	50	180	FLAT	
62	SS	0.71	60°	HPMC E5	6	414	40	180	FLAT	
63	WP	1.0	STD	HPMC E5	6	414	40	180	FLAT	
64	WP	1.0	STD	HPMC E5	9	414	50	180	FLAT	
65	SCH	0.8	STD	OPADRY	10	414	50	180	FLAT	
66	SCH	0.8	STD	OPADRY	20	414	30	180	FLAT	
67	SCH	0.8	STD	OPADRY	15	414	40	180	FLAT	
68	SCH	0.8	STD	OPADRY	15	414	30	180	FLAT	
69	SCH	0.8	STD	HPMC E5	9	414	40	180	FLAT	WITH 1%w/w PEG 400
70	SCH	0.8	STD	HPMC E5	12	414	40	180	FLAT	HPMC E5 batch 5
71	SCH	0.8	STD	HPMC E5	12	414	40	180	FLAT	HPMC E5 batch 3
72	SCH	0.8	STD	HPMC E5	9	414	50	180	10°CONE	[WITH 1%w/w PEG 400]
73	SCH	0.8	STD	HPMC E5	9	414	30	250	FLAT	[AND 3.5%w/w $CaCO_3$]
74	SS	0.51	45°	HPMC E5	9	414	40	180	FLAT	
75	SS	0.51	120	HPMC E5	6	276	28	200	CONE	INLET AIR 83°C/0.094m^3s^{-1}
76	SCH	0.8	STD	HPMC E5	9	414	40	180	FLAT	INLET AIR 0.088m^3s^{-1}
77	SCH	0.8	STD	HPMC E5	9	414	40	180	ELIPSE	
78	SCH	0.8	STD	HPMC E5	9	414	40	180	FLAT	INLET LIQUID TEMP 43°C
79	SCH	0.8	STD	HPMC E5	9	414	40	180	FLAT	INLET AIR TEMP 56°C

Except where stated, an inlet air temperature of between 64°C and 67°C and an inlet volume flow rate of 0.129m^3s^{-1} were used.

APPENDIX 2

COATED TABLET DEFECTS

RUN NO	15mm FLAT TABLETS			10mm FLAT TABLETS			10mm CONVEX TABLETS	
	STICKING	PICKING	EDGE SPLITTING	STICKING	PICKING	EDGE SPLITTING	PICKING	SPRAY DRYING
1	10	0	0	4	4	0	0	1,5
2	37	29	0	39	32	0	27	0
3	93	4	0	80	18	0	99	0
4	62	7	0	36	8	0	12	0
5	38	38	0	32	45	0	31	0
6	22	42	0	10	55	0	33	0
7	2	31	1	7	36	0	43	0,5
8	3	3	6	1	11	0	3	1
9	9	2	0	3	5	0	3	0,5
10	20	22	10	8	50	6	44	0
11	10	30	44	10	29	46	35	0
12	43	42	1	16	61	0	44	0
13	10	6	2	5	9	2	27	0,5
14	6	2	2	6	3	1	3	1,5
15	26	57	0	23	58	0	45	0
16	28	47	6	8	54	4	19	0
17	22	27	14	10	44	7	18	0
18	63	1	22	46	5	10	39	0
19	56	3	27	35	18	17	63	0
20	52	6	28	33	11	14	28	0
21	0	1	15	0	0	0	0	2
22	0	3	5	0	0	1	0	2
23	11	9	1	8	1	4	0	1,5
24	0	12	7	2	19	7	23	0
25	3	2	3	1	1	3	1	1,5
26	2	3	0	0	2	0	3	2
27	1	1	2	3	1	0	1	0,5
28	54	18	0	23	21	0	18	1
29	18	9	3	12	14	0	6	1,5
30	15	3	0	5	3	0	3	2
31	21	21	16	12	47	9	40	0
32	0	2	8	1	0	1	1	1
33	0	3	1	0	1	0	0	1
34	4	1	0	4	2	0	0	0,5
35	2	0	0	0	0	0	1	1
36	11	3	0	3	1	0	0	1
37	18	3	0	4	1	0	2	1,5
38	17	22	0	6	26	0	26	0,5
39	63	28	0	25	49	0	49	1
40	12	3	0	0	5	0	1	1

Defect values are expressed as percentages, except in the case of spray drying which is quantified on a scale between 0 and 3.

Full details of the coating runs are given in Appendix 1.

APPENDIX 2 (CONT)

COATED TABLET DEFECTS

RUN NO	15mm FLAT TABLETS			10mm FLAT TABLETS			10mm CONVEX TABLETS	
	STICKING	PICKING	EDGE SPLITTING	STICKING	PICKING	EDGE SPLITTING	PICKING	SPRAY DRYING
41	1	1	0	1	0	0	0	1
42	6	0	0	1	0	0	0	1.5
43	12	19	0	7	36	0	6	0
44	13	24	0	5	21	0	1	0.5
45	30	40	0	12	61	1	39	0
46	10	8	18	3	20	11	25	0.5
47	0	0	50	0	0	38	2	0.5
48	16	5	5	5	11	3	1	0.5
49	26	18	3	9	32	1	12	0
50	52	23	0	27	31	0	9	0
52	26	20	0	6	28	0	10	0
53	21	35	4	3	31	0	9	0
54	0	2	58	0	2	42	4	1
55	8	2	1	2	4	1	0	0.5
56	5	3	0	1	3	0	0	0.5
57	27	51	0	19	49	0	24	0
58	0	0	0	0	0	0	0	0.5
59	2	8	4	2	15	0	19	0
60	36	17	0	15	26	0	12	0.5
61	12	9	0	6	16	0	3	0.5
62	1	0	3	1	2	0	4	0
63	12	9	8	10	26	2	51	0
64	22	42	0	8	44	0	45	0
65	0	0	30	0	3	4	9	0
66	0	0	0	0	0	0	4	0.5
67	4	2	16	1	2	6	3	0.5
68	0	0	26	0	0	10	3	1
69	7	0	0	3	1	0	0	0.5
70	6	3	0	2	6	0	4	0.5
71	28	20	0	21	20	0	12	1.5
72	6	16	0	2	16	0	36	0
73	0	0	0	0	0	0	0	3
74	6	12	7	5	14	0	22	0
75	0	13	65	4	12	66	57	0
76	2	3	1	4	1	2	4	0
77	20	0	0	6	0	0	0	0
78	6	12	0	3	7	0	0	0.5
79	15	36	2	1	42	0	17	0

Defect values are expressed as percentages, except in the case of spray drying which is quantified on a scale between 0 and 3.

Full details of the coating runs are given in Appendix 1.

NB Twelve 10mm convex tablets from run 75 exhibited edge splitting.

APPENDIX 3

ARITHMETIC MEAN ROUGHNESS VALUES OF TABLETS TAKEN FROM MODEL 10 ACCELA-COTA COATING RUNS

COATING RUN NUMBER	ARITHMETIC MEAN SURFACE ROUGHNESS (Ra) ± s.d. (μm)
1	3.90 ± 0.26
2	2.00 ± 0.18
4	1.60 ± 0.13
6	1.90 ± 0.14
7	2.72 ± 0.26
8	2.29 ± 0.17
9	2.53 ± 0.12
10	2.16 ± 0.20
11	1.90 ± 0.15
12	2.54 ± 0.19
13	2.30 ± 0.21
14	3.40 ± 0.24
15	2.41 ± 0.22
16	2.10 ± 0.17
17	2.03 ± 0.17
18	1.29 ± 0.09
19	1.44 ± 0.15
20	1.68 ± 0.13
21	2.60 ± 0.19
22	2.71 ± 0.15
23	3.20 ± 0.24
24	2.08 ± 0.16
25	3.09 ± 0.25
26	3.26 ± 0.31
27	2.31 ± 0.21
28	4.08 ± 0.44
29	3.75 ± 0.48
30	4.17 ± 0.30
31	1.94 ± 0.17
32	2.23 ± 0.16
33	2.27 ± 0.15
34	3.51 ± 0.26
35	4.09 ± 0.32
36	4.06 ± 0.32
37	>5.00
38	3.26 ± 0.29
39	4.16 ± 0.38

All Ra values taken from at least 10 separate surfaces of the 15mm flat tablets. See Appendix 1 for coating run details.

ARITHMETIC MEAN ROUGHNESS VALUES OF TABLETS TAKEN FROM MODEL 10 ACCELA-COTA COATING RUNS

COATING RUN NUMBER	ARITHMETIC MEAN SURFACE ROUGHNESS (Ra) ± s.d. (μm)
40	4.67 ± 0.49
41	3.98 ± 0.30
42	4.24 ± 0.53
43	2.86 ± 0.18
44	1.90 ± 0.20
45	3.20 ± 0.22
46	1.90 ± 0.20
47	1.83 ± 0.22
48	2.98 ± 0.38
50	2.85 ± 0.46
52	3.99 ± 0.55
53	2.28 ± 0.23
55	2.31 ± 0.24
56	2.38 ± 0.14
57	2.43 ± 0.23
58	2.54 ± 0.56
59	2.07 ± 0.14
60	4.06 ± 0.18
61	3.56 ± 0.19
62	2.00 ± 0.22
63	1.75 ± 0.18
64	1.94 ± 0.21
65	2.20 ± 0.26
66	4.24 ± 0.32
67	3.11 ± 0.32
68	2.61 ± 0.15
69	2.93 ± 0.30
70	2.88 ± 0.29
71	3.99 ± 0.29
72	2.14 ± 0.20
73	3.14 ± 0.15
74	2.15 ± 0.31
75	1.45 ± 0.20
76	2.39 ± 0.16
77	2.19 ± 0.27
78	2.88 ± 0.23
79	2.47 ± 0.23

All Ra values taken from at least 10 separate surfaces of the 15mm flat tablets. See Appendix 1 for coating run details.

APPENDIX 4

LIST OF CONFERENCE PAPERS AND PUBLICATIONS

1. The influence of solution properties and atomisation parameters on the droplet size of HPMC film coating solutions: Presented at the 4th International Conference on Pharmaceutical Technology (1986), A.G.P.I., Paris and published in the proceedings as: Aulton, M.E., Twitchell, A.M. and Hogan, J.E. (1986) Proc. 4th A.G.P.I. Int. Conf. on Pharm. Tech., Paris, V, 133.

2. Estimated surface tensions of atomised droplets in aqueous film coating: Presented at the 123rd British Pharmaceutical Conference (1986), Jersey and later published as: Twitchell, A.M., Aulton, M.E. and Hogan, J.E. (1986) J. Pharm. Pharmacol., 38, 75P

3. The effect of atomisation conditions on the surface roughness of aqueous film coated tablets: Presented at the 124th British Pharmaceutical Conference (1987), Manchester and later published as: Twitchell, A.M., Aulton, M.E. and Hogan, J.E. (1987) J. Pharm. Pharmacol., 39, 128P